



Manuel Hollauf, BSc MSc

**Dye-Functionalized Polymers
via Ring Opening Metathesis Polymerization
for Photophysical Applications**

DISSERTATION

zur Erlangung des akademischen Grades

Doktor der technischen Wissenschaften

eingereicht an der

Technischen Universität Graz

Betreuer

Assoc. Prof. Dipl.-Ing. Dr. techn Trimmel Gregor

Institute for Chemistry and Technology of Materials - ICTM

Graz, Jänner 2017

EIDESSTATTLICHE ERKLÄRUNG

Ich erkläre an Eides statt, dass ich die vorliegende Arbeit selbstständig verfasst, andere als die angegebenen Quellen/Hilfsmittel nicht benutzt, und die den benutzten Quellen wörtlich und inhaltlich entnommenen Stellen als solche kenntlich gemacht habe. Das in TUGRAZonline hochgeladene Textdokument ist mit der vorliegenden Dissertation identisch.

Datum

Unterschrift

DANKSAGUNG

Als erstes möchte ich mich bei Herrn Assoc. Prof. Dr. Gregor Trimmel vom Institut für Chemische Technologie von Materialien (ICTM) der Technischen Universität Graz für die Bereitstellung der Doktorarbeit in einem überaus interessanten und anwendungsorientierten Forschungsbereich sowie für die hervorragende Betreuung bedanken.

Des Weiteren bedanke ich mich bei DI Dr. Stefan Köstler und DI Dr. Paul Hartmann von der Forschungsgesellschaft Joanneum Research (MATERIALS - Institute for Surface Technologies and Photonics) die dieses Projekt ins Leben gerufen haben sowie bei dem „Klima und Energiefonds“ (FFG: 841153) der die Finanzierung dieses Projektes ermöglicht hat.

Großer Dank geht an DI Peter Zach BSc. und Ass. Prof. kand Sergey Borisov vom Institut für Analytische Chemie und Lebensmittelchemie der Technischen Universität Graz welche mich tatkräftig bei der Auswahl der Farbstoffe sowie bei den spektroskopischen Messungen unterstützt und durchgeführt haben.

Im Besondern möchte ich mich auch bei DI Dr. Astrid-Caroline Knall bedanken welche mich beim Verfassen meiner wissenschaftlichen Publikationen sehr unterstützt hat.

Danke gilt auch meinen unzähligen Studenten welche mich beim Entwickeln meiner Farbstoffe und die daraus folgenden Polymere geholfen haben. Ins Besondere meinen Diplom Studenten DI David Beichel BSc. in dem ich auch einen neuen Freund und motivierten Kletterpartner gefunden habe.

Viele Untersuchungen, welche im Zusammenhang mit dieser Arbeit stehen, wären ohne Kollaborationen nicht möglich gewesen. Deshalb möchte ich mich bei Ao. Univ.-Prof. DI Dr. Hansjörg Weber vom Institut für Organische Chemie und DI Dr. Petra Kaschnitz vom Institut für Chemische Technologie von Materialien für die Zusammenarbeit sämtlicher NMR Experimente bedanken. Bei Ao. Univ.-Prof. DI Dr. Robert Saf und bei Ing. Karin Bartl vom Institut für Chemische Technologie von Materialien für die massenspektrometrische

Messungen bedanken. Und bei Ing. Josefine Hobisch vom Institut für Chemische Technologie von Materialien für die Gel-Permutations-chromatographischen Messungen bedanken.

Des Weiteren möchte ich mich beim gesamten ICTM-Team, im speziellen bei meiner Arbeitsgruppe für die jederzeit vorhandene Hilfsbereitschaft sowie die hervorragende Arbeitsatmosphäre bedanken. Besonderer Dank gilt hier Simon Leimgruber und Franz Pirolt, die ständig ein offenes Ohr für meine Anliegen und Probleme hatten.

Ich möchte mich auch bei meiner Band bedanken die mir zwar immer wieder sehr viele Nerven gekostet hat (und noch kosten werden wird) aber dennoch immer eine sehr gute Ablenkung und Aufmunterung zum teilweise stressigen und frustrierenden Laboraltag geboten hat. Danke Paul, Bure, Olli und Gerfried.

Meinen Eltern Ingrid und Kurt möchte ich ein besonders wertvolles Dankeschön für die Unterstützung und Ermöglichung des Studiums aussprechen. Ohne euch wäre dies keinesfalls möglich gewesen.

Zu guter Letzt möchte ich mich noch bei meiner Freundin Magdalena bedanken die ich im Zuge meiner Dissertation kennenlernen durfte und mich noch in den letzten Monaten mental gestärkt hat, meinen Wahnsinn erduldet und mich immer motiviert meine privaten sowie beruflichen Ziele zu erreichen. Danke Magda!

ABSTRACT

The preparation of dye-functionalized polymers is a very interesting but also challenging task in materials chemistry. There are countless possibilities of application, like the conversion of laser light, optimizations of the efficiency of solar cells, optical data storage and optical sensing for chemical reactions, to name just a few. In this context ring opening metathesis polymerization (ROMP) has received wide reception for the preparation of such special polymers. This technique is well-known for its high functional group tolerance and it is a well investigated living polymerization technique that allows the synthesis of different polymer architectures.

In this work the synthesis of several di- and tricopolymers, functionalized with different chromophores, by ROMP is presented. Furthermore different polymer architectures have been synthesized. Therefore, the chromophores have been equipped with norbornene moieties to ensure a covalent attachment into the macromolecule after polymerization. The incorporation of different porphyrin derivatives in combination with diphenylanthracene or perylene derivatives led to special polymers which were able to convert electromagnetic radiations of higher wavelengths to lower wavelengths via triplet-triplet annihilation (TTA). With these systems it was possible to transfer red to green and green to blue light. The TTA behavior was investigated in dependence of different polymeric architectures.

Additionally, highly fluorescent and photostable naphthalimide derivatives with a polymerizable norbornene scaffold have been synthesized and polymerized using ROMP. All obtained materials showed good film-forming properties and bright fluorescence caused by the incorporated push-pull chromophores. The naphthalimide derivative containing a methylpiperazine functionality showed protonation-dependent photoinduced electron transfer. Therefore, it was randomly copolymerized with a water-soluble norbornene matrix obtaining a pH-sensor. The sensor shows no emission in an alkaline environment and starts to emit a yellow light in acidic solutions.

In addition, platinum tetraphenylporphyrin was equipped with four termination functionalities for ROMP. Hence, it should be possible to prepare star-shaped polymers with the chromophore in the center.

KURZFASSUNG

Die Herstellung von farbstofffunktionalisierten Polymeren ist eine sehr interessante, aber auch herausfordernde Aufgabe in der Materialchemie. Diese Polymere können für eine Vielzahl von Einsatzmöglichkeiten verwendet werden, wie z.B. die Konversion von Laserlicht, Optimierungen der Effizienz von Solarzellen, optische Datenspeicherung und optische Messungen für chemische Reaktionen, um nur einige zu nennen. In diesem Zusammenhang hat sich die Ringöffnungsmetathesepolymerisation (ROMP) als hervorragende Herstellungsmethode um solche Spezialpolymere zu erhalten herausgestellt. Diese Technik ist bekannt für ihre hohe Toleranz gegenüber funktionellen Gruppen und ist eine gut untersuchte lebende Polymerisationstechnik, die die Synthese verschiedener Polymerarchitekturen ermöglicht. In dieser Arbeit wird die Synthese mehrerer, mit verschiedenen Chromophoren funktionalisierten, Di- und Tricopolymeren durch ROMP beschrieben. Zusätzlich wurden verschiedene Polymerarchitekturen synthetisiert und untersucht. Die Farbstoffe wurden mit Norbornen-Einheiten ausgestattet, um eine kovalente Bindung in das Makromolekül nach der Polymerisation sicherzustellen. Der Einbau von verschiedenen Porphyrinderivaten mit Diphenylanthracen- oder Perylenderivaten führte zu speziellen Polymeren, die in der Lage sind, elektromagnetische Strahlung höherer Wellenlängen in niedrigere Wellenlängen umzuwandeln. Mit diesen Systemen ist es möglich, rotes zu grünem und grünes zu blauem Licht zu konvertieren. Dieses Verhalten wurde in Abhängigkeit von unterschiedlichen Polymerarchitekturen untersucht. Zusätzlich wurden hochfluoreszierende und photostabile Naphthalimidderivate mit einem polymerisierbaren Norbornengerüst synthetisiert und unter Verwendung von ROMP polymerisiert. Alle erhaltenen Materialien zeigten gute filmbildende Eigenschaften und intensive Fluoreszenz, die durch die eingebauten „push-pull“ Chromophore verursacht wurden. Das Naphthalimidderivat, das eine Methylpiperazinfunktionalität enthielt, zeigte einen protonierungsabhängigen photoinduzierten Elektronentransfer. Daher wurde es mit einer wasserlöslichen Norbornen-Matrix copolymerisiert, wodurch ein pH-Sensor hergestellt wurde. Der Sensor zeigt keine Emission in einer alkalischen Umgebung und beginnt in sauren Lösungen ein gelbes Licht zu emittieren. Zusätzlich wurde Platintetraphenylporphyrin mit vier ROMP-Terminationseinheiten ausgestattet. Mit dieser Verbindung sollte es möglich sein, sternförmige Polymere mit dem Chromophor im Zentrum herzustellen.

LIST OF ABBREVIATIONS

| | |
|-------------------|--|
| $^1E^*$ | excited singlet state emitter |
| $^1S^*$ | excited singlet state sensitizer |
| $^3E^*$ | excited triplet state emitter |
| $^3S^*$ | excited triplet state sensitizer |
| ac | acetyl |
| acac | acetyl acetone |
| APT | Attached Proton Test |
| ATR-FTI | attenuated total reflection- Fourier transform infrared spectroscopy |
| b | broad |
| CH | cyclohexane |
| d | duplet |
| DCC | <i>N,N'</i> -Dicyclohexylcarbodiimide |
| DCM | dichloromethane |
| dd | doublet of doublets |
| DMAP | 4-(dimethylamino)-pyridine |
| DMF | dimethylformamide |
| DMSO | dimethyl sulfoxide |
| DSC | differential scanning calorimetry |
| EtOAc | ethyl acetate |
| EtOH | ethanol |
| Et ₃ N | trimethylamine |
| g | gram |
| GPC | gel permeation chromatography |
| GS | ground state |
| h | hours |

| | |
|----------------|--|
| Hz | hertz |
| ISC | intersystem crossing |
| m | multiplet |
| MALDI-TOF | matrix-assisted laser desorption ionization-time of flight |
| MeOH | methanol |
| NMR | nuclear magnetic resonance spectroscopy |
| PDI | polydispersity index |
| PdOEP | Pd-octaethylporphyrin |
| PdTPTBP | Pd-tetraphenyltetrabenzoporphyrin |
| PET | photoinduced electron transfer |
| PtOEP | Pt-octaethylporphyrin |
| PtTPTBP | Pt-tetraphenyltetrabenzoporphyrin |
| q | quadruplet |
| ROMP | ring opening metathesis polymerization |
| s | singlet |
| t | triplet |
| T _G | glass transition temperature |
| THF | tetrahydrofuran |
| TLC | thin layer chromatography |
| TPP | <i>meso</i> -tetraphenylporphyrin |
| TTA | triplet-triplet annihilation |
| TTA-UC | triplet-triplet annihilation up-conversion |
| TTET | triplet triplet energy transfer |
| UV | ultraviolet light |
| UV-Vis | ultraviolet–visible spectroscopy |

TABLE OF CONTENT

| | | |
|------------------|---|-----|
| | INTRODUCTION | 1 |
| CHAPTER 1 | DYE-FUNCTIONALIZED POLYMERS VIA RING OPENING METATHESIS POLYMERIZATION: PRINCIPLE ROUTES AND APPLICATIONS | 4 |
| CHAPTER 2 | A WAY TO PHOTOACTIVE COMPOUNDS – EMPIRICAL INVESTIGATION OF DYE-FUNCTIONALIZED POLYMERS ABLE TO CONVERT ELECTROMAGNETIC RADIATION VIA TRIPLET-TRIPLET ANNIHILATION | 33 |
| CHAPTER 3 | FIRST ROMP BASED TERPOLYMERS FOR THE USE AS A LIGHT UP-CONVERTING MATERIAL VIA TRIPLET-TRIPLET ANNIHILATION | 55 |
| CHAPTER 4 | SYNTHESIS AND CHARACTERIZATION OF NAPHTHALIMIDE – FUNCTIONALIZED POLYNORBORNENES | 84 |
| CHAPTER 5 | NAPHTHALIMIDE – FUNCTIONALIZED POLYNORBORNENES FOR THE USE AS PH-SENSOR | 101 |
| CHAPTER 6 | PREPARATION OF A NEWLY DEVELOPED DYE – FUNCTIONALIZED TERMINATION REAGENT FOR RING OPENING METATHESIS POLYMERIZATION | 109 |
| CHAPTER 7 | CONCLUSION | 121 |
| CHAPTER 8 | CURRICULUM VITAE | 128 |

INTRODUCTION

This PhD-thesis focuses on the investigation of dye-functionalized polymers which were prepared via ring opening metathesis polymerization (ROMP) and have been tested for various photophysical applications.

The preparation of dye-functionalized polymers is a very important topic for a large number of different applications in research and technology. A big advantage of such systems is that the polymer chain prevents leakage of the dye molecules reducing aggregation and thus leading to more homogeneous distributed chromophores within the matrix polymer. This consequently leads to functional polymeric materials for different optical applications. Another very important benefit is that aggregation state, rigidity and solubility of the chromophores can be modified through the use of different matrix monomers but still contain their photo physical characteristics. For example, it is possible to dissolve a previously hydrophobic chromophore in an aqueous media through the copolymerization with a water soluble matrix monomer.¹ Another advantage of dye-functionalized polymers is that the covalent attachment to a macromolecule seems to be not only the reduced toxicity or the possibility of better recovery and reusability but also improved quality characteristics such as high colour fastness in textile dyeing.² Typical applications are e.g. utilization of dye properties in medicine, for analytical purposes or as optical sensors in chemical research.

The main focus of this PhD-thesis lies on the preparation of terpolymers that allow the conversion of optical radiation into photons of higher energy. This was accomplished through a precise selection and preparation of chromophores that are able to induce an up-conversion (UC) via triplet-triplet annihilation (TTA). This process requires a combination of two chromophores, a so called sensitizer which is able to absorb light of a defined wavelength and an emitter which is then able to emit electromagnetic radiation of higher energies. The chromophores have been equipped with norbornene moieties to copolymerize with a matrix monomer via ring opening metathesis polymerization. The triplet-triplet annihilation was first demonstrated by Parker and Hatchard in 1962.³ They were able to prepare solutions of anthracene and phenanthrene to up-convert ultraviolet light. This process was limited to liquid solutions of a sensitizer-emitter pair for almost half a century. In 2007 the group of Castellano achieved a TTA induced up-conversion in solid polymer

matrices.⁴ Due to their process ability and mechanical characteristics these polymers were more suitable for many potential applications than liquid solutions. In particular, systems where the chromophores are attached to a polymer backbone will help to increase the concentration of dyes and control the architecture of the resulting material. This is crucial for an efficient TTA due to the fact that a controlled and precise distance between the dyes is absolutely essential. With these polymer-based TTA systems a lot of different and interesting applications are possible, like the conversion of laser light, optimizations of the efficiency of solar cells or oxygen sensing. Further possible areas of applications are the pharmaceutical industry (e.g. drug delivery), optical data storage, and many others. This thesis presents the selection and the preparation of two suitable chromophore pairs that are able to cause a TTA. A sufficiently molar ratio of the chromophores to each other within the macromolecule was investigated. Furthermore, an adequate concentration for the TTA measurements was determined. To investigate the TTA behavior in dependence of the distance between the chromophores, different polymeric architectures were synthesized.

This thesis also focuses on the preparation of naphthalimide-functionalized polynorbornenes to compare the photo-physical properties of the monomers and the corresponding polymers. Therefore, five different naphthalimide derivatives have been synthesized and equipped with a norbornene moieties for further ROMP. These compounds are highly fluorescent and photostable and are thus in the interest of various fields of technologies. Interesting applications of naphthalimide derivatives are related to organic electronics where they are especially applied in organic light emitting diodes (OLED) or in organic photovoltaics where they are especially applied in non-fullerene acceptors and n-type polymers. Naphthalimide-based systems were also applied as fluorescent markers in molecular biology and imaging applications. The naphthalimide derivative containing a methylpiperazine functionality shows a protonation-dependent photoinduced electron transfer. Therefore, it was randomly copolymerized with a water-soluble norbornene matrix obtaining a pH-sensor. It was tested in various phosphate buffer solutions.

The following section presents a general overview of all chapters of this dissertation.

The first chapter deals with the principle routes and applications for ROMP based dye-functionalized polymers and summarize the highlights from recent literature. It presents the different approaches to incorporate dyes during initiation, propagation and termination

steps in ROMP. Furthermore, applications in the field of chemical sensors, bioimaging, electroactive materials, photochromic and photo-reactive materials as well as self-assembly help to understand the versatility of ROMP as a technique to prepare complex functional materials.

Chapter two to five present the preparation of the dye-functionalized polymers.

The prepared polymers which are presented in chapter two and three are able to undergo a triplet-triplet annihilation induced up-conversion. Different polymeric architectures have been prepared to investigate differences in the behaviour of the TTA, depending on the arrangement of the chromophores.

In chapter four highly fluorescent and photo stable naphthalimide derivatives with a polymerizable norbornene scaffold have been synthesized and copolymerized with different matrix monomers. The monomers presented herein could be polymerized in a living fashion, using different comonomers and different monomer ratios. All obtained materials showed good film-forming properties and bright fluorescence caused by the incorporated push-pull chromophores. Additionally, one of the monomers containing a methyl-piperazine functionality showed protonation-dependent photo-induced electron transfer which opens up interesting applications for logic gates and sensing.

Therefore, chapter five shows copolymerization of that pH-sensitive monomer with a glycol-functionalized norbornene monomer to obtain a water-soluble polymer which shows different photo physical properties at different proton concentrations.

Chapter six presents the preparation of a newly developed tetraphenylporphyrin derivative for the use as a ROMP termination reagent with four termination moieties. With this compound it should be possible to obtain star shaped polymers with a porphyrin core.

Chapter seven gives a conclusion of all results and offers ideas for further experiments.

CHAPTER 1

Chapter 1 was originally published in **MONATSHEFTE FÜR CHEMIE - CHEMICAL MONTHLY**.

DYE-FUNCTIONALIZED POLYMERS VIA RING OPENING METATHESIS POLYMERIZATION: PRINCIPLE ROUTES AND APPLICATIONS

Manuel Hollauf • Gregor Trimmel • Astrid C. Knall

Monatshefte für Chemie - Chemical Monthly, 2015,146, 1063

DOI: 10.1007/s00706-015-1493-9

© Springer Science + Business Media S. A.



Abstract

Herein, highlights from the recent literature regarding functional dye-polymer conjugates via Ring Opening Metathesis Polymerization (ROMP) are presented and the different approaches to incorporate dyes during the initiation, propagation and termination step in ROMP are discussed. Applications in the field of chemical sensors, bioimaging, electroactive materials, photochromic and photoreactive materials as well as self-assembly are used to discuss the versatility of ROMP as a technique to prepare complex functional materials.

Introduction

Dye-functionalized polymers are useful in a plenitude of current applications in research and technology. Firstly, the covalent attachment of dye molecules to the polymer main chain prevents leakage of the dye molecules reducing aggregation and thus leading to more homogeneous distributed chromophores within the matrix polymer and consequently leads to functional polymeric materials for different optical applications. In addition, by attaching a dye to an amphiphilic block copolymer and using their self-assembly and aggregation behavior, hydrophobic and non-water-soluble materials can be introduced in an aqueous environment which enables dye-polymer conjugates to be used in labeling experiments, ranging from cell staining to *in vivo* applications.

Furthermore, additional functionalities such as biomarkers, photoreactive groups, nanoparticles or functional groups which allow an interaction with surfaces can be incorporated in dye-polymer conjugates. In addition to the principle question of the reliable attachment of the dye to the polymer, the location of the dye molecule on the polymer chain is of almost the same importance. Since an ideal polymerization technique for the preparation of such multifunctional materials requires precise control of the incorporation of two or more monomers with different functionalities, ring-opening metathesis polymerization (ROMP) has received wide reception for the preparation of such specialty polymers. The initiators for ROMP have evolved in a way which enables living polymerization (characterized by complete and rapid initiation, irreversible propagation steps and absence of chain termination or chain transfer reactions) allowing the preparation of polymers with a narrow molecular weight distribution, and, even more importantly, the preparation of block copolymers. This, in combination with a high functional group tolerance and mild reaction

conditions makes ROMP a very well suited method for the preparation of functional materials and specialty polymers.⁵⁻⁹

This concept paper is aimed at giving an overview of the different strategies to obtain dye-functionalized ROMP polymers, discussing their advantages and disadvantages based on selected examples for synthesis and applications found in literature.

Approaches towards defined dye-functionalization of ROMP-polymers

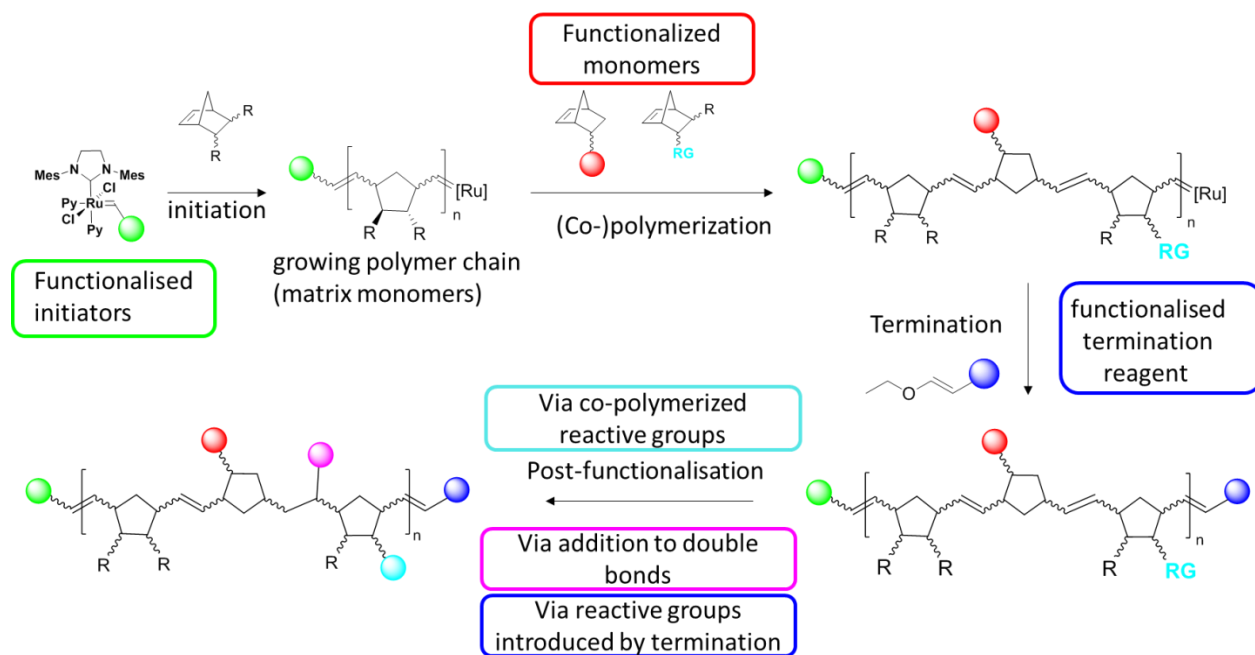


Figure 1 Schematic representation of possible ways to introduce dye-functionalities into a ROMP polymer: via initiation (green spheres), functionalized monomers (red spheres) or reactive groups (RG), termination (blue spheres) or post-functionalization reactions (pink spheres).

There are several strategies to introduce functionalities such as dyes into ROMP polymers (see Figure 1). Firstly, the carbenoid ligand of the initiator remains in the polymer chain so that suitably derivatized initiators can be used to label a polymer chain at its beginning with a dye molecule. Secondly, in the most common approach, monomers can be equipped with dye molecules and (co)polymerized to defined dye-functionalized (co)polymers. Thirdly, the termination reagents can be derivatized so that one dye molecule can be attached to the end of the polymer chains. Alternatively, reactive groups can be incorporated in the initiation, propagation and termination steps and the dye molecule is subsequently

immobilized in a post-polymerization functionalization approach. In addition to these methods, the double bonds in the polymer backbone are also available for post-polymerization functionalization.

With these various methods at hand, ROMP allows precise placement of dye molecules within polymer chains and materials. Table 1 gives an overview of different dye categories being incorporated in ROMP polymers using the aforementioned techniques.

Table 1 Different routes to dye-functionalized polymers and used dye categories

| Dye category | Homopolymers | Random copolymers | Block copolymers | Initiator | Termination reagent | Reactive groups | Post-functionalisation |
|---|---|--|---|---|--|-------------------------------|---|
| (Hetero)acenes | anthracene [17-19], pentacene [20], tetracene [20] | anthracene [17,19], pyrene [21], benzothienobenzothiophene [22] | - | - | anthracene [76] | - | fluorene [92] |
| (Hetero)cycles | perylenebisimides [23, 24, 25, 26], hexabenzocoronene [27, 28, 29], quinolone [30], pyrene [31] | phenanthroimidazole [32,33], perylene bisimides [23], quinizarine [34], phenoxynaphtacene [35] | perylene bisimides [23] | phenanthroimidazole [15], perylenebisimides [12], pyrene [13] | coumarin [81] | benzoxazole [83] | benzoxazole [78, 92]* |
| Triphenylmethane dyes | (dichloro)fluorescein [42], eosin [42] | eosin [43] | Oregon Green 488 [44], Rhodamin B [45], rhodamin [46], fluorescein [46], eosin [47, 48, 49] | fluorescein [14] | rhodamin, [14, 94] fluorescein, [14, 94] | - | Rhodamin Ba [79], Rhodamin 123a [80], fluoresceina [81] |
| Azo dyes | [50-54] | [50] | - | - | - | - | - |
| Polymethine dyes | Spiropyrans [55, 56, 57]b, spirooxazines [58]b | Spiropyrans [55, 59] b | - | - | - | Indocyanine green [86, 90,91] | Indocyanine green [87] |
| Transition metal coordination compounds | Al [60, 61], Ru [67], Fe [62,63], Ir [70] | Al [60], Pt [73], Zn [64, 65], Ir [71, 72], Eu [69] | Ru [67, 68], Pt [73, 74], Ir [71], Zn [66], Eu[69] | Tb[16] | - | - | Eu [93] |
| Conjugated oligomers and electroactive materials | oligo-EDOT [36], oligo-PPV [37], Fluorene-carbazole trimers [38], oligothiophene [39], triphenylamine [40,41] | oligo-EDOT [36] | - | - | oligothiophene [77] | 2PA Dyes [84] | oligo-PPV [37]a |

^aPost-functionalization of semi-telechelic polymers with reactive end groups; ^breversible photoreaction to merocyanines

It is also worth mentioning that ROMP also can be used to prepare conjugated polymers which can be considered as dye molecules themselves as covered in a recent review by Bunz et al.¹⁰. Another interesting class of materials are liquid crystalline ROMP polymers containing large polyaromatic and rigid moieties.¹¹ However, this work aims at giving examples on how the incorporation of functionalized dyes into ROMP polymers can be utilized to prepare functional materials which is why these topics will not be included in this work.

Functionalization by dye-modified initiators

The carbenoid ligand in the transition metal carbene initiators (typically a benzylidene or indenylidene group) remains at the beginning of the polymer chain. This has the advantage that all polymer chains are labeled so that polymerization kinetics and dye aggregation do not influence the dye content of the molecule. However, for certain applications, a higher dye content is required which cannot be achieved by this method (only one dye molecule per chain can be incorporated). Furthermore, for this functionalization technique, new initiators need to be synthesized for each dye class, which can be more challenging than monomer synthesis in some cases. A typical method for this is cross metathesis of a ROMP initiator with a suitable precursor. Also there is a potential interference between the initiator and the pending dye due to sterical hindrance or functional groups of the dye which could alter the polymerization kinetics, especially of the initiation step. Consequently, this route has not been used very often and only relative innocuous dyes like perylenebismides¹², pyrene¹³ or phenanthroimidazole¹⁵ have been employed whereas fluorescein¹⁴ could be only used after protecting the O-H functionalities, see also Figure 2.

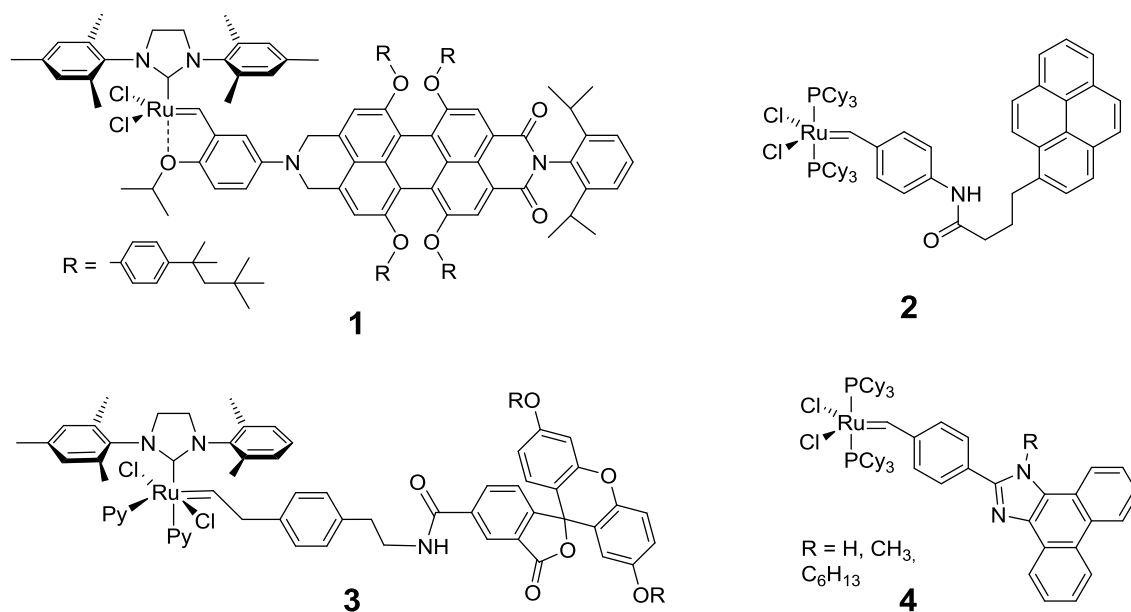


Figure 2 Chemical structures of dye-functionalized initiators: perylenebismides (**1**)¹², pyrene (**2**)¹³, fluorescein (**3**)¹⁴ and phenanthroimidazole (**4**).¹⁵

Alternatively, a ROMP initiator can be also grafted *in situ* via a terminal olefin, subsequently followed by polymerization which has been shown for a terbium coordination compound.¹⁶

Functionalization by dye-substituted monomers

Conceptually, the (co)polymerization of a suitably derivatized monomer is the most straightforward method to get to a highly functionalized polymer.

[2.2.1] Bicyclohept-5-ene-derivatives (norbornenes) are the most common monomers in ROMP, as a huge variety of different monomers can be produced by a [4 + 2]-cycloaddition (Diels-Alder reaction) of a dienophile (electron-deficient alkene) and a conjugated diene, in most cases cyclopentadiene or furan.

Alternatively, large and complex functionalities can be easily introduced by esterification or etherification reactions. E.g. for the anchoring of a dye via an ester group, norbornoyl chloride is usually prepared *in situ* from acryloyl chloride and cyclopentadiene, followed by reaction with the corresponding alcohol. Depending on the environment for the polymer to be applied in, esters as anchor groups might be subject to hydrolysis and could be replaced by ethers, amides, imides or aliphatic chains. However, one should consider that anchor groups have an influence on the polymerization rate and monomers which are sterically unhindered bear the inherent risk of backbiting via a cross metathesis mechanism leading to

ill-defined polymeric products. In addition to the nature of the anchoring groups, the polymerization rate constants also depend on the stereochemistry on the norbornene and thus on the configuration of the substituents in 2- and 3-position (*exo* or *endo*). To minimize these effects, bifunctional norbornene derivatives are often applied. These are typically prepared by [4 + 2]-cycloaddition of cyclopentadiene to *trans*-alkenes such as fumaric acid leaving a racemate of *endo*-, *exo*- substituted norbornenes. In contrast, mono-substituted alkenes lead to a mixture of *endo*- and *exo*- products with significant differences in their propagation rate. Nevertheless, the density of functional groups in the polymer can be additionally varied by changing between mono- and bi-functional norbornene derivatives. Another popular choice of monomer are norbornenes and 7-oxanorbornenes derived from maleimide and cyclopentadiene or furan, respectively. While, due to their easy synthetic availability, norbornenes are used in the majority of ROMP publications, other strained olefin monomers such as cyclobutene, cyclopentene or cyclooctene [12] have been used for special applications such as the synthesis of highly regular LDPE.

The majority of dye-functionalized ROMP polymers have been obtained following a functional monomer approach (Table 1). A wide range of suitable monomers has been copolymerized comprising (hetero)polyaromatic compounds¹⁷⁻³⁵, and more sophisticated functionalities like conjugated oligomers³⁶⁻⁴¹, triphenylmethane⁴²⁻⁴⁹, azo⁵⁰⁻⁵⁴ or polymethine⁵⁵⁻⁵⁹ dyes. Even transition metal coordination compounds of aluminium^{60, 61}, iron^{62, 63}, zinc⁶⁴⁻⁶⁶, ruthenium^{67, 68}, europium⁶⁹, iridium⁷⁰⁻⁷² and platinum^{73, 74} have been successfully incorporated in ROMP polymers.

Functionalization via the termination agent

To terminate a ring-opening metathesis polymerization, the active carbenoid species residing on the polymer chains needs to be converted into a less reactive species to avoid back-biting and other cross metathesis reactions.⁷⁵ One approach to this is to directly incorporate dyes by cross metathesis, either with difunctionalized alkenes¹⁴ or with dyes bearing acrylate or vinyl ether functionalities which convert the carbenoid species residing in a polymer chain into a less reactive, Fischer-type carbene. It should be noted that, while using dye-functionalized vinyl ether terminating agents results in quantitatively dye labeled polymer chains, acrylate - functionalized terminating reagents resulted in formation of a significant amount of methylene terminated polymer chains as side product.⁷⁶ Aldehydes

react with Schrock-type (molybdenum carbene) initiators as well as tungsten or titanium-based initiators in a Wittig-type reaction and can be used as terminating reagents for these systems.^{37, 75, 77}

The synthesis of dye functionalized termination reagents is, in most cases, as straightforward as for dye-functionalized monomers and initiator stability is obviously not an issue which is an advantage compared to functionalized initiators. While functional group placement is limited to one unit per polymer and the end of the respective polymer chain, this approach is complementary to the initiator route so that both ends can be labeled if desired. Alternatively, a reactive group such as activated esters, ketones or azides can be introduced via all of these reagents which can be then further used to attach dye molecules, an approach which has been quite frequently pursued.^{7, 78-81}

However, only living polymer chains are labeled at the end which leads to some polymer chains being possibly unlabeled - those which terminated during the polymerization process due to backbiting, impurities in the monomer or contaminants (e.g. oxygen) in the solvent.

Post-polymerization modification

With the increasing demand for multifunctional materials containing components which are even beyond the impressive substrate scope of ROMP initiators, post-polymerization functionalization has become increasingly attractive, also for polynorbornenes and other ROMP polymers. However, this more general method requires an efficient and chemoselective coordination or reaction step.

Frequently used reactive motifs for post-polymerization functionalization⁸² are hydroxyl, amino, carboxylic acid, activated ester (such as succinimidyl or pentafluorophenyl esters), azide, alkyne, alkene, thiol, or maleimide groups.

While activated esters^{14, 79, 83, 84} and maleimide functionalities can be straightforwardly (co)polymerized via ROMP, terminal alkynes would participate in a metathesis reaction and therefore need to be protected, typically by a trimethylsilyl group which can be conveniently cleaved after polymerization using tetrabutylammonium fluoride. Azides are also not compatible with ROMP but can be also introduced after polymerization by nucleophilic substitution of pendant alkyl halogenide chains.^{85, 86, 87} The triazolyl groups formed in copper catalyzed azide-alkyne click chemistry do not have a negative effect on ROMP.^{45, 88}

Another possibility is to introduce a derivatizable functionality by cross metathesis in direct precedence of polymerization, similar to the aforementioned *in situ* labeling of initiators. In most cases, protecting groups need to be applied to make sure the initiator does not change its reactivity.⁸⁹ In the termination step, more functionalities can be tolerated so that for example, it is possible to introduce azides^{79, 80} or ketones⁷⁹ via vinyl ether termination. More detailed information on the introduction of reactive groups in the termination step can be found in recent reviews by Kilbinger⁷⁵ and Nomura⁷.

Functionalization of double bonds in the poly(norbornene) backbone

In addition to derivatizable groups which may be introduced at any stage of the ROMP polymerization process, the double bonds of the polymer backbone can be used for introducing additional functionality, which was previously used for hydroxylation^{86, 87, 90, 91}, epoxidation¹⁹ and sulfonation¹⁹.

Exhaustive hydrogenation of polynorbornenes^{12, 31} was mainly performed to improve oxidative stability of the now aliphatic materials. Taking place under relatively mild reaction conditions, radical thiol-ene⁹² reactions have been recently used to attach dye molecules (fluorene and benzoxazole) directly to a polynorbornene backbone. In another novel approach, tetrazines were used to graft dipyridylpyridazine ligands in an inverse electron demand Diels-Alder reaction to a polydicyclopentadiene foam prepared by emulsion templating. Successful grafting of the ligands was proven by the formation of red phosphorescent europium complexes on the surface of the polymeric foams.⁹³

Selected applications of dye-functionalized polymers prepared by ROMP

In the second major part of this concept paper, we show some examples from recent literature which illustrate the ability of ROMP as a pathway to functional materials and thereby focus on different applications where ROMP polymers have made a significant contribution. Dye-polymer conjugates are the material of choice when sensing applications and bioimaging applications are targeted since they allow changing the solubility of dye molecules so that hydrophobic materials can be used in water. In addition, covalent immobilization of dyes reduces dye leaching, thereby improving, for example, sensor stability. In molecular probes, dyes can be combined with recognizable units and biocompatible materials and can therefore be used even *in vivo*. Another intriguing feature

of ROMP polymers is that crystalline materials can be rendered amorphous which is of interest in electroactive applications because of improved film-forming properties. On the other hand, large aromatic units which are likely to self-assemble can be polymerized so that self-assembled structures are conserved. Finally, poly(norbornene) backbones are virtually non-absorbing to UV-Vis irradiation which makes them a suitable candidate for the polymerization of photoreactive and photochromic compounds.

Chemosensors

Copolymerisation of dye molecules which change their optical properties upon an external stimulus (pressure/temperature change, presence/absence of an analyte) allows incorporating them into polymeric structures so that solubility and hydrophilicity can be adjusted to the application. Furthermore, self-assembly of amphiphilic block copolymers allows to incorporate these molecules into micelles and hierarchical bulk structures. Typically, norbornene polymers are characterized by a high polymerization yield, and easy monomer preparation, which makes combinatorial approaches possible.

As first example, azo dyes show a color change upon acidification which can be quantified as a bathochromic shift in the UV-Vis absorption spectrum. As opposed to radical polymerization techniques, ROMP is a facile way to incorporate these units in polymers and therefore, a number of polynorbornenes with azo dyes (**5**) have been synthesized.⁵⁰⁻⁵⁴ In Figure 3 monomers bearing such azo-dyes are shown as well as their color change at different pH-values in solution.

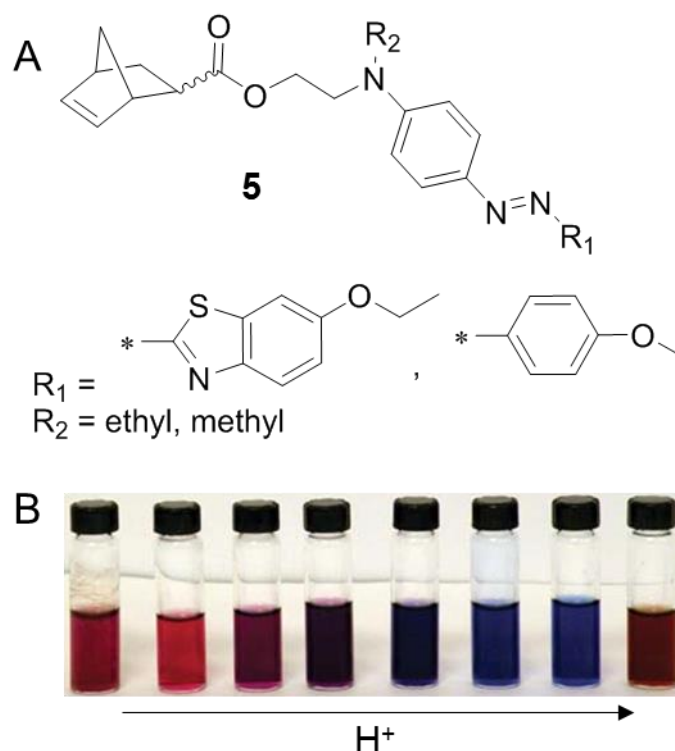


Figure 3 A) norbornene monomers bearing aryl- and heteroarylazo dyes (**5**) and B) their color change at different pH-values in DMF solution⁵⁰

Polynorbornenes with pendant 2-phenyl-1H-phenanthro[9,10-d]imidazoles showed a profound change of the photoluminescence of films upon exposure to HCl vapor.^{32, 33} Furthermore, xanthene functionalized (via copolymerization of fluorescein, dichlorofluorescein and eosin-bearing monomers (**6**)) ROMP polymers showed an acid/base sensitive behaviour when neat films were exposed to HCl or trimethylamine vapors, which makes them a promising material for sensing applications.⁴² The copolymerization of norbornenes with pendant europium(III)-containing side chains like **7** led to red phosphorescent materials, whose luminescence lifetime can be used to detect small amounts of water vapor [69]. The structures of the used dye-functionalized monomers are given in Figure 4.

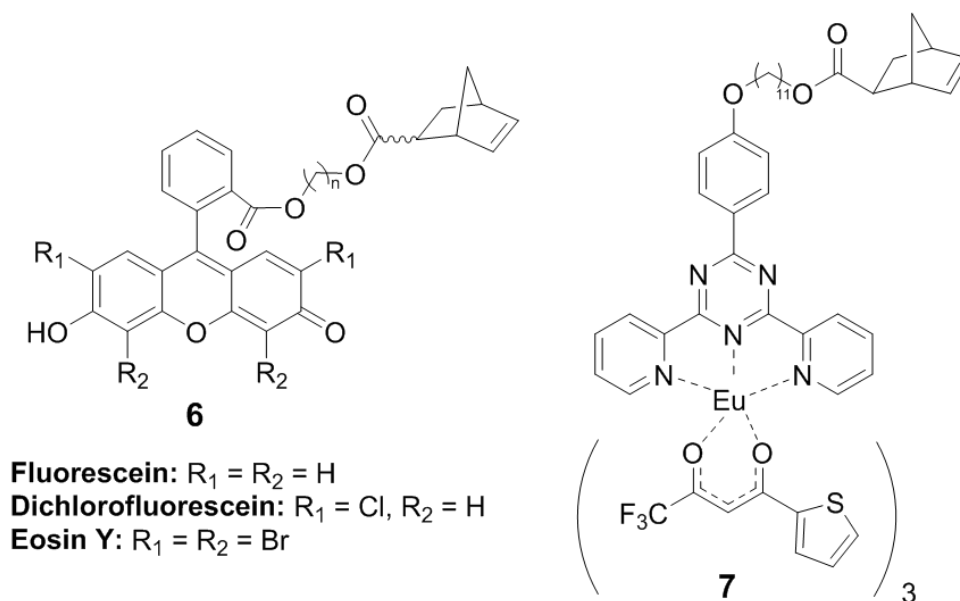


Figure 4 Xanthene⁴² and europium based⁶⁹ dyes used in ROMP sensor polymers.

The quenching of fluorescence by PET (photoinduced electron transfer) from moieties bearing free electron pairs, such as amines can be used for pH measurements while tetramethylpiperidine-1-oxyl units act as quenchers which can be applied for the detection of radical species. This approach of combining dyes and responsive units on a polymer backbone has the advantage that different sensing mechanisms can be straightforwardly accessed by combining according monomers via ROMP. Furthermore, oligo(ethyleneglycol)-functionalized norbornenes could be incorporated to render the resulting copolymers water-soluble. A key requirement is that the two functionalities are brought in proximity to each other, which was demonstrated by comparison of a blend system, random copolymers and block copolymers containing a perylene-based chromophore and trialkylamine and nitroxyl quenchers.²³

While several polymers derived from 8-hydroxyquinolinolato transition metal coordination compounds with pendant norbornenes have been obtained and characterized,^{60, 61, 65} it was only very recently that this effect was used for the detection of Hg^{2+} and Cu^{2+} ions.³⁰

Bioimaging

In the last few decades molecular imaging has become one of the most important topics in the fields of chemical biology, nanomedicine and noninvasive diagnosis of diseases. Due to the different solubility requirements in biological media, amphiphilic copolymers consisting

of hydrophobic and hydrophilic segments in combination with optical labelling and recognition sites have gained increasing importance in bioimaging, for example, the visualization of tumor cells.

For example Ohe et al. focused on the synthesis of amphiphilic ROMP polymers from a precursor to which oligo(ethylene) glycol chains were attached in a post-polymerization functionalization step using azide-alkyne click chemistry. Another monomer with a pendant 2-nitrobenzenesulfonyl group was incorporated to provide an orthogonal conjugation handle which was used to attach folic acid, glucosamine or an arginylglycylaspartic acid (RGD) peptide together with the near-infrared fluorescent (NIRF) dye indocyanine green (ICG).^{86, 87, 90, 91} The residual double bonds in these polymers whose number has been maximized (by using norbornadiene residues as ROMP-able group) were then perhydroxylated with K_2OsO_4 to form stable nanoparticles with a low critical micelle concentration in water. Different polymer architectures (for example **8**) were attempted depending on the application.

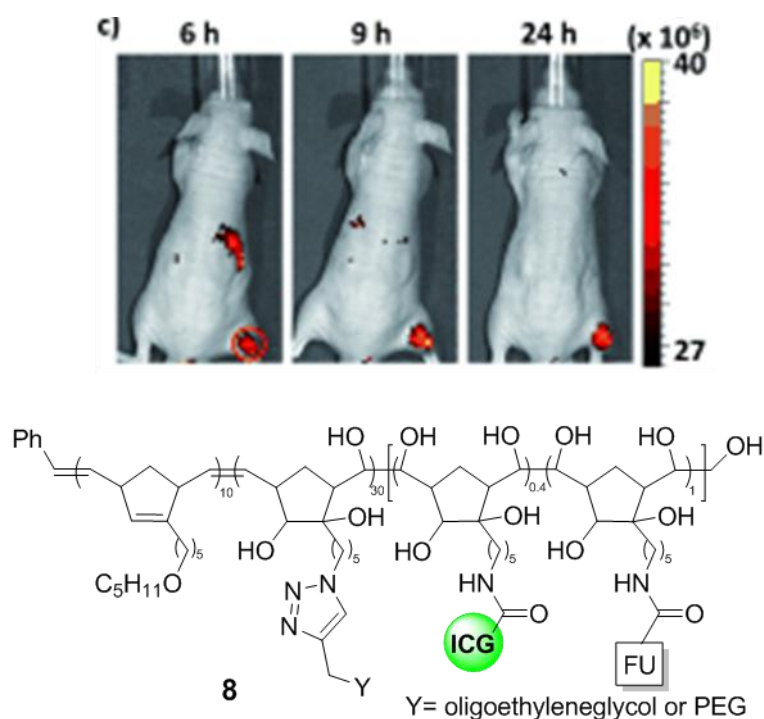
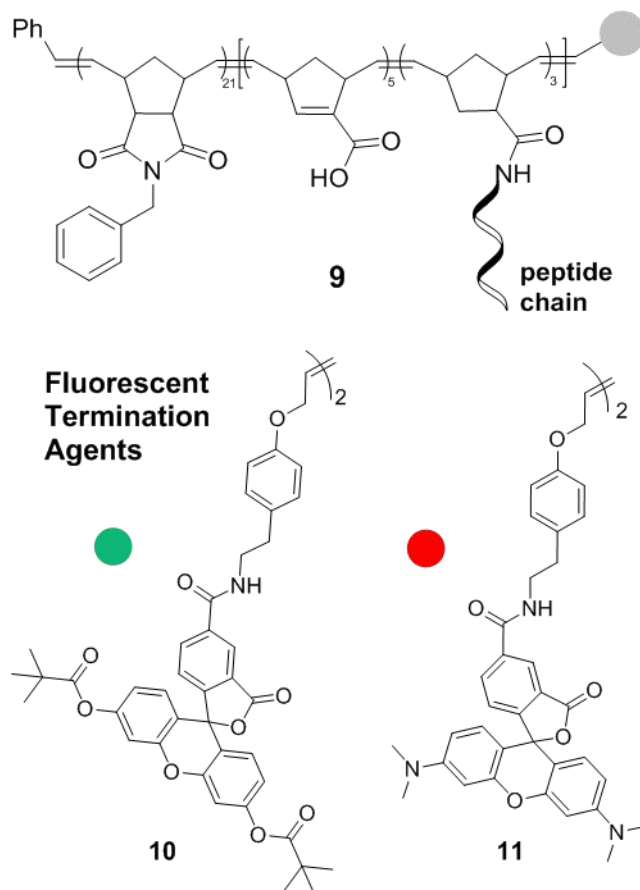


Figure 5 Perhydroxylated polynorbornenes labeled with dyes and recognizable units used as near-infrared fluorescent probes for cancer cell labeling in a mouse model. ICG= indocyanine green, FU=functional unit.⁹¹

Accumulation of these glycol chain bearing bioconjugated ROMP-based copolymers at tumor sites within several hours is possible and enables the visualization of cancer cells *in vivo* (mouse model, see Figure 5) using NIRF whereby the glucosamine- or RGD-derivatized probes had the advantage over the folate-derivatized ones of not being accumulated in other organs, such as the liver, but being preferably taken up by tumor tissue.⁹⁰ Belfield et al. attached two-photon fluorescent dyes and targeting RGD moieties to diblock ROMP copolymers with oligoethylenglycol chains via succinimide ester chemistry in a post-polymerization functionalization step.⁸⁴ These polymers form spherical micelles (about 100 nm diameter) in water which are able to target human $\alpha_v\beta_3$ integrin in glioblastoma cancer cells so that they can be made visible by two-photon fluorescence microscopy. Chien et al.⁴⁶ prepared block copolymers to which peptide chains were attached in a post-functionalization step and furthermore, a FRET (Förster resonance energy transfer) donor and acceptor couple was introduced to the end of the polymer chains via termination with dye substituted alkenes (bearing fluorescein (**10**) or rhodamin (**11**)) (Figure 6). Upon enzymatic hydrolysis by matrix metalloproteinases, which are overexpressed in certain tumor types, the peptide chains are cleaved so that the polymer chains form aggregates and resonance energy transfer takes place. Thus, enzymatic activity in tumor cells could be detected.⁹⁴



Peptide-polymer amphiphiles (PPAs) pack to form enzyme-responsive nanoparticles

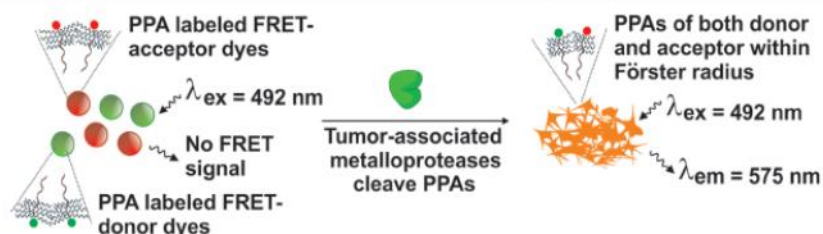


Figure 6 Matrix metalloproteinase-responsive fluorescent nanoparticles.⁹⁴

Organic Electronics

While there are some approaches using olefin metathesis polymerization for the preparation of organic semiconductor polymers, even short PPV oligomers which can be prepared by ROMP, were found to be insoluble. Therefore, several attempts to incorporate smaller electroactive units such as oligomers, emitters and hole- or electron-transporting side chains in ROMP polymers have been made. Some examples are shown in Figure 7.

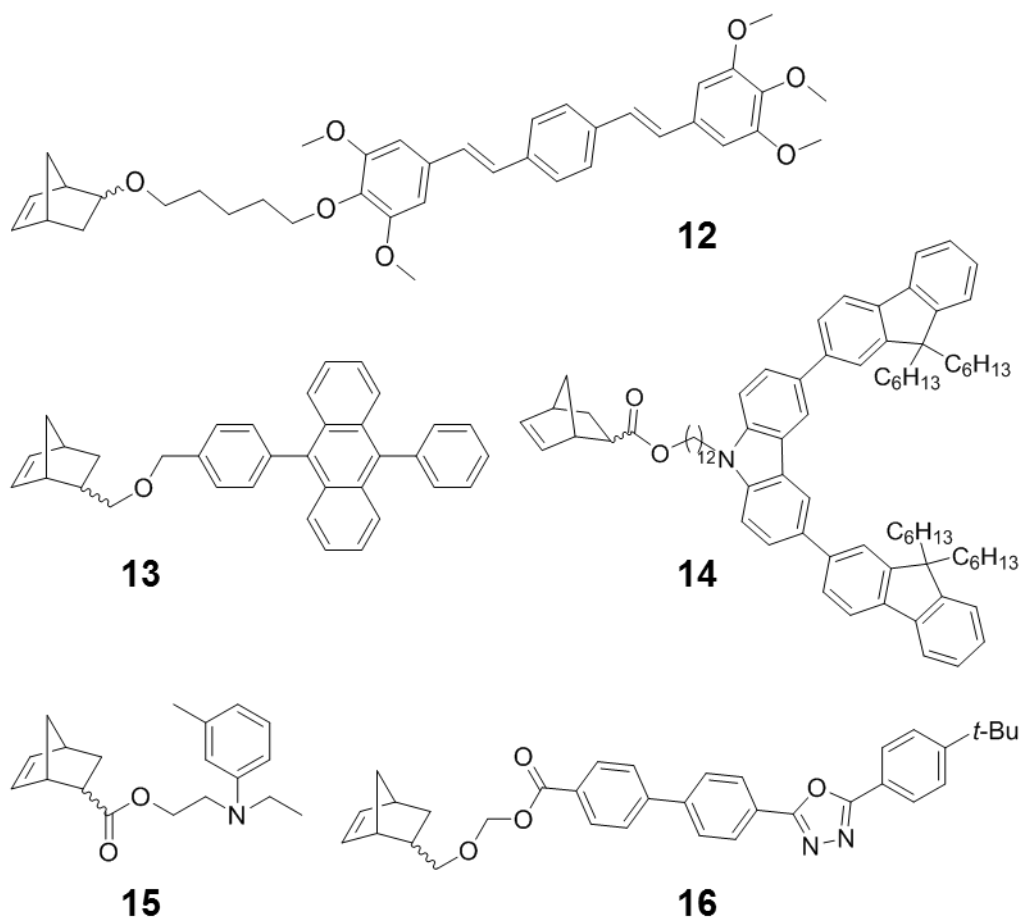


Figure. 7 ROMP monomers for OLEDs^{17, 19, 37, 38}

ROMP of **12** (Figure 7) using a [Mo] initiator led to a polymer with a maximum electroluminescence efficiency of about 0.55%.³⁷ Also, copolymerization can improve the film-forming properties of electroactive compounds which was demonstrated for diphenylanthracene. While pure diphenylanthracene cannot be used in electroluminescent devices, the polymers prepared by Schrock et al. (**13**) were successfully applied in organic light-emitting diodes (OLEDs). Similarly, 3,6-bis-(9,9-dihexyl-9H-fluoren-3-yl)-9-alkyl-9H-carbazole (**14**) was used in ROMP polymers prepared with a [Ru] initiator leading to good film-forming properties, thermal stability and good device performance.³⁸

An additional asset of ROMP in this context is that hole- (**15**) or electron transporting units (**16**) can be straightforwardly copolymerized (Fig. 7) which further improved device performance.¹⁷ Post-modification of such polymers (sulfonation and epoxidation of the double bonds in the polynorbornene backbone) was attempted. The polyanionic sulfonated polymer could be used for sequential layer-by layer adsorption with a

polycation (poly(allylamine·HCl)), while ring-opening of the epoxides with various nucleophiles failed.¹⁹

Triphenylamine containing polynorbornenes were used as emitter layers in OLEDs. The ester groups used to link these triphenylamine groups to the norbornenes, and consequently, the polymer backbone are photolabile, rendering the resulting polymer photoreactive (via a photodecarboxylation reaction) which was demonstrated by photolithography of thin films so that different patterns could be inscribed to obtain structured fluorescent surfaces and patterned OLEDs.⁴⁰ In another study, LEDs with poly(norbornene)-triphenylamine as hole transporter and tris(8-quinolinato)aluminum as emitter showed bright green emission with external quantum efficiencies of up to 0.77% (1.30 lm/W) for 20 nm thick films.⁴¹ Cross-linking by UV irradiation was found to decrease the performance of these devices from 0.77% to 0.37%. The substitution of ester groups by less polar ether anchoring groups for the triphenylamino functionality greatly enhances external quantum efficiencies, lowers the operating voltage, and improves the stability of the device.

A polynorbornene random copolymer with phthalocyanine donor and C₆₀ fullerene acceptor side chains (**17**) was synthesized in 2006 for the application in solar cells (Figure 8). Fluorescence quenching in this copolymer was enhanced compared to a phthalocyanine-containing homopolymer. Although these copolymers can harvest photons with wavelengths up to the infrared region and the fluorescence spectra of the copolymers indicated a strong excitonic coupling, only moderate conversion efficiencies could be achieved so far [64]. Another approach for the preparation of PV cells was carried out by Marder et al. where perylene-3,4,9,10-tetracarboxylic diimides have been linked to a norbornene moiety. Two different perylene monomers have been synthesized; one where the monomer moiety is linked via one of the imide nitrogen atoms (**18**) and another one where the norbornene moiety is linked via the “bay”-area of the perylene (**19**, Figure 8).

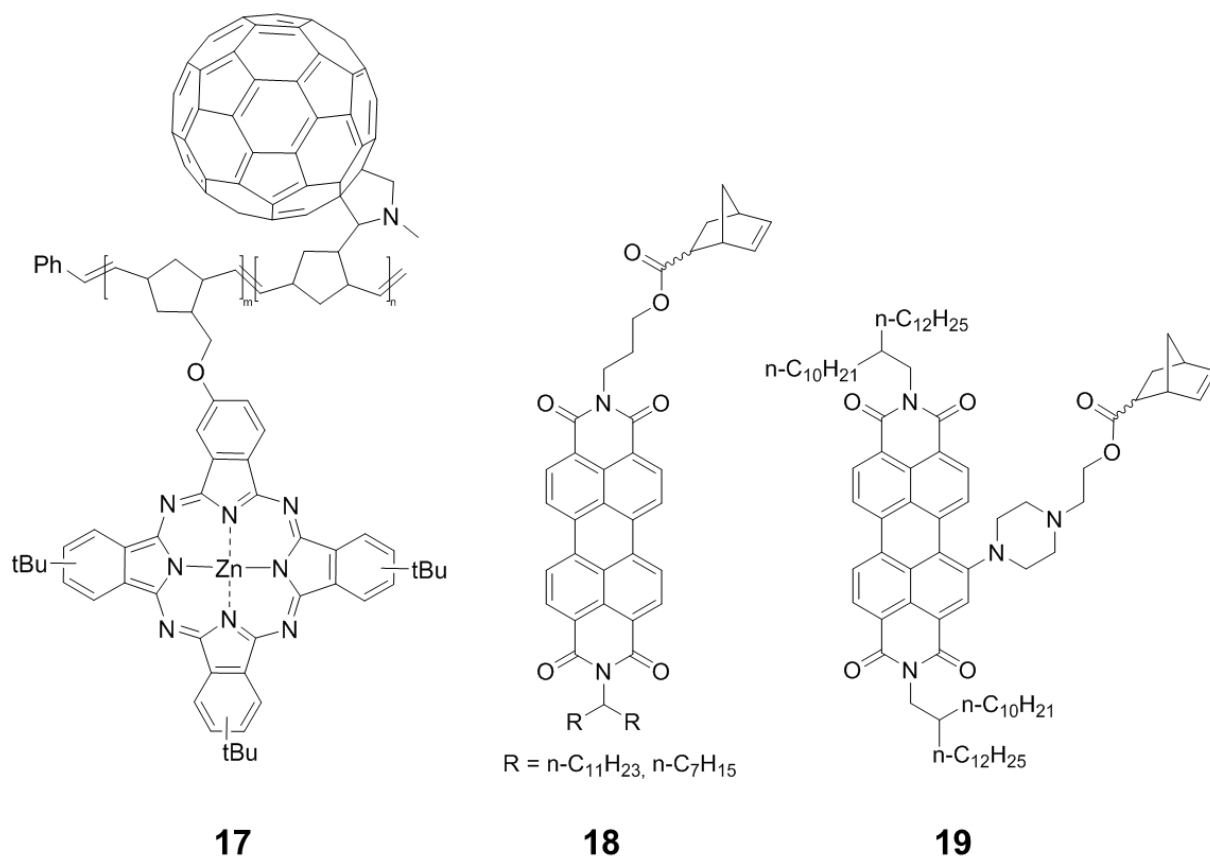


Figure 8 Zn-porphyrine/fullerene random copolymer⁶⁴ and perylenebisimide monomers for the preparation of PV cells²⁵.

After polymerization, UV-Vis spectroscopy of the polymer containing imide-immobilized perylenes (**18**) suggests aggregation which was supported by according peaks in powder X-ray diffraction. This π -stacking led to n channel field-effect transistor behavior whereas the perylene linked to the polymer chains via the bay region (**19**) showed a monomer-like UV-Vis spectrum, no evidence for π -stacking and no measurable transistor behavior. Using polymers of **18** as acceptors in bulk heterojunction solar cells in combination with poly(3-hexylthiophene), low power conversion efficiencies were obtained. The best performing device made from poly-**18** ($R = C_{11}H_{23}$) had a PCE (photoconversion efficiency) of 0.38%, whereas the PCE for polymers of **19** was one order of magnitude lower.²⁵

Generally speaking, the norbornene units necessary for polymerization result in a non-conductive polymer backbone which limits charge carrier transport, not only at a molecular level but also in the active layer which would be an explanation for the observed lower efficiencies in organic photovoltaics and lower performance in organic field effect

transistors. However, ROMP is an ideal technique to combine different functionalities in one polymer backbone.

Poly(norbornene-*exo*-dicarboximide) bottle brush-type polymers decorated with a pendant azobenzene dye were employed as polymer hosts for a phenyl vinylene thiophene vinylene chromophore guest resulting in bi-chromophore electrooptic (EO) blend materials, which changed their refractive index in dependence of an electric field. By attaching different substituents to the azobenzene moieties (methoxy or cyano groups), the authors were able to improve π -electronic polarization and the EO coefficient which is a measure for the change in refractive index upon applying an electric field.⁵¹

Flexible electrochromic devices were prepared from a ROMP polymer with pyrene and triphenylamine functionalities (**20**, Figure 9). The double bonds of the polymer back bone were hydrogenated to improve the thermal and oxidation stability. Furthermore, the polymer is characterized by remarkable solvatochromism, excellent electrochemical stability and reversible electrochromic behavior while adjusting the color (from yellow to green to dark-blue) can be done by applying different voltages.

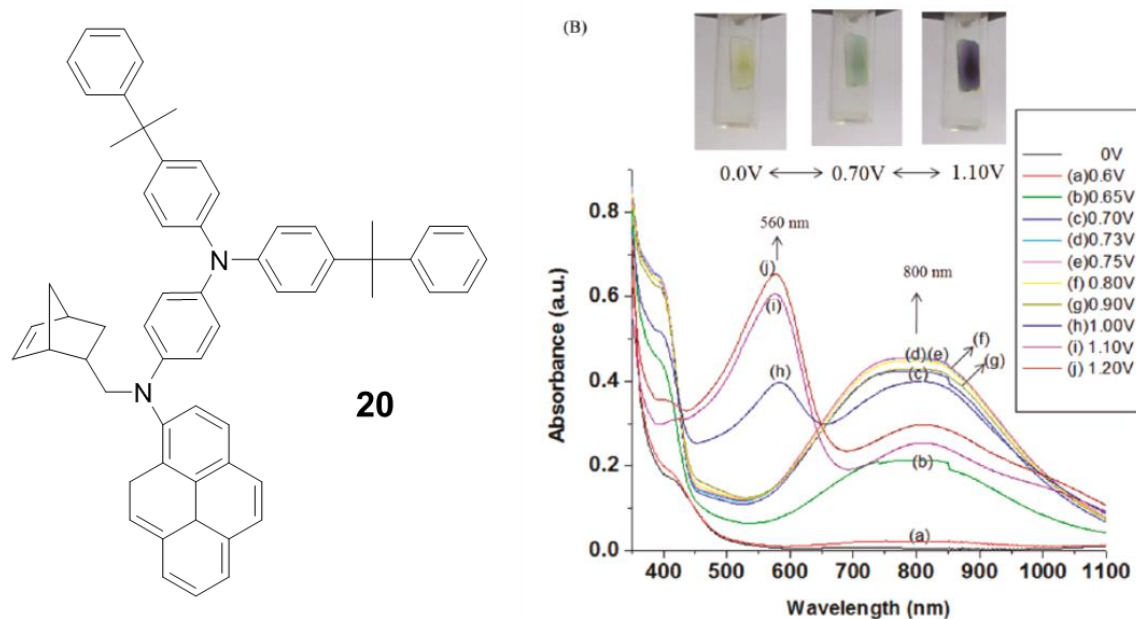


Figure 9 Electrochromic ROMP monomer (**20**) and optical images and UV-Vis spectra of the resulting polymer. Adapted with permission from.³¹ Copyright (2011) American Chemical Society.

Self-assembly/ nanocoils/ ladderphase (Hexabenzocoronenes/perylene)s

By tuning the polymer structure via ROMP, it is not only possible to define the quantity and the site of the dye within the polymer chain, but also to build up regular structures, i.e. di-block- and multiblock-copolymers. Thus, it is possible to create dye functionalized micelles or hierarchically ordered bulk materials and thin films by the self-assembly of amphiphilic block copolymers in solution and in the solid state.

Xanthene dyes (fluorescein, eosin, and dichlorofluorescein) have been incorporated into the core of amphiphilic block copolymer micelles. The self-assembly process in methanol is strongly influenced by the degree of ionization of the dye unit. The aggregation size was significantly smaller when the dye molecule was charged which is due to the ion pair formation of the charged molecule and the according counter ions, thus, inducing strongly attractive dipole-dipole interactions. Even a minor amount of ionogenic functional units influences the aggregation behavior drastically. The optical properties of the dye were preserved within the aggregates, which makes this material useful for sensor applications⁴⁹. The eosin containing micelle system was also investigated via SAXS (small angle X-ray scattering) measurements in solution, whereby the pH-sensitivity of the eosin dye was preserved within the accrued micelles.⁴⁷

Using the different approaches outlined above, precise placements of the dyes in either the hydrophilic or the hydrophobic block as well as on either chain is possible while the ratio of hydrophilic and hydrophobic blocks can be adjusted simply by employing adequate monomer/initiator molar ratios so that tailor-made block copolymers can be achieved easily.^{23,42-49} In addition to the tailored design of highly specific materials for bioimaging and visualization of tumor cells, even unspecifically labelled, self-assembled nanoparticles can be applied for e.g. drug delivery as shown for rhodamine-decorated micellar nanoparticles which were accumulated preferably in cervical cancer cells⁷⁹ or tumor cells⁴⁵.

Another intriguing approach is to have polymerizable moieties which can be used to conserve a self-assembled structure which is, since self-assembly is a thermodynamically controlled process, a good strategy to obtain kinetically favored self-assembled intermediate structures which arise only for a short period of time by polymerization of a backbone.

One example is the polymerization of self-assembled conductive nanocoils with uniform diameter and helical pitch from a norbornene-appended hexa-peri-hexabenzocoronene (HBC) [29]. After polymerization, the rearrangement of these nanocoils into nanotubes at

room temperature is no longer possible (**Fig. 10**). However, also the nanotubes can be obtained by post-annealing-ROMP of the self-assembled nanotubes. Furthermore, the π -stacked HBC arrays exhibited conductivity upon oxidative doping.

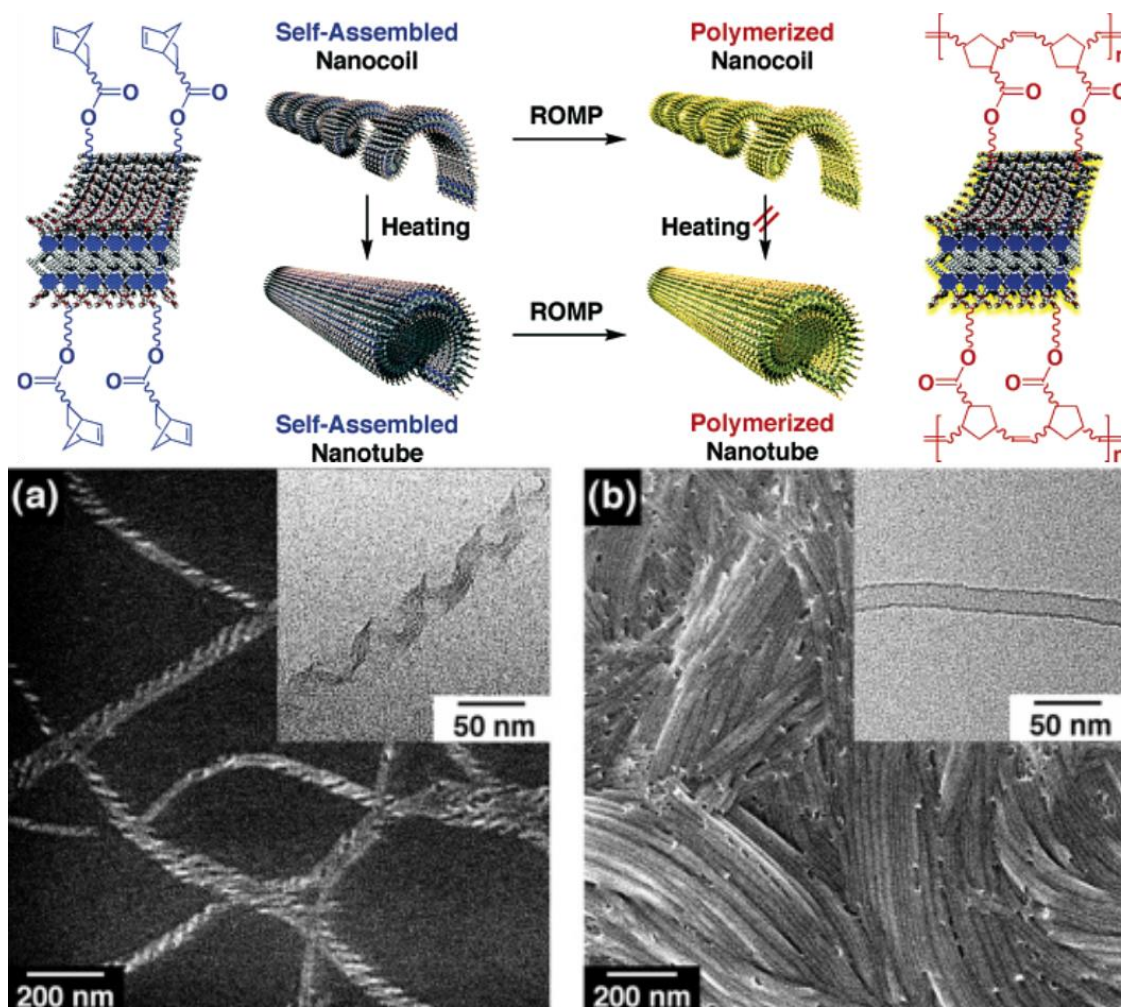


Figure 10 HBC nanocoils (a) and nanotubes (b) stabilized via ROMP. Adapted with permission from.²⁹ Copyright (2006) American Chemical Society.

By adding norbornenes with an enantiopure side chain to the hexabenzocoronene-decorated monomers, instead of a racemic mixture of right and left-handed coils, either version could be obtained selectively.²⁹

Later, double-stranded polymeric ladder polymers using HBC as linker (**21**, Figure 11) have been synthesized and self-assembled patterns were studied by STM (scanning tunneling microscopy).²⁷ While the monomers arranged into a similar pattern with face-on

morphology as observed for unsubstituted HBC, the ladder polymers attained a rod-like structure.

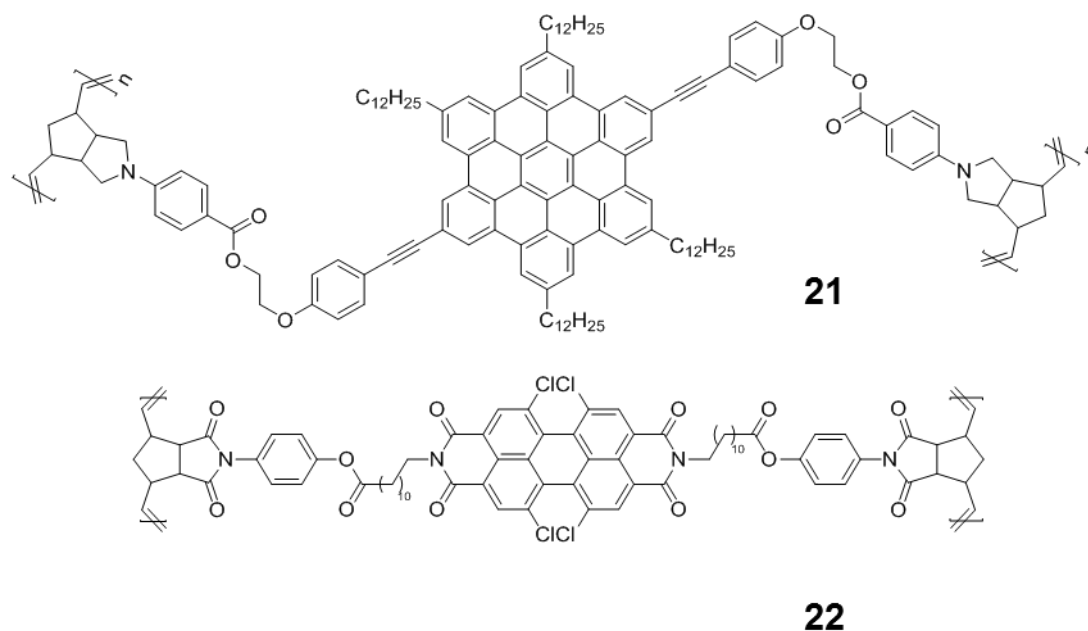


Figure 11 Ladder polymers based on HBC (**21**)²⁷ and perylenes (**22**)²⁶.

Perylenes are another class of polycyclic aromatic compounds which show interesting self-assembly behavior and were therefore also incorporated in ladder polymers (Figure 11). Unlike for the hexabenzocoronenes, the perylene moieties were aligned in different directions and the resulting ladder polymers ended up to be amorphous as shown by TEM analysis.²⁶ The aggregation of perylenes is varying depending on the chemical environment and this in turn influences the optical properties of a material in different solvents and in film.²⁴

Generally speaking, the polymerization and furthermore stabilization of such self-assembled dyes with pendant norbornene residues does not influence the spectroscopical characteristics. Therefore ROMP of self-assembled compounds is a great way to increase stability and also to lock energetically unfavorable self-assembled structures.

Photoreactive materials

Absorption of light can also induce changes in the materials properties, thus the incorporation of photoreactive dye molecules can be used to change the color in the material (irreversible e.g. by photobleaching – or reversible by photochromic dyes), to alter the surface energy (and thus the wettability and chemical reactivity of the surface) or solubility for applications as photoresist and to create relief structures and influence the morphology of materials. Using photolithographic methods, most of these changes can be realized locally and thus functional patterns can be inscribed by light.

Two different reaction types can be applied: irreversible photoreactions inducing a permanent change in color and the material's properties and reversible photoreactions creating a platform of materials responsive on light as external stimulus.

Regarding irreversible photoreactions, several approaches have been exploited. Examples are the photoisomerisation of benzylthiocyanates to benzylisothiocyanates⁹⁵, the photoisomerisation of aryl esters^{96, 97} or amides⁹⁸ via the photo-Fries rearrangement or the photocleavage of nitrobenzylesters (photo-acid generation)^{99, 100}, see Figure 12.

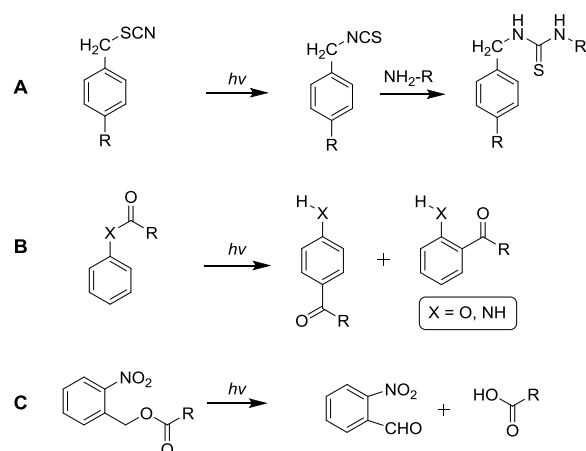


Figure 12 (A) Photoisomerisation of benzylthiocyanates to benzylisothiocyanates,⁹⁵ (B) photoisomerisation of aryl esters/amides⁹⁶⁻⁹⁸ and (C) photocleavage of nitrobenzylesters^{99, 100}.

The photochemistry of benzylthiocyanate (Figure 12 A) can be used to inscribe relief patterns into ROMP polymers by a subsequent addition of amines to the photogenerated isothiocyanate groups forming a thiourea-bond.⁹⁵ However, exactly this chemistry can also be used to immobilize dye molecules in a blend of this polymer and polyfluorene. Following this approach, an amino-functionalized ruthenium complex - Ru(bipyridine)₂(5-amino-

phenantroline)(PF₆)₂ - has been immobilized in thin films only in the irradiated areas leading to patterned fluorescent thin films as well as electroluminescent devices.¹⁰¹

The photo-Fries rearrangement (Figure 12 B) causes a significant change upon irradiation in the polymeric materials and thus can be used to create refractive index patterns with possible applications in optical data storage and transmission.^{96, 97, 102} Refractive index changes up to $n = 0.01$ have been obtained in polynorbornenes bearing aryl amides as pendant groups.⁹⁸ In addition, the photogenerated aromatic hydroxyketones and aminoketones can be easily post-functionalized with dye molecules. Following this route, dansyl chloride, thiocyanatoiron and hydrazones have been immobilized on the irradiated areas of polynorbornene dicarboxylic acid diphenyl ester¹⁰³ and fluorescamine using the corresponding phenyl amide functionalized polymer⁹⁸.

In the last years, also photoacid generators on the basis of the photocleavage of ortho-nitrobenzylesters (Figure 12 C) have been explored in regard to refractive index patterns.¹⁰⁰ Hydrogels cross-linked with ortho-nitrobenzylester units can be de-crosslinked upon irradiation.¹⁰⁴ This was also used for dissolving thin films prepared by layer-by-layer adsorption technique by disturbing the electrostatic balance within these films.¹⁰⁵ The change in surface polarity due to the formation of the carboxylic acid can also be used to influence electrical characteristics of organic thin film transistors based on pentacene, either via influencing the growth of pentacene from the vapor phase¹⁰⁶ or influencing the charge concentration in the conductive channel.¹⁰⁷

Another example of a photoreactive polynorbornene system was a tert-butyloxycarbonyl-protected quinizarin-functionalized polynorbornene which could be deprotected with the help of a photoacid generator (TPSOTf, triphenylsulfonium triflate) leading to a bathochromic shift of the absorption maximum from 350 to 490 nm in combination with arising red fluorescence (570-610 nm) after cleavage of the tert-butyloxycarbonyl protecting groups.³⁴ However, in this case the photoinitiator was not covalently linked to the polymer main chain.

Photoreactions have also been used to cross linked micelles leading to stable nanoparticles using the photodimerization of cinnamoyl groups via a photoinduced [2+2] cycloaddition. These groups have been introduced by the copolymerization of dye-functionalized monomers into the hydrophobic core of amphiphilic block copolymer micelles.^{48, 108} ROMP

was also used to prepare a macrophotoinitiator (eosin)-coinitiator (dimethylaminobenzoate) system for the UV curing of acrylates with improved migration stability and biocompatibility which was confirmed by leaching studies and improved adhesion of osteoblast cells.⁴³

Photochromic compounds undergo a reversible chemical reaction which changes their absorption properties upon an optical stimulus. Potential applications for such compounds are optical data-storage, ophthalmic lenses or photonic switches. Besides the two states being differently colored usually the two forms also significantly differ in other properties such as polarity or hydrophilicity.

The group of Branda uses photochromic phenoxynaphthacenequinone to regulate the luminescence of porphyrines both introduced into ROMP polymers via the monomer route, see Figure 13.¹⁰⁹ Isomer **23a** can quench the fluorescence of porphyrine as it is a much better electron acceptor. By switching between the two states **23a** and **23b** the luminescence can be reversibly turned on and off.

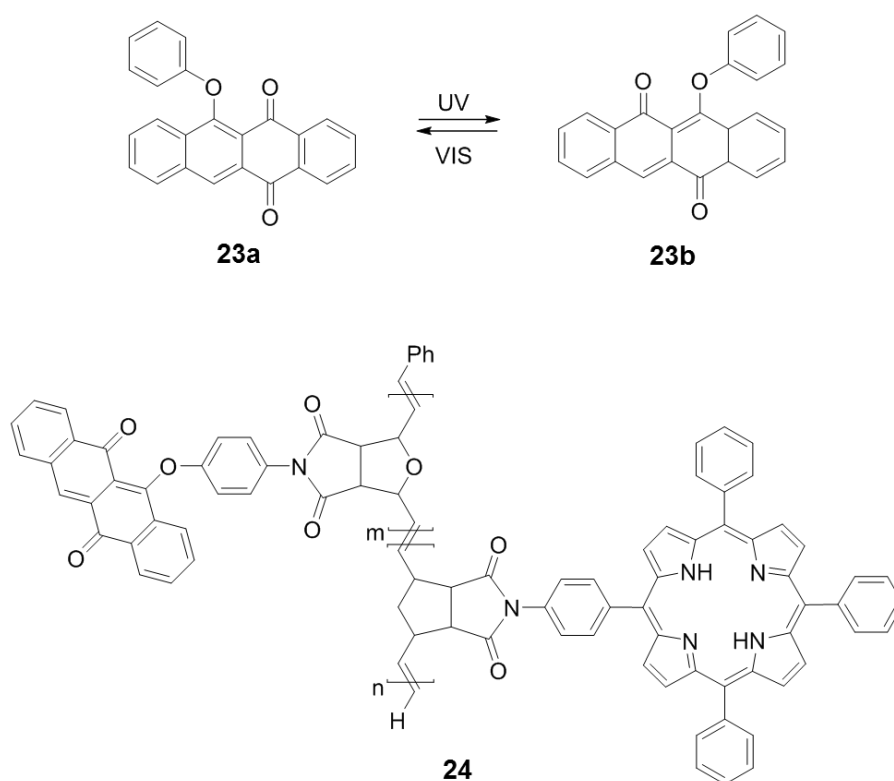


Figure 13 Photochromic ROMP polymers.

A series of homo- and copolymers containing various photochromic dithienylethenes (**25**) have been prepared by the same group. By blending or copolymerizing differently

substituted dithienylethenes the attained color can be adjusted over a broad range (Figure 14) and multiaddressable materials have been prepared with possible applications in multistate photochromic recordings and displays.^{110, 111}

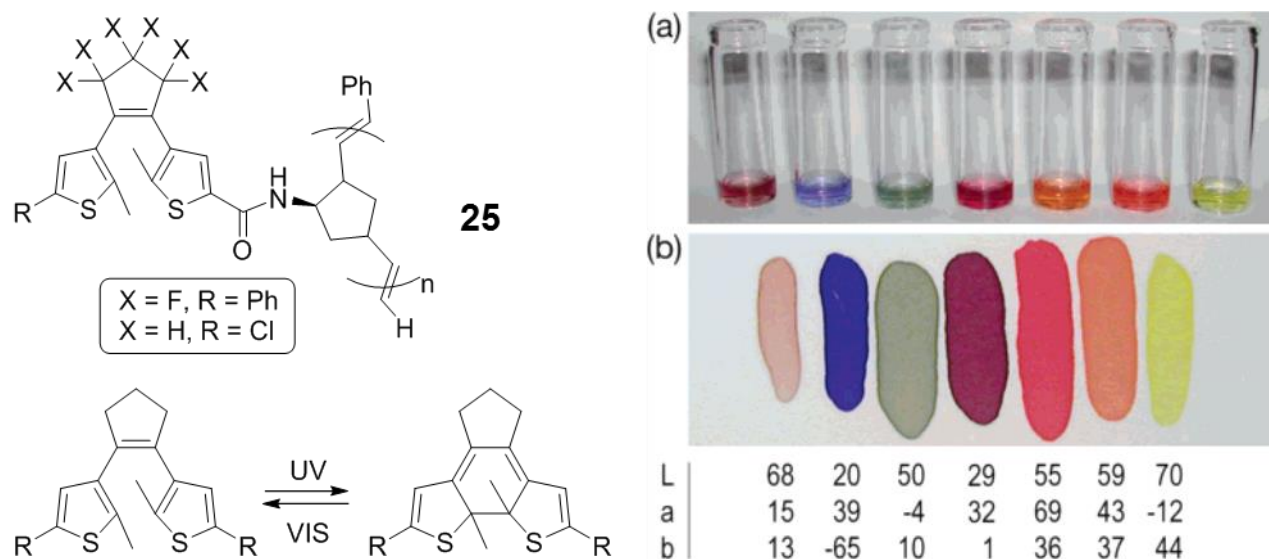


Figure 14 Photochromic dithienylethene-based ROMP polymers. Adapted with permission from.¹¹⁰ Copyright (2005) American Chemical Society.

The introduction of spiropyranes into ROMP-polymers also leads to photochromic materials.^{55, 112} Irradiation with UV light (e.g. 365 nm, Figure 15) leads to the cleavage of the C-O bond at the spiro center followed by the *cis* to *trans* isomerization of the adjacent C=C bond which results in a reversible formation of deeply blue colored merocyanines. This process is reversible for several reaction cycles and the back-reaction can be triggered thermally or by irradiation with long-wavelength light (>500 nm).

Amphiphilic random copolymers consisting of hydrophobic, hydrophilic and spiropyran monomers were prepared and showed self-assembly to micellar structures. Upon UV irradiation, the pendant spiropyran groups isomerize into their dipolar merocyanine form, which causes rupture of the micelles. Again, this process can be reverted by irradiation with longer wavelength light and this was used to encapsulate Nile Red serving as a lipophilic model substance for drug delivery applications, see Figure 15.⁵⁹

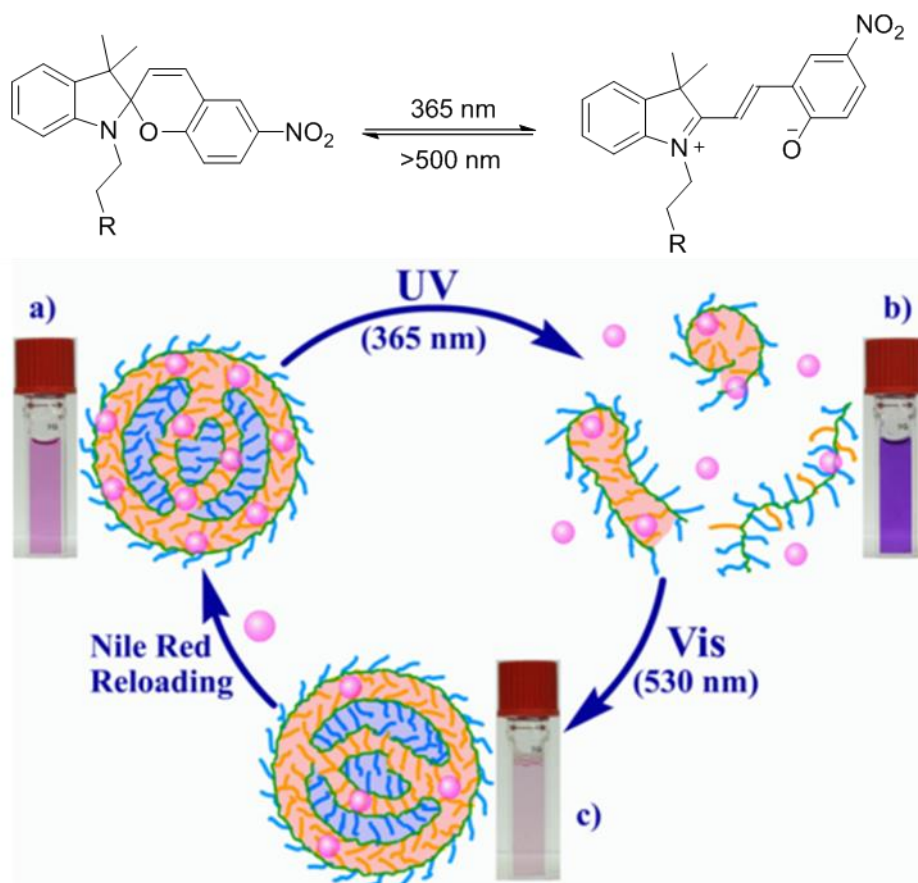


Figure 15 Reversible photochromism of spiropyrans^{55-57, 59} used for the light triggered encapsulation of Nile Red with spiropyran-functionalized random ROMP copolymers. Reprinted (adapted) with permission from.⁵⁹ Copyright (2012) American Chemical Society.

Structures with a resolution of down to 5 μm could be inscribed into thin films of a homopolymer containing pendant spiropyran units via contact photolithographic patterning.⁵⁵ Due to the dipolar nature of the formed merocyanines, a change in surface energy, confirmed by contact angle measurements^{55, 56} and friction force microscopy¹¹³ is imposed upon photoisomerization. The dipolar nature of the merocyanine zwitterions leads to them being favoured in a polar environment whereas spiropyrans are the preferred form in an apolar environment. This was used as a probe for solvent polarity using capillaries equipped with polymer brushes prepared in a SI(surface initiated)-ROMP approach.⁵⁷ Recently spiropyran-functionalized copolymers were used to control the charging properties from contact electrification in polymeric thin films.¹¹⁴

Tomasulo et al. synthesized a spirooxazine-bearing polymer via ROMP. The absorption maximum for the closed oxazin ring is about 310 nm, whereas the open form has an

absorption maximum of 440 nm. By transient absorption spectroscopy, it was demonstrated that UV irradiation opens the ring in less than 6 ns with a quantum yield of 0.09 in solution. However, the reversion speed was reduced from 20 ns up to 11 μ s on the polymeric backbone.⁵⁸

Lambeth and Moore used a homopolymer containing an azo dye in its side chain for photoisomerization experiments to inscribe surface relief gratings with a laser wavelength of 488 nm using interference of linearly polarized light which resulted in a sinusoidal diffraction grating.⁵² Furthermore, isotropic colloidal particles (prepared by gradual hydrophobic aggregation) were produced. These particles became deformed into ellipsoids when they were irradiated with linearly polarized light with the degree of stretching being proportional to the irradiation time. Different shapes could be inscribed in films of poly-**26** (Figure 16) by proximity field nanopatterning, again at a wavelength of 488 nm.⁵³ *Cis-trans* isomerization of such azo-dye bearing polymers was also achieved thermally.⁵⁰

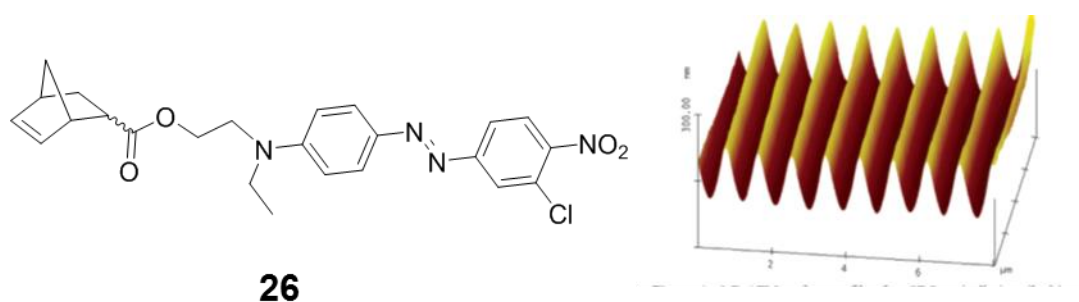


Figure 16 Azobenzene-derivatized monomer (**26**) and patterned photoisomerization of ROMP polymer thin film as visualized in AFM images. Adapted with permission from.⁵² Copyright (2007) American Chemical Society.

Another reversible photoreaction is the photoinduced $[4\pi + 4\pi]$ cycloaddition of anthracene, which was explored for crosslinking and thermal decrosslinking of polymeric materials. This photochromism was used for crosslinking of the macromolecules to generate a photolithographic pattern of thin polymer films. To achieve better solubility, copolymers with oligo(ethylenglycol) groups have been prepared and the principle to use this material as a photoresist have been shown.¹⁷

Overall, a vast variety of photoreactive materials has been prepared via ROMP, owing not only to the high functional group tolerance of this polymerization technique but also to the

beneficial properties for these applications such as good film formation and no interference with UV-Vis absorption of the functional dyes due to the poly(norbornene) backbones.

Conclusion

ROMP is a highly appropriate technique for the preparation of dye-functionalized polymers. The high functional group tolerance does not only allow the synthesis of polymers with a great density of functional groups on homopolymers, enabling one to study bulk properties such as photochromism, electron transport in devices or self-assembly leading to nanocoils, and ladder polymers. The living nature of ROMP, in addition to resulting in narrow polydispersity indices, also provides the opportunity to synthesize block copolymers while allowing precise placement of the dye molecules in either block. Furthermore, suitably derivatized initiators and termination reagents allow to selectively decorate either end of a polymer chain leading to precision polymers which have found use as polymeric sensor materials and furthermore, even as imaging probes which could be applied *in vivo* as well.

Moreover, reactive functionalities are easily incorporated in each of the three polymerization steps (initiation, propagation and termination) and can be then converted in post-polymerization functionalization steps. Prominent examples include azide-alkyne click chemistry and active ester chemistry, which have the advantage that a large variety of suitably functionalized dyes are already commercially available. The inherent double bonds in ROMP polymers provide an additional opportunity for functionalization via thiol-ene or inverse electron demand Diels-Alder chemistry which has been very recently also used for the immobilization of dyes on polymer chains.

We hope that this overview of recent developments of dye-derivatized ROMP polymers will stimulate further research in this exciting field.

Acknowledgements

ACK acknowledges the Austrian Science Fund (FWF):[T578-N19]. MH and GT are grateful to the Climate and Energy Fund of the Austrian Federal Government for financial support within the project PoTTA of the program Energy Mission Austria.

CHAPTER 2

A WAY TO PHOTOACTIVE COMPOUNDS –
EMPIRICAL INVESTIGATION OF DYE-FUNCTIONALIZED POLYMERS
ABLE TO CONVERT ELECTROMAGNETIC RADIATION
VIA TRIPLET-TRIPLET ANNIHILATION

Introduction

In this chapter, first experiments and results of a ring opening metathesis polymer (ROMP) based dye functionalized macromolecule will be presented. The used chromophores were functionalized with a norbornene moiety and were copolymerized with a matrix monomer obtaining photoactive di- and tri-copolymers. These newly developed substances are able to convert electromagnetic radiation of higher wavelengths to lower wavelengths. This process is called Up-Conversion (UC) which is induced via triplet-triplet annihilation.

Triplet-Triplet Annihilation

The triplet-triplet annihilation (TTA) is an effect which transfers electromagnetic radiation of higher wavelengths to lower wavelengths, such processes are called anti-Stokes shift. In contrast to that, the more common process is a Stokes-shift, which means that conversion of electromagnetic radiation of lower wavelengths to higher wavelengths takes place. Two well-known examples for that effect are fluorescence or phosphorescence (Figure 17).

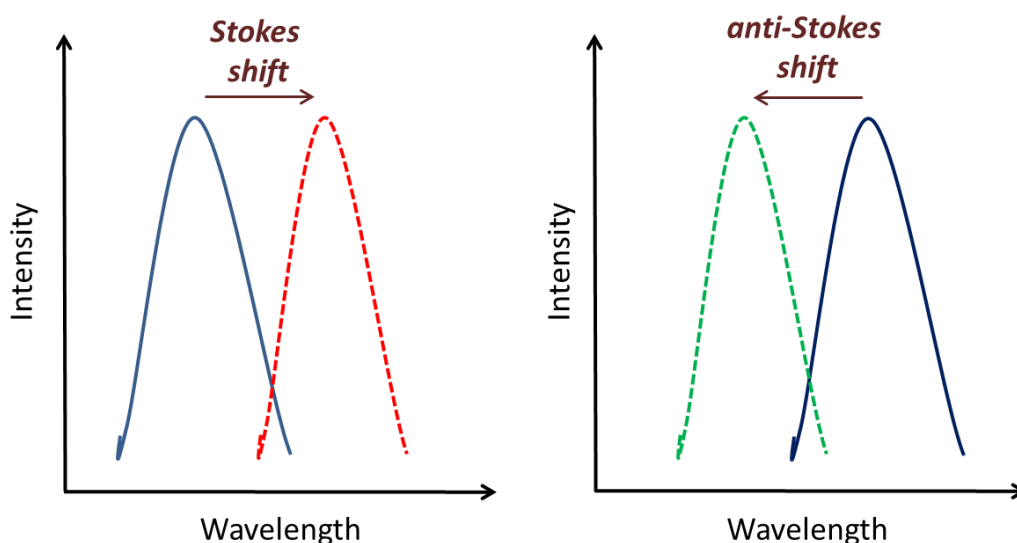


Figure 17 Schematic illustration of the Stokes (down-conversion) and anti-Stokes (up-conversion) shift. Solid lines represent the absorption spectra while dotted lines represent the emission spectra

To obtain a triplet-triplet annihilation (TTA) induced up-conversion (UC) a pair of chromophores involving a sensitizer and emitter which were able to interact in an intricate series of events is necessary. The current literature is still discussing on the TTA-UC

mechanism,¹¹⁵ but the generally accepted view is that the sensitizer is excited at a defined wavelength which then populates its first singlet excited state ($^1S^*$) followed by intersystem crossing (ISC) to its excited triplet state ($^3S^*$). The next step is the triplet-triplet energy transfer (TTET) to the emitter molecule. It is very important that the chromophores are in close proximity to each other, otherwise the TTET is not able to take place. The last step is the triplet-triplet annihilation (TTA) that involves two emitter molecules whereby one of them is able to populate the first singlet excited state ($^1E^*$) which finally results in radiative relaxation of the emitter singlet excited state in the form of anti-Stokes delayed fluorescence (Figure 17). The TTET is the crucial step for the TTA because both excited triplet states ($^3S^*$, $^3E^*$) are able to transfer their energy to oxygen and therefore are able to relax to their ground states. The energy level diagram is shown below in Figure 18.

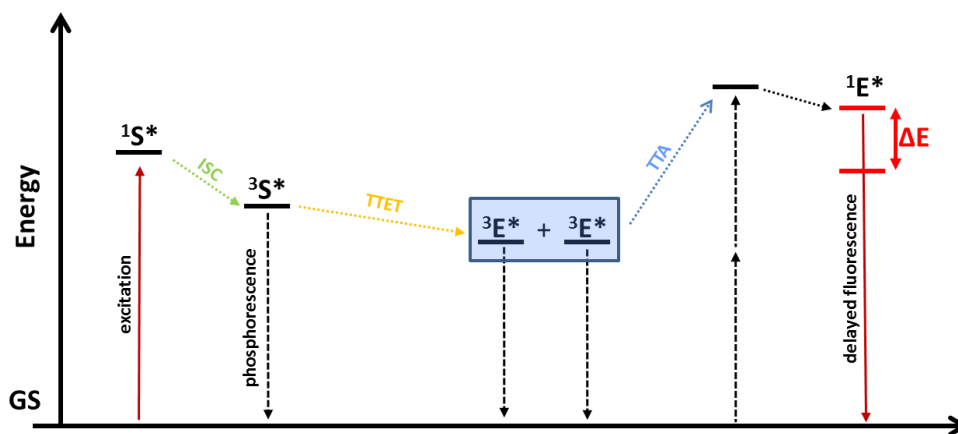


Figure 18 Jablonski energy level-diagram of TTA up-conversion.

(S stands for sensitizer and E for emitter. Coloured solid lines represent the intended radiative processes (absorption and emission). Vertical dashed lines represent undesired non radiative and radiative decay pathways. Slanted dotted arrows represent cascading energy transfer processes. GS denotes the ground states (for simplicity drawn at the same energy level) and ΔE is the energy difference between incident and emitted light)

The overall quantum yield of this process can be expressed by:¹¹⁶

$$\Phi_{UC} = 1/2 f \Phi_{ISC} \Phi_{ET} \Phi_{TTA} \Phi_E \quad (1)$$

where Φ_{ISC} , Φ_{ET} , Φ_{TTA} , and Φ_E are the quantum efficiencies for intersystem crossing, energy transfer, triplet–triplet annihilation, and emitter photoluminescence, respectively. The factor

$\frac{1}{2}$ expresses that two incident photons are combined into one and f is a factor that expresses the probability that the triplet–triplet annihilation results in a singlet (which can decay radiatively as desired) as opposed to a triplet or quintet excited state. As will become apparent from the discussion below, some of these quantities are largely dependent on the chromophores (i.e. f , Φ_{ISC} , and Φ_E), whereas others (Φ_{ET} , Φ_{TTA}) depend on external factors such as molecular mobility, the distance between chromophores, which in statistically mixed systems is a function of concentration, and also the concentration of triplet excited states, which amongst other factors also depends on the incident power density. Equation (1) does not explicitly account for back-transfer (i.e., energy transfer from the emitter to the sensitizer) and internal re-absorption such as quenching of the sensitizer or emitter triplet excited states by oxygen, which in fact represents a significant obstacle for efficient TTA-UC under ambient conditions.¹¹⁷

Chromophores (DPA/ TPP)

A well-known TTA chromophore system contains 9,10-diphenylanthracene (DPA) as emitter and porphyrin derivatives with Pt or Pd as metal ion. There are several approaches where a similar dye combination was used. The first publications dealing with this topic were blends of these chromophores in solution or within a polymeric matrix. The group of Castellano was the first who published a photon up-converting polymer system with blends of palladium (II) octaethylporphyrin (PdOEP) and DPA. They were using a quite powerful laser as excitation source with 2 mJ per pulse at 544 nm to investigate the increase of the up-conversion quantum yields at higher temperatures.¹¹⁸ Lee *et al.* were the first how prepared a terpolymer containing matrix, emitter and the sensitizer within one macromolecule. The chromophores where equipped with additional acrylate moieties so that a conventional free radical polymerization with methacrylate as matrix was performed. Quantum yields were quite low due to undesired electronic interactions between sensitizer and emitter.¹¹⁹ The highest quantum yields have been achieved by the working group of Ye *et al.*. It was possible to reach an up-conversion quantum yield of 36% due to enhancement of the phosphorescence lifetime of the sensitizer and the fluorescence quantum yield of the emitter. They dissolved Pd Tetraphenylporphyrin (Pt TPP) and DPA in propanol with addition of β -cyclodextrin. Excitation was done via LED with a low power density of 60 mW cm⁻² at 532 nm.¹²⁰

Due to the large knowledge and promising results for a porphyrin/ DPA system the preparation of platinum meso-tetraphenylporphyrin and a 9,10-diphenylanthracene derivatives with, norbornene moieties for further ring opening metathesis polymerization, was conducted. The developed chromophores are shown below in Figure 19.

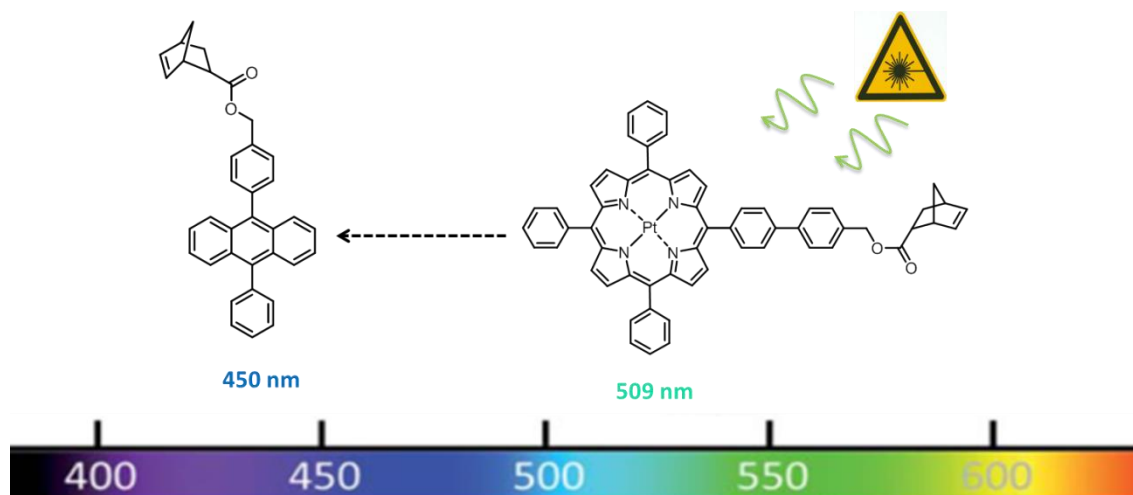


Figure 19 Developed TTA chromophores for further ROM polymerizations. Sensitizer was excited at 509 nm and emitter shows delayed fluorescence at 450 nm.

Results and Discussion

Emitter monomer (DPA_{mon})

A straightforward synthetic pathway for the preparation of the DPA_{mon} was designed and is shown below in Figure 20 (right). Only two reaction steps were necessary to obtain the desired monomer. First a Suzuki cross coupling with 9,10-dibromoanthracene, phenylboronic acid and 4-methoxyphenylboronic acid was performed obtaining (4-(10-phenylanthracen-9-yl)phenyl)methanol. The final step was the Einhorn variation of the Schotten-Bauman reaction where first 5-norbornoyl-2-carbonyl chloride was prepared *in situ* via Diels-Alder reaction with cyclopentadiene and acryloyl chloride followed by the addition of (4-(10-phenylanthracen-9-yl)phenyl)methanol. After purification via column chromatography the norbornene functionalized diphenylanthracene compound was obtained. For the absorption and emission measurements the chromophore was dissolved in DCM Figure 20 (left). Its global absorption maximum exhibits at 375 nm. It also has two local maxima at 357 and 396 nm. After excitation at a wavelength of 375 nm it shows a quite broad emission signal with its maximum at 436 nm.

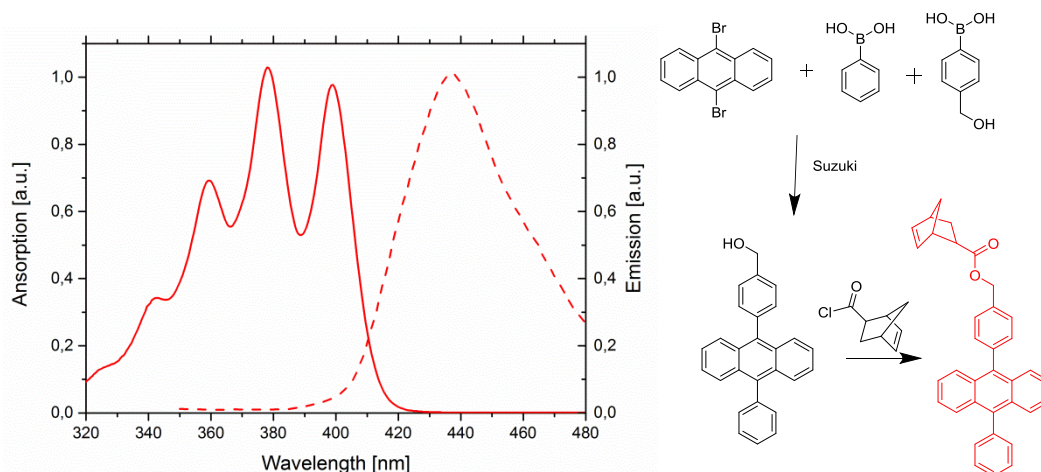


Figure 20 Normalized absorption (solid lines) and emission (dashed lines) spectra of **DPA_{monomer}** (left). Synthetic pathway for the preparation of **DPA_{monomer}** (right)

Sensitizer monomer (Pt TPP_{mon})

For the synthesis of the meso-tetraphenylporphyrin ligand (**TPP**) a well-know and very common way based on the work of Adler and Longo was chosen.¹⁷⁶ Therefore, freshly distilled pyrrole, freshly distilled benzaldehyde and 4-bromobenzaldehyde were dissolved in propionic acid and heated to reflux for 30 minutes. The reaction mixture turns dark violet due to the formation of a lot different by-products. Purification was done by recrystallization to obtain the tetraphenylporphyrin derivatives, bigger ring systems and polymers. Column chromatography was conducted several times to obtain the mono bromo functionalized compound (**BrTPP**). For the second step, the purple crystals were dissolved in benzonitrile and after addition of Pt(acac)₂ the mixture was placed into a microwave with a reaction temperature of 250°C. After 30 minutes the colour of the reaction mixture changed from purple to red and completion of the reaction was determined via TLC. The undesired by product, a green solid that was formed due to the protonation of the free ligand, was separated from the reaction mixture via decantation. To introduce a free accessibly hydroxyl group Suzuki cross-coupling with 4-methoxyphenylboronic acid was performed. For the last step an esterification with norbornoyl chloride was done, with same conditions as for the **DPA_{mon}**. This newly developed porphyrin derivative was dissolved in DCM for further absorption measurements. It exhibits its global maximum at 399 nm (Soret-band), while the Q-band appears at 509 nm. The reaction pathway as well as the UV/ Vis spectra is shown below in Figure 21. The related NMR and MS data are shown in the experimental part.

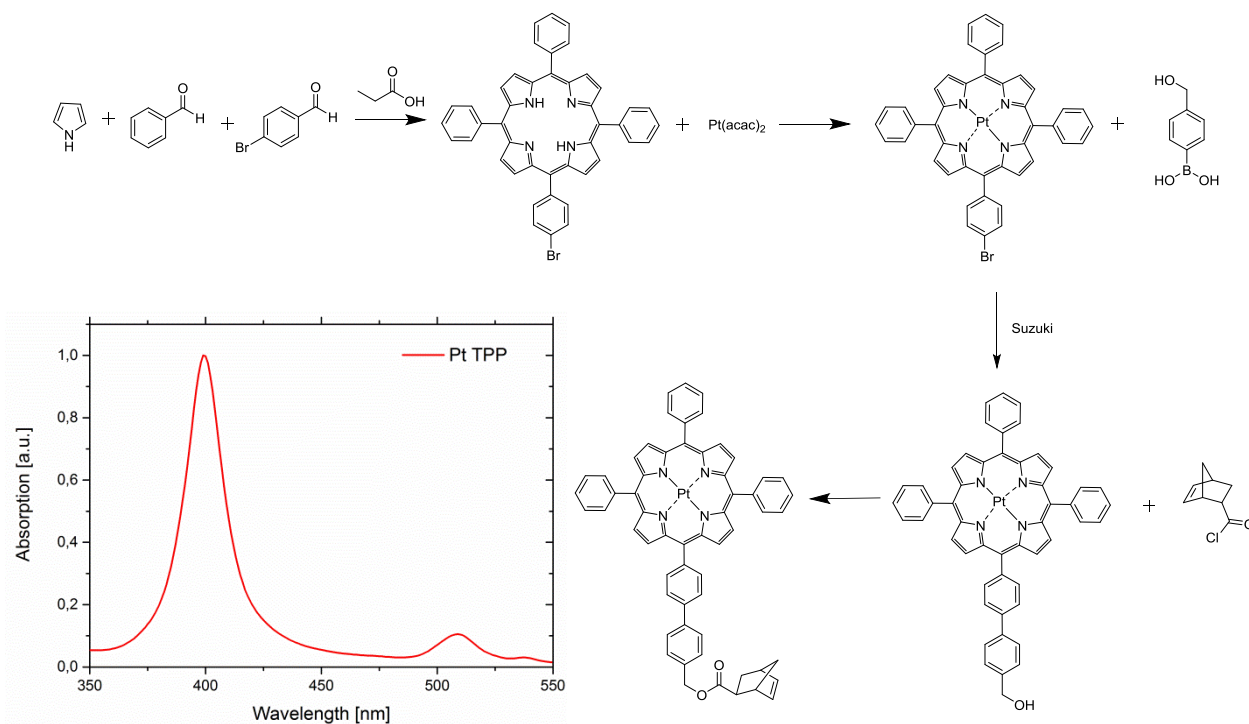


Figure 21 Normalized absorption spectra of **Pt TPP_{mon}** (bottom left). Synthetic pathway for the preparation of **Pt TPP_{mon}** (right)

Polymers and TTA UC measurements

A big variety of different chromophore ratios are known in literature hence determination of a perfect ratio was conducted first. Therefore a very wide concentration range was tested. For these preliminary experiments random copolymers containing the emitter monomer (**DPA_{mon}**) and the matrix monomer, 5-norbornene-2,3-dicarboxylate (**DME-N**), was synthesized via ROMP. The chain length for all polymers was adjusted to 500 units in total. M31 was used as initiator and ethyl vinyl ether was used for quenching the polymerisation.

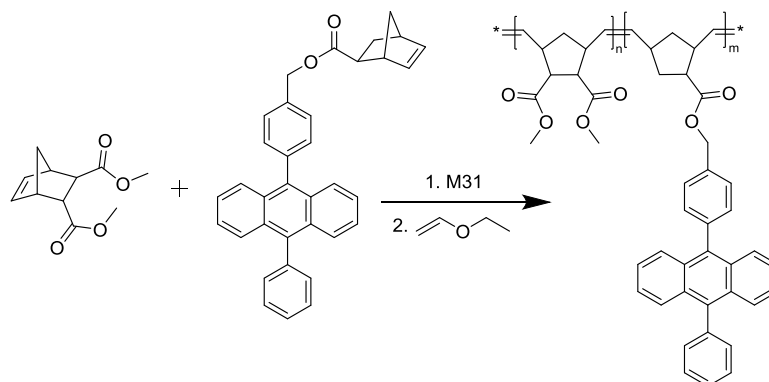


Figure 22 Preparation of a random emitter/matrix copolymer

The preparation of the copolymer is shown in Figure 22. The prepared copolymers had an emitter amount between 1 to 40 percentages by weight and the amounts of the sensitizers were tested between 0,005 to 5 percentages by weight. That leads to quite broad ratios of emitter to sensitizer, namely 3.3 / 1 up to 1 / 13700. An overview of all tested ratios is shown below in Table 2.

Table 2 Overview of emitter/ sensitizer ratios for the first TTA experiment

| Emitter | | Sensitizer | | Emitter/ Sensitizer |
|---------|----------|------------|-----------------------|---------------------|
| wt% | n [mmol] | wt% | n [mmol] | n/n [mol/mol] |
| 1 | 0.0021 | 5.000 | 4.835*10 ³ | 1 / 3.3 |
| 2 | 0.0042 | 5.000 | 4.835*10 ³ | 1 / 1.5 |
| 4 | 0.0084 | 5.000 | 4.835*10 ³ | 1.4 / 1 |
| 10 | 0.0210 | 5.000 | 4.835*10 ³ | 3.4 / 1 |
| 1 | 0.0021 | 0.500 | 4.835*10 ⁴ | 3.4/ 1 |
| 2 | 0.0042 | 0.500 | 4.835*10 ⁴ | 6.8 / 1 |
| 20 | 0.0420 | 5.000 | 4.835*10 ³ | 6.8 / 1 |
| 30 | 0.0620 | 5.000 | 4.835*10 ³ | 10.3 / 1 |
| 4 | 0.0084 | 0.500 | 4.835*10 ⁴ | 13.7 / 1 |
| 40 | 0.0830 | 5.000 | 4.835*10 ³ | 13.7 / 1 |
| 10 | 0.0210 | 0.500 | 4.835*10 ⁴ | 34.2 / 1 |
| 1 | 0.0021 | 0.050 | 4.835*10 ⁵ | 34.2 / 1 |
| 2 | 0.0042 | 0.050 | 4.835*10 ⁵ | 68.5 / 1 |
| 20 | 0.0420 | 0.500 | 4.835*10 ⁴ | 68.5 / 1 |
| 30 | 0.0620 | 0.500 | 4.835*10 ⁴ | 102.7 / 1 |
| 4 | 0.0084 | 0.050 | 4.835*10 ⁵ | 137.0 / 1 |
| 40 | 0.0830 | 0.500 | 4.835*10 ⁴ | 137.0 / 1 |
| 10 | 0.0210 | 0.050 | 4.835*10 ⁵ | 342.4 / 1 |
| 1 | 0.0021 | 0.005 | 4.835*10 ⁶ | 342.4 / 1 |
| 2 | 0.0042 | 0.005 | 4.835*10 ⁶ | 684.8 / 1 |
| 20 | 0.0420 | 0.050 | 4.835*10 ⁵ | 684.8 / 1 |
| 30 | 0.0620 | 0.050 | 4.835*10 ⁵ | 1027.2 / 1 |
| 4 | 0.0084 | 0.005 | 4.835*10 ⁶ | 1369.6 / 1 |
| 40 | 0.0830 | 0.050 | 4.835*10 ⁵ | 1369.6 / 1 |
| 10 | 0.0210 | 0.005 | 4.835*10 ⁶ | 3424.1 / 1 |
| 20 | 0.0420 | 0.005 | 4.835*10 ⁶ | 6848.2 / 1 |
| 30 | 0.0620 | 0.005 | 4.835*10 ⁶ | 10272.3 / 1 |
| 40 | 0.0830 | 0.005 | 4.835*10 ⁶ | 13696.4 / 1 |

Glass transition temperatures show an appropriate correlation with the amount of the emitter monomer. Polymerization of the matrix monomer on its own shows an T_g value of

90.5 °C whereas the polymer of the **DPA_{mon}** has a quite high glass transition temperature of 195.8 °C. All copolymers, of these two monomers, show an increase of the T_g with higher concentrations of the emitter monomer. Molecular mass distribution is for all macromolecules quite narrow, except for the pure DPA polymer due to stacking of the π - π system. A summary of all observed PDIs and T_g s are shown below in Table 3.

Table 3 Summary of PDIs and T_g s for the emitter/matrix copolymers

| Emitter amount | PDI [] | T_g [°C] | Matrix/Emitter |
|------------------|--------|------------|----------------|
| (DME-Polymer) 0% | 1.100 | 90.5 | - |
| 1% | 1.117 | - | 4.37 |
| 2% | 1.124 | 89.9 | 8.75 |
| 4% | 1.138 | 93.6 | 17.50 |
| 10% | 1.117 | 97.5 | 43.74 |
| 20% | 1.167 | 106.5 | 87.48 |
| 30% | 1.165 | 109.9 | 131.23 |
| 40% | 1.173 | 118.6 | 174.97 |
| 100% | - | 195.8 | - |

For the preliminary TTA-UC measurements the copolymers were dissolved in DMF and different amounts of **Pt TPP_{mon}** had been added to the polymer solution. A schematic illustration of these first TTA-UC experiments is shown below in Figure 23.

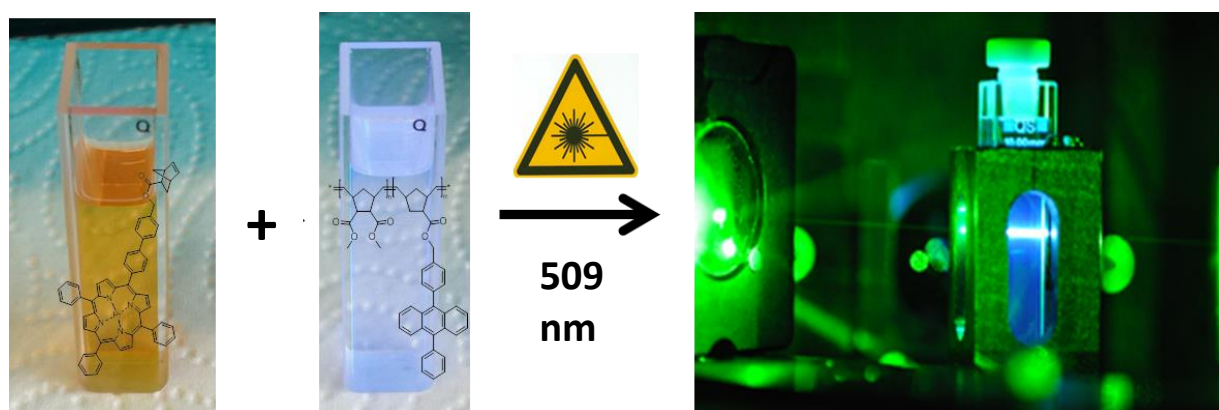


Figure 23 Schematic illustrations for the TTA-UC measurements. The Sensitizer solution was added to the emitter/matrix copolymer solution and was then excited with 509 nm obtaining blue emission

For these first TTA-UC measurements the emerging TTA emissions were recorded on a Shimadzu spectrofluorophotometer RF-5301PC without any further modifications. The compounds had been dissolved in DMF and degassed with argon for 10 minutes. The polymer concentration was set to 6.6 mg/ mL. Excitation wavelength was set to 509 nm and emission was detected in a right angle to the excitation source. The emission spectra are shown below in Figure 24.

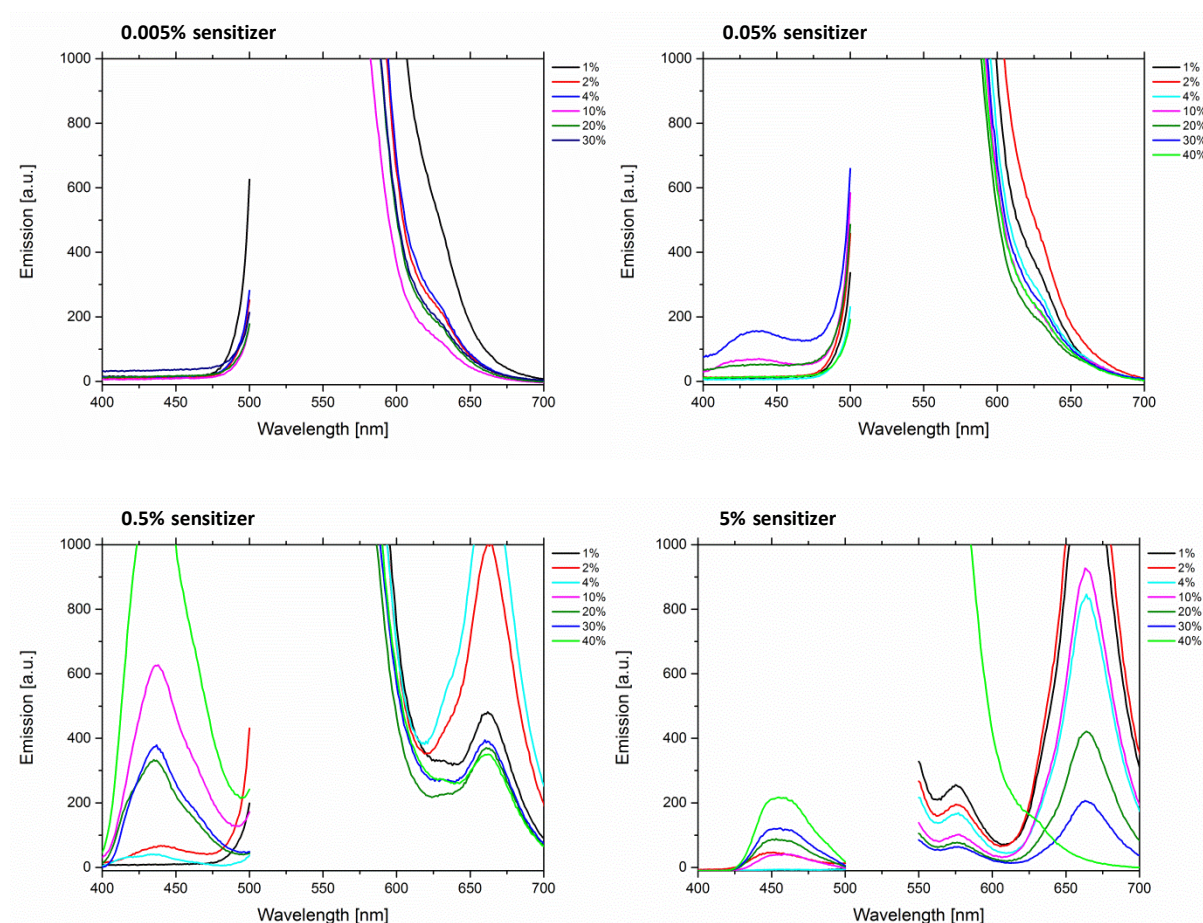


Figure 24 TTA-emission spectra of the matrix/emitter copolymer with blends of sensitizer. (Top-left 0.005 wt% sensitizer, top right 0.05 wt% sensitizer, bottom left 0.5 wt% sensitizer, bottom right 5 wt% sensitizer)

The polymer with 40 wt% of emitter and blends of 0.5 wt% sensitizer shows the highest intensity and also the lowest phosphorescence peak which indicates that the triplet-triplet energy transfer and the following annihilation works sufficiently. Therefore, terpolymers had been prepared were both chromophores were copolymerized with the matrix monomer to obtain a statistically distributed tri-copolymer. Sensitizer concentration was set to 0.5 wt%

and emitter concentration were tested in the range of 30 to 50 wt%. The Emitter concentration was increased because first experiments showed that a emitter concentration of 40% by weight always showed the highest emission signals. These prepared terpolymers have a chainlength of 500 in total. M31 was used as initiator and ethyl vinyl ether as quenching reagent. The synthetic pathway for the preparation of the terpolymers is shown below in Figure 25.

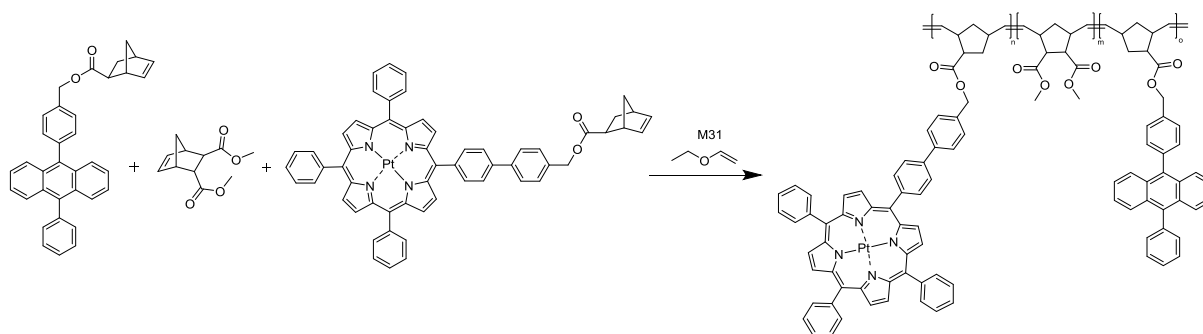


Figure 25 Preparation of a statistically distributed tri-copolymer

An overview of used the concentrations and ratios of emitter to sensitizer are shown below in Table 4.

Table 4 Overview of emitter/ sensitizer ratios for the statistically distributed tri-copolymers

| Emitter | | Sensitizer | | Emitter/ Sensitizer |
|---------|----------|------------|--------------------|------------------------|
| wt % | n [mmol] | wt % | n [mmol] | |
| 30 | 0.062 | 0.5 | $4.835 \cdot 10^4$ | 128.23 |
| 35 | 0.073 | 0.5 | $4.835 \cdot 10^4$ | 150.98 |
| 40 | 0.083 | 0.5 | $4.835 \cdot 10^4$ | 171.66 |
| 45 | 0.094 | 0.5 | $4.835 \cdot 10^4$ | 194.41 |
| 50 | 0.104 | 0.5 | $4.835 \cdot 10^4$ | 215.09 |

The measurement setup was similar to the copolymer/blend experiments and a comparison of the emission spectra is shown below in Figure 26. The highest emission signals were obtained with an emitter concentration of 40 wt% and 0.5 wt% of the sensitizer. This leads to an emitter to sensitizer ratio of 171 to 1.

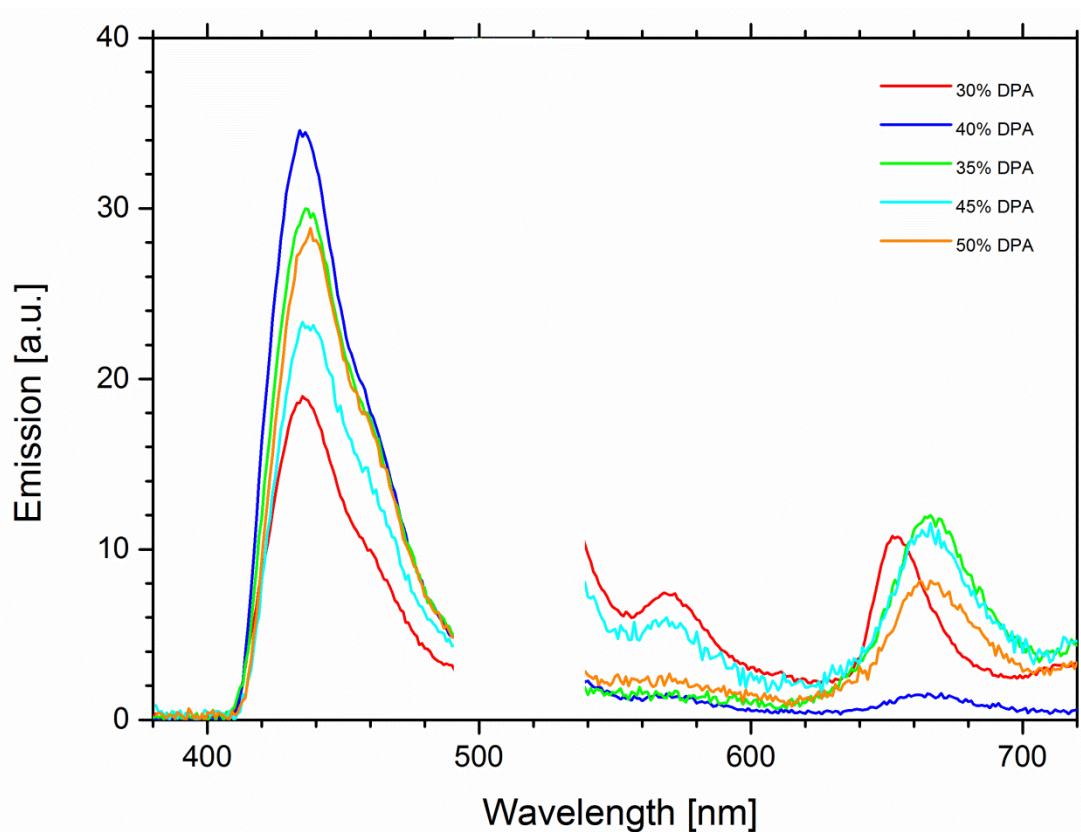


Figure 26 Comparison of emission spectra of terpolymers (Emitter: 30, 35, 40, 45 and 50 wt%; Sensitizer 0.5 wt%)

Due to these results we started the preparation of different polymeric architectures with a matrix/ emitter/ sensitizer ratio of 432/ 68/ 0.4. The different polymer architectures had been prepared in order to investigate the influence of the polymer architecture on the TTA induce photon up-conversion. The preparation of the polymers as well as the measurement setup and the calculation of the quantum yields were similar to the perylene/benzoporphyrin system (see chapter 3). A comparison of the polymeric architectures is shown below in Figure 27.






| Structure | Sample | Quantum Yield [%] |
|---|----------------------|-------------------|
|  | (DPA + Pt TPP) | 0.04 |
|  | DPA - DME - Pt TPP | 0.08 |
|  | DME - DPA - Pt TPP | 0.10 |
|  | (DPA + DME) - Pt TPP | 0.11 |
|  | (DME + DPA + Pt TPP) | 0.71 |

Figure 27 overview of the prepared terpolymers and comparison of its TTA quantum yields (red sphere: emitter, violet sphere: sensitizer, blue sphere: matrix)

The corresponding TTA-UC measurements are shown below in Figure 28.

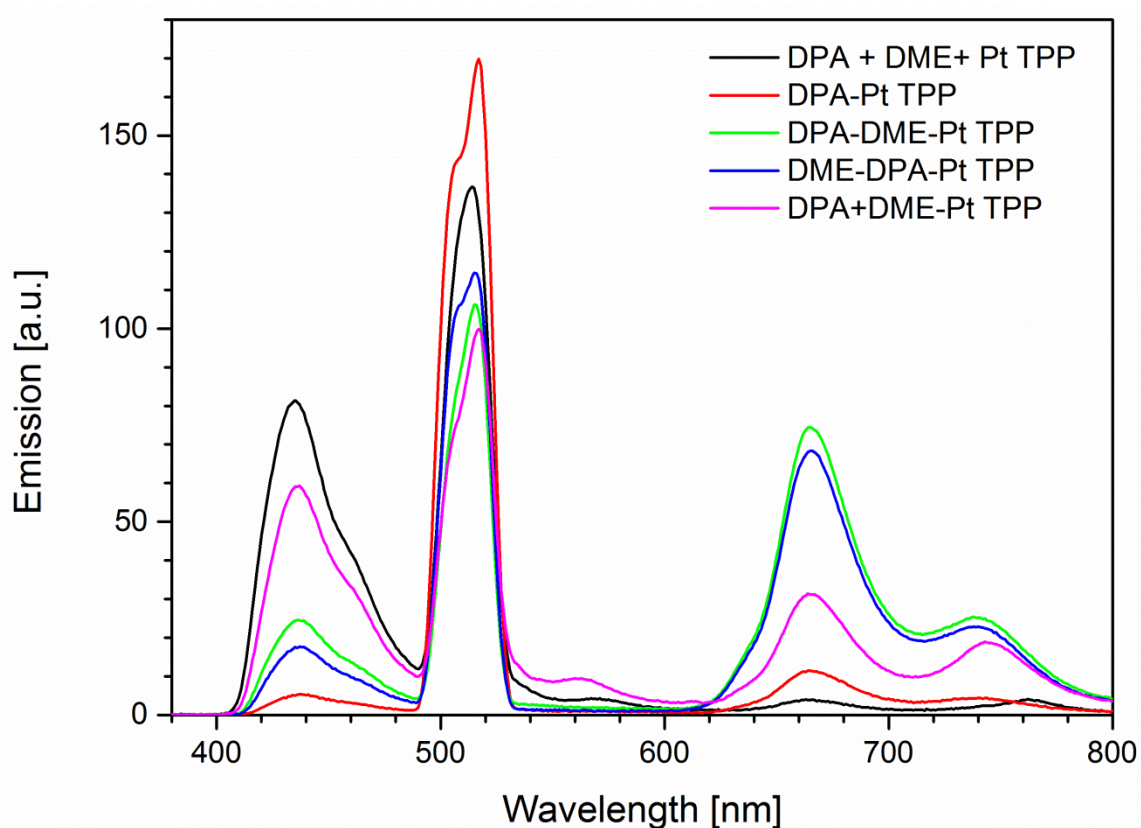


Figure 28 Comparison of TTA emission spectra of different polymer architectures

The characteristic TTA signal is quite broad and occurs between 410 to 480 nm approximately, its global maximum exhibits at 435 nm. The measurements have been carried out under room temperature. Excitation was done with a Xe 450W lamp with a

power density of $539 \text{ mol s}^{-1} \text{ m}^{-2}$. Calculations of the quantum yields (ϕ) are described in chapter 3. An overview of the polymer architecture and a comparison of the TTA-UC quantum yields are shown below in Figure 28.

The correlation between the architecture and the quantum yields is similar to the ones for the perylene/benzoporphyrin system (see chapter 3). There was no suitable laser available; therefore the polymers have been measured with a very low power source. Hence, the quantum yields are quite low for that terpolymer system. The light density dependent measurements (used filters: 100%, 50%, 30%, 10% and 5%) of the UC intensity show a quadratic dependence. This means that the system is not saturated; hence higher quantum yields are achievable with a higher power density.

Conclusion

This work describes the determination and preparation of a suitable chromophore system for a sufficiently working up-conversion via triplet-triplet annihilation. The chosen dyes are a platinum tetraphenylporphyrin derivative as sensitizer and a perylene derivative as emitter. Furthermore, determination of a suitable concentration for a polymer based TTA chromophore system was investigated. The used chromophores have been functionalized with norbornene moieties, preparing deionized- and terpolymers for further up-conversion measurements. First TTA measurements were conducted on a simple fluorometer with a emitter/matrix copolymer and blends of the sensitizer with DMF as solvent. These measurements showed that a emitter amount of 40 wt%, a sensitizer amount of 0.5 wt% and a total chain length of 500 had the highest intensity for the TTA up-conversion. Same results had been obtained for the corresponding terpolymer. Therefore the synthesis of different polymeric architectures was conducted. The best UC quantum yields had been obtained for the statistically distributed terpolymer. That polymer showed a quantum yield of more than 0.7%. The excitation source was a 450W Xe lamp that was set to 509 nm with a energy density of $539 \text{ mol s}^{-1} \text{ m}^{-2}$. The energy dependent measurements showed a quadratic dependence which is typical for a nonlinear process such as TTA-based up-conversion. The Logarithmic plot exhibits a slope of two which indicates that the system is not saturated. Hence, higher quantum yields could be obtained with a stronger light energy source. The next step is the investigation of these polymer systems with a stronger light

source (e.g. laser, LED) and the preparation of films via drop casting, spin coating or doctor blading.

Experimental

Materials and Methods

All reagents and solvents were purchased from commercial sources (ABCR or Sigma Aldrich) with reagent grade quality and used as received. Complex M31 [1. 3-bis (2, 4, 6-trimethylphenyl)-2-imidazolidinylidene] dichloro-(3-phenyl-1H-inden-1-ylidene)(pyridyl) ruthenium (II) for ring opening metathesis polymerisation (ROMP) was obtained from UMICORE AG Co. KG. NMR spectroscopy (^1H , ^{13}C , APT, COSY, HSQC) was performed on a Bruker Avance 300 MHz spectrometer. Deuterated solvents (Chloroform- d , DMSO- d_6 , D_2O) were obtained from Cambridge Isotope Laboratories Inc. and remaining solvent peaks were referenced according to literature.¹²¹ Peak shapes are specified as follows: s (singlet), bs (broad singlet), d (doublet), dd (doublet of doublets), t (triplet), q (quadruplet) and m (multiplet). Silica gel 60 F254 and aluminium oxide 60 F254 on aluminium sheets were used for thin layer chromatography. They were purchased from Merck. Visualization was done under UV light or by dipping into an aqueous solution of KMnO_4 (0.1 wt%). MALDI-TOF mass spectrometry was performed on Micromass TofSpec 2E Time-of-Flight Mass Spectrometer. The instrument was equipped with a nitrogen laser ($\lambda = 337 \text{ nm}$, operated at a frequency of 5 Hz) and a time lag focusing unit. Ions were generated just above the threshold laser power. Positive ion spectra were recorded in reflection mode with an accelerating voltage of 20 kV. The spectra were externally calibrated with a polyethylene glycol standard. Analysis of data was done with MassLynx-Software V3.5 (Micromass/Waters, Manchester, UK). The best ten shots were averaged to a spectrum. Samples were dissolved in acetone or DCM ($c = 1 \text{ mg/mL}$). Solutions were mixed in the cap of a microtube in the ratio of 1 μL : 10 μL . The resulting mixture (0.5 μL) was spotted onto the target and allowed to air-dry. The matrix was trans-2-[3-(4-tert-Butylphenyl)-2-methyl-2-propenylidene]malononitrile (DCTB). Absorption spectra were recorded on a Shimadzu spectrophotometer UV-1800. The emission was measured on a Hitachi F-7000 fluorescence spectrometer equipped with a red-sensitive photomultiplier R928 from Hamamatsu. For the TTA-measurements a Horiba Fluorolog-3 luminescence spectrometer was used. Excitation of the polymers was done either with a LED, LASER or a 450 W Xenon lamp at 617 nm. The Laser was purchased at

Roithner Laser. Relative luminescence quantum yields were determined according to Crosby and Demas¹²² using platinum(II)tetraphenyltetrabenzoporphyrin ($\phi = 0.51$)¹²³. Gel permeation chromatography (GPC) was used to determine molecular weights and the polydispersity index (PDI). These measurements were carried out, with dichloromethane as solvent, with the following instrument set up: Merck Hitachi L6000 (pump); Polymer Standards Service, 5 μm grade size (separation columns); Wyatt Technology (refractive index detector). Glass transition temperatures (T_g) have been measured on a Perkin Elmer Differential Scanning Calorimeter (Hyper DSC 8500). Two isothermal cycles were executed and the second scan was analysed. The scanning speed for cooling and heating was 20 $^{\circ}\text{C}/\text{sec}$.

Synthetic procedures

(4-(10-phenylanthracen-9-yl)phenyl)methanol A 250 mL three-neck round-bottom-flask was equipped with a stirring bar and reflux condenser. After addition of 18 mL toluene, 13 mL MeOH and 1 mL deionized water the mixture was deoxygenated for 1 hour with inert gas. The mixture was heated to 60 $^{\circ}\text{C}$ and (4-(hydroxymethyl)phenyl)boronic acid (0.339 g, 2.23 mmol) and phenylboronic acid (0.272 g, 14.9 mmol) were added to the mixture. After 30 minutes of stirring the acids had been entirely dissolved followed by addition of 9,10-dibromoanthracene (0.5 g, 1.49 mmol) and potassium carbonate (2.06 g, 14.9 mmol). The reaction was initiated with the addition of tetrakis(triphenylphosphine)palladium(0) (86 mg, $7.4 \cdot 10^{-2}$ mmol). After 24 hours under reflux the reaction was quenched with 15 mL deionized water. The product was extracted three times with DCM, the organic layer was dried with Na_2SO_4 , filtered off and concentrated *in vacuo* to obtain a yellowish solid. Purification was done by column chromatography (SiO_2 , DCM). Yield: 433 mg (80.5%). $^1\text{H-NMR}$ (δ , 20 $^{\circ}\text{C}$, CDCl_3 , 300 MHz): 7.75 – 7.30 (m, 17H, H_{Ar}), 4.91 (s, 2H, $-\text{CH}_2-$), 1.81 (bs, 1H, $-\text{OH}$), $^{13}\text{C-NMR}$ (δ , 20 $^{\circ}\text{C}$, CDCl_3 , 125 MHz): 140.2, 139.2, 138.7, 137.4, 136.9, 131.7, 131.5, 130.0, 128.6, 127.6, 127.3, 127.2, 127.0, 125.2, 125.2 (C_{Ar}), 65.5 ($-\text{CH}_2-$). **UV-Vis** (DCM) λ_{max} nm: 396, **375**, 357

4-(10-phenylanthracen-9-yl)benzyl-bicyclo[2.2.1]hept-5-ene-2-carboxylate (DPA_{mon}) A 500 mL three-neck round-bottom flask was filled with freshly distilled cyclopentadiene (0.825 g, 12.48 mmol) and was dissolved in 50 mL dry DCM. Acryloylchlorid (0.414 g, 4.58 mmol) was added dropwise while the mixture was ice-cooled. The reaction was finished after two

hours; completion was detected via TLC (CH: EtOAc 1:1). (4-(10-phenylanthracen-9-yl)phenyl)methanol (1.5 g, 4.16 mmol) was dissolved in 75 mL dry DCM and was added slowly to the previously prepared norbornoyl chloride solution. Afterwards, pyridine (336 μ L, 4.16 mmol) and a spatula tip of DMAP were added to the reaction and were stirred over night at room temperature. On the next day the reaction was quenched with 25 mL deionized water and stirred for 30 minutes. After addition of DCM extraction of the desired compound was done with 25 mL HCl (5%) and 50 mL saturated NaHCO₃ solution. The combined organic layers were dried with Na₂SO₄, filtered off and concentrated *in vacuo* to obtain a colourless solid. Purification was done by column chromatography (SiO₂, DCM). Yield: 1.62 g (81%). ¹H-NMR (δ , 20°C, CDCl₃, 300 MHz): 7.75 – 7.30 (m, 17H, H_{Ar}), 6.26 (m, 1H, H_{nb5}), 5.99 (m, 1H, H_{nb6}), 5.27 (s, 2H, -CH₂-), 3.35 (bs, 1H, H_{nb2}), 3.11 (bs, 1H, H_{nb1}), 2.97 (bs, 1H, H_{nb4}), 2.00 (bs, 1H, H_{nb3}), 1.60 – 1.35 (m, 2H, H_{nb7}), ¹³C-NMR (δ , 20°C, CDCl₃, 125 MHz): 138.1, 132.5, 131.6, 130.0, 128.6, 128.2, 127.6, 127.2, 127.0, 125.2, 125.2, (C_{Ar}, C=O, C_{nb5,6}), 49.8, 46.1, 43.6, 42.8, 29.5 (C_{nb1-4,7}), UV-Vis (DCM) λ_{max} , nm: 396, 375, 357. MALDI: m/z [M⁺]calc. for C₃₅H₂₈O₂: 480.2089; found 480.2060.

5-(4-bromophenyl)-10,15,20-triphenylporphyrin (BrTPP) A 1 L round-bottom flask was equipped with a magnetic stirring bar and a reflux condenser. The flask was filled with 650 mL propionic acid and heated to reflux. Freshly distilled benzaldehyde (12.75 mL, 0.125 mol) and 4-bromobenzaldehyde (7.73 g, 0.041 mol) was added to the mixture. After 10 minutes the substrates were dissolved completely and the dropwise addition of freshly distilled pyrrole (11.5 mL, 0.167 mol) was started. The addition was finished after 10 minutes and the mixture was then stirred for further 30 minutes under reflux. Completion of the reaction was detected via TLC (CH: EtOAc 5:1). The deep purple solution was cooled down to room temperature and left in the fridge over night at 4°C. On the next day the crude product was filtered off via suction filtration and washed with MeOH. The remaining solid was dissolved in DCM and extracted with deionized water and brine. The organic phase was dried with Na₂SO₄, filtered off and concentrated *in vacuo* obtaining a purple solid. To remove polymeric material, column chromatography with DCM as solvent was conducted. For the second column chromatography a mixture of CH and DCM (2:1) was used to obtain the mono substituted compound. After evaporation of the solvent, purple crystals were obtained. Yield: 1.22 g (4.3%). ¹H-NMR (δ , 20°C, CDCl₃, 300 MHz): 8.85 – 8.76 (m, 8H, H_{pyrrole}), 8.24 –

8.14 (m, 8H, H_{Ar-m}), 7.99 – 7.90 (m, 3H, H_{Ar-p}), 7.78 – 7.72 (m, 8H, H_{Ar-o}), -2.87 (bs, 2H, -NH)
UV/VIS (DCM): λ_{max} = 415, 512, 547, 589, 646.

Platinum (II) 5-(4-bromophenyl)-10,15,20-triphenylporphyrin (Pt BrTPP) A 20 mL microwave vessel was equipped with a stirring bar and filled with 12 mL benzonitrile. After addition of the porphyrin (120 mg, 0.173 mmol) and the metal salt (190.5 mg, 0.484 mmol) the vessel was sealed with a septum and placed into the microwave. The reaction temperature was set to 250°C for 30 minutes. The pressure was controlled by a load cell connected to the vessel via a non-invasive pressure measurement device above the septum surface. After completion of the reaction the remaining salts and the undesired protonated ligand were filtered off. The desired product was obtained via precipitation with a mixture of EtOH, DI water and brine. The red solid was filtered off and concentrated *in vacuo*. Purification was done by column chromatography (SiO₂, CH: DCM, 1:2). Yield: 73.6 mg, 48%, ¹H-NMR (δ , 20°C, CDCl₃, 300 MHz): 8.85 – 8.76 (m, 8H, $H_{pyrrole}$), 8.24 – 8.14 (m, 8H, H_{Ar-m}), 7.99 – 7.90 (m, 3H, H_{Ar-p}), 7.78 – 7.72 (m, 8H, H_{Ar-o}), **UV/VIS** (DCM): λ_{max} = 398.5, 508.

Platinum (II) (4'-(10,15,20-triphenylporphyrin-5-yl)-[1,1'-biphenyl]-4-yl)methanol A 100 mL Schlenk flask was filled with 45 mL of a 1:1 mixture DMF: toluene and was degassed for 30 minutes. Afterwards, the porphyrin (400 mg, 0.452 mmol), the boronic acid (137.4 mg, 0.904 mmol), potassium carbonate (498.7 mg, 3.61 mmol) and the catalyst (7.84 mg, 6.8*10⁻² mmol) were dissolved and the reaction mixture was stirred for 12 hours. Completion of the reaction was detected via TLC (DCM). After addition of 50 mL DCM the product was extracted with deionized water and brine. The organic layer was dried with Na₂SO₄, filtered off and concentrated *in vacuo* obtaining a red solid. Purification was done via column chromatography (SiO₂, DCM). Yield: 70 mg (17%). ¹H-NMR (δ , 20°C, CDCl₃, 300 MHz): 8.85 – 8.76 (m, 8H, $H_{pyrrole}$), 8.24 – 8.14 (m, 8H, H_{Ar-m}), 7.99 – 7.90 (m, 3H, H_{Ar-p}), 7.78 – 7.72 (m, 8H, H_{Ar-o}), 7.48 – 7.31 (m, 4H, H_{Ar}), 5.20 – 5.10 (m, 2H, Ph-CH₂-O-), **UV/VIS** (Aceton): λ_{max} = 390, 499.

Platinum (II) (4'-(10,15,20-triphenylporphyrin-5-yl)-[1,1'-biphenyl]-4-yl)methyl-bicyclo[2.2.1]hept-5-ene-2-carboxylate (Pt TPP_{mon}) A 10 mL Schlenk flask was purged with inert gas three times. Afterwards, cyclopentadiene (119 mg, 1.8 mmol) and acryloyl chloride (81 mg, 0.9 mmol) were dissolved in 40 mL dry DCM for the preparation of the corresponding norbornene acid chloride. After 2 hours the reaction was finished and the previously dissolved porphyrin (550 mg, 0.6 mmol) was dissolved in 20 mL dry DCM and was

added slowly to the same, ice cooled, reaction mixture. Addition of pyridine (72 mL, 0.6 mmol) and a spatula tip DMAP was necessary for a complete conversion. On the next day the reaction was finished, detection was done via TLC (DCM: MeOH, 20: 1). The reaction was quenched with 1 mL deionized water and was stirred for 30 minutes. The product was extracted with HCl (5%), saturated NaHCO₃ and deionized water. The organic phase was dried with Na₂SO₄ and concentrated *in vacuo* to obtain a red solid. Purification was done by column chromatography (SiO₂, DCM). Yield: 230 mg (37 %). ¹H-NMR (δ, 20°C, CDCl₃, 300 MHz): 8.85 – 8.76 (m, 8H, H_{pyrrole}), 8.24 – 8.14 (m, 8H, H_{Ar-m}), 7.99 – 7.90 (m, 3H, H_{Ar-p}), 7.78 – 7.72 (m, 8H, H_{Ar-o}), 7.48 – 7.31 (m, 4H, H_{Ar}), 6.27 – 6.22 (m, 1H, H_{nb6}), 5.99 – 5.95 (m, 1H, H_{nb5}), 5.20 – 5.10 (m, 2H, Ph-CH₂-O-), 3.32 (bs, 1H, H_{nb2}), 3.26 (bs, 1H, H_{nb1}), 2.96 (bs, 1H, H_{nb4}), 1.98 – 1.93 (m, 2H, H_{nb3}), 1.50 – 1.44 (m, 2H, H_{nb7}). MALDI: m/z [M⁺]calc. for C₅₉H₄₂O₂N₄Pt: 1033.2960; found 1033.2985. UV/VIS (acetone): λ_{max} = 399, 508.

Dimethyl-5-norbornene-2,3-dicarboxylate (N-DME)¹²⁴ Dimethyl fumarate (10.01 g, 0.0679 mol) was dissolved in ice cooled DCM (75 mL). Freshly distilled cyclopentadiene (6.43 mL, 0.0764 mol) was added slowly while the reaction mixture was stirred at room temperature for 15 hours. Purification was modified according to Lowe et al.. The solvent was removed under reduced pressure and crystallization was initiated by adding a seed crystal. After suction filtration the product was dried *in vacuo* and was used without any further purification steps. Yield: 12.47 g (87%). ¹H-NMR (δ, 20°C, CDCl₃, 300 MHz): 6.24 (dd, ³J_{HH} = 5.4, 3.1 Hz, 1H, H_{nb5}), 6.04 (dd, ³J_{HH} = 5.5, 2.7 Hz, 1H, H_{nb6}), 3.68 (s, 3H, -CH₃), 3.61 (s, 3H, -CH₃), 3.34 (t, ³J_{HH} = 4.1 Hz, 1H, H_{nb2}), 3.23 (bs, 1H, H_{nb1}), 3.09 (bs, 1H, H_{nb4}), 2.65 (dd, ³J_{HH} = 4.3, 1.4 Hz, 1H, H_{nb3}), 1.58 (d, ³J_{HH} = 8.8 Hz, 1H, H_{nb7b}), 1.43 (dd, ³J_{HH} = 8.8, 1.5 Hz, 1H, H_{nb7a}). ¹³C-NMR (δ, 20°C, CDCl₃, 75 MHz): 175.08 (C=O), 173.85 (C=O), 137.69, 135.27 (C_{nb5,6}), 52.16 (-CH₃), 51.88 (-CH₃), 47.94, 47.71, 47.40, 47.17, 45.70 (C_{nb1-4}, C_{nb7}).

Supporting Information

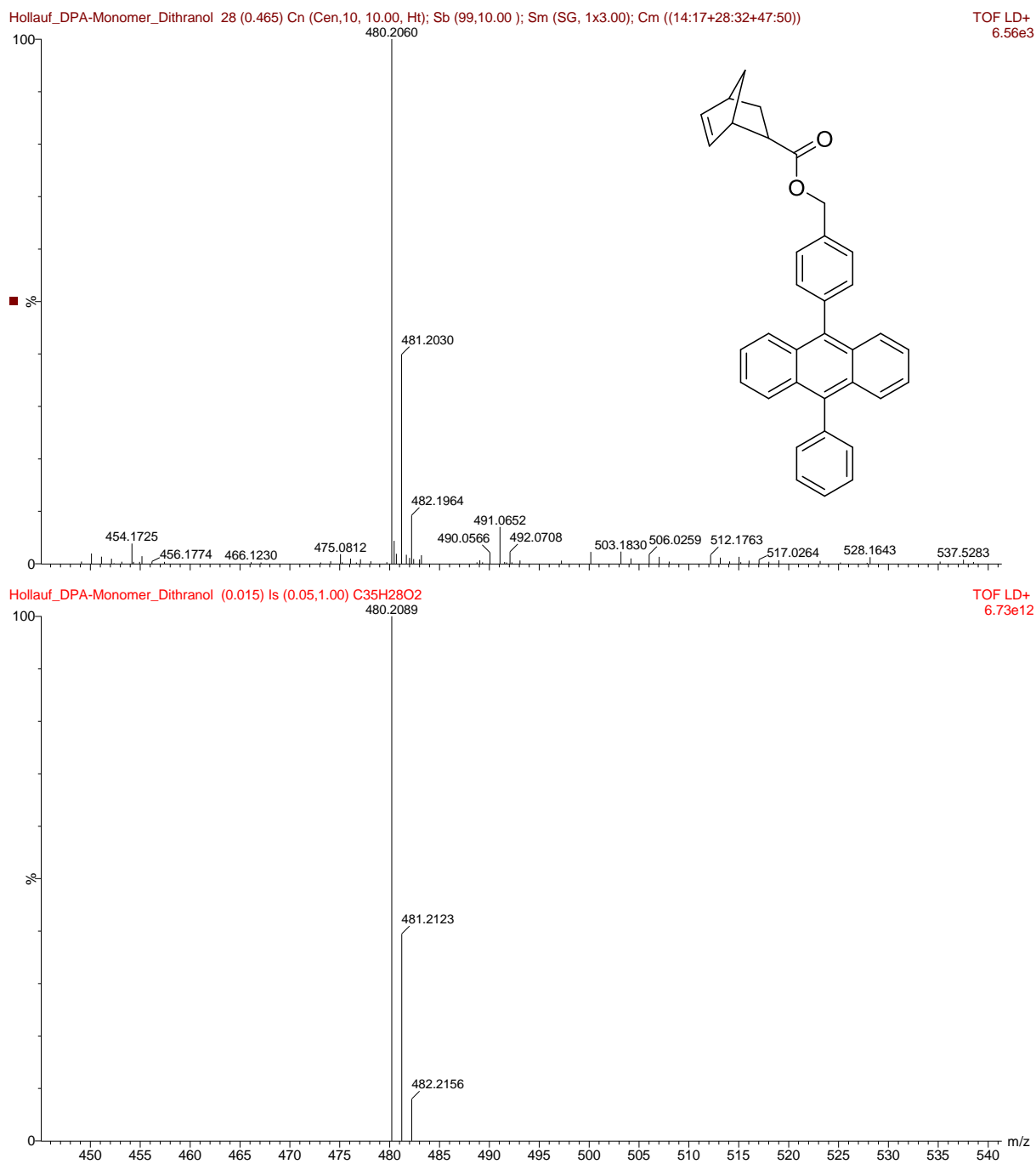


Figure 1S. Mass spectrum (MALDI) of **DPA_{monomer}**

C₃₅H₂₈O₂

calculated: 480.2089 g/mol

experimental: 480.2060 m/z

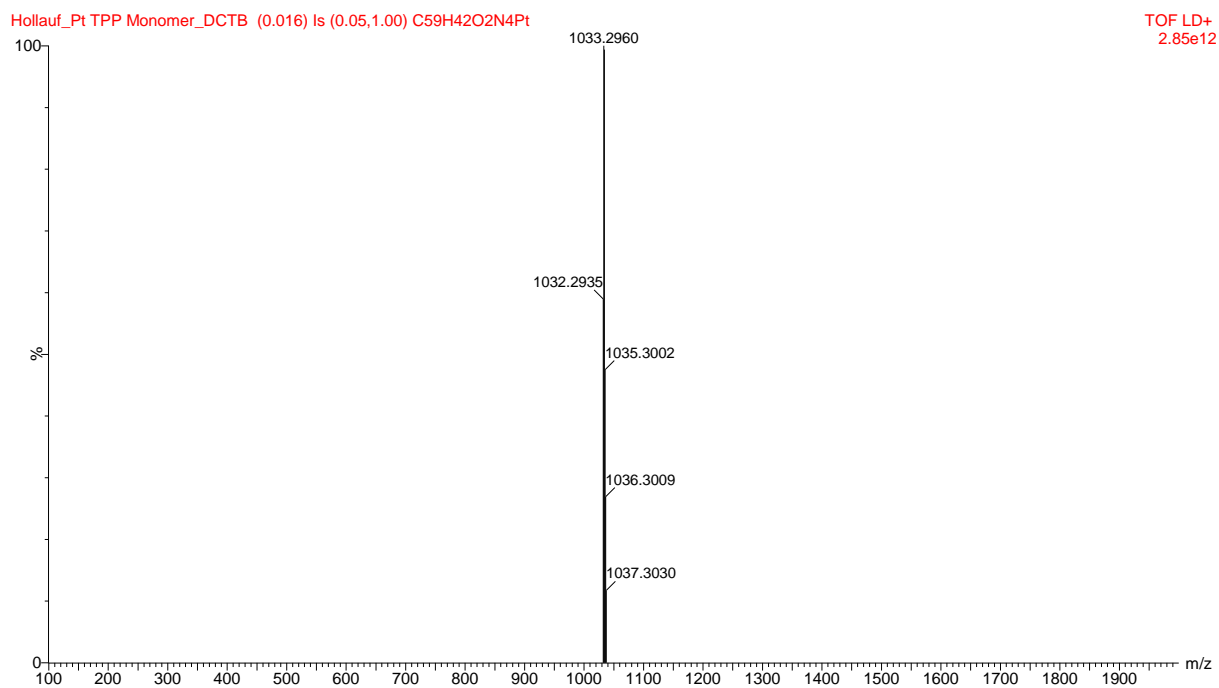
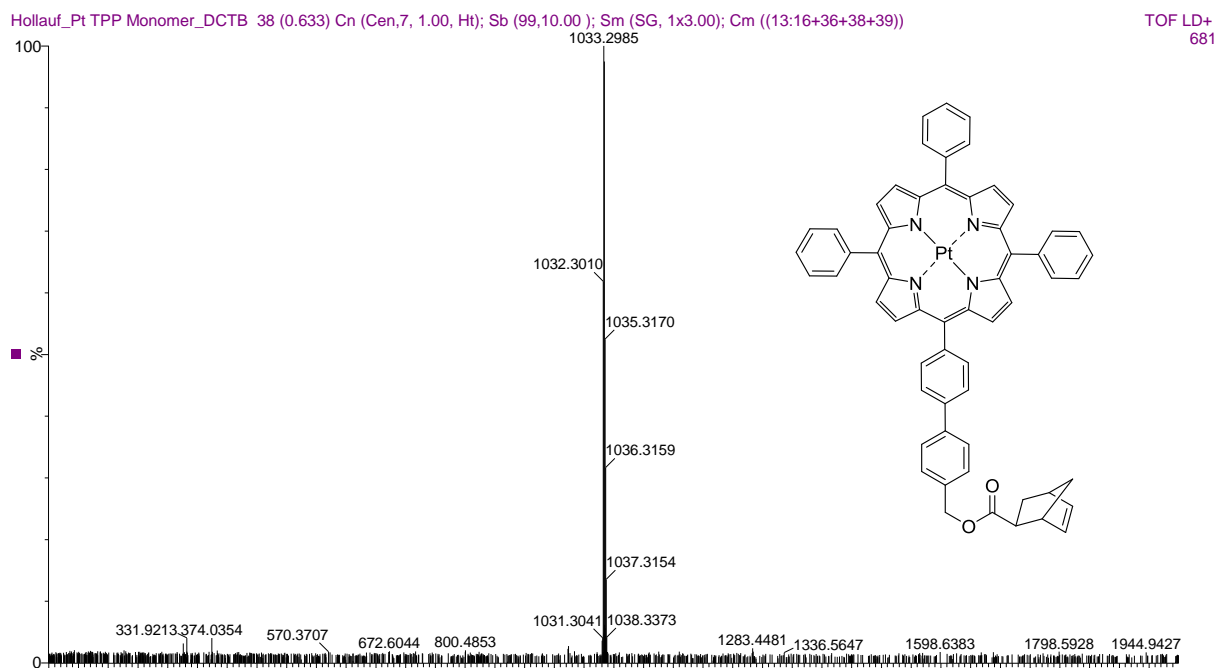


Figure 2S. Mass spectrum (MALDI) of TPP Pt_{monomer}

C₅₉H₄₂O₂N₄Pt

calculated: 1033.2960 g/mol

experimental: 1033.2985 m/z

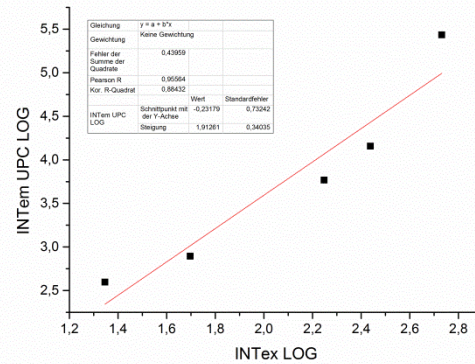
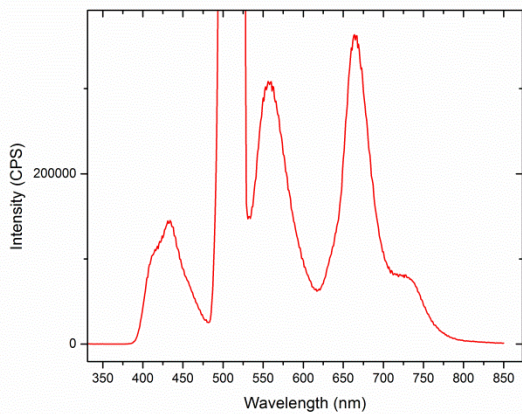


Figure 3S. TTA UC emission Spectra of polymer I and the corresponding double logarithmic plot of energy dependent UC measurements (Xe Lamp)

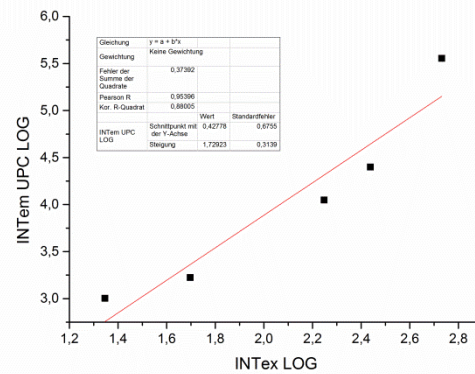
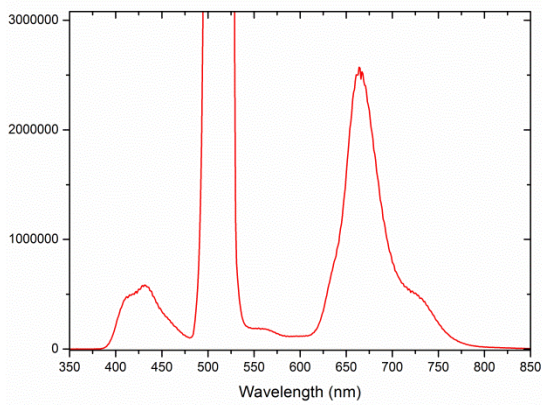


Figure 4S. TTA UC emission Spectra of polymer II and the corresponding double logarithmic plot of energy dependent UC measurements (Xe Lamp)

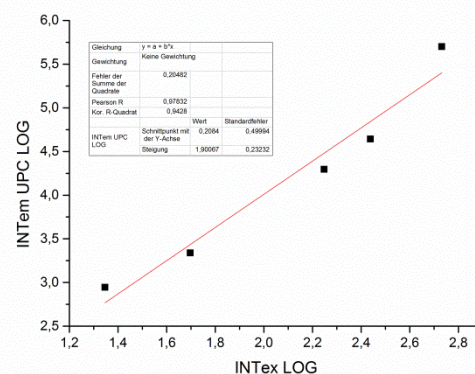
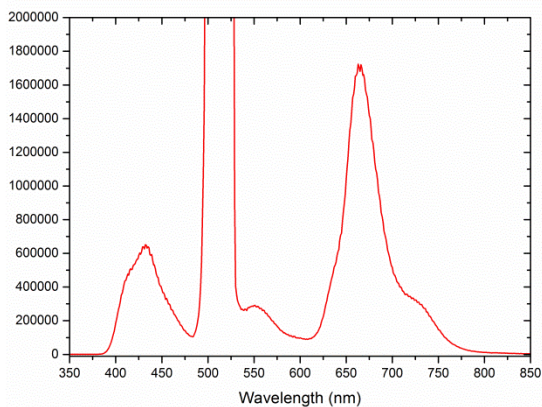


Figure 5S. TTA UC emission Spectra of polymer III and the corresponding double logarithmic plot of energy dependent UC measurements (Xe Lamp)

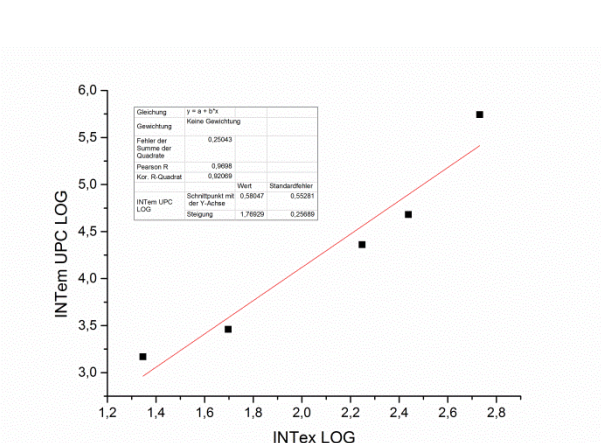
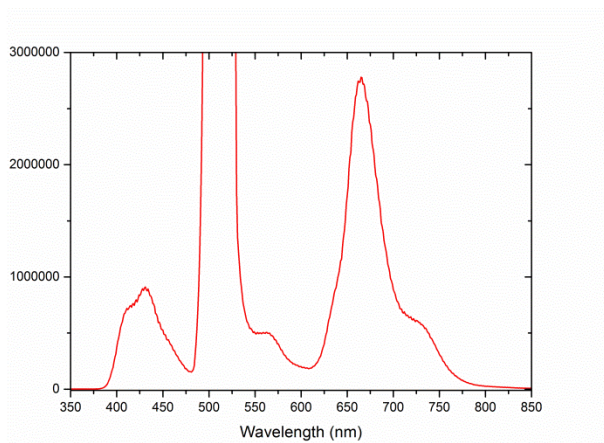


Figure 6S. TTA UC emission Spectra of polymer **IV** and the corresponding double logarithmic plot of energy dependent UC measurements (Xe Lamp)

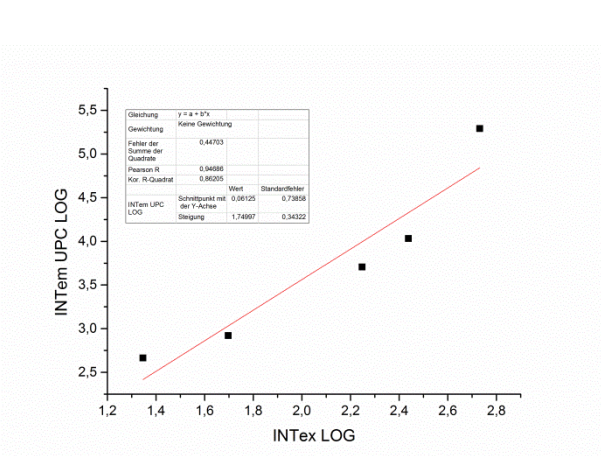
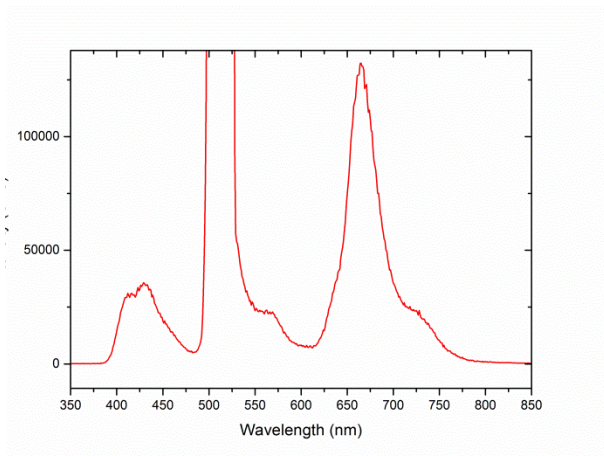


Figure 7S. TTA UC emission Spectra of polymer **V** and the corresponding double logarithmic plot of energy dependent UC measurements (Xe Lamp)

CHAPTER 3

Chapter 3 was submitted to **Journal of Materials Chemistry C**.

FIRST ROMP BASED TERPOLYMER FOR THE USE AS A LIGHT UP- CONVERTING MATERIAL VIA TRIPLET-TRIPLET ANNIHILATION

M. Hollauf • P. Zach • S. M. Borisov • B. J. Müller • D. Beichel •

M. Tscherner • S. Köstler • A. C. Knall • G. Trimmel

Journal of Materials Chemistry C, 2016, XXX, XXXX

DOI: XXXXXXXXXXXXX



Abstract

In this paper we present the preparation of the first ROMP terpolymer system comprising covalently attached sensitizer and emitter chromophores for the use as a light up-converting material via triplet-triplet annihilation. Due to the advantages of ROMP it was possible to prepare five different polymeric architectures to investigate the influence of polymer architecture and chromophore arrangement on photon up-conversion behaviour. Both chromophore containing monomer units were newly developed and demonstrated appropriate photophysical characteristics for photon up-conversion via triplet-triplet annihilation. The used chromophores are derivatives of Pt(II) meso-tetraphenyltetraabenzotetrabutylporphyrin Pt(II) and a perylenediester. Polymerisations were performed with the monomeric chromophores and a well-known norbornene matrix monomer, called dimethyl 5-norbornene-2,3-dicarboxylate. The best quantum yields have been achieved with a completely statistically distributed terpolymer and show in solution an up-conversion quantum yield of up to 3%.

Introduction

Anti-Stokes photoluminescence, the emission of photons at higher energy than the absorbed ones, also known as photon up-conversion (UC), is a very interesting effect due to the wide range of possible applications such as bioimaging, optical data storage, display devices, high-resolution optical microscopy, drug delivery, up-conversion layers for photovoltaics and many others.^{125,126,127} The field of anti-Stokes fluorescence imaging was traditionally dominated by inorganic crystals doped with luminescent lanthanide ions and by organolanthanide complexes, where the UC scheme requires the sequential absorption of two or more photons exciting the metastable states of the emitting ions.^{128,129} Today the most frequent ways to achieve a photon up-conversion are through second harmonic generation or two photon absorption (TPA).¹³⁰ A big disadvantage of the TPA mechanisms is that they usually require excitation irradiances in the order of MW cm^{-2} .¹³¹ In contrast to that, the UC based on triplet-triplet annihilation (TTA) is a promising low-power up-conversion process which already shows delayed fluorescence using excitation irradiances of less than 100 mW cm^{-2} (solar energy is enough).^{132,133} This effect requires two dyes which are called sensitizer and emitter or are also known as acceptor and annihilator. First the sensitizer absorbs incident photons that allow it to occupy its excited singlet state ($^1\text{S}^*$) that

quickly relaxes into a metastable excited triplet state ($^3S^*$) caused by a spin-forbidden intersystem crossing (ISC). In presence of suitable emitter molecules, that have excited triplet levels of similar energy, a triplet-triplet energy transfer (TTET) from the sensitizer to the emitter takes place. Annihilation of the two excited emitter species ($3E^*$) generates one emitter molecule in the singlet excited state ($1E^*$) which eventually results in TTA. Here one molecule relaxes to its ground state in a radiationless process while the other one shows delayed fluorescence. Hence, the TTA-UC represents another possibility to obtain anti-Stokes fluorescence. The corresponding Jablonski diagram is shown below in Figure 29.

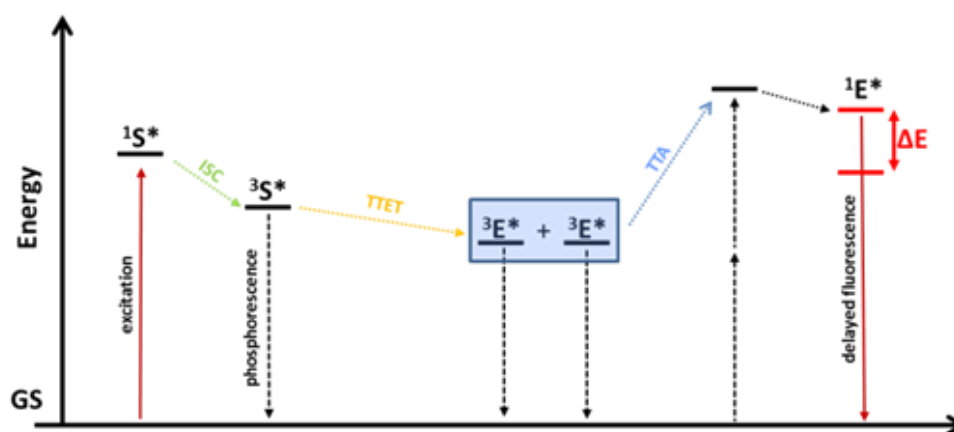


Figure 29 Jablonski energy level-diagram of TTA up-conversion

(S stands for sensitizer and E for emitter. Coloured solid lines represent the intended radiative processes (absorption and emission). Vertical dashed lines represent undesired non radiative and radiative decay pathways. Slanted dotted arrows represent cascading energy transfer processes. GS denotes the ground states (for simplicity drawn at the same energy level) and ΔE is the energy difference between incident and emitted light)¹²⁸

Regarding the chromophores, numerous chromophore combinations resulting in efficient TTA-UC have been established. The most commonly used dyes are perylenes, anthracenes, rubrene derivatives or borodipyrroles as emitters and porphyrin derivatives, supramolecular chromophores, phthalocyanines or cyclometallated Pt (II) complexes as a sensitizers to name just a few.^{134,135,136,137,138} To obtain photon up-conversion a chromophore pair, where the excited triplet state of the sensitizer is higher than the one of the emitter, has to be found. This is crucial for an efficient triplet triplet energy transfer (TTET).

Although TTA is known in solution since over 50 years¹³⁹ it has only recently been possible to realize this effect in solid polymeric films. The first examples were prepared in 2007 by the

working group of Castellano *et al.* and used blends of Pd 2,3,7,8,12,13,17,18-octaethylporphyrin (PdOEP) as sensitizer and diphenylanthracene (DPA) as emitter in an ethylene oxide/ epichlorohydrin copolymer to obtain a rubber like matrix.¹⁴⁰ Recent studies show that this effect is also possible with active polymeric structures^{141,142,143,144,145,146}, liposomes^{147,148}, ionogels¹⁴⁹, oil in water micro emulsions^{150,151,152}, micelles¹⁵³, dendrimers¹⁵⁴, nanocapsules^{155,156,157} and many more^{125,131,158}. The translational and rotational mobility of the chromophores is essential for an efficient photon light up-converting process, due to the fact that mobility influences all the implemented energy transfer processes. Hence, there are only a few examples where covalently bound dye molecules are involved for efficient TTA quantum yields. Nevertheless, a close distance and a defined position of sensitizer and emitter to each other are at least equally important to obtain a high TTA photon emission. There are a few examples of a direct covalent coupling of both dyes^{159,160,161,162}. Only very recent studies investigated the covalent binding of one of the dyes to a polymeric matrix^{163,164,165} or even both dyes^{126,166} considering the fact, that the sensitizer and emitter need to be in close proximity in order to efficiently undergo short-range interactions such as ET and TTA (Fig. 1). Following this idea, the influence of different emitter to sensitizer ratios on the TTA efficiency was studied in methacrylate based materials synthesised by free radical polymerisation.¹²⁶ Alternatively, the group of Ghiggino prepared star polymers with the sensitizer in the centre and emitter functionalized arms (2 and 6 arms) using RAFT as controlled polymerisation technique¹⁶⁷ demonstrating that the placement of dye molecules at distinct places using controlled polymerisation techniques or post-functionalisation approaches is a strategy to study the TTA-process in polymeric materials in detail. A straightforward synthetic pathway to prepare such dye functionalized polymers with a defined structure is ring opening metathesis polymerisation (ROMP). A big advantage of ROMP is that it is a powerful method for the synthesis of novel materials with well-defined structures such as statistically distributed copolymers, block copolymers, alternating copolymers, crosslinked copolymers, end-group functionalized polymers or graft copolymers to name just a few.¹⁶⁸ It is also known for its versatility, functional-group tolerance and for the preparation of special polymers.¹⁶⁹ In addition, ROMP offers different possibilities for the preparation of dye functionalized polymers for different applications in sensing, bio-imaging and other optoelectronic applications.¹⁷⁰ The easiest way for this is the use dye-functionalized

monomers, e.g. as shown by us in the synthesis of fluorescent polymeric materials using naphthalimide¹⁷¹ or xanthene¹⁷² containing norbornenes.

In this paper, we will investigate how the polymer architecture will influence the TTA efficiency using ROMP as polymerisation technique. In contrast to the work of Boutin, we will introduce both the sensitizer and the emitter via functionalized monomers. This allows the precise placement of both chromophore types in combination with a matrix monomer into defined terpolymer structures. As TTA-chromophore pair we chose the system: Pt(II)meso-tetraphenyltetrabenzoporphyrin (PtTPTBP) represents in combination with diisobutyl 3,9-perylene dicarboxylate, Solvent Green 5,¹⁷³ due to very high molar absorption coefficient of the former and matching energies of the triplet states of both dyes. As PtTPTBP shows reduced solubility due to π - π stacking of the porphyrin rings¹⁷⁴, the benzo moieties were equipped with additional *tert*-butyl groups to increase solubility and this structure was chosen as precursor for the synthesis of the corresponding sensitizer monomer in this study. Both the monomers are depicted in Figure 30.

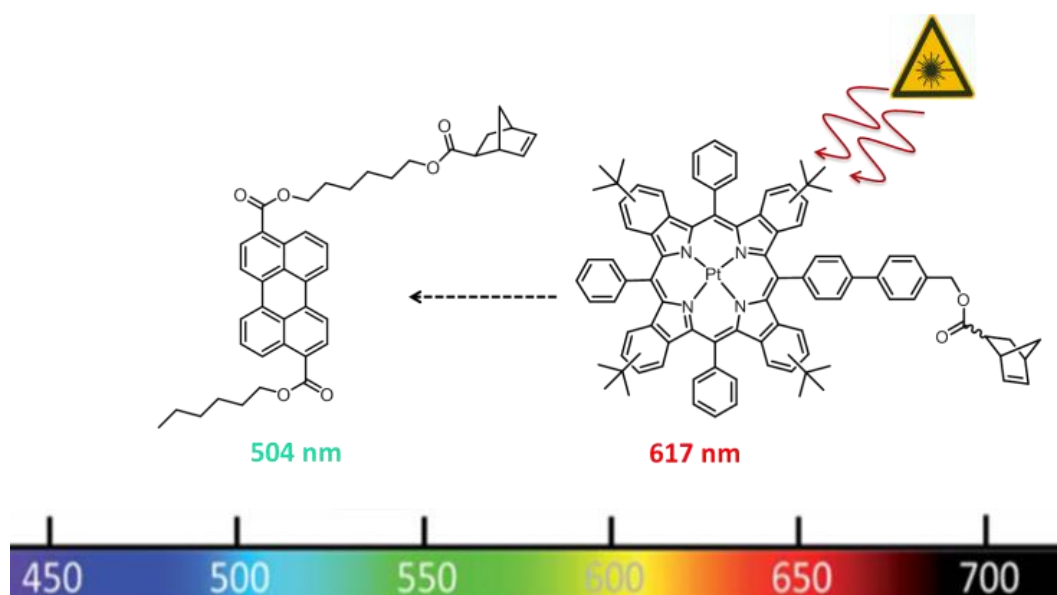


Figure 30 perylene dicarboxylate and Pt(II)meso-tetraphenyltetrabenzoporphyrin functionalized monomers used in this study

Results and Discussion

Synthesis of emitter monomer

To ensure a covalent attachment of the chromophores to the polymer backbone, a norbornene moiety has to be linked to the dyes (cf. Fig. 31).

The synthesis scheme for the preparation of the desired perylene emitter monomer is depicted in Scheme 3. The first reaction step was the saponification of diisobutyl 3,9-perylene dicarboxylate with potassium hydroxide to obtain potassium dicarboxylate (**PDC**). The second step was the unsymmetrical esterification with 1-bromobutane and 6-bromo-1-hexanol in water and tetra-n-butylammonium bromide as a phase transfer catalyst. Due to the differences in polarity of educts and product, the reaction products precipitate out of the reaction mixture and can be isolated by a simple filtration. The unsymmetrical perylene diester (**PDE**) can be separated from the two symmetrical esters via column chromatography. For the last step, **PDE** was added slowly to a solution of 5-norbornene-2-carbonyl chloride, which was prepared before in the same flask by an Diels-Alder reaction of cyclopenta-1,3-diene with 2-propenoyl chloride. The emitter monomer **PDE_{Mon}** was finally isolated using column chromatography.

The photophysical properties of **PDE_{Mon}** will be discussed.

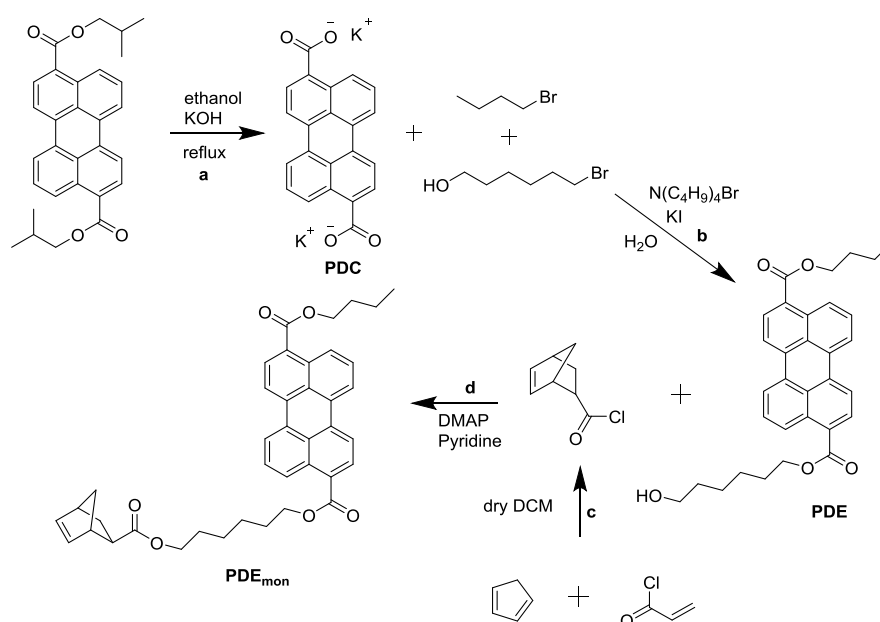


Fig. 31 Synthetic pathway of PDEmonomer

(a: saponification, b: esterification in water with a phase transfer catalyst, c: Diels-Alder reaction, d: Einhorn variation of the Schotten-Baumann reaction)

Synthesis of sensitizer monomer

The overall reaction scheme for the sensitizer monomer **TPTBTBPt_{Mon}** is shown in Fig. 32. There are many techniques for the preparation of porphyrin ligands. The first porphyrin synthesis was done by Rothmund in 1936¹⁷⁵. While today a very common way is based on the work of Adler and Longo¹⁷⁶ it is not the best method for the preparation of benzoporphyrins. Here, the Lindsay method became popular.^{177,178,179} Alternatively, the template condensation allows a preparation of tetrabenzoporphyrins in a single step starting from phthalimide and phenylacetic acid but this method results in a broad mixture of porphyrin byproducts which are very difficult to separate.¹⁸⁰ Recently, Hutter et al.¹⁸¹ demonstrated that substitution of phthalimide with 1,2-dicyanobenzene results in analytically pure benzoporphyrins. This synthetic methodology was adapted to prepare mono-bromo-substituted benzoporphyrin for further modification. Therefore, phenyl acetic acid, Zn-4-bromophenylacetate and 4-(*tert*-butyl)phthalonitrile were melted together to obtain the mono bromo functionalized tetraphenyltetrabutyl porphyrin forming a complex with Zn(II) as coordination centre. The introduction of *tert*-butyl moieties in the benzo core is highly advantageous, since these big sterically demanding moieties prevent noncovalent interactions of the aromatic macrocycles between each other (also known as π - π stacking) which would lead to poor solubility.

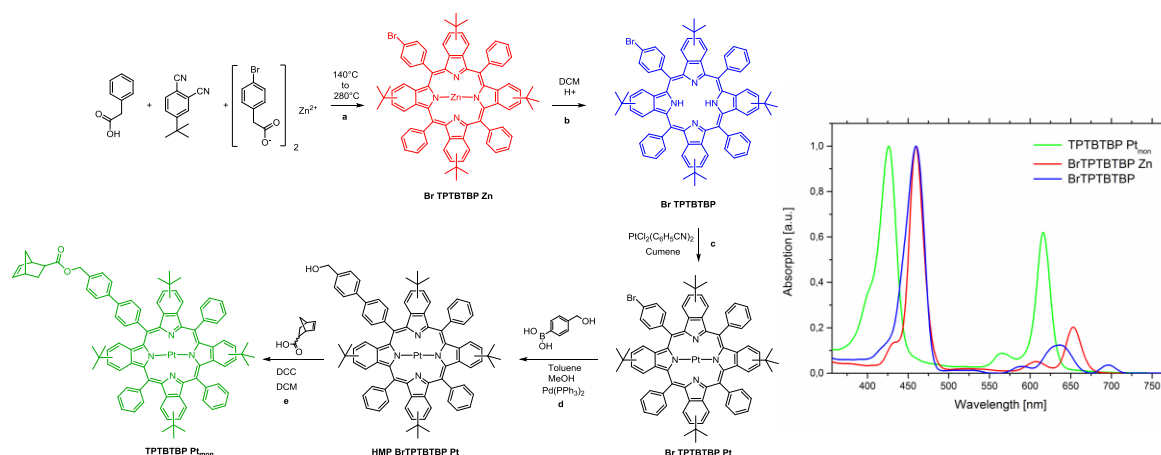


Fig. 32 Synthetic pathway of **TPTBTBPt_{Mon}** (a: melting process, b: demetallation, c: platinumation, d: Suzuki-cross coupling, e: Steglich esterification) right: Normalized absorption spectra of porphyrin derivatives. Absorption peak maximum of the monomer exhibits at 429 nm with a molar absorption coefficient of 155500 M cm^{-1}

However, due to the formation of different side products with similar physical properties, i.e. multiple substituted bromo derivatives, laborious work up steps, such as multiple precipitations and column chromatography are required. The yield for this first step was only 6.4%. However, this is rather good considering that the complete mono-functionalized benzoporphyrin ring system is formed in this single step reaction, instead of at least three steps (e.g. in case of the Lindsey Method). Further advantages are low costs of starting materials and simplicity of the procedure. Although Zn(II) benzoporphyrins can be used as sensitizers for TTA up-conversion,¹⁸² they neither possess high molar absorption coefficients for the Q-band nor show good energy match of the triplet excited state with that of the perylene emitter. Therefore, the Zn(II) complex was converted into the Pt(II) complex (**BrTPTBTBP Pt**) in two steps. First, demetallation of **BrTPTBTBP Zn** is conducted in acidic solution, followed by the metallation with Pt (C₆H₅CN)Cl₂ in the second step. For this reaction step extreme caution is required; as during the metallation the evolving HCl can protonate the remaining free ligand which then precipitates and is removed from the reaction due to low solubility in cumene. Therefore, it is essential to remove the emerging HCl, which was done via an inert gas flow through the reaction mixture. The norborne moiety was introduced via two further reaction steps. A Suzuki-cross coupling of **Pt(BrTPTBTBP** with (4-(hydroxymethyl)phenyl)boronic acid was performed, followed by a Steglich esterification with the corresponding norbornene carboxylic acid in dichloromethane. The Steglich esterification was chosen because of its very mild reaction conditions.¹⁸³ The original Zn porphyrine derivative differs significantly in the photophysical properties from the pure ligand and also from the Pt-containing ring, thus the demetallation and platination steps can be easily followed by measuring the absorption spectra, as shown in Figure 4, right image. The sensitizer monomer **TPTBTBP Pt_{Mon}** shows optical characteristics similar to previously published **TPTBP Pt**¹⁸⁴ and has identical absorption characteristics as the two platinated precursor (**BrTPTPTBP Pt** and HMP **BrTPTPTBP**) but displays a hypsochromic shift compared to the free ligand **BrTPTPTBP** and the Zinc derivative **BrTPTPTBP Zn**. The desired monomer exhibits a global absorption maximum at 429 nm (Soret-band), while the Q-bands appear at 567 and 618 nm. The molar absorption coefficient for the Soret-band is 155 500 M⁻¹ cm⁻¹. Due to the heavy atom effect, Pt-metalloporphyrins allow efficient intersystem crossing into excited triplet states leading to phosphorescence emission. The phosphorescence emission for this compound is in the near infrared area (λ_{max} 775 nm). A comparison of the absorption

and emission properties of **TPTBTBP Pt_{Mon}** with those of **PDE_{Mon}** is displayed in Figure 33. The perylene monomer shows a global absorption maximum at 464 nm, a blue shifted local maximum at 438 nm and a slight shoulder at 413 nm with half of the intensity of the global maxima. The molar absorption coefficient for its global maximum is 29000 M⁻¹ cm⁻¹. The compound is highly fluorescent, emitting green light (λ_{max} 509 nm). Furthermore, it has to be noted that the emission peak area is quite broad. It reaches from 476 to 540 nm with half of the intensity of the global maximum.

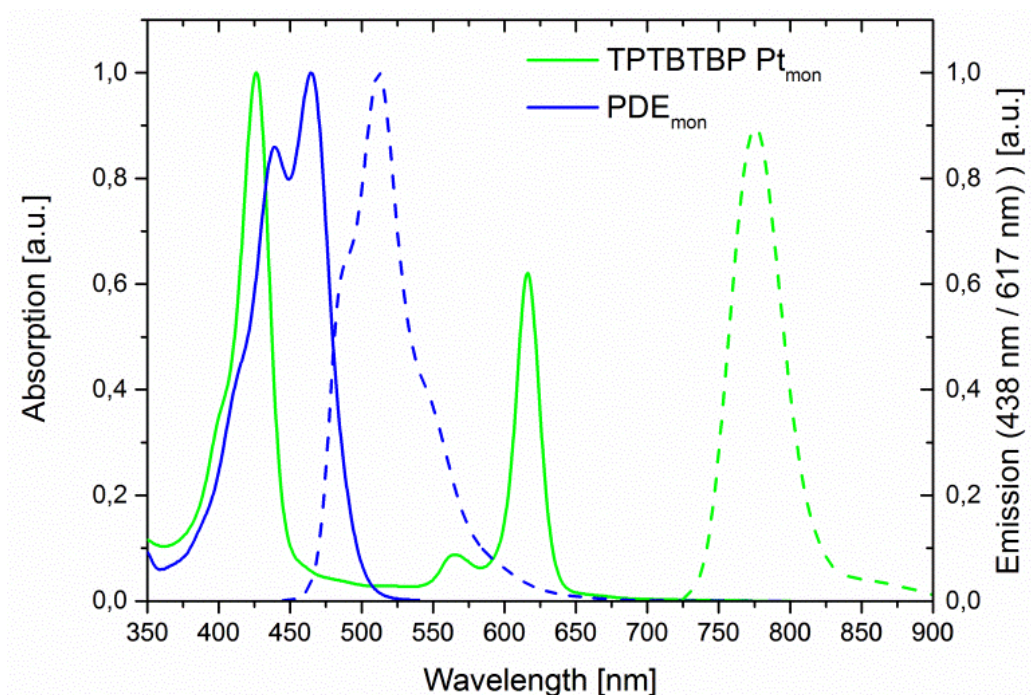


Fig. 33 Normalized absorption (solid lines) and emission (dashed lines) spectra of **PDE_{mon}** and **TPTBTBP Pt_{mon}**. **PDE_{mon}**: Absorption peak maximum exhibits at 464 nm with a molar absorption coefficient of 29200 M⁻¹ cm⁻¹ **TPTBTBP Pt_{mon}**: Absorption peak maximum of the monomer exhibits at 429 nm with a molar absorption coefficient of 155500 M cm⁻¹

Polymers

Five different polymer architectures have been prepared with this two monomers and dimethyl-5-norbornene-2,3-dicarboxylate (**N-DME**) as matrix monomer in order to investigate the influence of the polymer architecture on the triplet-triplet annihilation induced photon up-conversion (Figure 34). Due to its stability and wide functional group tolerance [1,3-Bis(2,4,6-trimethylphenyl)-2-imidazolidinylidene]dichloro(3-phenyl-1H-inden-

1-ylidene)(pyridyl)ruthenium(II) [(SIMes)Ru(py)(Ind)Cl₂] (also known as **M31**) was used for all polymerisations.¹⁸⁵

The ratio of the emitter to sensitizer was fixed to a ratio of 5:1, in accordance to the up-conversion study reported for this chromophore pair (10:1 or 5:1).¹⁷³ The following polymers were prepared: First a random copolymer of the emitter and sensitizers monomers in the ration **PDE_{Mon}:TPTBTBP Pt_{Mon}** of 500:100 has been prepared (polymer **I**). In addition terpolymers (**II** to **V**) were prepared with **N-DME** as matrix monomer and the chromophore system in a ratio **N-DME:PDE_{Mon}:TPTBTBP Pt_{Mon}** of 500:5:1. Polymer **II** is a tri-block copolymer where the matrix block is separating the sensitizer and emitter. Polymer **III** is also a triblock copolymer, but now, emitter and sensitizer are directly linked to each other. Polymer **IV** is a diblock-copolymer, where the emitter is randomly distributed in the matrix block and the sensitizer is added as the second “block”. It has to be noted, that in our series, the average block length of the sensitizer is only 1, thus, that some of the macromolecules will contain more than 1 but others contain no sensitizer molecule. Finally, polymer **V** is a random terpolymer of all three monomers. The GPC and DSC data of all polymers are summarized in Table 5.

Table 5 Overview of Mn, PDI, and the up-conversion quantum yields in anoxic dioxane solution (ϕ). Excitation was done via Diode-Laser at 635 nm (36200 $\mu\text{mol s}^{-1}\text{m}^{-2}$)

| Polymer | M _n (GPC) [g/mol] | PDI | ϕ [%] |
|------------|---------------------------------|------|------------|
| I | 580 000 | 1.63 | 0.06 |
| II | 81 040 | 1.21 | 0.16 |
| III | 81 100 | 1.23 | 0.10 |
| IV | 80 950 | 1.16 | 0.52 |
| V | 81 050 | 1.14 | 2.95 |

The polydispersity index (PDI) of polymer **I** is quite high with a value of 1.6 due to sterical hinderance during polymerisation. The characteristics of polymer **II-V** are very similar. The PDI values are always below 1.23 and all polymers exhibit very similar molar masses of approx. 81 kg/mol.

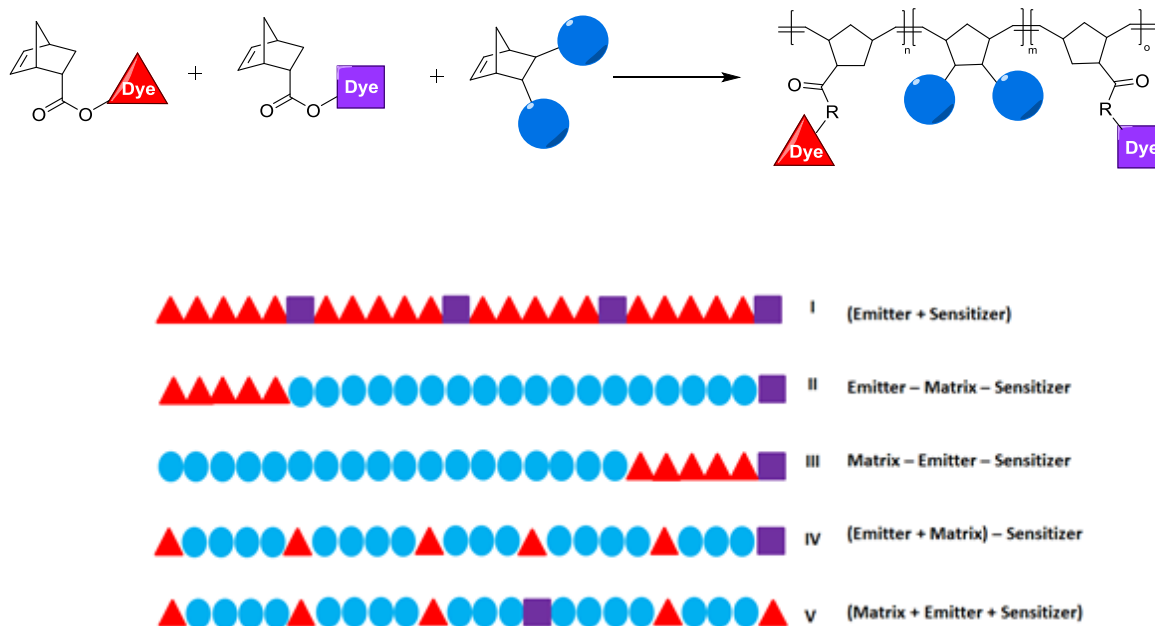


Fig. 34 Overview of different polymer architectures
(red triangles = emitter, purple squares = sensitizer, blue spheres = matrix)

TTA-UC

For the characterization of up-conversion properties of the prepared chromophore functionalized terpolymer systems the concentration of acceptor and annihilator were adjusted to the values used previously for dissolved indicators.¹⁷³ The chosen concentration of PDE_{mon} was $5 \cdot 10^{-4}$ M and $1 \cdot 10^{-4}$ M for $\text{TPTBTBP Pt}_{\text{mon}}$. Hence, the investigated polymer concentration of copolymer I was 0.46 g/L. For polymers II to V the prescribed concentration leads to a copolymer concentration of 10.5 g/L. All measurements were carried out in 1,4-dioxan as solvent. To ensure complete dissolution of the polymer, the mixtures were left in the ultrasonic bath for 30 minutes. Before the measurements were started deoxygenation with argon for 10 minutes is essential to prevent quenching of the triplet states of the sensitizer and annihilator by molecular oxygen.

The polymers have been excited with a 450W Xe lamp ($244 \mu \text{mol s}^{-1} \text{m}^{-2}$) at 617 nm and a 635 nm laser diode ($36200 \mu \text{mol s}^{-1} \text{m}^{-2}$). All TTA spectra show a broad phosphorescence signal with a peak maximum at 775 nm, which means that the triplet-triplet energy transfer can be improved further. The characteristic TTA signal is very broad and occurs between 480 to 550 nm approximately, the maximum appears at 504 nm. The TTA spectrum of polymer V is illustrated below (Fig. 35).

For laser excitation of polymers **IV** and **V**, the up-converted green fluorescence from TTA can be observed with the naked eye. For illustration purposes polymer **II**, **IV** and **V** have been excited with a laser diode at 635 nm ($36200 \mu \text{ mol s}^{-1} \text{ m}^{-2}$) which is shown below in Figure 36.

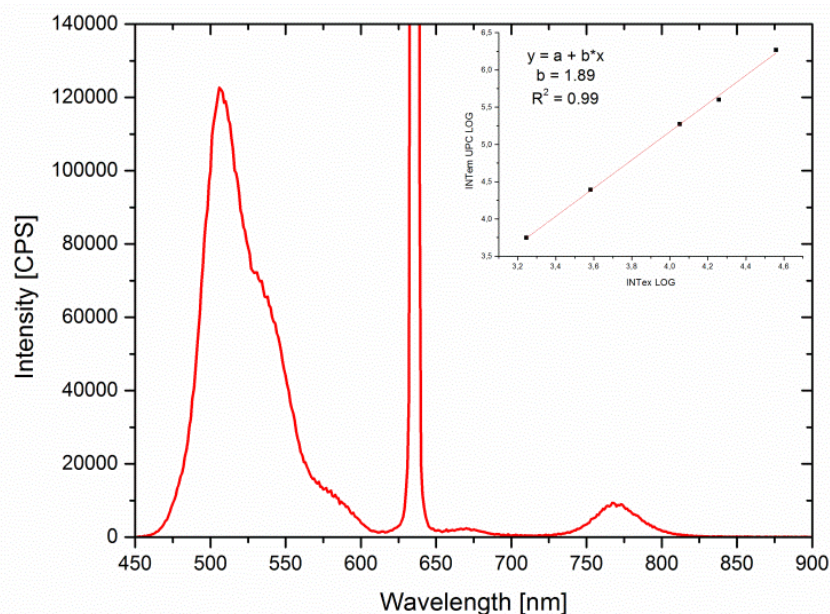


Fig. 35 TTA emission spectrum of polymer **V**. The graph shows up-converted fluorescence where the peak maximum was detected at 509 nm and phosphorescence of the sensitizer which appears at 775 nm. The polymer was dissolved in 1,4-dioxane with a concentration of 10.5 g/L ($C_{\text{emitter}} = 5 * 10^{-4} \text{ M}$, $C_{\text{sensitizer}} = 1 * 10^{-4} \text{ M}$). Excitation wavelength was set at 635 nm with a power density of $36200 \mu \text{ mol s}^{-1} \text{ m}^{-2}$. Light irradiance dependent measurements are shown in the additional window on the right top. The logarithmic plot exhibits a slope of 1.89.

For the estimation of the quantum yields of the delayed up-converted fluorescence a comparison of the peak area of the emission of a polymerized matrix/sensitizer system (ratio of matrix to sensitizer: 500/1) with the TTA polymers was done. Excitation was done in solution via laser. The measurements have been carried out under room temperature. The quantum yield of polymer **I** shows by far the lowest value compared to the other polymers (0.06%). Due to very short distances between the chromophores it is very likely that the chromophores tend to aggregation which results in self-quenching. The next lowest quantum yields were obtained for block-copolymers **II** and **III** ($\phi = 0.16\%$ and $\phi = 0.10\%$); this correlates with the investigations of Xinjun Yu and co-workers.¹⁸⁶ They reported a sharp

maximum of the TTA-UC efficiency as a function of the emitter concentration and the interchromophore distance. Furthermore, they also suggested that self-quenching of the excited singlet state became significant at high dye concentrations. Thus, UC emission is even lower for polymer **III**, where both chromophores are next to each other. Polymer **IV** shows the second highest up-conversion ($\phi = 0.52\%$), since the statistical distribution of the emitter within the polymer chain avoids the previously described undesired effects. The best result by far was achieved with a statistical distribution of all three monomers in Polymer **V** ($\phi = 2.95\%$). As in both polymers, **IV** and **V** one could argue that effects like aggregation or self-quenching have been avoided, the result that there is still a big difference in terms of quantum yield is somehow surprising. The main difference between those two architecture systems is that the sensitizer is fixed to the end of the polymer chain instead of appearing somewhere inside the chain. This leads obviously to a significant decrease of the TTA up-conversion quantum yield. Therefore, it seems that selectively positioning the sensitizer chromophore at the very end of the polymer chain facilitates nonradiative deactivation processes such as self-quenching, collisional quenching, etc.. In contrast, if the sensitizer chromophore is located somewhere within the polymer backbone the probability for efficient triplet-triplet transfer seems to be enhanced. Furthermore, it cannot be argued that every single macromolecule of polymer **IV** has exactly one sensitizer monomer on each end. However in reality they are also statistically distributed, containing polymer chains with zero, one or even two sensitizer units on one end. Hence, it can be suggested that it is easier to transfer the energy of the excited triplet states of the sensitizer intermolecularly instead of intramolecularly. Furthermore, this leads again to self-aggregation and self-quenching effects, which also decrease the quantum yield considerably. An overview of the observed ϕ values is shown in Table 5.

Further investigations of excitation light irradiance dependent up-conversion intensity (stepwise reduction of excitation light intensity using transmission filters: 50%, 30%, 10% and 5%) show a quadratic dependence (see supporting information Fig. 4S – 13S). This is typical for a nonlinear process such as TTA-based up-conversion. The logarithmic plot, for that measurement, exhibits a slope of two. This indicates that the triplet decay pathway is (quasi) first order (phosphorescence, quenching and inter system crossing).¹⁸⁷ Furthermore, this means that all measured ϕ values were below saturation. Hence, all values can be higher if higher excitation irradiance is used. Furthermore, increasing of the concentration of

the polymers by 2-fold did not have much influence on the quantum yields (see Table 3S). All presented ϕ values were obtained with Diode Laser excitation at 635 nm (at power density of $36200 \mu \text{ mol s}^{-1} \text{ m}^{-2}$); in addition we tested the system with a Xe lamp at 617 nm with a two orders of magnitude lower power density compared to the laser. As expected a tremendous decrease of the up-conversion emission was detected. The logarithmic plot of power density to UC emission still exhibits a slope of two (see supporting information).

It can be summarized that the investigated terpolymer systems with covalently bound sensitizer and emitter chromophores can emit up-converted delayed fluorescence by TTA even upon irradiation with relatively low intensity excitation sources. But the threshold for achieving linear dependence of the TTA generated on excitation intensity.

As final test, films of polymer **V** have been prepared via drop casting in order to examine the TTA up-conversion behaviour in the solid state. First preliminary measurements demonstrated that up-conversion by TTA is in principal also possible in a solid, fully covalently bound polymer system, (see Figure 13S). Nevertheless, in the solid state the intensity of up-converted emission is still very weak compared to the phosphorescence emission. This is not surprising considering the strongly restricted mobility of the chromophores and relatively high T_g of the polymers. So for achieving solid state TTA up-conversion further optimization of the polymer structure by e.g. using lower T_g matrix monomer can be pursued.

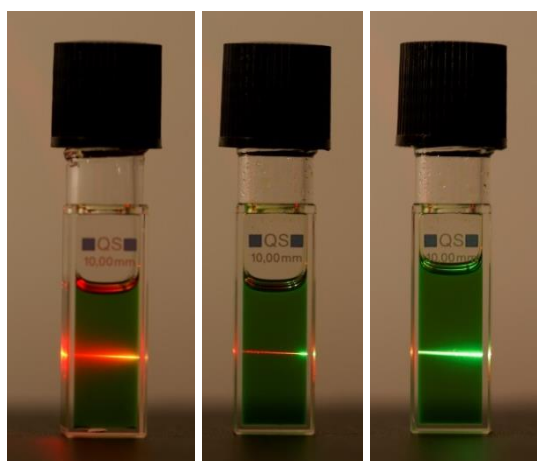


Fig. 36 Photographic images of solutions of polymer II, IV and V (left to right). Polymers have been dissolved in deoxygenated 1,4-dioxane and were excited with an red laser at 635 nm.

Conclusion

We presented the preparation of the first ROMP based dye functionalized polymer which is able to undergo triplet-triplet annihilation. The highest quantum yield was achieved for the macromolecule having statistically distributed sensitizer and annihilator, with a value of $\phi \approx 3\%$, after excitation with a red Laser diode (635 nm). For this compound up-conversion was even detectable with the naked eye, in solutions of 1,4-dioxane. The structural studies of the copolymers showed that an addition of a matrix monomer is essential for an efficient up-conversion; otherwise the chromophores are in too close proximity which results in self-quenching and aggregation, and consequently very low up-conversion efficiency. The same effect is observed for the prepared block-copolymers. Up-conversion for all polymers was below saturation under the given experimental conditions which means that TTA up-conversion efficiency could be further enhanced if a higher light irradiance is used. Due to coiling of the matrix polymer, influences of different polymer matrixes have to be investigated.

Such polymer architectures capable of up-converted light emission and consisting of fully covalently bound chromophores are highly attractive if the functional polymers are used in solution e.g. for certain fluorescence microscopy and imaging techniques. The class of polymeric materials investigated here could e.g. be highly promising for applications in bioimaging (cell imaging, in-vivo imaging, etc.). Therefore they could be easily modified by using water soluble matrix monomer in the ROMP process.

It was also possible to prepare a polymer film which showed solid state up-conversion, albeit with very low efficiency. Optimizations like using a different polymer matrix, varying temperatures while measurement, using different chain lengths, using a higher power density, varying in the thickness of the films, using different manufacturing methods or the addition of different softening agents will be done and presented in further investigations.

Experimental

Materials and Methods

All reagents and solvents (except dry DCM) were purchased from commercial sources (ABCR or Sigma Aldrich) with reagent grade quality and used as received. The dry DCM was obtained through distillation over a drying agent (Na/K) and degassed with nitrogen. Zinc-4-bromophenylacetate was prepared according to Ritveld *et al.*¹⁸⁸ Complex M31 [1. 3-bis (2, 4,

6-trimethylphenyl)-2-imidazolidinylidene] dichloro-(3-phenyl-1H-inden-1-ylidene)(pyridyl) ruthenium (II) for ring opening metathesis polymerisation (ROMP) was obtained from UMICORE AG Co. KG. NMR spectroscopy (^1H , ^{13}C , APT, COSY, HSQC) was performed on a Bruker Avance 300 MHz spectrometer. Deuterated solvents (Chloroform- d , DMSO- d_6 , D_2O) were obtained from Cambridge Isotope Laboratories Inc. and remaining solvent peaks were referenced according to literature.¹⁸⁹ Peak shapes are specified as follows: s (singlet), bs (broad singlet), d (doublet), dd (doublet of doublets), t (triplet), q (quadruplet) and m (multiplet). Silica gel 60 F254 and aluminium oxide 60 F254 on aluminium sheets were used for thin layer chromatography. They were purchased from Merck. Visualization was done under UV light or by dipping into an aqueous solution of KMnO_4 (0.1 wt%). MALDI-TOF mass spectrometry was performed on Micromass TofSpec 2E Time-of-Flight Mass Spectrometer. The instrument was equipped with a nitrogen laser ($\lambda = 337$ nm, operated at a frequency of 5 Hz) and a time lag focusing unit. Ions were generated just above the threshold laser power. Positive ion spectra were recorded in reflection mode with an accelerating voltage of 20 kV. The spectra were externally calibrated with a polyethylene glycol standard. Analysis of data was done with MassLynx-Software V3.5 (Micromass/Waters, Manchester, UK). The best ten shots were averaged to a spectrum. Samples were dissolved in acetone or DCM ($c = 1$ mg/mL). Solutions were mixed in the cap of a microtube in the ratio of 1 μL : 10 μL . The resulting mixture (0.5 μL) was spotted onto the target and allowed to air-dry. The matrix was trans-2-[3-(4-tert-butylphenyl)-2-methyl-2-propenylidene]malononitrile (DCTB). Absorption spectra were recorded on a Shimadzu spectrophotometer UV-1800. The emission was measured on a Hitachi F-7000 fluorescence spectrometer equipped with a red-sensitive photomultiplier R928 from Hamamatsu. For the TTA-measurements a Horiba Fluorolog-3 luminescence spectrometer was used. The ring opening metathesis polymers have been measured in solutions of 1,4-dioxane and excitation was done either with a 635 nm-laser diode or with a 450 W Xenon lamp at 617 nm. The Laser diode was purchased at Roithner Laser (LDM 635/5LJM, 635 nm 5 mW, focusable, 3-5 V, \varnothing 12x30.5 mm). Relative luminescence quantum yields were determined according to Crosby and Demas¹⁹⁰ using platinum(II)tetraphenyltetrabenzoporphyrin ($\phi = 0.51$)¹⁹¹ as reference compound. Gel permeation chromatography (GPC) was used to determine molecular weights and the polydispersity index (PDI). These measurements were carried out, with dichloromethane as solvent, with the following instrument set up: Merck Hitachi L6000 (pump); Polymer

Standards Service, 5 μm grade size (separation columns); Wyatt Technology (refractive index detector). Glass transition temperatures (T_g) have been measured on a Perkin Elmer Differential Scanning Calorimeter (Hyper DSC 8500). Two isothermal cycles were executed and the second scan was analysed. The scanning speed for cooling and heating was 20 $^{\circ}\text{C}/\text{min}$.

Synthetic procedures

Potassium perylene 3,9 – dicarboxylate (PDC) A 250 mL round-bottom flask was filled with diisobutyl perylene-3,9-dicarboxylate (3.00 g, 6.63 mmol) and 100 mL ethanol. After slow addition of KOH (1.49 g, 26.52 mmol), the mixture was heated to reflux for 3 days. A significant change of colour from orange to yellow was noticed and a yellow solid was formed. The solid was filtered off, washed with ethanol and CH_2Cl_2 several times, dried *in vacuo* and was used without further purification. Yield: 93 %. $^1\text{H-NMR}$ (δ , 20 $^{\circ}\text{C}$, D_2O , 300 MHz): 8.19 – 8.13 (m, 4H, H_{pery}), 8.05 – 8.02 (m, 2H, H_{pery}), 7.59 – 7.45 (m, 4H, H_{pery}). UV-Vis (Water): λ_{max} , nm (rel. int.): 420 (0.83), 446 (1).

Butyl – (6-hydroxyhexyl) perylene-3,9-dicarboxylate (PDE)¹⁹² PDC (500 mg, 1.2 mmol), potassium carbonate (696.5 mg, 5.04 mmol), tetra-n-butylammonium bromide (348.2 mg, 1.08 mmol) and potassium iodide (tip of spatula) were filled into a 50 mL two-neck-round-bottom flask and dissolved in 18 mL deionized water. After addition of 1-bromobutane (128.5 μL , 1.2 mmol) and 6-bromo-1-hexanol (157.0 μL , 1.2 mmol) the solution was heated to reflux for 12 hours. An orange solid was formed which was collected via suction filtration. The product was purified by flash chromatography (SiO_2 , CH_2Cl_2 :methanol, 20:1). Yield: 59.2%. $^1\text{H-NMR}$ (δ , 20 $^{\circ}\text{C}$, CDCl_3 , 300 MHz): 8.94 – 8.91 (d, $^3J_{\text{HH}} = 8.4$ Hz, 1H, H_{pery}), 8.85 – 8.83 (d, $^3J_{\text{HH}} = 8.4$ Hz, 1H, H_{pery}), 8.31 – 8.16 (m, 6H, H_{pery}), 7.67 – 7.61 (m, 2H, H_{pery}), 4.45 – 4.41 (t, $^3J_{\text{HH}} = 6.5$ Hz, 4H, $-\text{COO}-\text{CH}_2-$), 3.71 – 3.67 (t, $^3J_{\text{HH}} = 6.3$ Hz, 2H, $-\text{CH}_2-\text{OH}$) 1.87 – 1.43 (m, 12H, H_{alkyl}) 1.05 – 1.01 (t, $^3J_{\text{HH}} = 7.3$ Hz, 3H, $-\text{CH}_2-\text{CH}_3$). UV-Vis (DCM) λ_{max} , nm (rel. in.): 437 (0.84), 464 (1).

3-((6-((bicyclo[2.2.1]hept-5-ene-2-carbonyl)oxy)hexyl) 9-butyl perylene-3,9-dicarboxylate (PDE_{mon}) A 100 mL Schlenk flask was evacuated and purged with nitrogen three times. After addition of 20 mL dry CH_2Cl_2 , freshly distilled cyclopentadiene (131.7 mg, 1.99 mmol) and acryloyl chloride (66.2 mg, 0.73 mmol), the mixture was stirred overnight, obtaining norbornoyl chloride on the next day. PDE (330 mg, 0.67 mmol) was dissolved in 20 mL dry DCM and added dropwise to the previously prepared norbornoyl chloride solution.

Immediately after addition pyridine (72.5 μL , 0.90 mmol) and a catalytic amount of DMAP was added. The reaction mixture was stirred overnight. Afterwards the reaction was quenched with 10 μL distilled water which caused the mixture to turn cloudy. The organic layer was extracted with HCl (5%), sodium bicarbonate (saturated) and dried over sodium sulphate. The crude product was concentrated under reduced pressure and purified via column chromatography (SiO_2 , dichloromethane). Yield: 52%. $^1\text{H-NMR}$ (δ , 20°C, CDCl_3 , 300 MHz): 8.94 – 8.91 (d, $^3J_{\text{HH}} = 8.6$ Hz, 1H, H_{pery}), 8.85 – 8.82 (d, $^3J_{\text{HJ}} = 8.6$ Hz, 1H, H_{pery}), 8.31 – 8.15 (m, 6H, H_{pery}), 7.67 – 7.61 (m, 2H, H_{pery}), 6.14 – 6.08 (m, 2H, H_{nb5} , H_{nb6}), 4.45 – 4.41 (m, 4H, $-\text{COO}-\text{CH}_2-$), 4.14 – 4.10 (t, $^3J_{\text{HH}} = 6.6$ Hz, 2H, $-\text{CH}_2-\text{OH}$), 3.49 (bs, 1H, H_{nb2}), 3.03 (bs, 1H, H_{nb1}), 2.91 (bs, 1H, H_{nb4}), 2.17 (bs, 2H, H_{nb3}), 1.94 – 1.35 (m, 14H, H_{alkyl} , H_{nb7}), 1.05 – 1.01 (t, $^3J_{\text{HH}} = 7.3$ Hz, 3H, $-\text{CH}_2-\text{CH}_3$). $^{13}\text{C-NMR}$ (δ , 20°C, CDCl_3 , 125 MHz): 153.63 (C=O), 138.06, 135.78, 130.85, 130.47, 128.24, 122.10, 121.33, 120.40 (C_{pery}), 65.12, 64.37 ($-\text{COO}-\text{CH}_2-$), 46.64, 46.39, 43.23, 41.65, 30.87, 30.36, 28.68, 25.89, 25.76 (C_{alkyl} , C_{nb}), 19.42 ($-\text{CH}_2-\text{CH}_3$), 13.83 ($-\text{CH}_3$). MALDI: m/z [M⁺] calc. for $\text{C}_{40}\text{H}_{40}\text{O}_6\text{Na}$: 639.2723; found, 639.2746. UV-Vis (DCM) λ_{max} , nm (rel. in.): 438 (0.86), 464 (1). $\lambda_{\text{emission}}$ nm: 509.

Monobromo meso-tetraphenyl tetrabenzo tert-butyl porphyrin Zn (II) (BrTPTBTBP Zn)¹⁸¹
 Phenylacetic acid (17.6 g, 129.3 mmol), Zn-4-bromophenylacetate (7.98 g, 16.2 mmol) and 4-(tert-butyl)phthalonitrile (11.9 g, 64.6 mmol) were mixed and homogenized using a pestle and mortar. Portions of about 1 g each were weighed into 4 ml vials with a stirring bar, compressed with a glass rod and sealed with a metal screw cap. The vials were placed into a preheated metal block and melted at 140°C while the temperature was slowly increased to 280°C. The reaction progress was monitored via UV-Vis spectroscopy and thin layer chromatography. After 40 minutes TLC showed full conversion of the substrates, stirring was stopped and the mixture was cooled down. The mixture was dissolved in EtOH (500 mL) and product was precipitated with dropwise addition of a NaHCO_3 solution (0.3 M, 150 mL). The green precipitate was filtered and dried under reduced pressure. The precipitation was repeated twice. The product was additionally purified by column chromatography (Al_2O_3 , DCM) and dried *in vacuo* obtaining a green solid. Yield: 6.4 %. $^1\text{H-NMR}$ (δ , 20°C, CDCl_3 , 300 MHz): 8.49 – 6.88 (m, 31H, $\text{H}_{\text{porphyrin}}$, H_{Ar}), 1.40 – 1.12 (m, 36H, $(\text{CH}_3)_3$). UV-Vis (acetone) λ_{max} , nm (rel. in.): 460 (1), 606 (0.05), 652 (0.20).

Monobromo meso-tetraphenyltetrabenzotetrabutylporphyrin (BrTPTBTBP) A mixture of BrTPTBTBP Zn (400 mg, 0.32 mmol) and methanesulfonic acid (1.5 mL, 23.1 mmol) was

dissolved in acetone (5 mL). The mixture was stirred for 30 min. and was diluted with DCM (100 mL) afterwards. The organic layer was washed several times with H₂O/ sat. NaHCO₃ (2:1, 100 mL) and dried with Na₂SO₄. The solvent was removed under reduced pressure to obtain a green solid. Yield: 99%. ¹H-NMR (δ, 20°C, CDCl₃, 300 MHz): 8.41– 6.90 (m, 31H, **H_{Porphyrin}**, **H_{Ar}**), 1.36 – 1.13 (m, 36H, (CH₃)₃), -1.4 (bs, 2H, -NH-). UV-Vis (acetone) λ_{max}, nm (rel. in.): 464 (1), 592 (0.05), 642 (0.17), 696 (0.06).

Monobromo meso-tetraphenyl-tetrabenzotetrabutylporphyrin Pt (BrTPTBTBP Pt) [*The precursor Pt (C₆H₅CN)Cl₂ was obtained by stirring PtCl₂ in boiling benzonitrile for one hour and precipitating the resulted product with hexane. The yellow product is filtrated, washed with hexane and dried at 60°C*]¹⁸¹ A three-neck-round bottom flask equipped with a reflux condenser, a dropping funnel and a glass tube to induce nitrogen gas to the reaction mixture was filled with the free porphyrin ligand (550 mg, 0.49 mmol) and dissolved in cumene (200 mL). Pt(C₆H₅CN)₂Cl₂ (562 mg, 1.19 mmol) was suspended in cumene (200 mL) and added in portions of 3 mL over 10 hours. (Due to the formation of HCl gas an appropriate nitrogen flow is very important.) The reaction progress was monitored via UV-Vis spectroscopy and thin layer chromatography. After full conversion the solution was decanted and the solvent was removed under reduced pressure. The product was purified by column chromatography (SiO₂, CH:DCM 3:1) and dried *in vacuo* to obtain a dark green solid. Yield: 49.5%. ¹H-NMR (δ, 20°C, CDCl₃, 300 MHz): 8.45 – 6.80 (m, 31H, **H_{Porphyrin}**, **H_{Ar}**), 1.19 – 1.01 (m, 36H, (CH₃)₃). UV-Vis (acetone) λ_{max}, nm (rel. in.): 426 (1), 564 (0.09), 616 (0.62).

Hydroxymethylphenyl monobromo meso-tetraphenyltetrabenzotetrabutylporphyrin Pt (HMP BrTPTBTBP Pt)¹⁹³ BrTPTBTBP Pt (300 mg, 0.23 mmol) was dissolved in the mixture of toluene (15 mL) and MeOH (5 mL). The solution was deoxygenised for 30 minutes. After deoxygenation, boronic acid (126 mg, 0.23 mmol) and Pd(PPh₃)₄ (16 mg, 1.38•10⁻⁵ mmol) were added. The reaction mixture was stirred under inert atmosphere at 65 °C for 72 hours. The mixture was diluted with DCM (50 mL) and the organic phase was washed with H₂O (25 mL) and sat. NaHSO₄-solution (25 mL) and dried over Na₂SO₄. The solvent was removed under reduced pressure to obtain a green residue. The product was isolated by column chromatography (SiO₂, CH:EtOAc, 10:1) Yield: 37.5 %. ¹H-NMR (δ, 20°C, DMSO-d₆, 300 MHz): 8.35 – 6.81 (m, 35H, **H_{Porphyrin}**, **H_{Ar}**), 5.34 (dd, ³J_{HH} = 8.9, 5.1 Hz, 1H, -OH), 4.62 (d, ³J_{HH} = 5.4 Hz, 2H, CH₂-OH), 1.20 – 1.01 (m, 36H, (CH₃)₃). MALDI: m/z [M⁺] calc. for C₈₃H₇₄N₄O₂:

1338.5535; found, 1338.6215. UV-Vis (acetone) λ_{\max} , nm (rel. in.): 426 (1), 564 (0.09), 616 (0.62).

Meso tetraphenyltetra-benzotetra-butylporphyrin monomer (TPTBTB Pt_{mon})¹⁹⁴ A 50 mL round-bottom flask was filled with HMP BrTPTBTBP Pt (340 mg, $8.22 \cdot 10^{-2}$ mmol), norbornene-2-carboxylic acid (244 mg, 1.62 mmol) and DMAP (catalytic amount) were dissolved in dry, ice-cooled DCM (15 mL). After addition of DCC (342 mg, 1.58 mmol) the reaction was heated to reflux and stirred overnight. On the next day the precipitate was filtered off and the solvent was removed under reduced pressure. The product was purified by column chromatography (SiO₂, CH:DCM 1:1) and dried *in vacuo*. Yield: 88%. ¹H-NMR (δ , 20°C CDCl₃, 300 MHz): 8.46 – 6.90 (m, 35H, H_{porphyrin}, H_{Ar}), 6.28 (dd, ³J_{hh} = 5.1, 3.0 Hz, 1H, H_{nb5}), 6.06 – 5.98 (m, 1H, H_{nb6}), 5.25 (s, 2H, -O-CH₂), 3.35 (bs, 1H, H_{nb2}), 3.11 (dd, ³J_{HH} = 9.2, 3.7 Hz, 1H, H_{nb1}), 2.99 (bs, 1H, H_{nb4}), 2.11 – 1.88 (m, 2H, H_{nb3}), 1.62 – 1.11 (m, 38H, H_{nb7}, -CH₃)₃. MALDI: m/z [M⁺] calc. for C₉₁H₈₂N₄O₂Pt: 1458.6111; found, 1458.769. UV-Vis (acetone) λ_{\max} , nm (rel. in.): 426 (1), 564 (0.09), 616 (0.62).

Dimethyl-5-norbornene-2,3-dicarboxylate (N-DME)¹⁹⁵ Dimethyl fumarate (10.01 g, 0.0679 mol) was dissolved in ice cooled DCM (75 mL). Freshly distilled cyclopentadiene (6.43 mL, 0.0764 mol) was added slowly while the reaction mixture was stirred at room temperature for 15 hours. The solvent was removed under reduced pressure and crystallisation was initiated by adding a seed crystal. After suction filtration the product was dried *in vacuo* and was used without any further purification steps. Yield: 87%. ¹H-NMR (δ , 20°C, CDCl₃, 300 MHz): 6.24 (dd, ³J_{HH} = 5.4, 3.1 Hz, 1H, H_{nb5}), 6.04 (dd, ³J_{HH} = 5.5, 2.7 Hz, 1H, H_{nb6}), 3.68 (s, 3H, -CH₃), 3.61 (s, 3H, -CH₃), 3.34 (t, ³J_{HH} = 4.1 Hz, 1H, H_{nb2}), 3.23 (bs, 1H, H_{nb1}), 3.09 (bs, 1H, H_{nb4}), 2.65 (dd, ³J_{HH} = 4.3, 1.4 Hz, 1H, H_{nb3}), 1.58 (d, ³J_{HH} = 8.8 Hz, 1H, H_{nb7b}), 1.43 (dd, ³J_{HH} = 8.8, 1.5 Hz, 1H, H_{nb7a}).

¹³C-NMR (δ , 20°C, CDCl₃, 75 MHz): 175.08 (C=O), 173.85 (C=O), 137.69, 135.27 (C_{nb5,6}), 52.16 (-CH₃), 51.88 (-CH₃), 47.94, 47.71, 47.40, 47.17, 45.70 (C_{nb1-4}, C_{nb7}).

Polymer preparation

To ensure a precise ratio of monomers and initiator, stock solutions in DCM have been prepared (N-DME: $1.01 \cdot 10^{-1}$ g/L, PDE_{mon}: $1.74 \cdot 10^{-2}$ g/L, TPTBTBP Pt_{mon}: $1.04 \cdot 10^{-2}$ g/L, M31: $2.10 \cdot 10^{-2}$ g/L). The stock solutions have been filled into evacuated 10 mL Schlenk flasks purged with nitrogen and equipped with a stirring bar, amounts of the used monomers are

shown in Table 6. First all stock solutions have been degassed. For polymer **I** 1.153 mL **PDE_{mon}** solution, 0.9096 mL **TPTBRBP Pt_{monomer}** solution and 0.023 mL M31 have been filled, all at once, into the flask. Amounts of stock solutions for polymers **II** to **V** are listed below: 0.9865 mL **N-DME** solution, 0.1666 mL **PDE_{mon}** solution, 0.1335 mL **TPTBTBP Pt_{mon}** solution and 0.339 mL **M31**. For the preparation of block-copolymers **II** and **III** just one monomer was added to the initiator solution. The following monomers have been added not until full conversion of the prior added ones was shown by thin layer chromatography. Polymer **IV** was prepared by adding initiator, matrix and emitter at once and after full conversion of these monomers the sensitizer solution was added. The statistically distributed polymer **V** was prepared by adding the corresponding amount of the stock solutions at once. Yield \approx 90%. $^1\text{H-NMR}$ (δ , 20°C, CDCl_3 , 300 MHz): 5.54 – 5.11 (m, 2H, **CH=CH**), 3.68 – 3.59, 3.32 – 2.62 (m, 4H, **H_{cp1-4}**), 1.98 (bs, 1H, **H_{cp5a}**), 1.47 (bs, 1H, **H_{cp5b}**). $^{13}\text{C-NMR}$ (δ , 20°C, CDCl_3 , 75 MHz): 174.6 – 173.3 (**C=O**), 133.3 – 129.0 (**HC=CH**), 53.4 – 51.4 (**C_{cp1-5}**), 40.8 (**-CH₃**). (**PDE_{mon}** and **TPTBTBP Pt_{mon}** could not be detected, due to the low concentration of chromophores) UV-Vis (DCM) λ_{max} , nm (rel. in.): 428 (1), 567 (0.1), 616 (0.6) Polymers **II** to **V**: PDI: 1.14. M_n : $8.105 \cdot 10^4$ g/mol. T_g : 93,7

Table 6 Used amounts for TTA monomers and initiator

| | | Matrix | PDE_{monomer} | TPTBTBP Pt_{monomer} | M31 |
|----------|-----------------------|---------------|------------------------------|-------------------------------------|-------------------|
| m [mg] | Polymer I | / | 20 | 9.46 | $4.9 \cdot 10^3$ |
| n [mmol] | | / | $3.24 \cdot 10^2$ | $6.49 \cdot 10^3$ | $6.55 \cdot 10^5$ |
| ratio | | / | 500 | 100 | 1 |
| m [mg] | Polymer II - V | 100 | 2.89 | 1.39 | 0.72 |
| n [mmol] | | 0.476 | $4.76 \cdot 10^3$ | $9.52 \cdot 10^4$ | $9.52 \cdot 10^4$ |
| ratio | | 500 | 5 | 1 | 1 |

Acknowledgements

This project "PoTTA" (FFG: 841153) is funded by the Austrian "Klima und Energiefonds" within the program Energy Emission Austria.

Supporting Information

Table S1. Preparation list of the stock solutions

| | M [g/mol] | m [g] | n [mmol] | Solvent [mL] | Stock solution [g/L] |
|-----------------|---------------------|--------------|--------------------|------------------------|-----------------------------|
| <i>Matrix</i> | 210.23 | 0.5068 | 2.4107 | 5.00 | 0.10136 |
| <i>PdE</i> | 616.75 | 0.0347 | 0.0563 | 2.00 | 0.01735 |
| <i>Pt TPTBP</i> | 1458.77 | 0.0208 | 0.0143 | 2.00 | 0.01040 |
| <i>M31</i> | 747.71 | 0.0042 | 0.0056 | 2.00 | 0.00210 |

Table S2. Table for GPC data of the Polymers

| Polymer | Mn [g/mol] | Mw [g/mol] | Mz [g/mol] | PDI |
|----------------|-------------------|-------------------|-------------------|------------|
| I | 580000 | 662080 | 745660 | 1.63 |
| II | 81040 | 92510 | 104190 | 1.21 |
| III | 81100 | 92580 | 104265 | 1.23 |
| IV | 80950 | 92405 | 104070 | 1.16 |
| V | 81050 | 92520 | 104200 | 1.14 |

Table 3S. Comparison of UC quantum yields

| Polymer | Xe Lamp [%] | Laser [%] | Laser (polymer * 2) [%] |
|----------------|--------------------|------------------|------------------------------------|
| I | 0.01 | 0.06 | / |
| II | 0.02 | 0.16 | 0.18 |
| III | 0.01 | 0.10 | 0.08 |
| IV | 0.06 | 0.52 | 0.35 |
| V | 0.43 | 2.95 | 2.80 |

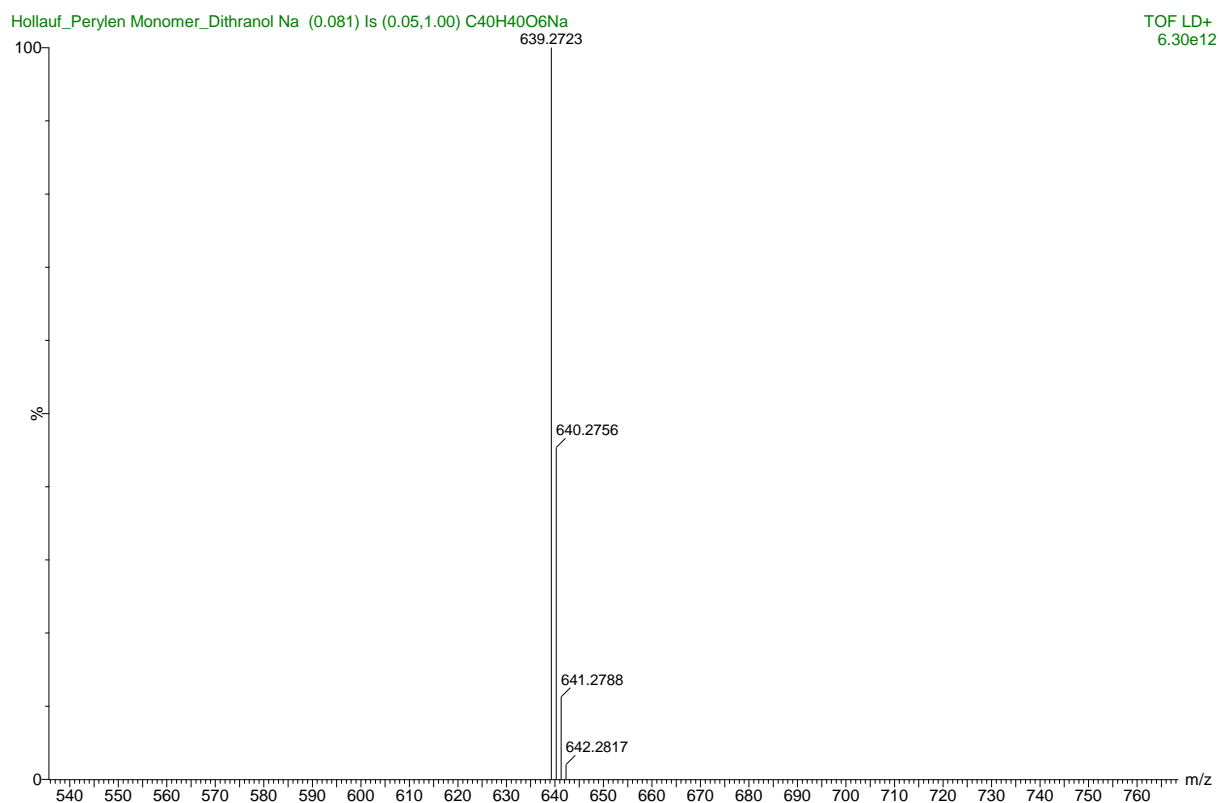
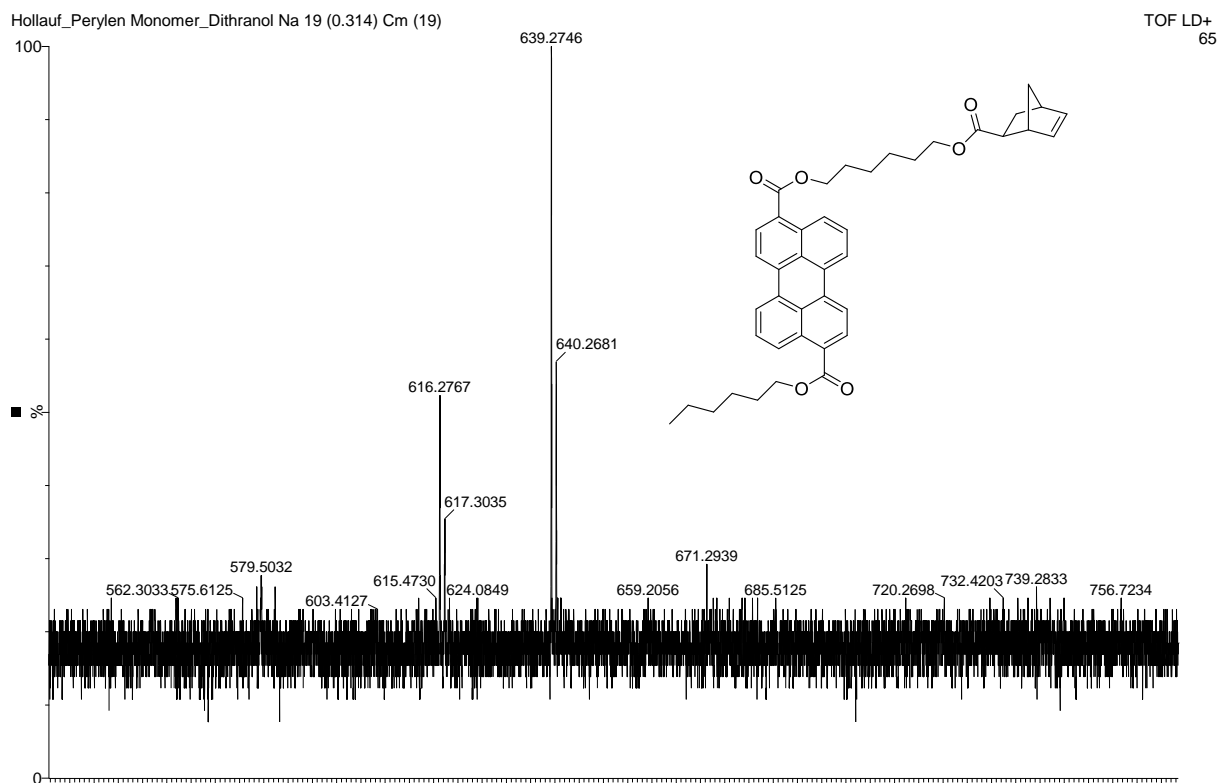


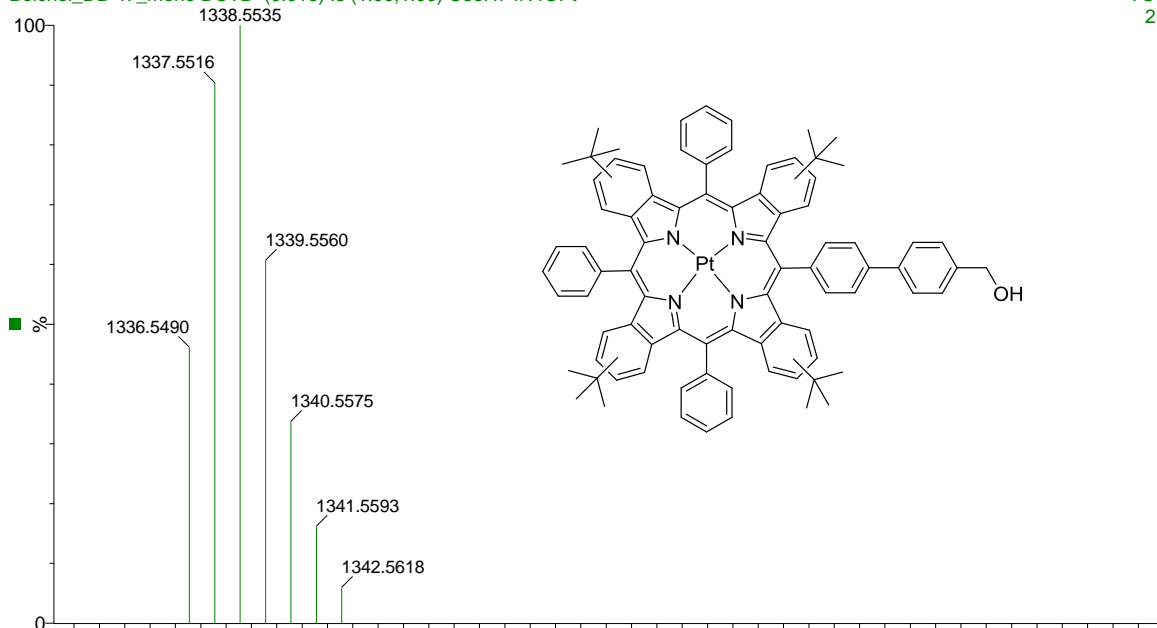
Figure 1S. Mass spectrum (MALDI) of PdE_{monomer}

C₄₀H₄₀O₆Na calculated: 639.2723 g/mol

experimental: 639.2746 m/z

Beichel_DB 47_mono DCTB (0.016) Is (1.00,1.00) C₈₃H₇₄N₄O_{Pt}

TOF LD+
2.80e12



Beichel_DB 47_mono DCTB 44 (0.733) Cn (Cen,3, 70.00, Ht); Sb (99,10.00); Sm (SG, 1x3.00); Cm ((21:26+41:45+65:70))

TOF LD+
719

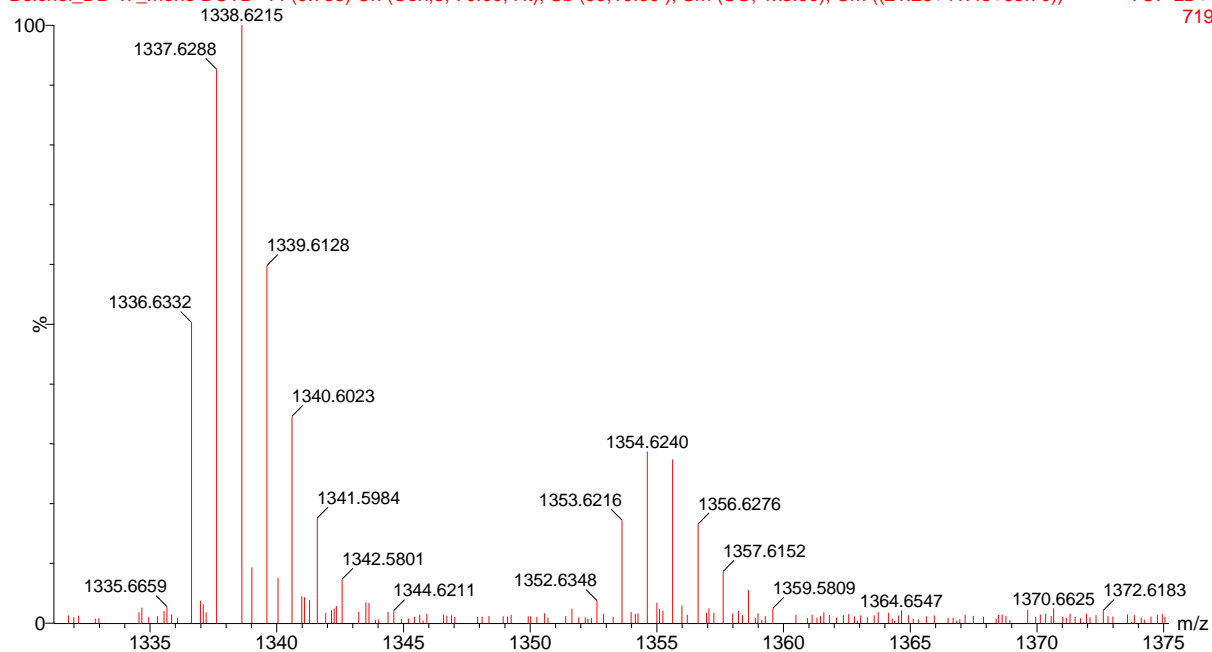


Figure 2S. Mass spectrum (MALDI) of HMP BrTPTBTBP Pt

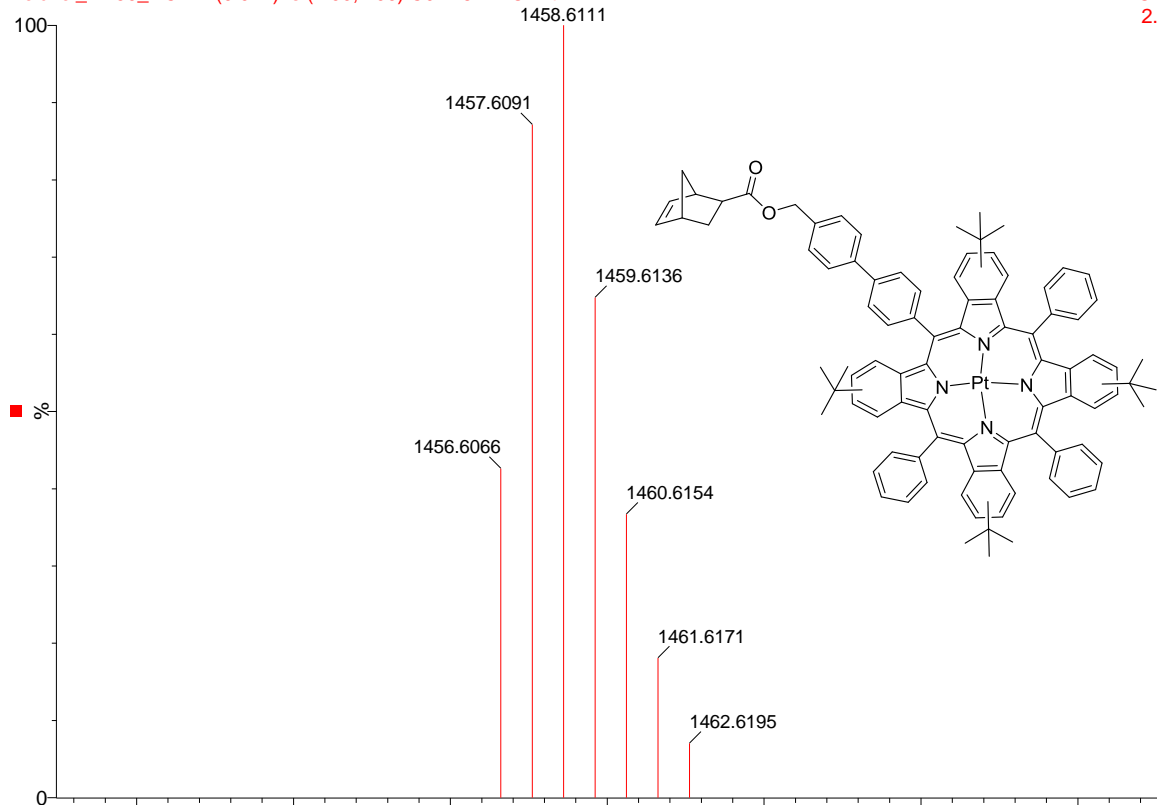
C₈₃H₇₄N₄O

calculated: 1338.5535 g/mol

experimental: 1338.6215 m/z

Beichel_DB50_DCTB (0.014) Is (1.00,1.00) C₉₁H₈₂N₄O₂Pt

TOF LD+
2.77e12



Beichel_DB50_DCTB 26 (0.431) Sb (99,10.00); Sm (SG, 1x3.00); Cm (26:36)

TOF LD+
486

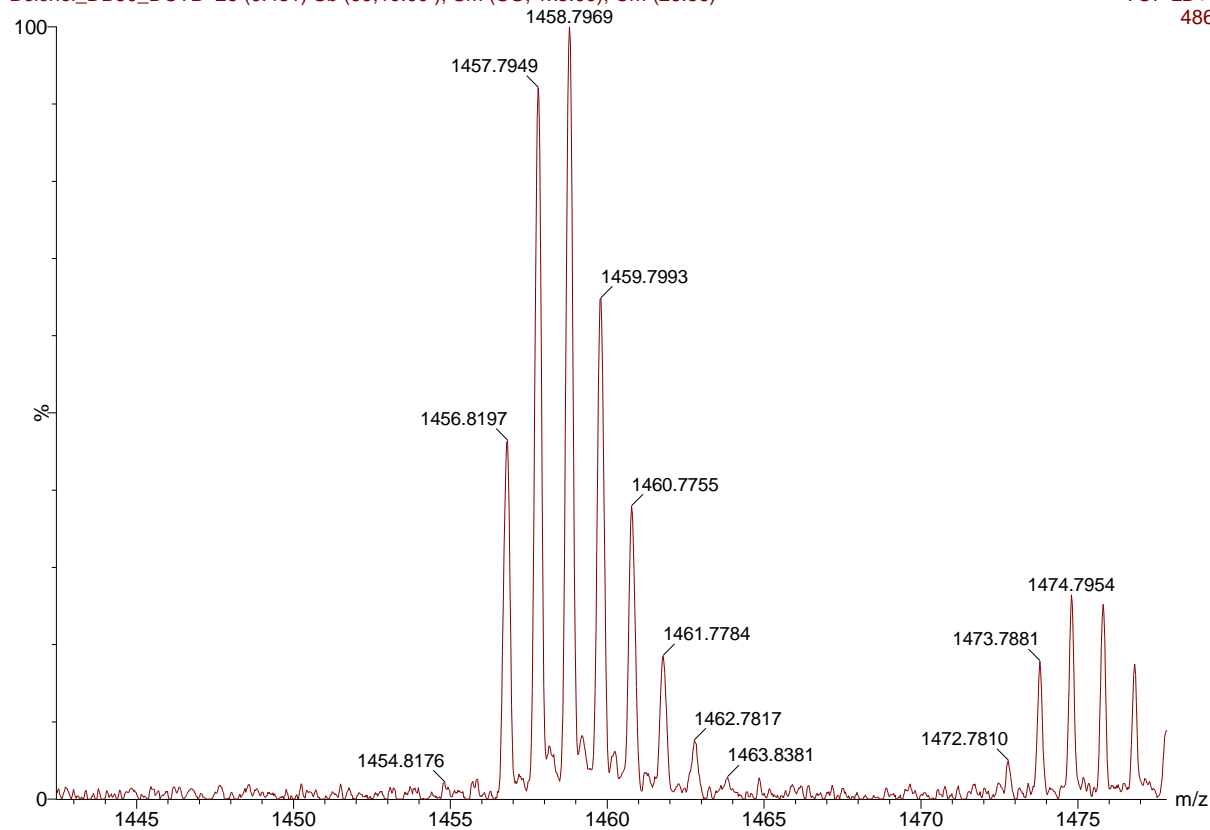


Figure 3S. Mass spectrum (MALDI) of TPTBTBP Pt_{monomer}

C₉₁H₈₂N₄O₂Pt

calculated: 1458.6111

experimental: 1458.769

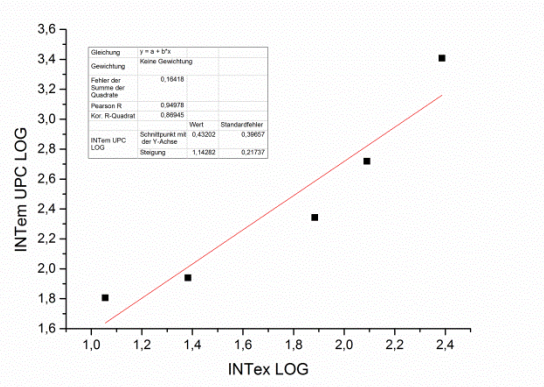
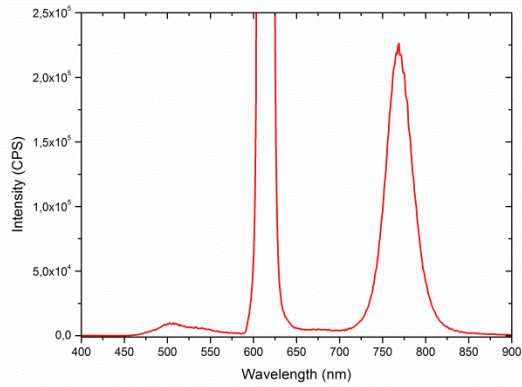


Figure 4S. TTA UC emission Spectra of polymer I and the corresponding double logarithmic plot of energy dependent UC measurements (Xe Lamp)

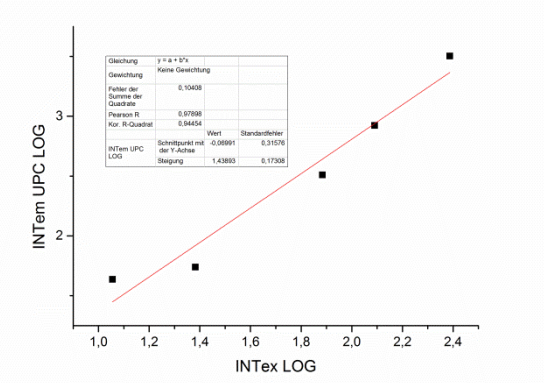
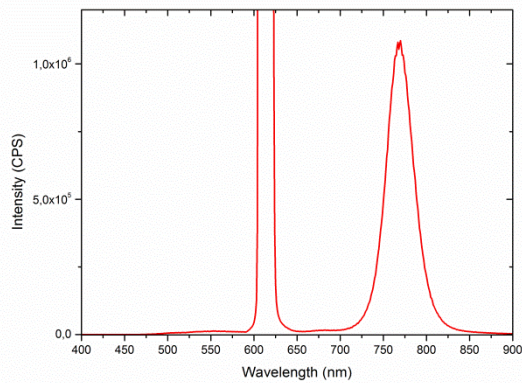


Figure 5S. TTA UC emission Spectra of polymer II and the corresponding double logarithmic plot of energy dependent UC measurements (Xe Lamp)

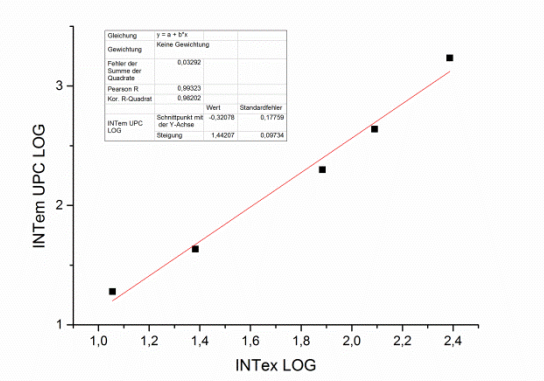
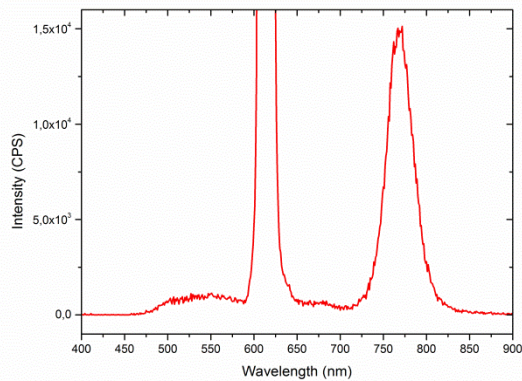


Figure 6S. TTA UC emission Spectra of polymer III and the corresponding double logarithmic plot of energy dependent UC measurements (Xe Lamp)

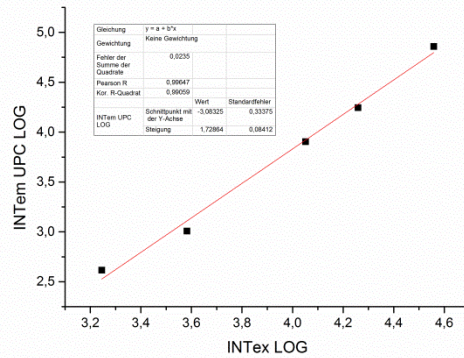
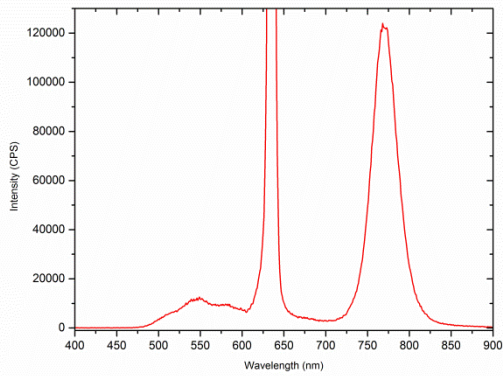


Figure 10S. TTA UC emission Spectra of polymer II and the corresponding double logarithmic plot of energy dependent UC measurements (Laser)

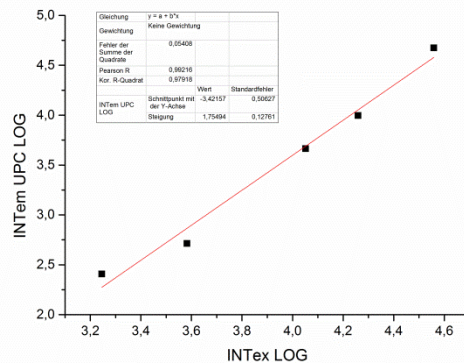
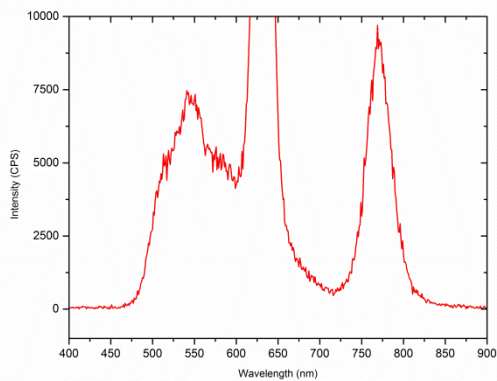


Figure 11S. TTA UC emission Spectra of polymer III and the corresponding double logarithmic plot of energy dependent UC measurements (Laser)

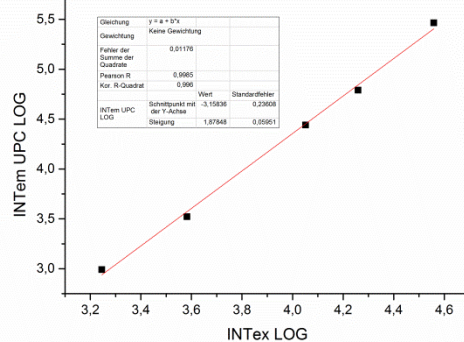
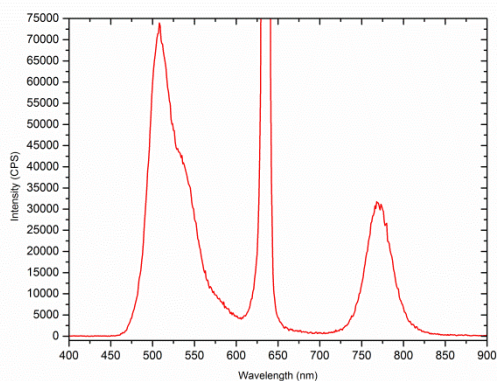


Figure 12S. TTA UC emission Spectra of polymer IV and the corresponding double logarithmic plot of energy dependent UC measurements (Laser)

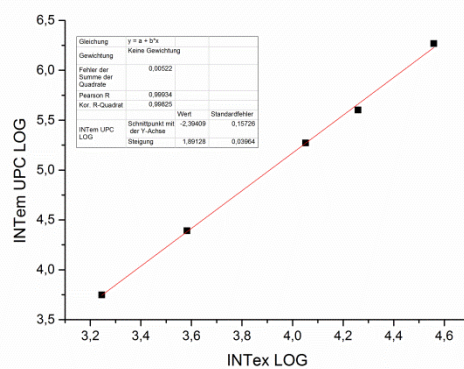
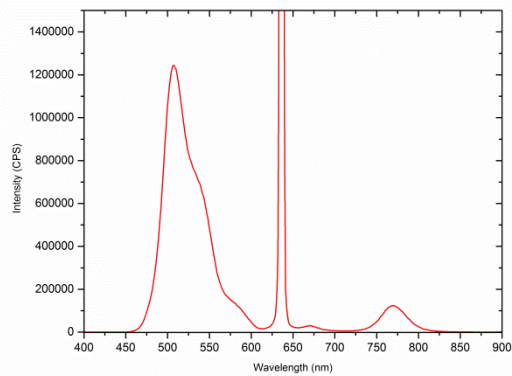


Figure 13S. TTA UC emission Spectra of polymer **V** and the corresponding double logarithmic plot of energy dependent UC measurements (Laser)

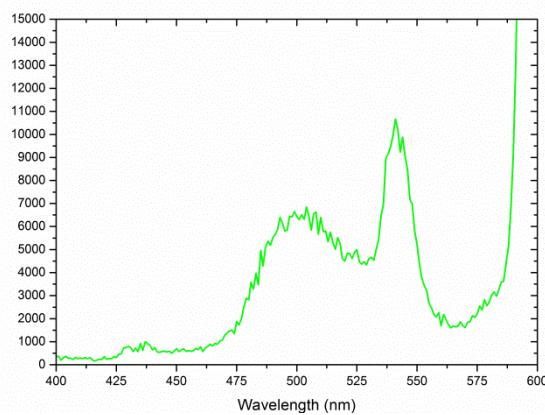
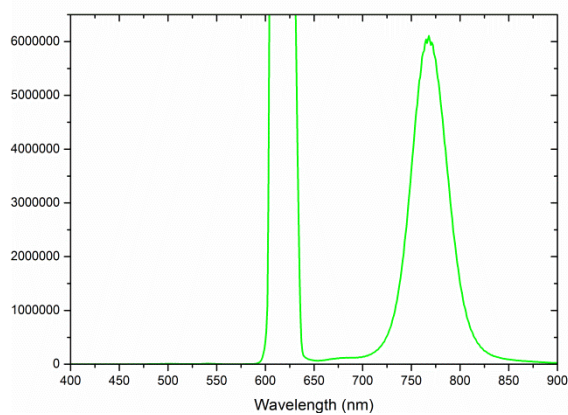


Figure 13S. TTA UC emission Spectra of the drop casted polymer **V**

CHAPTER 4

Chapter 4 was originally published in **Monatshefte für Chemie - Chemical Monthly**.

SYNTHESIS AND CHARACTERIZATION OF NAPHTHALIMIDE-FUNCTIONALIZED POLYNORBORNENES

Manuel Hollauf • Merima Cajlakovič • Martin Tscherner •

Stefan Köstler • Astrid-Caroline Knall • Gregor Trimmel

Monatshefte für Chemie - Chemical Monthly, 2016, 148, 121

DOI: 10.1007/s00706-016-1887-3

© Springer Science + Business Media S. A.



Abstract

Highly fluorescent and photostable (2-Alkyl)-1H-benzo[de]isoquinoline-1,3(2H)-diones with a polymerizable norbornene scaffold have been synthesized and polymerized using ring-opening metathesis polymerization (ROMP). The monomers presented herein could be polymerized in a living fashion, using different comonomers and different monomer ratios. All obtained materials showed good film-forming properties and bright fluorescence caused by the incorporated push-pull chromophores. Additionally, one of the monomers containing a methylpiperazine functionality showed protonation-dependent photoinduced electron transfer which opens up interesting applications for logic gates and sensing.

Introduction

(2-Alkyl)-1H-benzo[de]isoquinoline-1,3(2H)-diones (better known as 1,8-naphthalimides) are highly fluorescent and photostable compounds and are thus in the interest of various fields of technologies. For example, naphthalimides can be used as photoreactive polymerization initiators.¹⁹⁶

Other interesting potential applications of naphthalimide derivatives are related to organic electronics where they are especially applied in organic light emitting diodes (OLED)^{197, 198} or in organic photovoltaics where they are especially applied in non-fullerene acceptors and n-type polymers.¹⁹⁹

By utilizing the readily synthetically available 4-bromonaphthalic anhydride as a starting material, substituents can be straightforwardly introduced²⁰⁰ yielding push-pull chromophores whose photophysical properties strongly depend on the substituents in 6-position. These relationships, together with solvent effects and other effects (e.g. π - π stacking) have been thoroughly studied.^{200, 201, 202, 203}

Furthermore, chemically responsive functionalities which modulate this intramolecular charge transfer can be attached leading to functional fluorophores which can be used for sensors or imaging.^{204, 205, 206, 207, 208, 209, 210, 211, 212} Furthermore, the photophysical properties can be further tuned by e.g. connecting a second dye molecule in 6-position as demonstrated in chitosan based fluorescent materials.²¹³

Similarly, naphthalimide-based systems were applied as fluorescent markers in molecular biology and imaging applications.²¹⁴

Another opportunity of modify naphthalimide-type dyes is to introduce functionalities via the imide nitrogen, which is typically utilized to tune solubility and compatibility or to attach naphthalimides to other materials.^{213, 215} Alternatively, polymerizable groups can be attached to obtain functional polymers. One interesting approach is to molecularly imprint these naphthalimide-decorated materials again leading to optochemical probes.^{216, 217}

All of the above mentioned modification techniques can be combined, leading to photoswitchable, pH sensitive polymers which were used to detect lysosomes in cancer cells.²¹⁸

In many applications, a covalent attachment to the polymer matrix controls the distribution of the dye within the material and prevents the dye from leaching out. In particular, for biological labelling or special sensing applications, the dye molecules should be placed at a distinct location of the polymer chain, thus making a rational polymerisation and labelling process necessary.

Ring-opening metathesis polymerization (ROMP)²¹⁹ has been recognized as a powerful polymerization technique due to its high functional group tolerance. Thus, a number of dye-functionalized polymers have been successfully obtained^{220, 221} while the living nature of ROMP allowed the precise placement of dye molecules in dedicated segments of block copolymers and combining them with stimuli-responsive comonomers.²²² This renders ROMP the method of choice for the synthesis of naphthalimide-functionalized polymers which is the objective of this work. Furthermore, the photophysical properties of the obtained materials are characterized and discussed.

Results and Discussion

The overall reaction scheme is depicted in Scheme 1. Starting from 1,8-naphthalic anhydride, imides are prepared which are typically used for tuning the solubility of the dye or connecting the naphthalimide to a material. We use this imide functionality to link the functional naphthalimide chromophores to a norbornene residue which can be polymerized using ring-opening metathesis polymerization (ROMP). In the resulting 4-substituted 1,8-naphthalimide (formally, 6-substituted (2-alkyl)-1H-benzo[de]isoquinoline-1,3(2H)-dione) system, substituents are introduced in 6-position which can be varied and have a strong influence on the photophysical properties.^{223, 224}

Therefore, we used 4-bromo-1,8-naphthalic anhydride **1** as precursor for all synthesized naphthalimide dyes, which is then converted into 6-bromo-2-(2-hydroxyethyl)-1*H*-benzo[de]isoquinoline-1,3(2*H*)-dione **2**, which can be straightforwardly obtained by refluxing **1** with monoethanolamine in ethanol.²²⁵

Due to the fact that bromine is a good leaving group, 2-(2-Hydroxyethyl)-6-methoxy-1*H*-benzo[de]isoquinoline-1,3(2*H*)-dione(**3**), and 2-(2-Hydroxyethyl)-6-(piperazin-1-yl)-1*H*-benzo[de]isoquinoline-1,3(2*H*)-dione (**4**) could be obtained using quite mild conditions. **4** was then alkylated using paraldehyde in formic acid [226] which led to 2-(2-Hydroxyethyl)-6-(4-methylpiperazin-1-yl)-1*H*-benzo[de]isoquinoline-1,3(2*H*)-dione (**5**), see Figure 37.

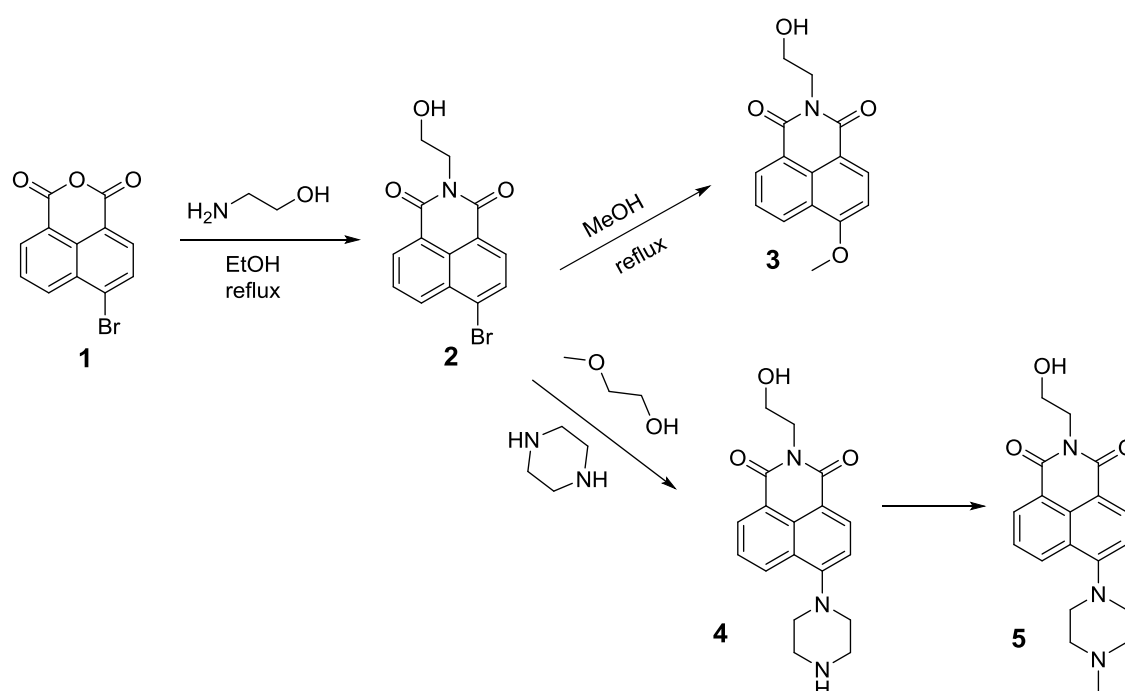


Figure 37 Synthetic pathway for the preparation naphthalimide derivatives

Monomers **6** (2-(6-Bromo-1,3-dioxo-1*H*-benzo[de]isoquinolin-2(3*H*)-yl)ethyl bicyclo[2.2.1]hept-5-ene-2-carboxylate), **7** (2-(6-methoxy-1,3-dioxo-1*H*-benzo[de]isoquinolin-2(3*H*)-yl)ethyl bicyclo[2.2.1]hept-5-ene-2-carboxylate), **8** (2-(1,3-dioxo-6-(piperazin-1-yl)-1*H*-benzo[de]isoquinolin-2(3*H*)-yl)ethyl bicyclo[2.2.1]hept-5-ene-2-carboxylate) and **9** (2-(6-(4-methylpiperazin-1-yl)-1,3-dioxo-1*H*-benzo[de]isoquinolin-2(3*H*)-yl)ethyl bicyclo[2.2.1]hept-5-ene-2-carboxylate)) were obtained by esterification of the hydroxyl moiety of **2-5**, respectively, with 5-norbornene-2-carbonyl chloride using Schotten-Baumann conditions (which is shown in **Figure 38**).

As shown in **Figure 39** and **40**, the substituent at position 6 in the *N*-alkyl-1*H*-benzo[de]isoquinoline-1,3(2*H*)-dione system has a strong influence on the spectroscopic characteristics. Replacing the bromine substituent in **6** with electron-donating substituents creates a donor-acceptor system where the naphthalimide moiety acts as an acceptor, leading to a bathochromic shift which is even more pronounced in the case of amine-substituted **8-10** compared to methoxy-substituted **7**. Furthermore, the UV-Vis absorption of naphthalimide-type chromophores is very sensitive to the conformation of the amino moiety which is reflected in **8** having a significantly red-shifted absorption maximum compared to **9** and **10** which, expectedly show similar UV-Vis spectra.²²⁷ Comparing the absorption maxima of **6-10** in DMSO (see Table 6), the absorption maximum of the methoxy-substituted derivative **7** is red-shifted by about 20 nm which is a consequence of the increased solvent polarity. Notably, this effect was not as pronounced for the amino-substituted compounds **8-10**.

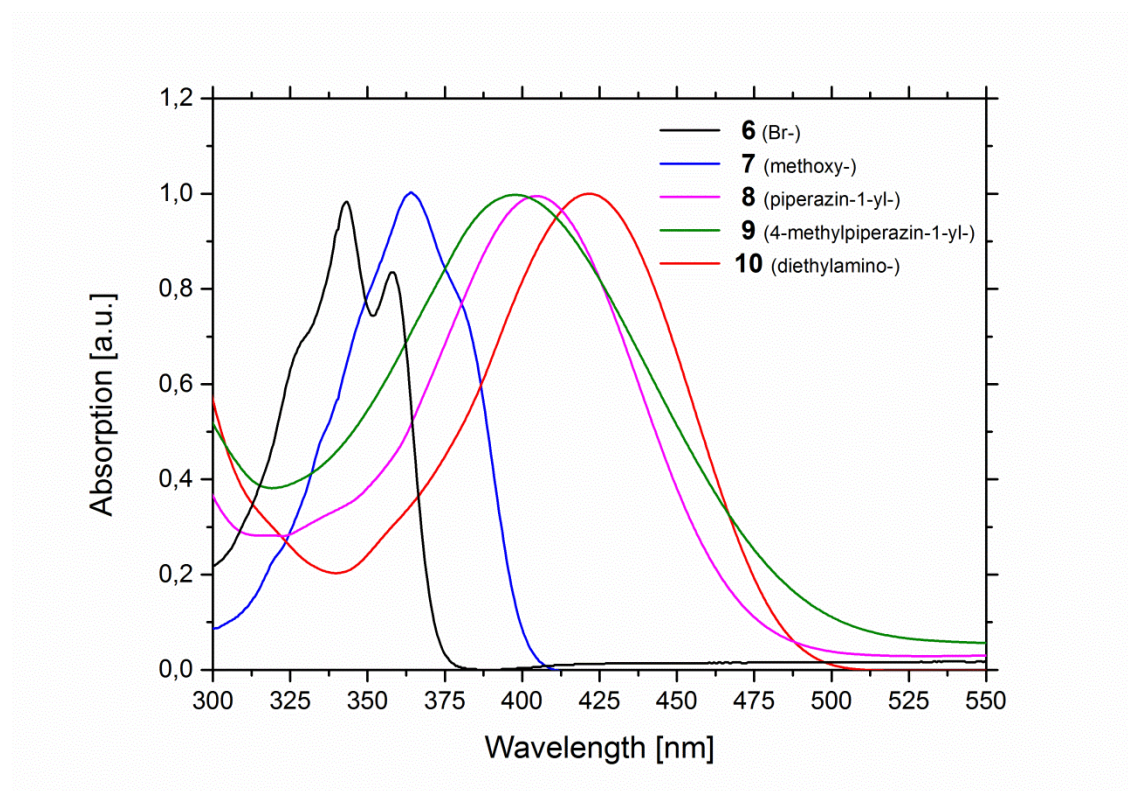


Figure 40 Normalized UV-Vis absorption and fluorescence spectra of monomers **6-10** in dichloromethane

The fluorescence spectra of **6-10** are shown in Figure 4. Due to the heavy bromine substituent, the fluorescence of **6** is quenched via intersystem crossing. **7-10** show intense fluorescence and the Stokes shifts are between 70 and 100 nm for all compounds. The

emission maximum of diethylamino-substituted compound **10** is bathochromically shifted compared to **7-9**, **7** being the emitter with the lowest emission wavelength maximum.

Table 7 Absorption and emission spectra of naphthalimide functionalized monomers in different solvents at room temperature

| | $\lambda_{\max}^{\text{abs}}$ [nm] | | | ϵ [l mol cm ⁻¹] | $\lambda_{\max}^{\text{em}}$ [nm] | |
|----|------------------------------------|------|-----------|--------------------------------------|-----------------------------------|-----------|
| | CH ₂ Cl ₂ | DMSO | thin film | | CH ₂ Cl ₂ | thin film |
| 6 | 343 | 340 | 343 | 21000 | /* | |
| 7 | 363 | 363 | 365 | 13700 | 433 | 424 |
| 8 | 392 | 396 | 407 | 9500 | 505 | 496 |
| 9 | 399 | 402 | 397 | 7400 | 497 | 485 |
| 10 | 422 | 428 | 422 | 6200 | 532 | 509 |

*6 is nonfluorescent

Monomers **7-10** were copolymerized with dimethyl bicyclo[2.2.1]hept-5-ene-2,3-dicarboxylate **11** in different ratios (1/499, 5/495, 10/490, 50/450) using [1,3-bis(2,4,6-trimethylphenyl)-2-imidazolidinylidene]dichloro(3-phenyl-1H-inden-1-ylidene)ruthenium(II) (**M31**) as initiator to yield random copolymers. For the pH-sensitive monomer **9**, additional matrix monomers (bicyclo[2.2.1]hept-5-ene-2,3-diyl)bis(phenylmethanone) (**12**) and 5,6-bis(ethoxymethyl)bicyclo[2.2.1]hept-2-ene (**13**) were selected for copolymerization. An overview of the used matrix monomers is shown in Figure 41.

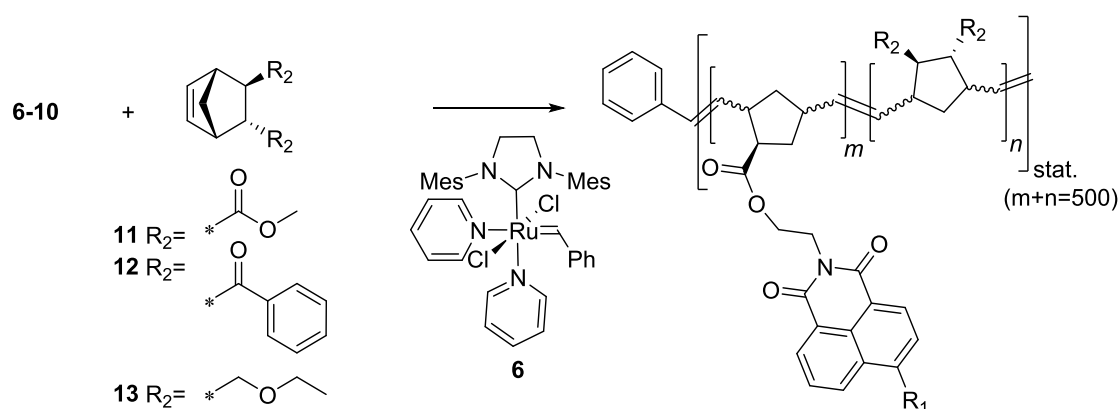


Figure 41 Overview of used matrix monomer and corresponding polymers

Table 8 Polymerization data of random copolymers of dye monomers **8-11** and matrix monomers **10-13**

| polymer | Yield [%] | Mn ^a [kDa] | PDI ^a | Tg [°C] ^b |
|--|-----------|-----------------------|------------------|----------------------|
| co(6 ₁ - 11 ₄₉₉) | 85 | 115.7 | 1.16 | 93.6 |
| co(6 ₅ - 11 ₄₉₅) | 82 | 110.1 | 1.20 | 94.3 |
| co(6 ₁₀ - 11 ₄₉₀) | 80 | 106.5 | 1.40 | 97.5 |
| co(6 ₅₀ - 11 ₄₅₀) | 78 | 96.7 | 1.80 | 97.8 |
| co(7 ₁ - 11 ₄₉₉) | 84 | 118.3 | 1.13 | 95.3 |
| co(7 ₅ - 11 ₄₉₅) | 83 | 105.1 | 1.28 | 95.9 |
| co(7 ₁₀ - 11 ₄₉₀) | 80 | 121.3 | 1.15 | 98.6 |
| co(7 ₅₀ - 11 ₄₅₀) | 82 | 151.7 | 1.40 | 99.1 |
| co(8 ₁ - 11 ₄₉₉) | 75 | 116.4 | 1.55 | 94.8 |
| co(8 ₅ - 11 ₄₉₅) | 68 | 118.7 | 3.04 | 95.3 |
| co(8 ₁₀ - 11 ₄₉₀) | 65 | 59.1 | 2.38 | 96.1 |
| co(9 ₁ - 11 ₄₉₉) | 75 | 49.9 | 1.12 | 94.4 |
| co(9 ₅ - 11 ₄₉₅) | 76 | 49.7 | 1.10 | 95.5 |
| co(9 ₁₀ - 11 ₄₉₀) | 74 | 58.3 | 1.22 | 96.2 |
| co(9 ₅ - 12 ₄₉₅) | 80 | 49.9 | 1.12 | 150.1 |
| co(9 ₅ - 13 ₄₉₅) | 78 | 58.3 | 1.22 | 28.3 |
| co(10 ₁ - 11 ₄₉₉) | 73 | 53.2 | 1.62 | 94.4 |
| co(10 ₅ - 11 ₄₉₅) | 75 | 74.8 | 1.70 | 93.5 |
| co(10 ₁₀ - 11 ₄₉₀) | 70 | 73.5 | 2.00 | 90.9 |

^a determined by size exclusion chromatography (SEC); ^b determined by differential scanning calorimetry (DSC)

Overall, we observed an increasing polydispersity index (PDI) and shorter chain lengths with increasing dye load. This was especially the case for monomer **8** and **10**, however, dye functionalized polymeric materials could be successfully prepared using these monomers. Monomer **9**, was successfully copolymerized with two additional comonomers (**12** and **13**, see Scheme 3) as indicated by similar polydispersity indices for all three copolymers. DSC (differential scanning calorimetry) measurements revealed that the glass transition

temperature (T_g) was expectedly mainly governed by the bulk comonomers. A small increase in T_g was detected for monomers **6-7** with increasing dye load, whereas increased dye loadings for **8-10** led to a decreased T_g .

UV-Vis absorption and photoluminescence spectra ($\lambda_{ex}=395$ nm) of drop-casted films of polymers **co(M₁-11₄₉₉)** (M = 6,7,8,9, or 10) are shown in **Figure 42**. Since **6** and its copolymers did not show any fluorescence, no data is shown for polymer **co(6₁-11₄₉₉)**.

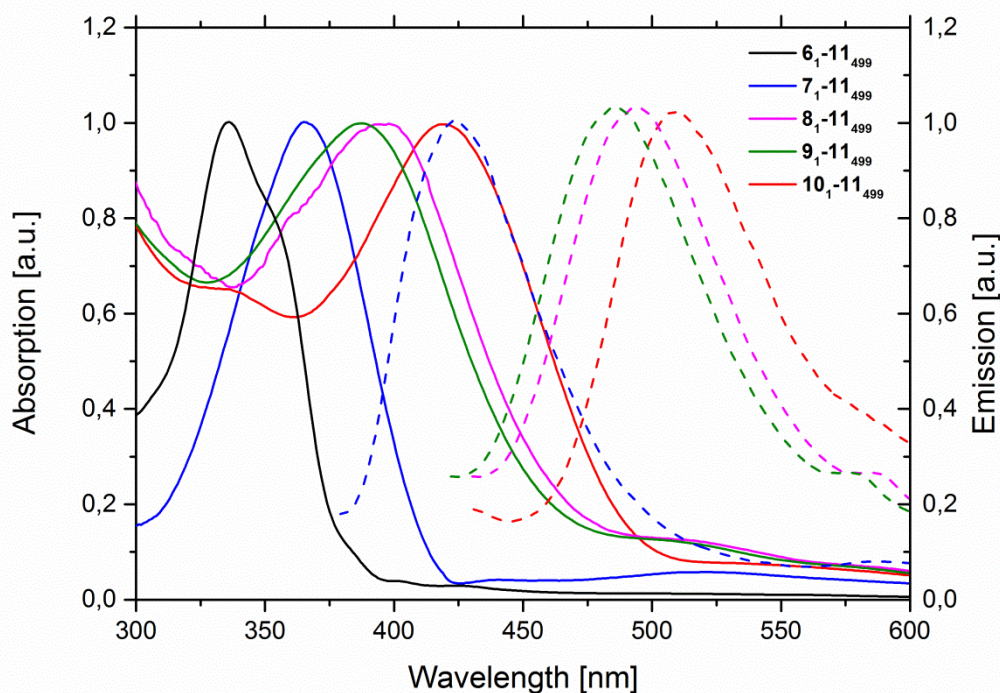


Figure 42 UV-Vis absorption and photoluminescence emission spectra of drop cast polymer films of **co(M₁-11₄₉₉)** M = 6,7,8,9 or 10 (10 mg cm⁻³ in DCM)

The absorption and photoluminescence of the dye functionalized-monomers and the derived polymers are very similar to the free dye molecules **2-6**. Thus, stacking of the naphthalimides which would lead to strong shifts in the photophysical properties is avoided.

In addition, monomer **9** and all related copolymers with this monomer are pH-sensitive due to the possibility to protonate the pyrazine group. In Fig. 5 this is shown by the UV-Vis spectra of the protonated and unprotonated form of the monomer. The absorption maximum of **9** at 402 nm is blue shifted to 375 nm if the pyrazine is protonated, e.g. by the addition of trifluoro acetic acid. This is reversible and addition of a base (e.g. triethylamine) lead to the appearance of the original color. Thus co-polymers with **9** are possible candidates

for polymer based pH-sensing materials, using similar read-out techniques as proposed by Trupp et al. using the same dye functionality in a hydrogel matrix.²²⁹ The possibility to use copolymers of **9** as sensor materials will be exploited in future.

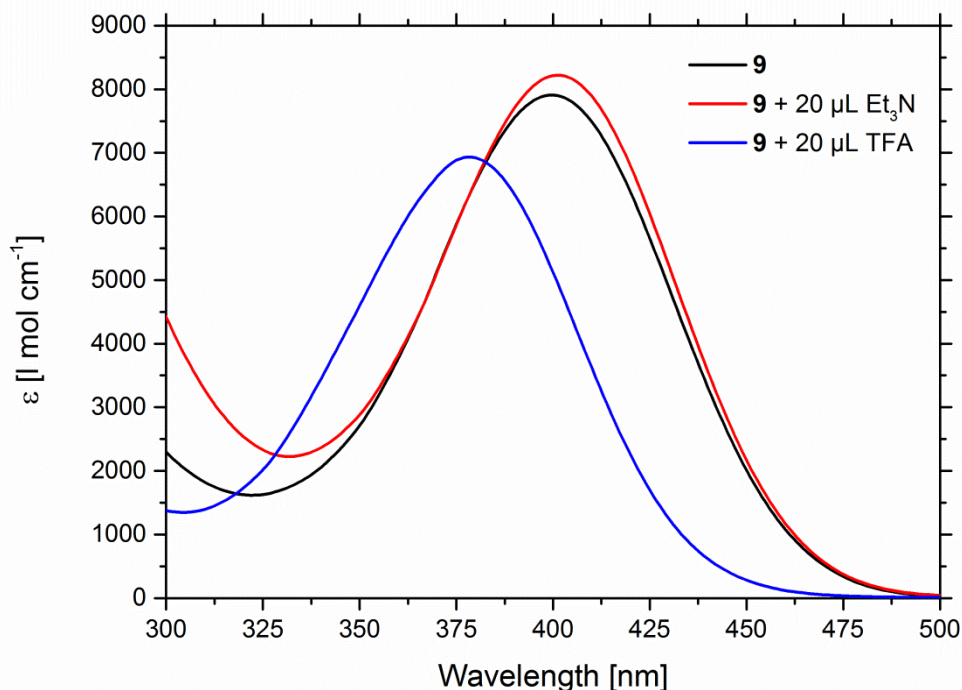


Figure 43 UV-Vis spectra of monomer **9** in DMSO, after addition of trifluoroacetic acid (TFA) and after addition of triethylamine

Conclusion

In this contribution, different naphthalimide dyes have been successfully linked to norbornene monomers and subsequently polymerized with methyl norbornene dicarboxylate to random copolymers. All derivatives could be copolymerized with different norbornene monomers leading to random copolymers. Narrow polydispersity indices and good control of the molecular weight suggest a living polymerization which can be used to design special macromolecular architectures. The optical properties of the monomers and the polymers are practically identical to those of the pure unsubstituted dye molecules showing that π - π stacking of the naphthalimide dyes is avoided.

Experimental

UV-Vis spectroscopy

Absorption spectra were recorded on a Shimadzu spectrophotometer UV-1800. The emission was measured on a Hitachi F-7000 fluorescence spectrometer equipped with a photomultiplier R928 from Hamamatsu. NMR Spectroscopy (^1H , APT) was done on a Bruker Avance 300 MHz spectrometer. Deuterated solvents (Chloroform-d, DMSO-d⁶) were obtained from Cambridge Isotope Laboratories Inc. and remaining peaks were referenced according to literature. Peak shapes are specified as follows: s (singlet), bs (broad singlet), d (doublet), dd (doublet of doublets), t (triplet), q (quadruplet), m (multiplet). Gel permeation chromatography (GPC) was used to determine molecular weights and the polydispersity index (PDI) of the polymers. Measurements were carried out in THF with the following arrangement: a Merck Hitachi L6000 pump, separation columns of Polymer Standards Service (5 μm grade size) and a refractive-index detector from Wyatt Technology. For calibration, polystyrene standards purchased from Polymer Standard Service were used.

The T_g was measured on a PerkinElmer Differential Scanning Calorimeter Hyper DSC 8500. Three isothermal cycles were executed, the second scan was analysed. The scanning speed for cooling and for heating was set to 20°C/min and the temperature range was set between 20 to 200°C. MALDI-TOF mass spectrometry was Performed on a Micromass TofSpec 2E Time-of-Flight Mass Spectrometer. The instrument is equipped with a nitrogen laser (337 nm wavelength operated at a frequency of 5 Hz) and a time lag focusing unit. Ions were generated by irradiation just above the threshold laser power. Positive ion spectra were recorded in reflectron mode applying an accelerating voltage of 20 kV and externally calibrated with a suitable mixture of poly (ethyleneglycol)s (PEG). Analysis of data was done with massLynx-Software V3.5 (Micromass/Waters, Manchester, UK). Samples were dissolved in THF (c=1 mg/mL). Solutions were mixed in the cap of a Microtube in the ratio of μL :10 μL . 0.5 μL of the resulting mixture were spotted onto the target and allowed to air dry.

6-Bromo-2-(2-hydroxyethyl)-1H-benzo[de]isoquinoline-1,3(2H)-dione (**2**, $\text{C}_{14}\text{H}_{10}\text{BrNO}_3$) [320.14] 2.002 g (7.226 mmol, 1.0 equiv.) of **1** were dissolved in 110 cm^3 of EtOH in a 250 cm^3 two-necked round bottom flask equipped with a stirrer bar upon heating to reflux. Then, 467 mm^3 ethanolamine (7.949 mmol, 1.1 equiv.) was added and the reaction mixture was stirred for 4h. The solution turned from pale beige to dark brown and was cooled to room temperature. The formed precipitate was filtered off, washed three times with dest. H_2O /

EtOH and was dried under vacuum. Yield: 1.804 g (78%) of **2** ^1H NMR (300 MHz, DMSO- d_6): δ = 8.60 – 8.52 (m, 2H, H_{naph7} , H_{naph9}), 8.34 – 8.31 (d, 1H, $^3J_{\text{HH}}$ = 8.1 Hz, H_{naph4}), 8.23 – 8.20 (d, 1H, $^3J_{\text{HH}}$ = 8.1 Hz, H_{naph8}), 8.02 – 7.97 (t, $^3J_{\text{HH}}$ = 7.9 Hz 1H, H_{naph5}), 4.83 – 4.79 (t, 1H, $^3J_{\text{HH}}$ = 5.7 Hz, $\text{OH-CH}_2\text{-}$), 4.16 – 4.12 (t, 2H, $^3J_{\text{HH}}$ = 6.4 Hz, $\text{-N-CH}_2\text{-CH}_2\text{-}$), 3.65 – 3.59 (m, 2H, $\text{OH-CH}_2\text{-CH}_2\text{-}$) ppm; ^1H NMR spectra were found to be identical with the ones described in Ref.²²⁵

2-(2-Hydroxyethyl)-6-methoxy-1H-benzo[de]isoquinoline-1,3(2H)-dione (3, C₁₅H₁₃NO₄)

A 50 mL round bottom flask equipped with magnetic stir bar and reflux condenser was filled with 207 mg of **2** (0.64 mmol, 1 equiv.) and potassium hydroxide (45.6 mg, 0.81 mmol, 1.27 equiv.) and dissolved in 5 cm³ MeOH. The reaction mixture was stirred at 70°C for 4 days. The colourless slurry turned pale yellow. After cooling down to room temperature 15 cm³ H₂O was added and stored overnight in the fridge (-5°C). On the next day the yellow precipitate was recovered by filtration and dried in vacuo. Yield: 163.2 mg (94%) of **3**.

^1H NMR (300 MHz, CDCl₃): δ = 8.62 – 8.55 (m, 3H, H_{naph4} , H_{naph7} , H_{naph9}), 7.73 – 7.68 (t, $^3J_{\text{HH}}$ = 7.9 Hz, 1H, H_{naph8}), 7.06 – 7.04 (d, $^3J_{\text{HH}}$ = 8.1 Hz, 1H, H_{naph5}), 4.46 – 4.43 (t, 2H, $^3J_{\text{HH}}$ = 5.0 Hz, $\text{OH-CH}_2\text{-CH}_2\text{-}$), 4.00 – 3.94 (m, 2H, $\text{-N-CH}_2\text{-CH}_2\text{-}$), 2.63 – 2.60 (t, 1H, $^3J_{\text{HH}}$ = 5.5 Hz, $\text{OH-CH}_2\text{-CH}_2\text{-}$) ppm; ^1H NMR spectra were found to be identical with the ones described in Ref.²³⁰

2-(2-Hydroxyethyl)-6-(piperazin-1-yl)-1H-benzo[de]isoquinoline-1,3(2H)-dione (4, C₁₈H₁₉N₃O₃) [205]

2 (1 g, 3.12 mmol, 1 equiv.) and piperazine hexahydrate (1.015 g, 5.23 mmol, 1.68 equiv.) were dissolved in 20 cm³ methoxyethanol, and heated to reflux. After one hour the reaction mixture started to turn yellow and after continuing the reaction overnight, a yellow solid was formed which was isolated via suction filtration and recrystallized from aqueous ethanol. The crude was further purified by column chromatography (DCM:MeOH 4/1). After evaporation of the solvent the product was dried in vacuo. Yield: 485 mg (48%) of **4** ^1H NMR (300 MHz, DMSO- d_6): δ = 8.57 – 8.47 (m, 2H, H_{naph7} , H_{naph9}), 8.43 – 8.40 (d, 1H, $^3J_{\text{HH}}$ = 8.1 Hz, H_{naph4}), 7.85 – 7.81 (t, 1H, H_{naph8}), 7.50 – 7.40 (m, 1H, $^3J_{\text{HH}}$ = 8.1 Hz, H_{naph5}), 4.80 (bs, 1H, -CH-OH), 4.16 – 4.11 (m, 2H, $\text{-N-CH}_2\text{-}$), 3.62 – 3.57 (m, 2H, $\text{-CH}_2\text{-O-}$), 3.38 (s, 8H, $\text{N-(CH}_2\text{)}_2$) ppm; MALDI-TOF MS m/z : Compound **4** calcd. for [C₁₈H₁₉N₃O₃ + H] 326,1505; found, 326,1505.

2-(2-Hydroxyethyl)-6-(4-methylpiperazin-1-yl)-1H-benzo[de]isoquinoline-1,3(2H)-dione (5, C₁₉H₂₁N₃O₃) [205]

Compound **4** (100 mg, 0.31 mmol, 1 equiv.) and paraldehyde (18.6 mg, 0.62 mmol, 2 equiv.) were dissolved in 4 cm³ formic acid (88-91%) and stirred at 80°C overnight. On the next day the solvent was evaporated. The yellow solid was purified via column

chromatography (100:10:1 DCM/MeOH/Et₃N) and dried in vacuo to yield 45 mg (0,13 mmol; 42%) of **5**. ¹H NMR (300 MHz, CDCl₃): δ = 8.88 – 8.76 (m, 2H, H_{naph7}, H_{naph9}), 8.70 – 8.67 (m, 1H, H_{naph4}), 8.02 – 7.94 (m, 1H, H_{naph8}), 7.52 – 7.47 (t, ³J_{HH} = 7.5 Hz, 1H, H_{naph5}), 4.23 – 4.20 (m, 2H, -N-CH₂-), 4.14 (bs, 1H, -CH₂-OH), 4.01 – 3.98 (m, 2H, -CH₂-OH), 3.53 – 3.49 (m, 8H, N-(CH₂)₂-), 2.57 (s, 3H, CH₃) ppm;

2-(6-Bromo-1,3-dioxo-1H-benzo[de]isoquinolin-2(3H)-yl)ethyl bicyclo[2.2.1]hept-5-ene-2-carboxylate (6, C₂₂H₁₈BrNO₄) 799 mg of **2** (2.5 mmol) were dissolved in 30 cm³ DCM and added dropwise to 1.1 equiv. of norbornoyl chloride prepared *in situ* in 25 cm³ dry DCM (from 225 mm³ acryloyl chloride and 625 mm³ (excess) freshly distilled cyclopentadiene). Immediately after the addition 203 mm³ (2.5 mmol, 1 equiv.) pyridine and 20 mg (catalytic amount) of DMAP was added. The reaction mixture was stirred overnight. On the next day the reaction was quenched with 12 cm³ distilled water which caused the mixture to turn cloudy. The organic layer was extracted with HCl (5%), 2% sodium bicarbonate and dried over sodium sulphate. The crude product was concentrated under reduced pressure and purified via column chromatography (100:1 dichloromethane/methanol). Yield: 748.5 mg (63 %) **6**. ¹H NMR (300 MHz, CDCl₃): δ = 8.69 – 8.66 (d, 2H, ³J_{HH} = 8.9 Hz, H_{naph7}), 8.61 – 8.58 (d, 1H, ³J_{HH} = 8.9 Hz, H_{naph9}), 8.45 – 8.42 (d, 1H, ³J_{HH} = 7.8 Hz, H_{naph4}), 8.07 – 8.05 (d, 1H, ³J_{HH} = 7.8 Hz, H_{naph8}), 7.89 – 7.84 (t, 1H, ³J_{HH} = 7.3 Hz, H_{naph5}), 6.08 – 6.05 (d, 1H, ³J_{HH} = 2.8 Hz, H_{nb6}), 5.83 – 5.80 (d, 1H, ³J_{HH} = 2.8 Hz, H_{nb5}), 4.40 – 4.36 (m, 2H, -N-CH₂-CH₂-), 4.50 – 4.46 (m, 2H, -N-CH₂-CH₂-), 3.11 (bs, 1H, H_{nb2}), 2.91 – 2.85 (m, 1H, H_{nb1}), 2.83 (bs, 1H, H_{nb3^b}), 1.89 – 1.80 (m, 1H, H_{nb4}), 1.37 – 1.19 (m, 3H, H_{nb7^{a,b}}, H_{nb3^a}) ppm; No exo-compound was detected due to column chromatography.

¹³C-NMR (75 MHz, CDCl₃): δ = 174.79 (1C, -COO-), 163.70 (2C, O=C-N-C=O), 137.75, 133.55, 132.28, 131.45, 131.28, 130.58, 129.17, 128.25, 123.03, 122.16 (10C, C_{naph}), 132.55, 130.80 (2C, C_{nb5}, C_{nb6}), 61.44 (1C, -COO-CH₂-CH₂-), 49.69 (1C, C_{nb7}), 45.69 (1C, C_{nb1}), 43.33 (1C, C_{nb2}), 42.61 (1C, C_{nb4}), 39.38 (1C, -N-CH₂-CH₂-), 29.41 (1C, C_{nb3}) ppm; MALDI-TOF MS m/z: Compound **6** calcd. for [C₂₂H₁₈BrNO₄ + Na] 465,0331; found, 465,0382.

2-(6-methoxy-1,3-dioxo-1H-benzo[de]isoquinolin-2(3H)-yl)ethyl bicyclo[2.2.1]hept-5-ene-2-carboxylate (7, C₂₃H₂₁NO₅), [391.42] 1.5 g of **3** (5.53 mmol) were dissolved in 200 cm³ DCM and added dropwise to 1.1 equiv. of norbornoyl chloride prepared *in situ* (from 493 mm³ acryloyl chloride and 1.37 cm³ (excess) freshly distilled cyclopentadiene). Immediately after the addition 445 mm³ (5.53 mmol, 1 equiv.) pyridine and 50 mg (catalytic amount) of DMAP

was added. The reaction mixture was stirred overnight. On the next day the reaction was quenched with 35 cm³ distilled water which caused the mixture to turn cloudy. The organic layer was extracted with HCl (5%), 2% sodium bicarbonate and dried over sodium sulphate. The crude product was concentrated under reduced pressure and purified via column chromatography (5:1 cyclohexane/ethyl acetate). Yield: 1.4 g (65 %) **7**. ¹H NMR (300 MHz, CDCl₃): δ = 8.61 – 8.54 (m, 3H, **H_{naph}4**, **H_{naph}7**, **H_{naph}9**), 7.73 – 7.67 (t, 1H, ³J_{HH} = 8.4 Hz, **H_{naph}8**), 7.05 – 7.03 (d, 1H, ³J_{HH} = 8.4 Hz, **H_{naph}5**), 6.07 – 6.04 (m, 1H, **H_{nb}6**), 5.83 – 5.79 (m, 1H, **H_{nb}5**), 4.48 – 4.35 (m, 4H, -N-**CH₂-CH₂-**), 4.13 (s, 3H, -O-**CH₃**), 3.11 (bs, 1H, **H_{nb}2**), 2.93 – 2.87 (m, 1H, **H_{nb}1**) 2.82 (bs, 1H, **H_{nb}3^b**), 1.88 – 1.80 (m, 1H, **H_{nb}4**), 1.38 – 1.32 (m, 2H, **H_{nb}3^a**, **H_{nb}7^a**), 1.21 – 1.18 (d, ³J_{HH} = 8.0 Hz, 1H, **H_{nb}7^b**) ppm; No exo-compound was detected due to column chromatography. ¹³C-NMR (75 MHz, CDCl₃): δ = 174.77 (1C, -COO-), 164.61, 163.98, (2C, O=C-N-C=O), 161.06 137.68, 132.62, 131.80, 128.93, 123.68, 122.36, 115.03, 105.37 (10C, **C_{naph}**), 133.72 (2C, **C_{nb}5**, **C_{nb}6**), 61.60 (1C, -COO-CH₂-CH₂-), 56.36 (1C, -O-CH₃), 49.68 (1C, **C_{nb}7**), 45.71 (1C, **C_{nb}1**), 43.33 (1C, **C_{nb}2**), 42.62 (1C, **C_{nb}4**), 39.00 (1C, -N-CH₂-CH₂-), 29.38(1C, **C_{nb}3**) ppm; MALDI-TOF MS m/z: Compound **7** calcd. for [C₂₃H₂₁NO₅ + Na] 414,3137; found, 414,1042.

2-(6-(diethylamino)-1,3-dioxo-1H-benzo[de]isoquinolin-2(3H)-yl)ethyl bicyclo[2.2.1]hept-5-ene-2-carboxylate (10, C₂₆H₂₈N₂O₄) [432.52] 300 mg (0.96 mmol, 1 equiv.) of **6** were placed in a 50 cm³ round-bottom flask and dissolved in 10 cm³ DMF. After addition of diethylamine (498 mg, 6.81 mmol, 10 equiv.) the mixture was stirred overnight. On the next day the solvent was removed by distillation and the product was purified via column chromatography (10/1 DCM/ MeOH) yielding 240 mg (57 %) of **10**.

¹H NMR (300 MHz, CDCl₃): δ = 8.58 – 8.56 (d, 2H, **H7**, **H9**) 8.50 – 8.44 (t, 1H, ³J_{HH} = 8.5 Hz, **H4**), 7.68 – 7.63 (t, 1H, ³J_{HH} = 8.0 Hz, **H8**), 7.22 – 7.19 (d, 1H, ³J_{HH} = 8.0 Hz, **H5**), 6.07 – 6.05 (m, 1H, **H_{nb}6**), 5.84 – 5.81 (m, 1H, **H_{nb}5**), 4.47 – 4.34 (m, 4H, -N-**CH₂-CH₂-**), 3.45 – 3.38 (m, 4H, -N-**CH₂-CH₃**), 3.10 – 3.05 (m, 2H, **H_{nb}1**, **H_{nb}2**), 2.78 - 2.88 (bs, 1H, **H_{nb}3^b**), 1.87 – 1.80 (m, 1H, **H_{nb}4**), 1.52 – 1.47 (t, 6H, ³J_{HH} = 7.4 Hz, -N-CH₂-CH₃), 1.36 – 1.32 (m, 3H, **H_{nb}3^a**, **H_{nb}7^{a,b}**) ppm; Characteristic exo-signals could not be detected due to peak broadening. ¹³C-NMR (75 MHz, CDCl₃): δ = 174.82 (1C, -COO-), 164.72 (2C, O=C-N-C=O), 137.67, 131.31, 131.21, 125.32, 116.93, (10C, **C_{naph}**), 132,64, 132.33 (2C, **C_{nb}5**, **C_{nb}6**), 61.63 (1C, -COO-CH₂-CH₂-), 49.68 (1C, **C_{nb}7**), 47.40 (2C, -N-CH₂-CH₃), 45.71 (1C, **C_{nb}1**), 43.33 (1C, **C_{nb}2**), 42.48 (1C, **C_{nb}4**), 38.96 (1C, -N-CH₂-CH₂-), 29.39(1C, **C_{nb}3**), 12.37 (2C, -N-CH₂-CH₃) ppm; Characteristic exo-signals could

not be detected due to peak broadening. MALDI-TOF MS m/z: Compound **10** calc. for $[C_{26}H_{28}N_2O_4]$ 432,2049; found, 432,2079.

2-(1,3-dioxo-6-(piperazin-1-yl)-1H-benzo[de]isoquinolin-2(3H)-yl)ethyl bicyclo[2.2.1]hept-5-ene-2-carboxylate (8, $C_{26}H_{27}N_3O_4$) [445.52] 300 mg of **4** (0.92 mmol) were dissolved in 40 cm³ DCM and added dropwise to 1.1 equiv. of norbornoyl chloride prepared *in situ* in 10 cm³ dry DCM (from 99 mm³ acryloyl chloride and 227 mm³ (excess) freshly distilled cyclopentadiene). Immediately after the addition 75 mm³ (0.92 mmol, 1 equiv.) pyridine and 10 mg (catalytic amount) of DMAP was added. The reaction mixture was stirred overnight. After full consumption of the starting material had been detected by TLC (DCM/Methanol 20/1), 12 mL of water were to quench the reaction which was then stirred for 90 minutes. The organic layer was extracted with HCl (5%) and 2% sodium bicarbonate and subsequently dried over sodium sulphate. After solvent removal under reduced pressure, the product was purified using column chromatography (40/1 DCM/MeOH). 269 mg (68%) of **8** were retrieved. ¹H NMR (300 MHz, DMSO-d₆): δ = 8.62 – 8.39 (m, 3H, **H4**, **H7**, **H9**), 7.73 (t, 1H, ³J_{HH} = 7.9 Hz, **H8**), 7.27 – 7.17 (m, 1H, **H5**), 6.11 – 6.08 (m, 1H, **H_{nb}6**), 5.65 – 5.62 (m, 1H, **H_{nb}5**) 4.38 – 4.24 (m, 4H, -N-CH₂-CH₂-O-), 3.33 (bs, 8H, N-(CH₂)₂-(CH₂)₂), 3.09 (bs, 1H, **H_{nb}2**) 3.00 – 2.75 (m, 3H, **H_{nb}1**, **H_{nb}3^b**, **H_{nb}4**), 1.52 – 1.27 (m, 3H, **H_{nb}3^a**, **H_{nb}7^{a,b}**) ppm; Characteristic exo-signals: 6.00 – 5.88 (m, 0.2H). ¹³C-NMR (75 MHz, DMSO-d₆): δ = 173.07 (1C, -COO-), 163.84 (2C, O=C-N-C=O), 155.37, 137.58, 136.78, 132.99, 132.54, 130.02, 126.11 (10C, **C_{naph}**), 131.38 (2C, **C_{nb}5**, **C_{nb}6**), 61.48 (1C, -O-CH₂-CH₂-), 50.01 (1C, **C_{nb}7**) 45.78 (2C, -N-(CH₂)₂-), 45.00 (1C, **C_{nb}1**), 43.21 (2C, -N-(CH₂)₂-), 42.89 (1C, **C_{nb}2**), 42.57 (1C, **C_{nb}4**), 39.01 (-N-CH₂-CH₂-), 31.05 (1C, **C_{nb}3**) ppm;

MALDI-TOF MS m/z: Compound **8** calcd. for $[C_{26}H_{27}N_3O_4]$ 445,2002; found, 445,2049.

2-(6-(4-methylpiperazin-1-yl)-1,3-dioxo-1H-benzo[de]isoquinolin-2(3H)-yl)ethyl bicyclo[2.2.1]hept-5-ene-2-carboxylate (9, $C_{27}H_{29}N_3O_4$) [459.55] published? New 300 mg of **5** (0.884 mmol) were dissolved in 40 cm³ dry DCM and added dropwise to 10 cm³ dry DCM of 1.2 equiv. norbornoyl chloride prepared *in situ* (from 94.3 mm³ acryloyl chloride and 219 mm³ (excess) freshly distilled cyclopentadiene). Immediately after the addition 71.4 mm³ (0.884 mmol, 1 equiv.) pyridine and 20 mg (catalytic amount) of DMAP was added. The reaction mixture was stirred overnight. Progress of the reactions was monitored via TLC (DCM:MeOH 20/1). The esterification was completed on the next day and excess acid chloride was quenched with 7 cm³ water. The organic layer was then extracted with

saturated sodium bicarbonate and dried over sodium sulphate. The drying agent was removed via filtration and the solvent was evaporated to yield a sticky yellow solid which was purified via column chromatography (10/1 DCM/MeOH) yielding 212 mg (52%) of **9**. ¹H NMR (300 MHz, DMSO-d₆): δ = 8.62 – 8.56 (d, 3H, **H4**, **H7**, **H9**), 8.02 – 7.97 (t, 1H, ³J_{HH} = 7.8 Hz, **H8**), 7.53 – 7.50 (d, ³J_{HH} = 7.8 Hz, 1H, **H5**), 6.17 – 6.14 (m, 1H, **H_{nb}6**), 5.85 – 5.81 (m, 1H, **H_{nb}5**), 4.47 (bs, 4H, -N-CH₂-CH₂-O, -), 3.53 (bs, 4H, N-(CH₂)₂-), 3.43 (bs, 3H, -CH₃) 3.17 (bs, 1H, **H_{nb}2**), 2.96 (bs, 1H, **H_{nb}1**) 2.86 – 2.80 (m, 2H, **H_{nb}3^b**, **H_{nb}4**), 2.70 (s, 4H, N-(CH₂)₂-), 1.48 – 1.30 (m, 3H, **H_{nb}3^a**, **H_{nb}7^{a,b}** CH₃-) ppm; Characteristic exo-signals: 6.23 – 6.19 (m, 0.15H), 5.95 – 5.91 (m, 0.15H) ¹³C-NMR (75 MHz, CDCl₃): δ = 173.69 (1C, -COO-), 163.62, 163.03 (2C, O=C-N-C=O), 155.75, 137.43, 129.19, 125.98, 125.25, 115.29, 115.04 (10C, **C_{naph}**), 132.25, 130.65 (2C, **C_{nb}5**, **C_{nb}6**), 60.78 (1C, -COO-CH₂-CH₂-), 54.49 (1C, **C_{nb}7**), 54.59 (2C, -N-(CH₂)₂-), 52.51 (2C, -N-(CH₂)₂-), 48.97 (2C, -N-CH₂-CH₃), 45.72 (1C, **C_{nb}1**), 44.95 (1C, **C_{nb}2**), 42.48 (1C, **C_{nb}4**), 41.83 (1C, -N-CH₃) 28.68(1C, **C_{nb}3**) ppm; MALDI-TOF MS m/z: Compound **9** calcd. for [C₂₇H₂₉N₃O₄ + H⁺] 460,2236; found, 460,2236.

General procedure for ring-opening metathesis polymerization

100 mg (0.48 mmol, 499 equiv.) of matrix monomer **11** and 0.42 mg (9.5×10⁻⁴ mmol, 1 equiv.) of naphthalimide monomer **6** were placed in a Schlenk tube and dissolved in 4 cm³ of absolute dichloromethane. After degassing, the polymerization was initiated with 1.15 mg (0.0016 mmol, 1 equiv.) of modified second-generation Grubbs initiator RuCl₂(H₂IMes)(pyridine)₂(CHPh) (**M31**). TLC (CH₂Cl₂ + EtOAc, 5 + 1, KMnO₄) after 2 h proved full turnover. Subsequently, the polymerization was quenched with 200 mm³ of ethyl vinyl ether and stirred for 1 h at room temperature. Afterwards, the volume of the reaction mixture was reduced to 1 cm³ and the polymer was precipitated by dropwise addition of this solution to 200 cm³ of chilled, vigorously stirred methanol. After having repeated this process twice, the precipitated polymer was collected and dried in vacuo. Copolymerization T7

Yield: ≈ 99%

Open access funding provided by Graz University of Technology. This work is funded by the Austrian “Klima und Energiefonds” within the program Energy Emission Austria “PoTTA” (FFG: 841153). ACK acknowledges the Austrian Science Fund (FWF): T578-N19. The authors

would like to thank Karin Bartl for MS-measurements and Kurt Stubenrauch for carrying out preliminary works on the synthesis of naphthalimide dyes.

CHAPTER 5

NAPHTHALIMIDE – FUNCTIONALIZED POLYNORBORNENES FOR THE USE AS A PH-SENSOR

Introduction

In addition to the investigations of the photo physical properties of the naphthalimide-functionalized polynorbornens, also pH depended spectroscopic measurements had been carried out with methyl-piperazine-naphthalimide as chromophore. Due to the work of de Silva et al.²³¹ it is known that amine functionalized naphthalimides show a tremendous change in these properties in dependency of different pH values. Therefore, methyl-piperazine-naphthalimide was copolymerized with a water soluble norbornene matrix monomer. Ring opening metathesis polymerization was again used as method of choice due to the high functional group tolerance and also already existing norbornene moieties. The previously prepared naphthalimide derivative responds to different proton concentration because the lone pair of the amino group is able to covalently bind protons, forming a quaterization of the amine, which then results in the elimination of charge transfer or photo-induced electron transfer (PET). The photo-induced transfer is a process that describes a transfer of excited electrons from a donor to an acceptor. Due to this process a charge separation is generated, which means that a redox reaction takes place in an excited state. Therefore, protonation of that compound will “switch off” the PET path and recover the fluorescence of the fluorophore.²³² Hence, the spectral properties as a function of pH values were investigated. A schematic illustration of that effect is shown below in Figure 44.

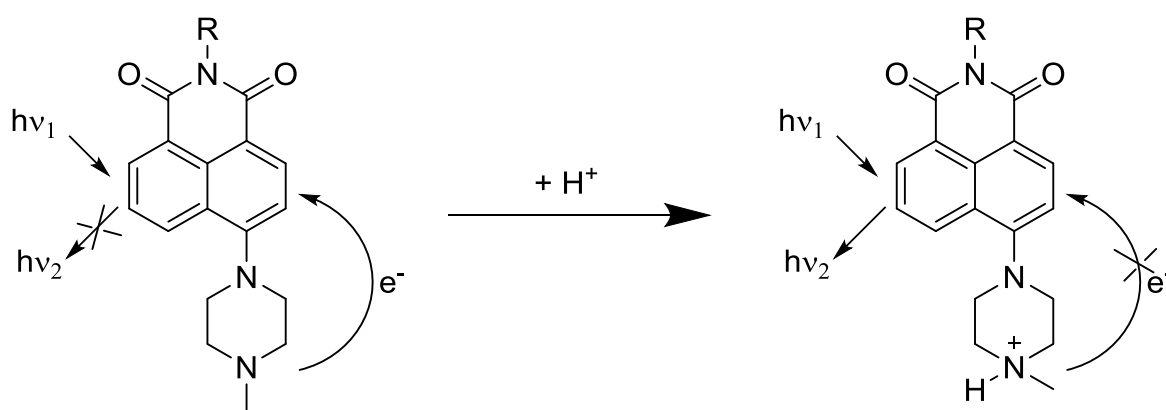


Figure 44 Deprotonated compound undergoes photo-induced electron transfer which quenches the fluorescence (left), protonated compound has no electron left for the PET effect and therefore show fluorescence (right)

These model substances are constructed in the form of donor-spacer-fluorophore, in which the tertiary amine is selected as the donor the piperazine moiety serves as spacer and the naphthalimide is the fluorophore.

Results and Discussion

The preparation of 2-(6-(4-methylpiperazin-1-yl)-1,3-dioxo-1H-benzo[de]isoquinolin-2(3H)-yl)ethyl which will be used as pH sensor is described in chapter 4.

For the preparation of the water soluble norbornene monomer the Einhorn variation of the Schotten-Baumann reaction was used for the esterification of 5-Norbornene-2,3-dicarbonyl chloride with two equivalents of triethylene glycol monomethyl ether. With those two norbornene monomers a statistically distributed copolymer with a chain length of 500 was prepared via ROMP. The Synthetic pathway for the preparation of the matrix monomer and the corresponding polymer is shown in Figure 45.

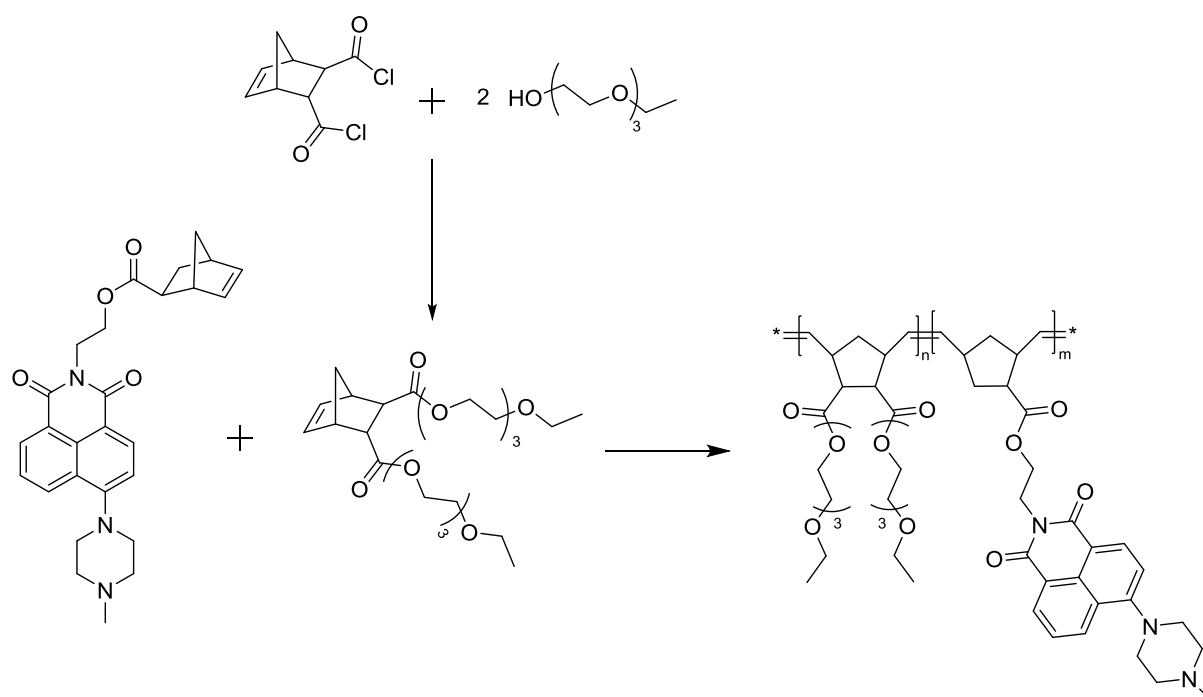


Figure 45 Synthetic pathway for the preparation of the pH sensor

The ratio of matrix to chromophore was set to 100 to 1. The polymerization was done in dry DCM with M31 as initiator and ethyl vinyl ether was used as termination reagent. In contrast to other norbornene monomers where the polymerization was finished after 60 minutes, these polymers were usually stirred over night and were also heated to 35°C. After

GPC measurements a polydispersity index of 1.05 was obtained and the polymer has an average molecular weight of 447 kDa. The theoretical molecular weight should exhibit with a value of 501 kDa, hence the actual chain length is 89 units long. The obtained polymer is a yellow-green highly viscose oil with a glass transition temperature of 21.9°C. For the photo physical measurements 1 mL of the aqueous polymer solution with a concentration of 5g/ L was mixed with 1 mL of an aqueous phosphate buffer. For the preparation of the phosphate buffer three aqueous solutions (0.1 M H₃PO₄, 0.1 M KH₂PO₄ and 0.1 M K₂HPO₄ solution) have been prepared and mixed in different ratios and were adjusted with an pH-meter to obtain 14 different buffer solutions, thus 14 different pH values were tested. The range of the buffer solutions reaches from very acidic with a value of 1.3 to highly basic media with a value of 10.7. The emission spectra of all pH sensitive polymers show a very broad peak with their peak maximum at 528 nm and were excited at 400 nm. The highest emission intensity was detected with a pH value of 4.2. Lower pH values almost show no influence on the brightness of the chromophore emission. A comparison of the pH depended emission spectra is shown in Figure 46.

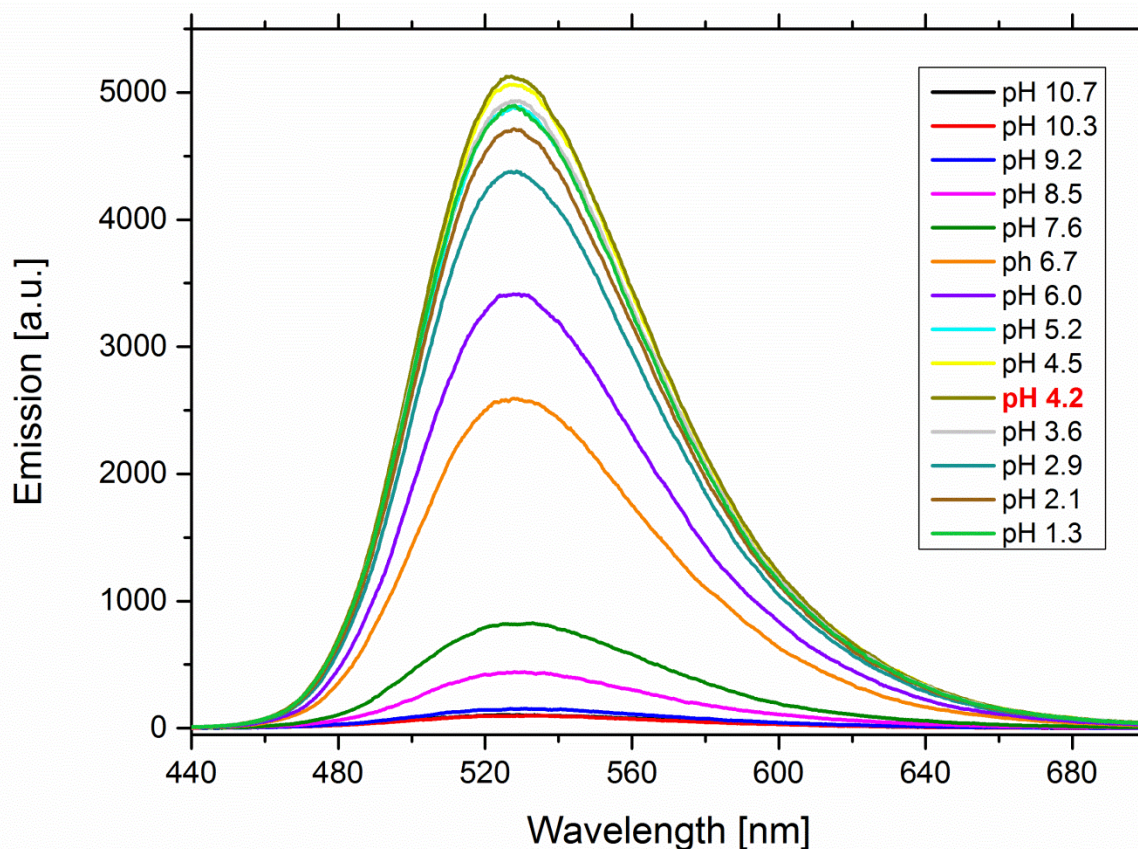


Figure 46 Comparison of the pH depended emission spectra

The following figure 47 shows a comparison of the emission intensity at 528 nm with different pH values. In that figure it clearly can be seen that the highest intensity was achieved with a pH value of 4.2 and immediately starts to decrease drastically after a value of 5.2. The emission is almost vanished within slightly basic solutions. The pH value of 7.6 decreases the emission intensity to one fifth compared to the maximum intensity at a pH value of 4.2. Almost no emission signals were detected with a pH Value of 8.5 or higher. Figure 48 shows a photographic illustration of the dye-functionalized polymer in different phosphate buffer solutions. That picture clearly illustrates that a rapid emission decrease occurred with a pH value of 6.0. With a pH value of 8.5 and higher almost no detection of the emission by naked eye was possible anymore.

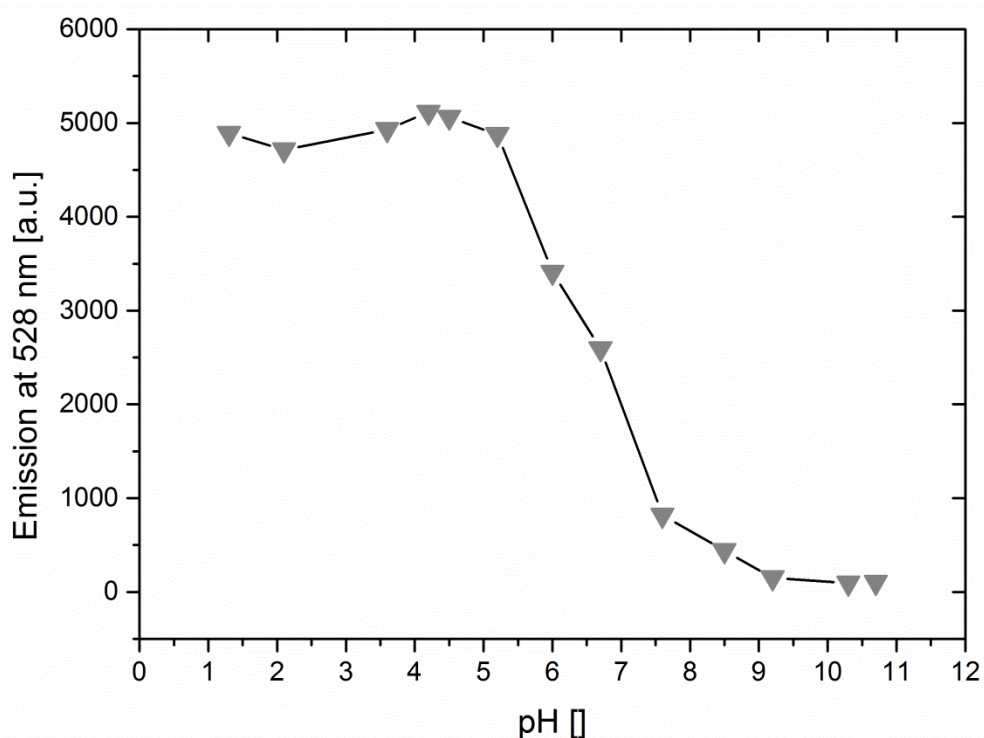


Figure 47 Comparison of the pH depended emission spectra at 528 nm

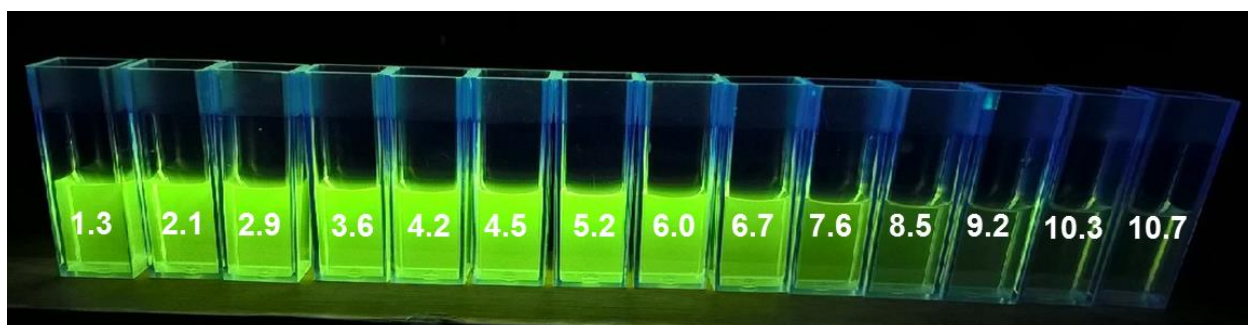


Figure 48 Photographic illustration of polymer solutions with different pH values (white numbers) excited at 365 nm

The same solutions had been used for the absorption measurements. The peak maximum exhibits at a wavelength of 389 nm and shows a bathochromic shift at higher pH values which goes up to 406 nm. This is due to changes in polarity caused by different proton concentrations.²³³ Furthermore, a tremendous decrease of intensity is noted within basic solutions. A comparison of the absorption spectra with different pH values and a comparison of the absorption intensity at 400 nm with different pH values is shown below in Figure 49.

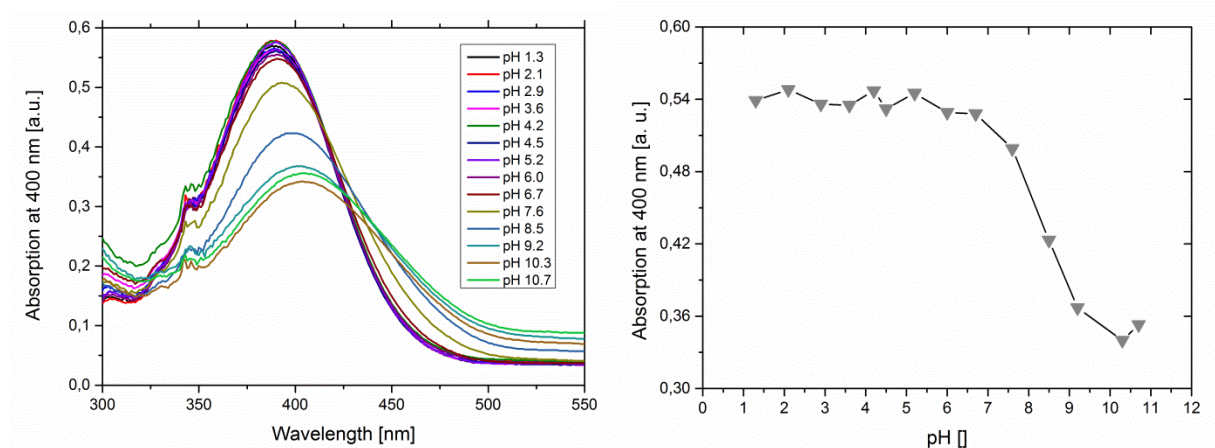


Figure 49 Comparison of the pH depended absorption spectra (left) and comparison of pH dependent absorption intensity at 528 nm (right)

Conclusion

In this chapter the preparation of a naphthalimide functionalized water soluble polynorbornene for the use as a pH sensor was described. Methyl-piperazine-naphthalimide was synthesized and functionalized with norbornene for further ring opening metathesis polymerization. Norbornene-diglycol-ester was used as matrix and shows great solubility in water due to its glycol moieties. The polymer has a theoretical chain length of 100 with an average amount of 1 naphthalimide units per macromolecule. The pH sensitivity was tested with different phosphate buffers and excitation wavelength was set to 400 nm. Highest emission signal was detected with a pH value of 4.2 and decreases immediately with a value of 5.2. Almost no emission was detected with a pH value of 8.5 and higher. The piperazine moiety has also the ability to interact with metal ions. Hence, this newly developed pH-responsive polymer may also find use as a sensor for metal ions and has to be investigated in further experiments.

Experimental

Materials and Methods

All reagents and solvents were purchased from commercial sources (ABCR or Sigma Aldrich) with reagent grade quality and used as received. Complex M31 [1. 3-bis (2, 4, 6-trimethylphenyl)-2-imidazolidinylidene] dichloro-(3-phenyl-1H-inden-1-ylidene)(pyridyl) ruthenium (II) for ring opening metathesis polymerisation (ROMP) was obtained from UMICORE AG Co. KG. Absorption spectra were recorded on a Shimadzu spectrophotometer UV-1800. The emission was measured on a Hitachi F-7000 fluorescence spectrometer equipped with a photomultiplier R928 from Hamamatsu. NMR Spectroscopy (^1H , APT) was done on a Bruker Avance 300 MHz spectrometer. Deuterated solvents (Chloroform- d , DMSO- d^6) were obtained from Cambridge Isotope Laboratories Inc. and remaining peaks were referenced according to literature. Peak shapes are specified as follows: s (singlet), bs (broad singlet), d (doublet), dd (doublet of doublets), t (triplet), q (quadruplet), m (multiplet). Gel permeation chromatography (GPC) was used to determine molecular weights and the polydispersity index (PDI) of the polymers. Measurements were carried out in THF with the following arrangement: a Merck Hitachi L6000 pump, separation columns of Polymer Standards Service (5 μm grade size) and a refractive-index detector from Wyatt Technology. For calibration, polystyrene standards purchased from Polymer Standard Service were used.

The T_g was measured on a PerkinElmer Differential Scanning Calorimeter Hyper DSC 8500. Three isothermal cycles were executed, the second scan was analysed. The scanning speed for cooling and for heating was set to 20°C/min and the temperature range was set between 20 to 200°C.

Synthetic procedure

Preparation of 2-(6-(4-methylpiperazin-1-yl)-1,3-dioxo-1H-benzo[de]isoquinolin-2(3H)-yl)ethyl (1R,4R)-bicyclo[2.2.1]hept-5-ene-2-carboxylate is described in chapter 4.

Tris(2-ethoxyethyl)-bicyclo[2.2.1]hept-5-ene-2,3-dicarboxylate²³⁴

A 100 mL Schlenk flask was evacuated and purged with nitrogen three times. Afterwards triethylene glycol monomethyl ether (3.8 mL, 21.7 mmol), DMAP (catalytic amount) and pyridine (2 mL, 24.8 mmol) were dissolved in 40 mL dry DCM. Norbornen-2,3-dicarbonyl dichloride (1.6 mL, 9.86 mmol) was dissolved in 10 mL dry DCM and was added dropwise via

dropping funnel to the ice cooled solution. After addition, the mixture was stirred overnight. On the next day the reaction was monitored via TLC and after completion it was quenched with 2 mL of DI water and stirred for 30 minutes. The organic layer was extracted with 2M HCl, saturated NaHCO₃ solution and water, dried with Na₂SO₄, filtered off and dried *in vacuo*. The slightly yellow oil was purified via column chromatography with a solvent mixture of DCM + MeOH (20 + 1) filtered through activated carbon and after evaporation of the solvent colorless oil was obtained. Yield: 4.12 g (96.5%). ¹H-NMR (δ, 20°C, CDCl₃, 300 MHz): 1.41 – 1.46 (d, ³J_{HH} = 9.0 Hz, 1H, H_{nb7a}), 1.58 – 1.64 (d, ³J_{HH} = 9.0 Hz, 1H, H_{nb7b}), 2.72– 2.74 (m, 1H, H_{nb3}), 3.14 (bs, 1H, H_{nb4}), 3.28 (bs, 1H, H_{nb1}), 3.41 – 3.44 (t, ³J_{HH} = 3.81 Hz, 1H, H_{nb2}), 3.48 – 3.73 (m, 12H, 2x -O-CH₂-CH₂-O-), 4.12 – 4.31 (m, 4H, 2x -OOC-CH₂-), 6.04 - 6.09 (m, 1H, H_{nb6}), 6.25 - 6.28 (m, 1H, H_{nb5}). ¹³C-NMR (δ, 20°C, CDCl₃, 75 MHz): 174.4, 173.1 (C=O), 137.5, 135.2 (C_{nb5,6}), 70.8, 70.6, 69.8, 69.1, 66.7, 63.9, 63.7 (-O-CH₂-CH₂-), 47.9, 47.7, 47.2, 47.1, 45.8 (C_{nb1-4,7}), 15.1 (-CH₃).

Polymer preparation

A 10 mL Schlenk flask was evacuated and purged with nitrogen three times. The flask was equipped with a stirring bar and was filled with 3 mL dry DCM. The pH sensitive chromophore (1.85 mg, 4*10⁻³ mmol) and the glycol norbornene monomer (200 mg, 0.4 mmol) were added to the flask. An evacuated 4 mL vial was filled with initiator M31 (0.6 mg, 8*10⁻⁴ mmol) dissolved in 500 μL dry DCM and was then added to the monomer solution. The reaction mixture was stirred at 35°C for 20 hours. The polymerisation was terminated with a drop of ethyl vinyl ether. Purification was done via precipitation in ice cold pentane and decanted to obtain a yellowish oil. Yield: 150 mg. ¹H-NMR (δ, 20°C, CDCl₃, 300 MHz): 5.54 – 5.11 (m, 2H, CH=CH), 3.68 – 3.59 (m, 6H, -CH₃), 3.32 – 2.62 (m, 4H, H_{cp1-4}), 1.98 (bs, 1H, H_{cp5a}), 1.47 (bs, 1H, H_{cp5b}). ¹³C-NMR (δ, 20°C, CDCl₃, 75 MHz): 174.6 – 173.3 (C=O), 133.3 – 129.0 (HC=CH), 53.4 – 51.4 (C_{cp1-5}), 40.8 (-CH₃). UV/Vis (water): 391.5.

CHAPTER 7

PREPARATION OF A NEWLY DEVELOPED DYE – FUNCTIONALIZED

TERMINATION REAGENT FOR

RING OPENING METATHESIS POLYMERIZATION

Introduction

In addition to the mono norbornene functionalized **Pt TPP** (see chapter 2), a tetra methoxyacrylic functionalized **Pt TPP** was synthesized for the use as a termination reagent for ring opening metathesis polymerization, for a selective end-group functionalization.

For the termination of functional group tolerant Ru-based ROMP polymers only a few papers have been published.²³⁵ The most common termination reagents are enol ethers, acrylates or molecular oxygen.²³⁶ According to Lexer *et al.* a termination with acrylates leads to poor yields, because of the property of its double bond to react with the Ru-complex in two stereo-mechanistic paths where one leads to the undesired methylene product (Figure 50) Usually this occurs with a ratio of the desired ester product to the methylene product of 75 to 25.²³⁷

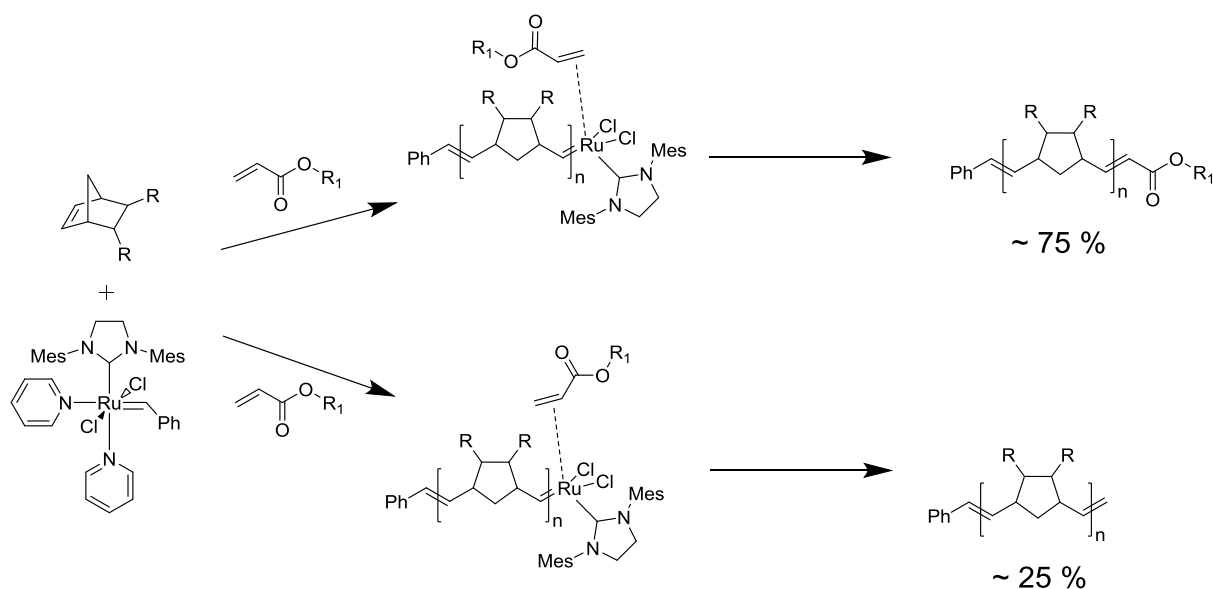


Figure 50 Synthesis of semi-telechelic polymers

This effect does not occur if enol ethers were used as termination reagent,²³⁸ but preparation of dyes with a enol ether moiety often leads to a very complex, expensive and time-consuming synthetic pathways.

Results and Discussion

To avoid an unselective termination as well as a too difficult synthetic pathway a new termination reagent was synthesized and tested. Therefore, we started with a cheap commercially available compound, namely methyl-3-methoxyacrylate. After saponification

with KOH the carboxylic acid was obtained which can be used for further esterification reactions with DCC and DMAP as co-reagent (Steglich-esterification). As a first preliminary test the carboxylic acid was used for an esterification with benzyl alcohol. The reaction scheme is shown below in Figure 51.

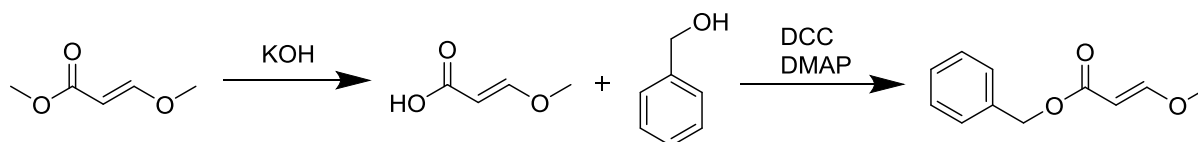


Figure 51 Preparation of benzyl-3-methoxyacrylate

Benzyl-3-methoxyacrylate was then used for the termination of a dimethyl-5-norbornene-2,3-dicarboxylate oligomer with a chain length of 10. The short chain length was chosen to verify the termination via $^1\text{H-NMR}$, if a longer chain would have been prepared integration of the aromatic protons will become challenging due to the low ester concentration. After the termination the oligomer was purified with column chromatography with dichloromethane as solvent. Considering the proton NMR spectrum a complete termination took place. There are several signs for that assumption; like that no methyl signals of the methoxyacrylate moiety appear any more, the aromatic signals appear in an broader area than before and that the acrylate double bond proton shows an integration value of 0.10 which correlates perfect with the prepared chain length of 10. The NMR spectrum is shown in the supporting information in Figure 3S. For a better understanding of these statements the termination with benzyl-3-methoxyacrylate is shown below in Figure 52.

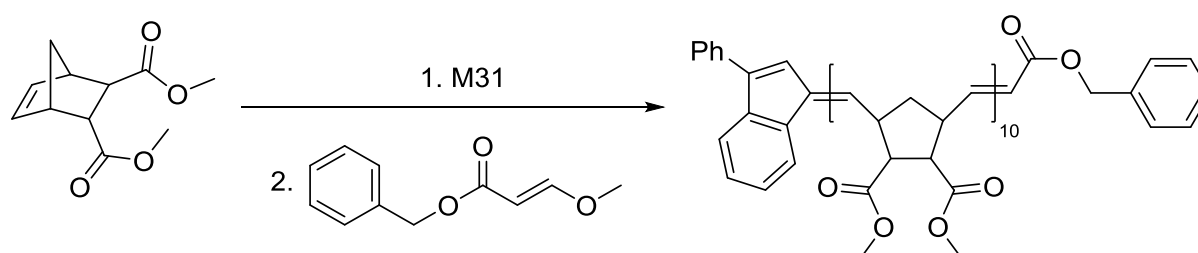


Figure 52 Preparation of a Norbornene oligomer followed by termination with benzyl-3-methoxyacrylate

Due to these experiments the synthesis of a **Pt TPP** with four termination moieties was prepared, for the preparation of star shaped polymer with the chromophore in the center. A schematic illustration of the desired star shaped polymer is shown below in Figure 53.

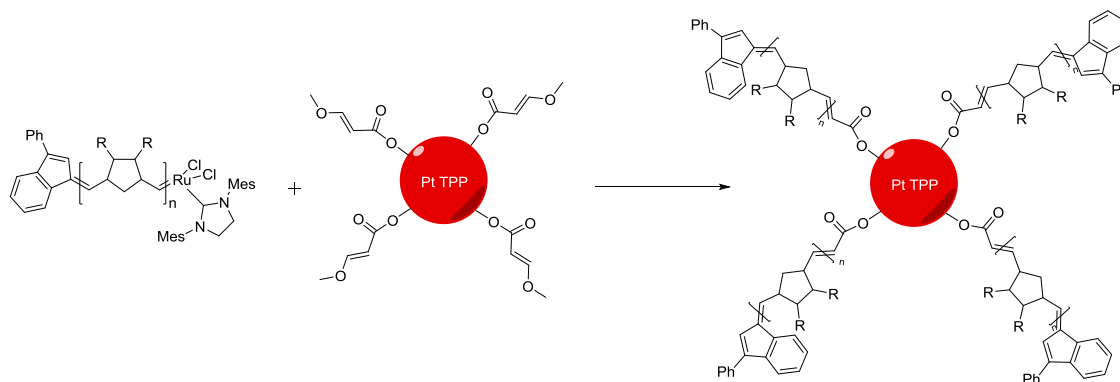


Figure 53 Schematic illustration of a star shaped polymer

The preparation of that compound is very similar to the preparation of the norbornene functionalized porphyrin but with one major difference, the preparation of a tetra bromo functionalized ligand. The first reaction step was again inspired by the work of Adler and Longo, whereby freshly distilled pyrrole and 4-bromobenzaldehyde was dissolved in propionic acid and heated to reflux for 50 minutes. Purification was done by column chromatography to obtain the tetra bromo functionalized compound. Next step was the platination with the microwave. Therefore, the porphyrin and $\text{Pt}(\text{acac})_2$ were dissolved in benzonitril and heated to 250 °C. After 30 minutes the reaction was finished and after purification via column chromatography a Suzuki cross-coupling with 4 equivalents of 4-(hydroxymethyl)-phenylboronic acid was conducted. To obtain higher yields for the tetra functionalized compound aliquot was used as co-reagent. The last step was the Steglich esterification with the priviosly prepared 3-methoxyacrylic acid. The synthesis pathway is shown below in Figure 54. This newly prepared porphyrin show the exact same photo physical properties like the norbornene functionalized compound. The absorption measurement was done with DCM as solvent. Its Soret-band exhibits at 399 nm, while the Q-band appears at 509 nm.

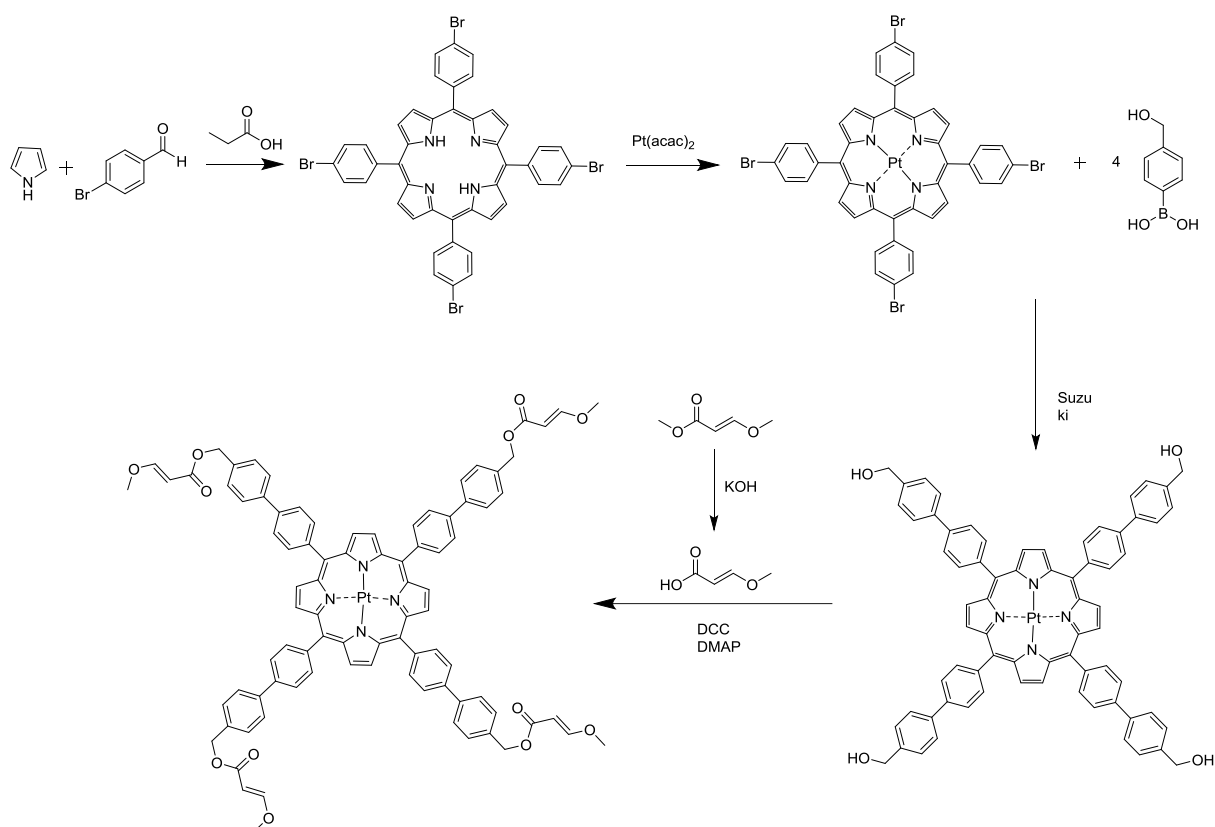


Figure 54 Synthetic pathway for the **Pt TPP** termination reagent

Conclusion

The preparation of a newly developed tetra methylene-3-methoxyarylate functionalized tetraphenyltetraporphyrin was presented. First experiments where benzyl-3-methoxyacrylate was used as a quenching reagent for ROMP showed that a termination with a test substance is possible. The test substance was a simple DME-N oligomere with a chain length of ten. Further experiments have to be carried out, but the porphyrin derivative seems to be a promising reagent for the preparation of ROMP based star shaped polymers with the chromophore moiety as core for the prepared macromolecule.

Experimental

Materials and Methods

All reagents and solvents were purchased from commercial sources (ABCR or Sigma Aldrich) with reagent grade quality and used as received. Complex M31 [1. 3-bis (2, 4, 6-trimethylphenyl)-2-imidazolidinylidene] dichloro-(3-phenyl-1H-inden-1-ylidene)(pyridyl)

ruthenium (II) for ring opening metathesis polymerisation (ROMP) was obtained from UMICORE AG Co. KG. NMR spectroscopy (^1H , ^{13}C , APT, COSY, HSQC) was performed on a Bruker Avance 300 MHz spectrometer. Deuterated solvents (Chloroform- d , DMSO- d_6 , D_2O) were obtained from Cambridge Isotope Laboratories Inc. and remaining solvent peaks were referenced according to literature.²³⁹ Peak shapes are specified as follows: s (singlet), bs (broad singlet), d (doublet), dd (doublet of doublets), t (triplet), q (quadruplet) and m (multiplet). Silica gel 60 F254 and aluminium oxide 60 F254 on aluminium sheets were used for thin layer chromatography. They were purchased from Merck. Visualization was done under UV light or by dipping into an aqueous solution of KMnO_4 (0.1 wt%). MALDI-TOF mass spectrometry was performed on Micromass TofSpec 2E Time-of-Flight Mass Spectrometer. The instrument was equipped with a nitrogen laser ($\lambda = 337 \text{ nm}$, operated at a frequency of 5 Hz) and a time lag focusing unit. Ions were generated just above the threshold laser power. Positive ion spectra were recorded in reflection mode with an accelerating voltage of 20 kV. The spectra were externally calibrated with a polyethylene glycol standard. Analysis of data was done with MassLynx-Software V3.5 (Micromass/Waters, Manchester, UK). The best ten shots were averaged to a spectrum. Samples were dissolved in acetone or DCM ($c = 1 \text{ mg/mL}$). Solutions were mixed in the cap of a microtube in the ratio of $1 \mu\text{L} : 10 \mu\text{L}$. The resulting mixture ($0.5 \mu\text{L}$) was spotted onto the target and allowed to air-dry. The matrix was trans-2-[3-(4-tert-Butylphenyl)-2-methyl-2-propenylidene]malononitrile (DCTB). Absorption spectra were recorded on a Shimadzu spectrophotometer UV-1800. The emission was measured on a Hitachi F-7000 fluorescence spectrometer equipped with a red-sensitive photomultiplier R928 from Hamamatsu.

Synthetic procedures

3-Methoxyacrylic acid A 50 mL round bottom flask was filled with methyl (E)-3-methoxyacrylate (5 g, 43 mmol) and dissolved in 30 mL NaOH (2N) solution. The mixture was stirred under reflux for 2 days. For the workup the solution was neutralized with approximately 1 g citric acid. The product was extracted 8 times with EtOAc. The organic phase was dried with Na_2SO_4 and concentrated *in vacuo*. The product was used without further purification. Yield: 897 mg (20 %). $^1\text{H-NMR}$ (δ , 20°C , CDCl_3 , 300 MHz): 12.22 (s, 1H, -COOH), 7.71 – 7.67(d, $J = 12.6 \text{ Hz}$, 1H, -CH=CH-O-), 5.19 – 5.14 (d, $J = 12.6 \text{ Hz}$, 1H, -CH=CH-O), 3.70 (bs, 3H, - CH_3).

Benzyl-3-methoxyacrylate Phenylmethanol (500 mg, 4.625 mmol), 3-methoxyacrylate (472 mg, 4.625 mmol), DCC (953.5 mg, 4.625 mmol) and a spatula tip DMAP was dissolved in 40 mL dry DCM. The reaction mixture was stirred for 15 hours. To remove undesired by-products extraction was done with HCl (5%), saturated NaHCO₃ solution and deionized water. The organic phase was dried with Na₂SO₄ and concentrated *in vacuo*. Purification was done by column chromatography (SiO₂, CH₂/ EtOAc, 5+1). Yield: 897 mg (20%). ¹H-NMR (δ, 20°C, CDCl₃, 300 MHz): 7.71 – 7.67(d, J = 12.6 Hz, 1H, -CH=CH-O-), 7.37 (bs, 5H, H_{Ar}), 5.28 – 5.24 (d, J = 12.6 Hz, 1H, -CH=CH-O-), 5.18 (bs, 2H, Ph-CH₂-O-) 3.67 (bs, 3H, -CH₃).

5,10,15,20-tetrakis(4-bromophenyl)porphyrin (TBrTPP) A 250 mL two-neck-round bottom flask was filled with 10 g of freshly distilled pyrrole (149 mmol) and 18.18 g of 4-brom benzaldehyde (99.4 mmol). The substrates were dissolved in 250 mL propionic acid and heated to reflux at 120°C. The progress of the reaction was monitored via TLC (CH₂ + DCM, 3 + 2). After 50 minutes the reaction was stopped and the solvent was cooled to room temperature. The Solvent was evaporated and the remaining black oil was dissolved in 50 mL DCM. The product was extracted with water and saturated NaHCO₃ solution. The greenish red organic solution was dried with Na₂SO₄ and evaporated afterwards. The residue was purified using column chromatography with 3 + 2, Cy + DCM mixture. The process was monitored using TLC in the same solvent. The product was collected, condensed under reduced pressure, and dried under vacuum. The porphyrin was dissolved in acetone and precipitated in MeOH. The purple crystals were collected via suction filtration and dried under vacuum. Yield: 2.52 g (2.8 %). ¹H-NMR (δ, 20°C, CDCl₃, 300 MHz): -2.78 (bs, 2H, -NH), 7.75 – 7.79 (m, 8H, H_{phenyl}), 8.20 – 8.23 (m, 8H, H_{phenyl}), 8.85 (bs, 8H, H_{pyrrole}). ¹³C-NMR (δ, 20°C, CDCl₃, 75 MHz): 119.16, 112.81 (C(5), C(10), C(15), C(20)), 130.16 (C_{pyrrole}), 135.99 (C_{ortho}, C_{meta}), 140.97 (-C-Br). UV/VIS (CHCl₃): λ_{max} = 418, 513, 550, 590.

Platinum (II) 5,10,15,20-tetrakis(4-bromophenyl)porphyrin (Pt TBrTPP) A 20 mL microwave vessel was equipped with a stirring bar and filled with 16 mL benzonitrile. After addition of the porphyrin (200 mg, 0.215 mmol) and the metal salt (211 mg, 0.538 mmol) the vessel was sealed with a septum and placed into the microwave. The reaction temperature was set to 250°C for 30 minutes. The pressure was controlled by a load cell connected to the vessel via a non-invasive pressure measurement device above the septum surface. After completion of the reaction the remaining salts and the undesired protonated ligand were filtered off. The desired product was obtained via precipitation with a mixture of EtOH, DI water and brine.

The red solid was filtered off and concentrated in vacuo. Purification was done by column chromatography (SiO₂, CH/ DCM, 1+2). Yield: 105 mg (43.5 %). ¹H-NMR (δ, 20°C, CDCl₃, 300 MHz): 8.75 (s, 8H, H_{pyrrol}), 8.01 (d, J = 8.3 Hz, 8H, H_{Ar}), 7.89 (d, J = 8.3 Hz, 8H, H_{Ar}). ¹³C-NMR (δ, 20°C, CDCl₃, 75 MHz): 140.7 (Cq), 140.0 (Cq), 135.2 (CH), 130.8 (CH), 130.1 (CH), 122.7 (Cq), 121.2 (Cq). **UV/VIS** (CHCl₃): λ_{max} = **401**, 510.

(Platinum (II) porphyrin-5,10,15,20-tetrayltetrakis([1,1'-biphenyl]-4',4-diyl))tetramethanol Pt TBrTPP (130 mg, 0.12 mmol) was dissolved in a mixture of toluol/ THF/ H₂O (2 + 2 + 1). The solution was deoxygenised for 30 minutes. Subsequently 4-(Hydroxymethyl)-phenylboronic acid (703.4 mg, 4.63 mmol), potassium carbonate (192.4 mg, 1.4 mmol), Pd(PPh₃)₄ (5.4 mg, 5*10⁻³ mmol) and Aliquat (catalytic amount) was added. The reaction mixture was stirred under inert atmosphere at 65 °C for 18 hours. DCM was added and the organic phase was washed with H₂O and sat. NaHCO₃-solution and dried over Na₂SO₄. The solvent was removed under reduced pressure. The products were isolated by column chromatography (SiO₂). The porphyrin was eluted with DCM + MeOH (20+1). Yield: 125 mg (87.4%). ¹H-NMR (δ, 20°C, CDCl₃, 300 MHz): 4.75 (bs, 8H, -CH-CH₂-OH), 7.43 - 7.63 (m, 16H, H_{phenyl}), 7.90 - 7.99 (m, 8H, H_{por-phenyl}), 8.21 - 8.25 (m, 8H, H_{por-Phenyl}), 8.80 - 8.92 (bs, 8H, H_{pyrrole}). ¹³C-NMR (δ, 20°C, CDCl₃, 75 MHz): 119.16, 112.81 (C(5), C(10), C(15), C(20)), 130.16 (C_{pyrrol}), 135.99 (C_{ortho}, C_{meta}), 140.97 (-C-Br). **UV/VIS** (CHCl₃): λ_{max} = 401, 510. MALDI: m/z [M⁺]calc. for C₇₂H₅₂N₄O₄Pt: 1230.3616; found 1230,2498.

Platinum (II) (porphyrin-5,10,15,20-tetrayltetrakis([1,1'-biphenyl]-4',4-diyl))tetrakis(methylene) tetrakis(3-methoxyacrylate) (Pt TPP_{ter}) A 50 ml round-bottom flask was filled with the tetra hydroxyl functionalised porphyrin (50 mg, 4.1*10⁻² mmol), (E)-3-methoxyacrylic acid (16.74 mg, 0.164 mmol), DCC (33.8 mg, 0.164 mmol) and a spatula tip of DMAP and was dissolved in 10 mL dry DCM. The reaction was ice-cooled and stirred for 3 days. Completion of the reaction was detected via TLC (DCM). The emerging by-product (1,3-dicyclohexylurea) was filtered off and the product was extracted with HCl (5%), NaHCO₃ and Brine. The organic layer was dried with Na₂SO₄ and concentrated *in vacuo* obtaining a red solid. The product was purified by column chromatography (SiO₂, DCM). Yield: 8 mg (12%). ¹H-NMR (δ, 20°C, CDCl₃, 300 MHz): 8.90 - 7.38 (m, 44H, H_{porphyrin}, H_{Ar}, -CH=CH-O), 5.51 (bs, 8, -Ph-CH₂-O-), 5.34 - 5.09 (m, 4H, -CH=CH-O), 3.75 - 3.69 (m, 12H, -O-CH₃). MALDI: m/z [M⁺]calc. for C₈₈H₆₈N₄O₁₂Pt: 1568.4507; found 1581.7202. **UV/VIS** (CHCl₃): λ_{max} = **401**, 510.

Supporting Information

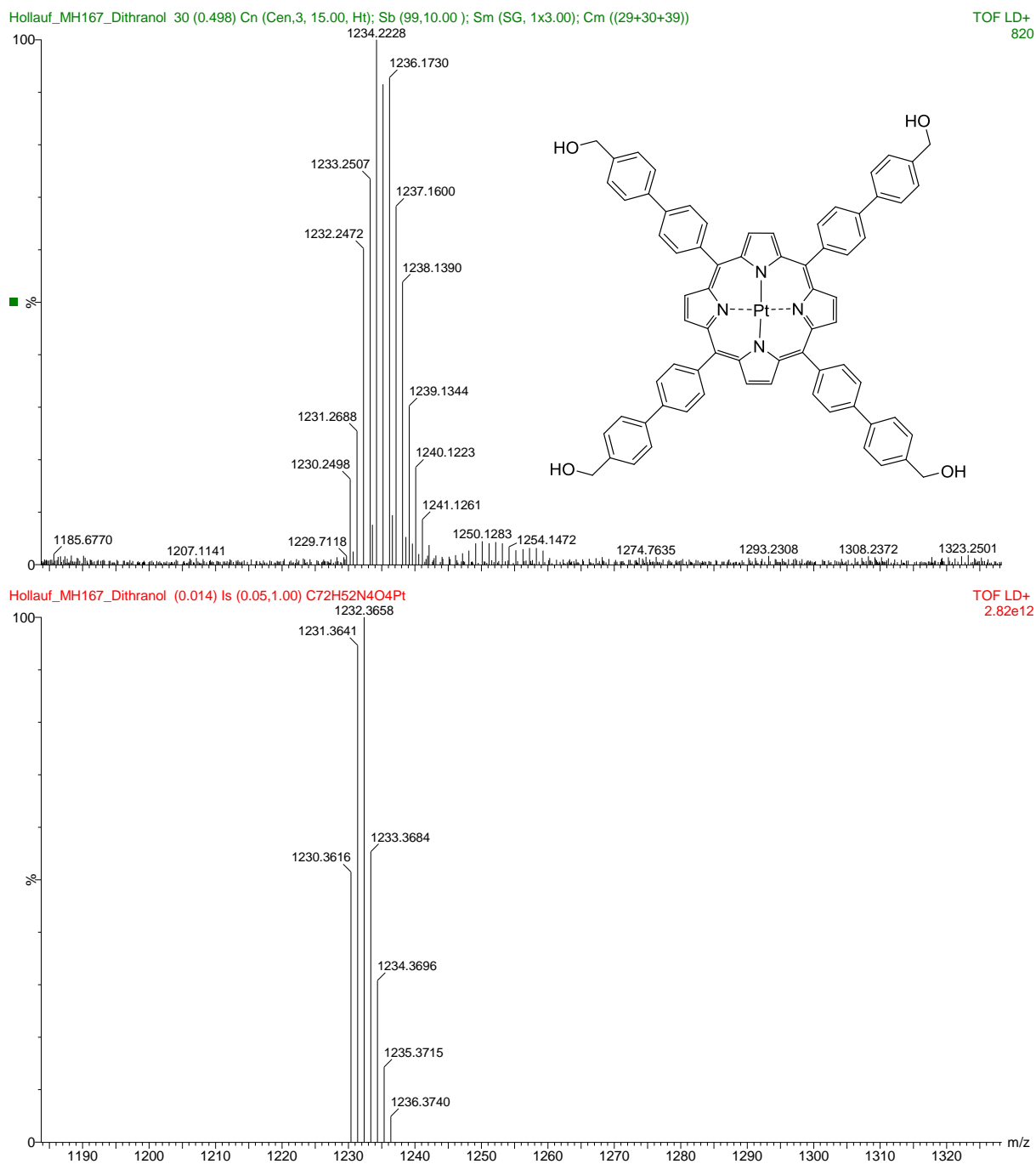


Figure 1S Mass spectrum (MALDI) of **tetra hydroxyl TPP Pt**

$C_{72}H_{52}N_4O_4Pt$

calculated: 1230.3616 g/mol

experimental: 1230,2498 m/z

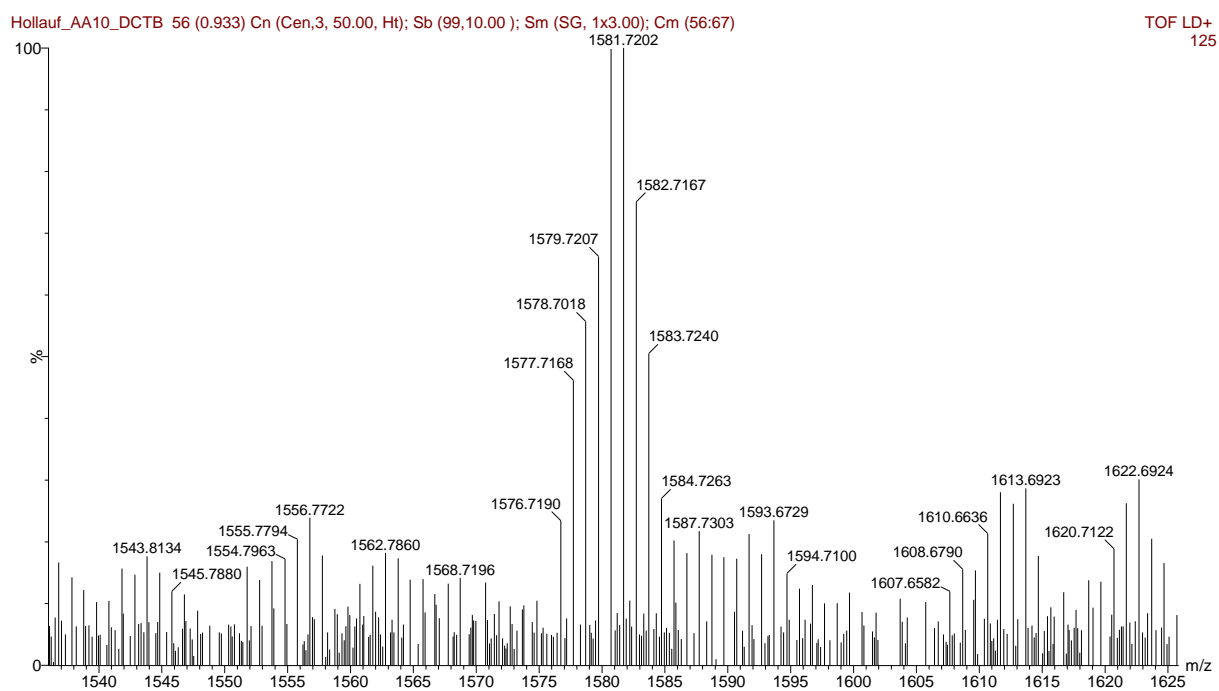
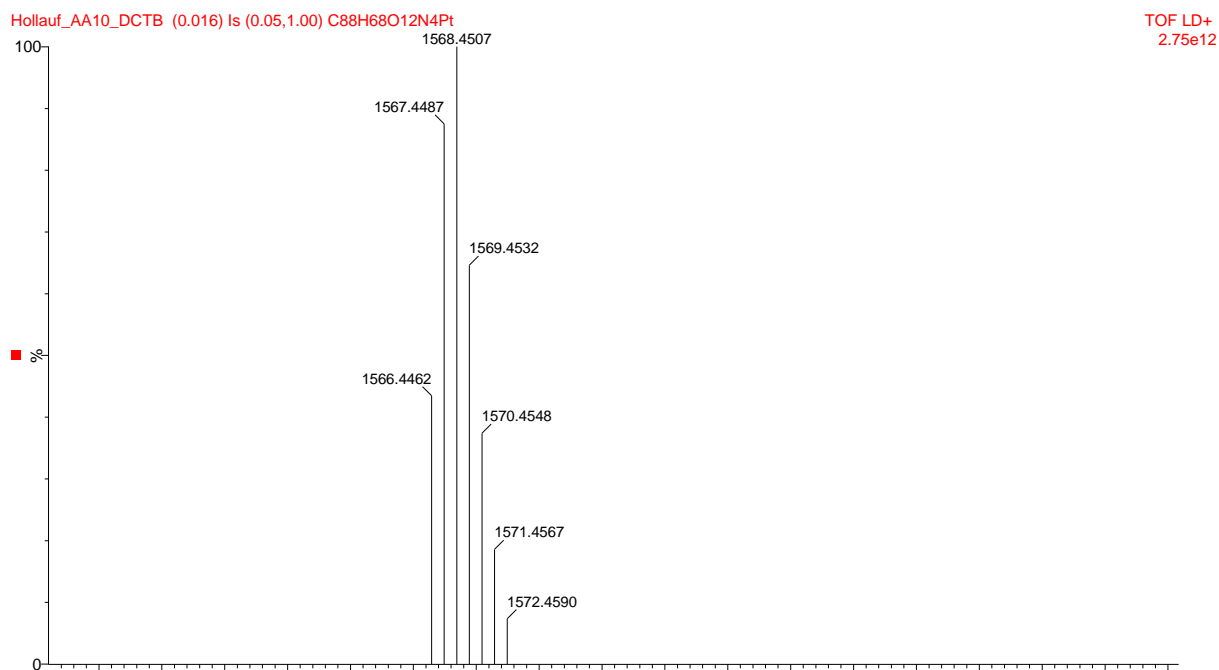


Figure 2S Mass spectrum (MALDI) of TPP Pt_{termination} reagent

C₈₈H₆₈N₄O₁₂Pt calculated: 1568.4507g/ mol found 1581.7202m/z

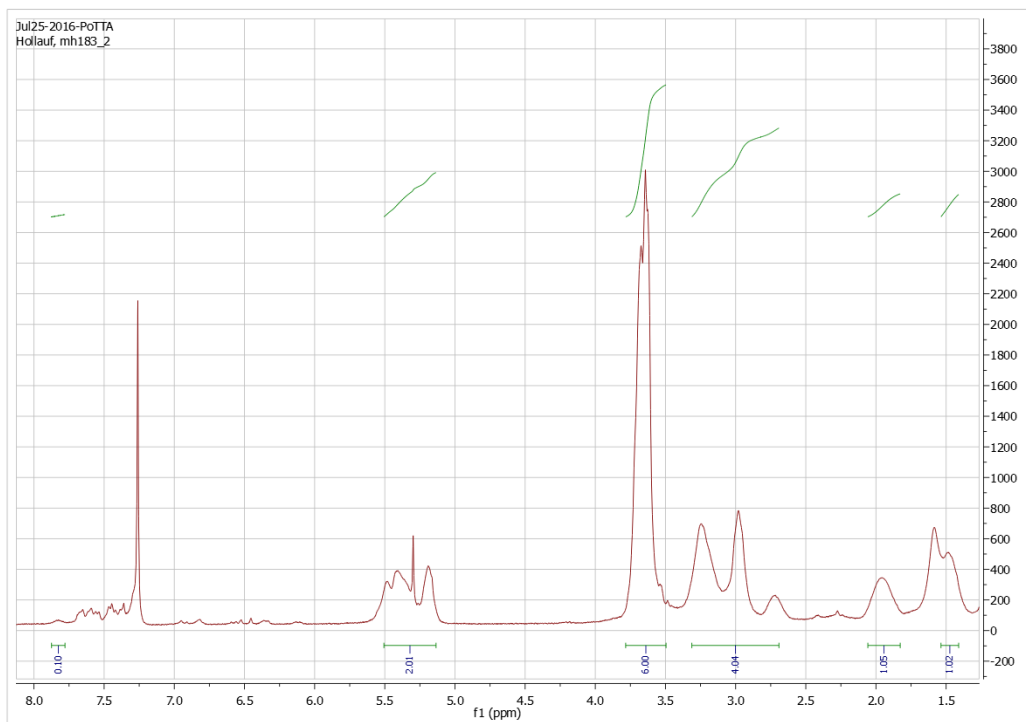


Figure 3S NMR spectrum of an DME oligomer (chain length = 10) after termination with benzyl-3-methoxyacrylate

CHAPTER 7

CONCLUSION

The first chapter showed that ROMP is a highly suitable technique for the preparation of dye-functionalized polymers. The high functional group tolerance does allow the synthesis of polymers with a great density of functional groups on homopolymers, enabling to study bulk properties such as photochromism, electron transport and self-assembly leading to nanocoils and ladder polymers. The living nature of ROMP supports the preparation of block copolymers while allowing precise placement of the dye molecules in either block. It is also possible to selectively decorate the prepared macromolecules at the end of its polymer chain with the help of suitable derivatized initiators and termination reagents. Moreover, reactive functionalities are easily incorporated in each of the three polymerization steps (initiation, propagation and termination) and then can be converted in post-polymerization functionalization steps.

Chapter two and three presented the first ROMP based dye-functionalized terpolymers which are able to undergo a triplet-triplet annihilation induced up-conversion. These systems were able to convert red to green light and green to blue light which is shown in Figure 55 below.

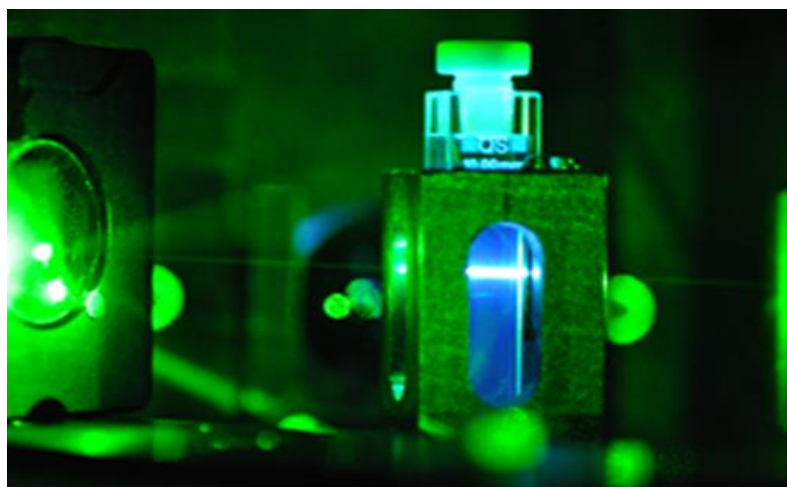


Figure 55 photographic illustration of an triplet-triplet annihilation induced up-conversion

The first system consists of a diphenylanthracene (**DPA**) derivative as emitter, a Pt tetraphenylporphyrin (**Pt TPP**) as sensitizer and dimethyl 5-norbornene-2,3-dicarboxylate (**DME-N**) as matrix. Preliminary experiments showed that the highest quantum yields were achieved with a concentration of 40 wt% of the emitter and 0.5 wt% of the sensitizer. Hence a molar ratio of 171 to 1 of emitter to sensitizer was prepared. The second system consists of a perylene derivative (**PDE**) as emitter, Pt tetraphenyltetrabenzoporphyrin (**Pt TPTBP**) as

sensitizer and dimethyl 5-norbornene-2,3-dicarboxylate (**DME-N**) as matrix. For that system a concentration which is already well-known from literature was used. Therefore, the molar ratio of emitter to sensitizer was set to 5 to 1. For both systems five different polymeric architectures have been prepared (Polymer **I - V**) which are shown below in Figure 56.

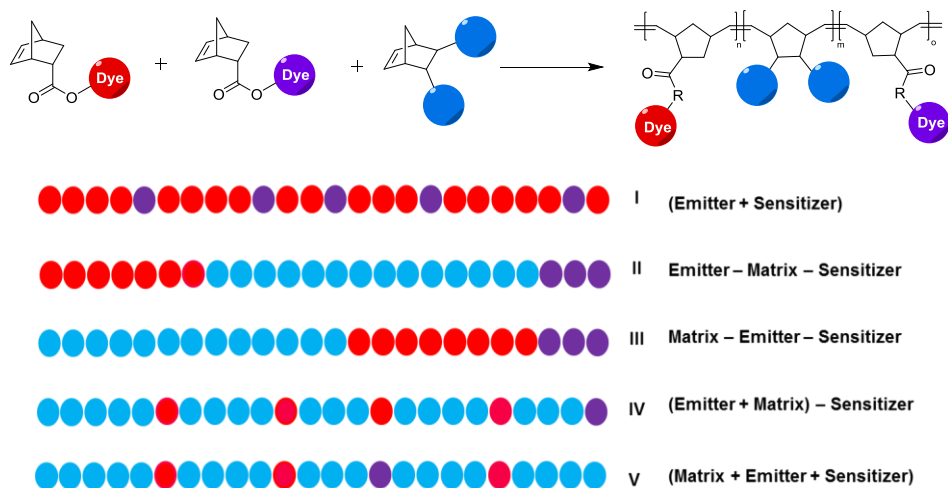


Figure 56 Overview of the prepared polymer architectures

Polymer **I** is a statistically distributed copolymer consisting of only the chromophores with the corresponding emitter to sensitizer ratio and a chain length of 500. Polymer **II** and **III** were block-copolymers in the form of emitter-matrix-sensitizer and matrix-emitter-sensitizer. Polymer **IV** exhibits a statistically distribution of emitter and matrix and a sensitizer block at the end of the macromolecule. For polymer **V** a statistically distribution of all three monomers was obtained.

The TTA-UC measurements showed that the architecture has a strong influence on the delayed fluorescence. The varying quantum yields are summarized below in Table 8.

Table 9 Summarized quantum yields

| Polymer | DPA/ Pt TPP | PDE/ Pt TPTPTBP |
|------------|-------------|-----------------|
| | Φ [%] | Φ [%] |
| I | 0.04 | 0.06 |
| II | 0.08 | 0.16 |
| III | 0.10 | 0.10 |
| IV | 0.11 | 0.52 |
| V | 0.71 | 2.95 |

The polymer without the matrix monomer (polymer **I**) showed the lowest quantum yield and a statistically distribution of all three monomers (polymer **V**) showed the highest quantum yield. The quantum yield of polymer **II** and **III** are almost as low as for polymer **I**. A reason for the low quantum yields might be aggregation of the chromophores leading to a close proximity which is detrimental to the TTA-UC.

Due to the fact that the **DPA/ Pt TPP** system was excited with a low photon density source ($540 \text{ mol s}^{-1} \text{ m}^{-2}$) at 509 nm, the obtained quantum yields were quite low ($\phi \approx 0.04$ to 0.71 %). The **PDE/ Pt TPTBP** system was excited with a green laser at 617 nm ($36\,200 \mu\text{mol s}^{-1} \text{ m}^{-2}$) and was able to exhibit red light that was detectable with the naked eye. The highest quantum yield for this system was almost 3%. Figure 57 shows a photographic illustration of the polymers **II**, **IV** and **V** which were excited with a red laser.

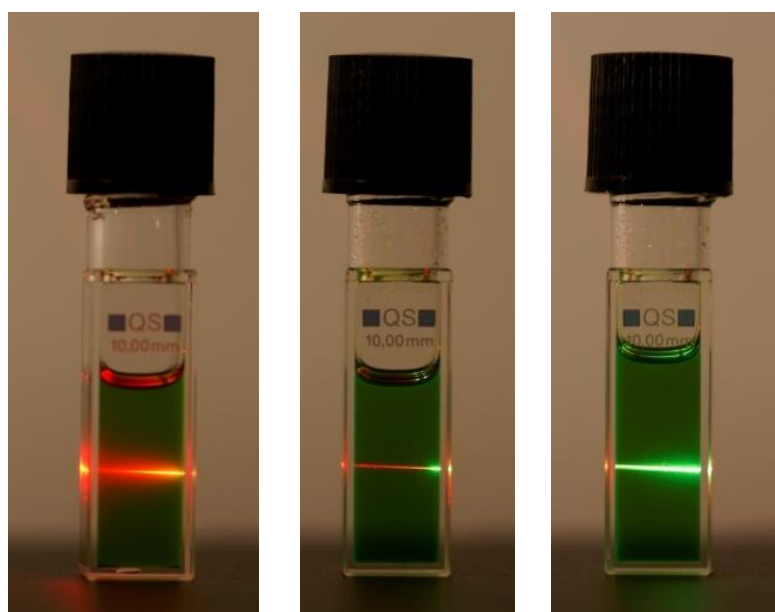


Figure 57 Photographic images of solutions of polymer **II**, **IV** and **V** (left to right). Polymers have been dissolved in 1,4-dioxane and were excited with a red laser at 617 nm.

For both systems energy dependent measurements were carried out, whereby both showed a quadratic dependence. This is typical for a nonlinear process such as TTA-based up-conversions. The logarithmic plot exhibits a slope of two which indicates that the system is not saturated. Therefore it is possible to achieve higher quantum yields with a stronger energy source.

The next step is the investigation of these polymer systems with a stronger light source and the preparation of films via drop casting, spin coating or doctor blading. First TTA polymer

films have already been prepared for the second system (see chapter 3) which could be used as a light up-converting solid material. Due to low quantum yields, optimizations like using a different polymer matrix, using different chain lengths, varying temperatures during the measurement, using a higher photon density, varying the thickness of the films, using different manufacturing methods or the addition of different softening agents will be done and presented in further investigations.

The naphthalimide investigation shows that it is possible to link different naphthalimide dyes to norbornene monomers and that subsequently polymerization with a norbornene matrix to random copolymers was successful. Narrow polydispersity indicates good control over the molecular weight which can be used to design special macromolecular architectures. The optical properties of the monomers and the polymers are practically identical to those of the pure unsubstituted dye molecules showing that π - π stacking of the naphthalimide dyes is avoided. A photographic illustration of all monomers dissolved in DMSO is shown below in Figure 58.



Figure 58 Monomers **6-10** in solution (DMSO) under visible light (top) and under UV irradiation at 365 nm (bottom)

Furthermore, the photo physical behaviour of methyl-piperazine-naphthalimide was investigated as a function of the proton concentration. Therefore, this compound was synthesized and functionalized with a norbornene moiety for further ring opening metathesis polymerization. This naphthalimide was copolymerized with a water-soluble matrix obtaining a pH sensitive macromolecule. It shows the highest emission intensity with a pH value of 4.2 and decreases immediately with a value of 5.2. Almost no emission was detected with a pH value of 8.5 and higher which is shown below in Figure 59. This newly developed pH-responsive polymer may also find use as a sensor for various metal ions, due to the accessible and responsive lone pair of the piperazine moiety, and has to be investigated in further experiments.

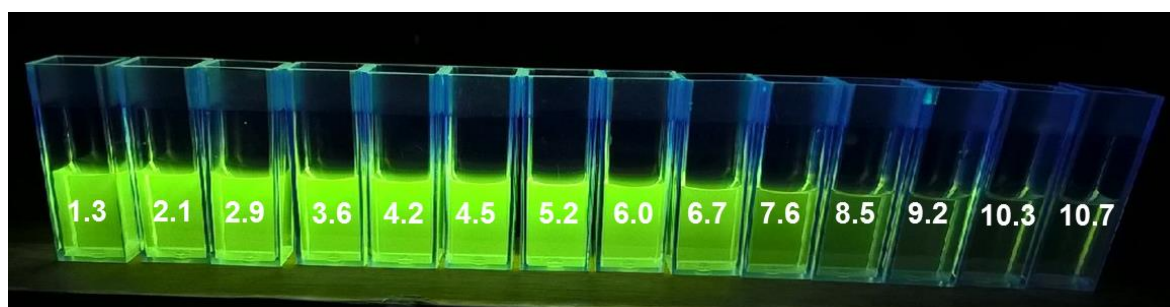


Figure 59 Photographic illustration of polymer solutions with different pH values (white numbers) excited at 365 nm

The final step was the preparation of a newly developed tetra methylene-3-methoxyarylate functionalized tetraphenylporphyrin. Preliminary experiments showed that benzyl-3-methoxyacrylate is able to terminate ROMP reactions. Further experiments have to be carried out, but the porphyrin derivative seems to be a promising reagent for the preparation of ROMP based star-shaped polymers with the chromophore moiety as core for the prepared macromolecule.

This thesis presented new strategies for the preparation of dye-functionalized ring opening metathesis polymers.

CHAPTER 8

CURRICULUM VITAE

LEBENS LAUF

Persönliche Angaben:

Familienname, Vorname: Hollauf Manuel, BSc. MSc.
Staatsangehörigkeit: Österreich
Familienstand: Ledig
Adresse: Wiener Straße 58, 8020 Graz
Kontakt: manuel.hollauf@tugraz.at;
+43 664/ 57 96 713

Ausbildung:

2/2014 – 2/2017 PhD Student (Wissenschaftlicher Mitarbeiter)
an der Technischen Universität Graz am Institut für Chemische Technologie
von Materialien (ICTM) mit dem Titel: „Dye-Functionalized Polymers via
Ring Opening Metathesis Polymerization for Photophysical Applications“

10/2011 – 12/2013 Masterstudium der Chemie
an der Karl-Franzens Universität Graz (KFU) und an der Technischen
Universität Graz (TUG)

2/2013 – 9/2013 Masterarbeit
an der Technischen Universität Graz am Institut für Chemische Technologie
von Materialien (ICTM) mit dem Titel: „Orthogonally "Clickable"
Norbornenes for the Preparation of Functional Polymers and Kinetic Studies
of inverse electron demand Diels-Alder (iEDDA) reactivities“

10/2008 – 9/2011 Bachelorstudium der Chemie
an der Karl-Franzens Universität Graz (KFU) und an der Technischen
Universität Graz (TUG)

9/2007 – 5/2008 Zivildienst LKH Graz West

9/2003 – 6/2007 ORG der Schulschwestern Graz, Eggenberg (Matura)

9/1999 – 7/2003 ÜHS Hasnerplatz Graz

9/1995 – 7/1999 ÜVS Lendplatz Graz

Sonstige Aktivitäten:

- Wintersemester 2011/2012, Wintersemester 2012/2013, Wintersemester 2013/2014: studentischer Mitarbeiter im Lehrbetrieb an der Karl-Franzens-Universität für das Grundlagen Praktikum (CHE.115: LU aus Allgemeiner Chemie)
- Sommersemester 2012 und Sommersemester 2013: studentischer Mitarbeiter im Lehrbetrieb an der Karl-Franzens-Universität für das Organik Praktikum (CHE.144: LU aus Organischer Chemie)
- Summer Student im März und April 2012 an der Karl-Franzens-Universität unter Univ. Prof. DI Dr. Wolfgang Kroutil mit dem Arbeitstitel: Chemische und enzymatische Herstellung von beta chiralen Amininen
- Genehmigung eines Förderstipendiums gemäß § 63 Studienförderungsgesetz (StudFG) im Zuge der Diplomarbeit (Orthogonally "Clickable" Norbornenes for the Preparation of Functional Polymers and Kinetic Studies of inverse electron demand Diels-Alder (iEDDA) reactivities) im Sommersemester 2013
- Sommersemester 2016: studentischer Mitarbeiter im Lehrbetrieb an der Technischen Universität Graz für das Technische Praktikum (CHE. 161 LU aus Technischer Chemie)
- Genehmigung eines Förderstipendiums gemäß § 63 Studienförderungsgesetz (StudFG) im Zuge der Dissertation () im Sommer 2016
- Genehmigung eines Reisestipendiums – Travel Grands gemäß § 63 Studienförderungsgesetz (StudFG) im Zuge der Dissertation () im Sommer 2016
- Im Rahmen der Zeitschrift Monatshefte für Chemie/ Chemical Monthly des Springer-Verlages wurde im Sommer 2016 der Young Scientists Best Paper Award verliehen für die herausragende Recherche und Verfassung eines Reviews
- Im Zuge als Wissenschaftlicher Mitarbeiter (PhD Student) an der TU Graz von 02.2014 bis 02.2017 wurden 2 Erasmus Studenten, 8 Projektlaboranten, 5 Bachelorstudenten und ein Diplom Student betreut und ausgebildet

Wissenschaftliche Veröffentlichungen:

- ▶ **M. Hollauf**, P. Zach, S. M. Borisov, B. J. Müller, D. Beichel, M. Tscherner, S. Köstler, P. Hartmann, A. C. Knall, G. Trimmel
Dye functionalized-ROMP based terpolymer for the use as a light up-converting material via triplet-triplet annihilation
Submitted

- ▶ **Hollauf Manuel**, Cajlakovic Merima, Tscherner Martin, Koestler Stefan, Knall Astrid-Caroline, Trimmel Gregor
Synthesis and characterization of naphthalimide-functionalized polynorbornenes
Monatshefte fuer Chemie (2017), 148(1), 121-129

- ▶ Knall Astrid-Caroline, **Hollauf Manuel**, Saf Robert, Slugovc Christian
A trifunctional linker suitable for conducting three orthogonal click chemistries in one pot
Organic & Biomolecular Chemistry (2016), 14(45), 10576-10580

- ▶ **Hollauf M.**, Knall A.-C., Trimmel G
Dye-functionalized polymers via ring opening metathesis polymerization: principal routes and applications
Monatshefte für Chemie/ Chemical monthly 146 (2015) 7, S. 1063 - 1080

- ▶ Fuchs C. S., **Hollauf M.**, Meissner M., Simon R. C., Besset T., Reek J. N., Riethorst W., Zepeck F., Kroutil W
Dynamic kinetic resolution of 2-phenylpropanal derivatives to yield β -chiral primary amines via bioamination . in: Advanced synthesis & catalysis 356 (2014) 10, S. 2257 - 2265

- ▶ Knall A.-C., **Hollauf M.**, Slugovc C.
Kinetic studies of inverse electron demand Diels-Alder reactions (iEDDA) of norbornenes and dipyrudin-2-yl-1,2,4,5-tetrazine. in: Tetrahedron letters 55 (2014) , S. 4763 - 4766

- ▶ Knall A.-C., **Hollauf M.**, Saf R., Slugovc C.
1, 2,4,5-Tetrazines as click chemistry reagents - towards orthogonal conjugation reactions. in: Abstracts of Papers, 248th ACS National Meeting & Exposition, San Francisco, CA, United States, (2014), S. 2014

- ▶ Knall A.-C., Kovacic S., **Hollauf M.**, Reishofer D. P., Saf, R., Slugovc C.
Inverse electron demand Diels-Alder (iEDDA) functionalisation of macroporous poly(dicyclopentadiene) foams. in: Chemical communications 49 (2013) , S. 7325 – 7327

Vorträge an internationalen Konferenzen:

- ▶ Hollauf M.; Beichel B.; Tscherner M.; Köstler S.; Hartmann P.; Knall A. C.; Trimmel G.;
Influence of different polymeric architectures on the efficiency of the triplet-triplet annihilation
40th Anniversary of the Polymer Society of Korea (Iupac-PSK40).
Jeju (Korea) am. 4.10.2016

- ▶ Hollauf M.; Beichel B.; Tscherner M.; Köstler S.; Hartmann P.; Trimmel G.;
ring-opening-metathesis-polymers as an up-converting material via triplet-triplet-annihilation:
6th EuCheMS Chemistry Congress.
Seville (Spanien) am: 12.9.2016

- ▶ Hollauf, M.; Trimmel, G.; Beichel, D.; Köstler, S.; Cajlakovic, M.; Hartmann, P.:
Preparation of dye functionalized ring-opening-metathesis-polymers for the use as an up-
converting material via triplet-triplet-annihilation
Nawi Graz_Doc Days 2016.
Graz (Österreich) am: 5.4.2016

- ▶ Hollauf, M.; Trimmel, G.; Beichel, D.; Köstler, S.; Cajlakovic, M.:
Photon Up-Conversion by Dye Functionalized Ring-Opening-Metathesis-Polymers via Triplet-
Triplet-Annihilation
**11th International Conference on Advanced Polymers via Macromolecular Engineering (APME
2015).**
Yokohama (Japan) am: 18.10.2015

- ▶ Hollauf, M.; Köstler, S.; Cajlakovic, M.; Trimmel, G. :
Farbstoff-funktionalisierte Polymere für Lichtkonversionsschichten.:
12. Österreichische Photovoltaik - Tagung.
Linz (Österreich) am: 04.11.2014

Poster:

- ▶ A new dye functionalized polymer system for the use as an up-converting material
Hollauf, M., Trimmel, G., Beichel, D., Hartmann, P., Cajlakovic, M. & Köstler, S. 2015

- ▶ Dye functionalized Polymer architectures
Hollauf, M., Trimmel, G., Cajlakovic, M., Köstler, S. & Hartmann, P. 2014

- ▶ Farbstoff-funktionalisierte Polymere für Lichtkonversionsschichten
Trimmel, G., **Hollauf, M.**, Cajlakovic, M., Köstler, S. & Hartmann, P. 2014

- ▶ Highly fluorescent naphthalimide-functionalized polymers by ring opening metathesis
polymerisation
Hollauf, M., Trimmel, G., Cajlakovic, M., Köstler, S. & Hartmann, P. 2015

- ▶ iEDDA as a tool for tailored macromolecule synthesis and material modification

- Knall, A-C., **Hollauf, M.**, Reishofer, D. P., Kovacic, S. & Slugovc, C. 2013
- ▶ Inverse electron demand Diels-Alder (iEDDA) reactions used for the preparation of polymer-grafted dipyrido(pyridazines) and their metal-binding ability

Knall, A-C., Reishofer, D., **Hollauf, M.**, Kovacic, S. & Slugovc, C. 2014
 - ▶ Inverse Electron Demand Diels-Alder Reaction (iEDDA) for the Post-Polymerization Functionalization of Unsaturated Polymers

Grumm, B., Knall, A-C., Reishofer, D., **Hollauf, M.** & Slugovc, C. 2015
 - ▶ Inverse electron demand Diels-Alder (iEDDA)-based reactions in precision polymer synthesis

Knall, A-C., **Hollauf, M.**, Reishofer, D. P., Kovacic, S. & Slugovc, C. 2013
 - ▶ Kinetic studies of inverse electron demand Diels-Alder (iEDDA) reactivities

Hollauf, M., Knall, A-C., Schlögl, C. & Slugovc, C. 2013
 - ▶ Kinetic studies on tetrazine-alkene inverse-electron demand (iEDDA) click chemistry and implications for polymer synthesis and modification

Knall, A-C., **Hollauf, M.** & Slugovc, C. 2014
 - ▶ Naphthalimide-functionalized polynorbornenes for highly fluorescent sensor materials

Hollauf, M., Tscherner, M., Köstler, S. & Trimmel, G. 20 Mär 2016
 - ▶ Naphthalimide-functionalized Polymers via ring opening metathesis polymerisation

Hollauf, M., Trimmel, G., Cajlakovic, M., Hartmann, P. & Köstler, S. 2015
 - ▶ Orthogonally "Clickable" Norbornenes for the Preparation of Functional Polymers

Hollauf, M., Knall, A-C. & Slugovc, C. 2013
 - ▶ Perylen functionalized polymers via ring-opening metathesis polymerisation with a high dye content

Hollauf, M., Beichel, D., Cajlakovic, M., Hartmann, P., Köstler, S. & Trimmel, G. 2015
 - ▶ Polymerizable, fluorescent perylene derivatives for the use in ring opening metathesis polymerisation

Hollauf, M., Beichel, D., Cajlakovic, M., Köstler, S., Hartmann, P. & Trimmel, G. 2015
 - ▶ Post-polymerization Functionalization of Unsaturated Polymers by Inverse Electron Demand Diels-Alder Reaction (iEDDA)

Grumm, B., Knall, A-C., Reishofer, D., **Hollauf, M.** & Slugovc, C. 2015

References

- [1] Hollauf M, Trimmel G, Knall A C (2015) *Monatsh. Chem.* 146:1063-1080
- [2] Fleischmann C, Lievenbrück M, Ritter H (2015) *Polymers* 7:717-746
- [3] Parker C A, Hatchard C G (1962) *Proc. Chem. Soc.* 147
- [4] Islangulov R R, Lott J, Weder C, Castellano F N (2007) *J. Am. Chem. Soc.* 129:12652-12653
- [5] Leitgeb A, Wappel J, Slugovc C (2010) *Polymer* 51:2927–2946
- [6] Bielawski CW, Grubbs RH (2007) *Progr Polym Sci* 32:1-29
- [7] Nomura K, Abdellatif MM (2010) *Polymer* 51:1861–1881
- [8] Knall AC, Slugovc C (2014) In: Grela K (ed) *Olefin Metathesis: Theory and Practice*, K Grela 1st edn, John Wiley & Sons, Inc, Hoboken, NJ, USA
- [9] Grubbs RH, Wenzel AG, O'Leary DJ, Khosravi E (2015) *Handbook of Metathesis* 2nd ed, John Wiley & Sons, New Jersey
- [10] Bunz UHF, Mäcker D, Porz M (2010) *Macromol Rapid Commun* 33: 886–910
- [11] Trimmel G, Riegler S, Fuchs G, Slugovc C, Stelzer F (2005) *Adv Polym Sci* 176:43-87
- [12] Scheinhardt B, Trzaskowski J, Baier MC, Baier MC, Stempfle B, Oppermann A, Wöll D, Mecking S (2013) *Macromolecules* 46:7902–7910
- [13] Gómez FJ, Chen RJ, Wang D, Waymouth RM, Dai H (2003) *Chem Commun* 190–191
- [14] Thompson MP, Randolph LM, James CR, Davalos AN, Hahn ME, Gianneschi NC (2014) *Polym Chem* 5:1954–1964
- [15] Burtscher D, Saf R, Slugovc C (2006) *J Polym Sci Part A Polym Chem* 44:6136–6145
- [16] Zhang Z, Feng H, Liu L, Yu C, Lü X, Zhu X, Wong WK, Jones RA, Pan M, Su C (2015) *Dalton Trans* 44:6229–6241
- [17] Radl SV, Roth M, Gassner M, Wolfberger A, Lang A, Hischmann B, Trimmel G, Kern W, Griesser T (2014) *European Polymer Journal* 52:98-104
- [18] Boyd TJ, Geerts Y, Lee JK, Fogg DE, Lavoie GG, Schrock RR, Rubner MF (1997) *Macromolecules* 30:3553–3559
- [19] Boyd TJ, Schrock RR (1999) *Macromolecules* 32:6608–6618
- [20] Porz M, Paulus F, Höfle S, Lutz T, Lemmer U, Colsmann A, Bunz UHF (2013) *Macromol Rapid Commun* 34:1611–1617
- [21] Gorodetskaya IA, Gorodetsky AA, Vinogradova EV, Grubbs RH (2009) *Macromolecules* 42:2895–2898
- [22] Combe CMS, Biniek L, Schroeder BC, McCulloch I (2014) *J Mater Chem C* 2:538-541
- [23] Gallas K, AC, Scheicher SR, Fast DE, Saf R, Slugovc C (2014) *Macromol Chem Phys* 215:76–81
- [24] Glaz MS, Biberdorf JD, Nguyen MT, Travis JJ, Holliday BJ, Vanden Bout DA (2013) *J Mater*

-
- Chem C 1:8060-8065
- [25] Huang C, Potscavage WJ, Tiwari SP, Sutcu S, Barlow S, Kippelen B, Marder SR (2012) *Polym Chem* 3:2996-3006
- [26] Song W, Han H, Wu J, Xie M (2014) *Chem Commun* 50:12899–12902
- [27] Chen CW, Chang HY, Lee SL, Lee SL, Hsu IJ, Lee JJ, Chen CH, Luh TY (2010) *Macromolecules* 43:8741–8746
- [28] Yamamoto T, Fukushima T, Kosaka A, Jin W, Yamamoto Y, Ishii N, Aida T (2008) *Angew Chemie - Int Ed* 47:1672–1675
- [29] Yamamoto T, Fukushima T, Yamamoto Y, Kosaka A, Jin W, Ishii N, Aida T (2006) *J Am Chem Soc* 128:14337–14340
- [30] Yao PS, Cao QY, Peng RP, Liu JH (2015) *J Photochem Photobiol A Chem* 305:11–18
- [31] Lian WR, Huang YC, Liao YA, Wang KL, Li LJ, Su CY, Liaw DJ, L KR, Lai JY (2011) *Macromolecules* 44:9550–9555
- [32] Noormofidi N, Slugovc C (2007) *Macromol Chem Phys* 208:1093–1100
- [33] Noormofidi N, Slugovc C (2010) *Eur Polym J* 46:694–701
- [34] Ahn KD, Lee JH, Cho I, Park KH, Kang JH, Han DK, Kim JM (2000) *J Photopolym Sci Technol* 13:493–496
- [35] Myles AJ, Gorodetsky B, Branda NR (2004) *Adv Mater* 16:922–925
- [36] Nantalaksakul A, Krishnamoorthy K, Thayumanavan S (2010) *Macromolecules* 43:37–43
- [37] Lee JK, Schrock RR, Baigent DR, Friend RH (1995) *Macromolecules* 28:1966–1971
- [38] Zaami N, Slugovc C, Pogantsch A, Stelzer F (2004) *Macromol Chem Phys* 205:523–529
- [39] Qiao Y, Islam MS, Yin X, Han K, Yan Y, Zhang J, Wang Q, Ploehn HJ, Tang C (2015) *Polymer* doi: 10.1016/j.polymer.2015.02.011
- [40] Griesser T, Rath T, Stecher H, Saf R, Kern W, Trimmel G (2007) *Monatshefte für Chemie* 138:269–276
- [41] Bellmann E, Shaheen S (1998) *Chem Mater* 10:1668–1676
- [42] Sandholzer M, Lex A, Trimmel G, Saf R, Stelzer F, Slugovc C (2007) *J Polym Sci Part A Polym Chem* 45:1336–1348
- [43] Sandholzer M, Schuster M, Varga F, Liska R, Slugovc C (2008) *J Polym Sci Part A Polym Chem* 46:3648–3661
- [44] Roberts KS, Sampson NS (2004) *Org Lett* 6:3253–3255
- [45] Gueugnon F, Denis I, Pouliquen D, Colette F, Delatouche R, Héroguez V, Grégoire M, Bertrand P, Blanquart C (2013) *Biomacromolecules* 14:2396–2402
- [46] Chien MP, Thompson MP, Lin EC, Gianneschi NC (2012) *Chem Sci* 3:2690-2694

-
- [47] Sandholzer M, Fritz-Popovski G, Slugovc C (2008) *J Polym Sci Part A Polym Chem* 46:401–413
- [48] Sandholzer M, Bichler S, Stelzer F, Slugovc C (2008) *J Polym Sci Part A Polym Chem* 46:2402–2413
- [49] Sandholzer M, Slugovc C (2009) *Macromol Chem Phys* 210:651–658
- [50] Abd-El-Aziz AS, Shipman PO, Shipley PR, Boden BN, Aly S, Harvey PD (2009) *Macromol Chem Phys* 210:2099–2106
- [51] Jia Y, Spring AM, Qiu F, Yu F, Yamamoto K, Aoki I, Otomo A, Yokoyama S (2014) *Jpn J Appl Phys* 53:01AF04
- [52] Lambeth RH, Moore JS (2007) *Macromolecules* 40:1838–1842
- [53] Lambeth RH, Park J, Liao H, Shir DJ, Jeon S, Rogers JA, Moore JS (2010) *Nanotechnology* 21:165301
- [54] Abd-El-Aziz AS, Okasha RM, Afifi TH, Todd EK (2003) *Macromol Chem Phys* 204:555–563
- [55] Hauser L, Knall AC, Roth M, Trimmel G, Edler M, Griesser T, Kern W (2012) *Monatshefte für Chemie* 143:1551–1558
- [56] Samanta S, Locklin J (2008) *Langmuir* 24:9558–9565
- [57] Florea L, Benito-Lopez F, Hennart A, Diamond D (2011) *Procedia Eng* 25:1545–1548
- [58] Tomasulo M, Deniz E, Benelli T, Sortino S, Raymo F (2009) *Adv Funct Mater* 19:3956–3961
- [59] Feng K, Xie N, Chen B, Zhang LP, Tung CH, Wu LZ (2012) *Macromolecules* 45:5596–5603
- [60] Meyers A, Weck M (2003) *Macromolecules* 36:1766–1768
- [61] Meyers A, Weck M (2004) *Chem Mater* 16:1183–1188
- [62] Abd-El-Aziz AS, Okasha RM, Afifi TH (2004) *Macromol Symp* 209:195–205
- [63] Abd-El-Aziz AS, Okasha RM, Afifi TH, Todd EK (2003) *Macromol Chem Phys* 204:555–563
- [64] De La Escosura A, Martínez-Díaz MV, Torres T, Grubbs RH, Guldi DM, Heugebauer H, Winder C, Drees M, Sariciftci NS (2006) *Chemistry - An Asian J* 1:148–154
- [65] Meyers A, South C, Weck M (2004) *Chem Commun* 1176–1177
- [66] Charvet R, Acharya S, Hill JP, Akada M, Liao M, Seki S, Honsho Y, Saeki A, Ariga K (2009) *J Am Chem Soc* 131:18030–18031
- [67] Chen B, Sleiman HF (2004) *Macromolecules* 37:5866–5872
- [68] Chen B, Metera K, Sleiman HF (2005) *Macromolecules* 38:1084–1090
- [69] Knall AC, Schinagl C, Pein A, Noormodifi N, Saf R, Slugovc C (2012) *Macromol Chem Phys* 213:2618–2627
- [70] Carlise JR, Wang XY, Weck M (2005) *Macromolecules* 38:9000–9008
- [71] Bochkarev LN, Begantsova YE, Platonova EO, Basova GV, Rozhkov AV, Il'ichev VA, Baranov

-
- EV, Abakumov GA, Bochkarev MN (2014) *Russ Chem Bull* 63(4):1001-1008
- [72] Tefashe UM, Metera KL, Sleiman HF, Mauzeroll J (2013) *Langmuir* 29:12866–12873
- [73] Niedermair F, Noormofidi N, Lexer C, Saf R, Slugovc C (2011) *Polymer* 52:1874–1881
- [74] Niedermair F, Sandholzer M, Kremser G, Slugovc C (2009) *Organometallics* 28:2888–2896
- [75] Hilf S, Kilbinger AFM (2009) *Nat Chem* 1:537–546
- [76] Lexer C, Saf R, Slugovc C (2009) *J Polym Sci Part A Polym Chem* 47:299–305
- [77] Takamizu K, Nomura K (2012) *J Am Chem Soc* 134:7892–7895
- [78] Madkour AE, Koch AHR, Lienkamp K, Tew GN (2010) *Macromolecules* 43:4557–4561
- [79] Kolonko EM, Pontrello JK, Mangold SL, Kiessling LL (2009) *J Am Chem Soc* 131:7327–7333
- [80] Mangold SL, Carpenter RT, Kiessling LL (2008) *Org Lett* 10:2997–3000
- [81] Gordon EJ, Gestwicki JE, Strong LE, Kiessling LL (2000) *Chem Biol* 7:9–16
- [82] Romulus J, Henssler JT, Weck M (2014) *Macromolecules* 47:5437–5449
- [83] Tezgel AÖ, Telfer JC, Tew GN (2011) *Biomacromolecules* 12:3078–3083
- [84] Biswas S, Wang X, Morales AR, Ahn HY, Belfield KD (2011) *Biomacromolecules* 12:441–449
- [85] Johnson JA, Lu YY, Burts AO, Lim YH, Finn MG, Koberstein JT, Turro NJ, Tirrell DA, Grubbs RH (2011) *J Am Chem Soc* 133:559–566
- [86] Miki K, Oride K, Kimura A, Kuramochi Y, Matsuoka H (2011) 3536–3547
- [87] Miki K, Kuramochi Y, Oride K, Inoue S, Harada H, Hiraoka M, Ohe K (2009) *Bioconjugate Chem* 6:511–517
- [88] Johnson JA, Lu YY, Burts AO, Xia Y, Durrell AC, Tirrell DA, Grubbs RH (2010) *Macromolecules* 43:10326–10335
- [89] Hanik N, Kilbinger AFM (2013) *J Polym Sci Part A Polym Chem* 51:4183–4190
- [90] Miki K, Kimura A, Oride K, Kuramochi Y, Matsuoka H, Harada H, Hiraoka M, Ohe K (2011) *Angew Chemie - Int Ed* 50:6567–6570
- [91] Miki K, Oride K, Inoue S, Kuramochi Y, Najak RR, Matsuoka H, Harada H, Hiraoka M, Ohe K (2010) *Biomaterials* 31:934–942
- [92] Van Hensbergen JA, Burford RP, Lowe AB (2013) *J Polym Sci Part A Polym Chem* 51:487–492
- [93] Knall AC, Kovačič S, Hollauf M, Reishofer D, Saf R, Slugovc C (2013) *Chem Commun* 49:7325–7327
- [94] Chien MP, Thompson MP, Barback CV, Ku TH, Hall DJ, Gianneschi C (2013) *Adv Mater* 25:3599–3604
- [95] Lex A, Trimmel G, Kern W, Stelzer F (2006) *J Mol Catal A Chemical* 254:174-179
- [96] Höfler T, Griesser T, Gstrein X, Trimmel G, Jakopic G, Kern W, (2007) *Polymer* 48:1930-1939
- [97] Köpplmayr T, Cardinale M, Jakopic G, Trimmel G, Kern W, Griesser T (2011) *J Mater Chem*

-
- 21:2965-2973
- [98] Griesser T, Kuhlmann JC, Wieser M, Kern W, Trimmel G (2009) *Macromolecules* 42:725-731
- [99] Thomas III SW (2012) *Macromol Chem Phys* 213:2443–2449
- [100] Edler M, Mayrbrugger S, Fian A, Trimmel G, Radl S, Kern W, Griesser T, (2013) *J Mater Chem* 1:3931-3938
- [101] Koeplmayr T, Cardinale M, Rath T, Trimmel G, Rentenberger S, Zojer E, Kern W, Griesser T, (2012) *Macromol Chem Phys* 213:367–373
- [102] Griesser T, Höfler T, Jakopiec G, Belzik M, Kern W, Trimmel G (2009) *J Mater Chem* 19:4557-4565
- [103] Griesser T, Höfler T, Temmel S, Kern W, Trimmel G (2007) *Chem Mater* 19:3011-3017
- [104] Gumbley P, Hu X, Lawrence III JA, Thomas III SW, (2013) *Macromol Rapid Commun* 34:1838–1843
- [105] Koylu D, Thapa M, Gumbley P, Thomas III SW, (2012) *Adv Mater* 24:1451–1454
- [106] Marchl M, Golubkov AW, Edler M, Griesser T, Pacher P, Haase A, Stadlober B, Belegriatis MR, Trimmel G, Zojer E (2010) *Appl Phys Lett*, 96:213303
- [107] Marchl M, Edler M, Haase A, Fian A, Trimmel G, Griesser T, Stadlober B, Zojer E (2010) *Adv Mater* 22:5361–5365
- [108] Matson JB, Grubbs RH (2008) *J Am Chem Soc* 130:6731–6733
- [109] Myles AJ, Gorodetsky B, Branda NR (2004) *Adv Mater* 16:922–925
- [110] Wigglesworth TJ, Branda NR (2005) *Chem Mater* 17:5473-5480
- [111] Myles AJ, Branda NR (2003) *Macromolecules* 36:298-303
- [112] Sam-Rok Keum SR, Su-Mi Ahn SM, Se-Jung Roh SJ, So-Young Ma SY (2010) *Dyes and Pigments* 86:74-80
- [113] Shen Q, Edler M, Griesser T, Knall AC, Trimmel G, Kern W, Teichert C (2014) *Scanning* 36:590–598
- [114] Gumbley P, Thomas III SW (2014) *ACS Appl Mater Interfaces* 6:8754–8761
- [115] (a) S Balushev, V Yakutkin, G Wegner, B Minch, T Miteva, G Nelles and A Yasuda, *J Appl Phys*, 2007, 102, 076103 (b) RP Steer, *J Appl Phys*, 2007, 102, 076102
- [116] A Monguzzi, R Tubino, S Hoseinkhani, M Campione and F Meinardi, *Phys Chem Chem Phys*, 2012, 14, 4322–4332
- [117] Y Simon and C Weder, *J Mater Chem*, 2012, 22, 20817
- [118] T N Singh-Rachford, J Lott, C Weder and F N Castellano, *J Am Chem Soc*, 2009, 17, 12007
- [119] S H Lee, H Soo, D C Thévenaz, C Weder and Y C Simon, *J Polym Sci Pol Chem*, 2015, 53, 1629
- [120] C Ye, J Wang, X Wang, P Ding, Z Liang and X Tao, *Phys Chem Chem Phys*, 2016, 18, 3430

-
- [121] GR Fulmer, AJM Miller, NH Sherden, HE Gottlieb, A Nudelman, BM Stoltz, JE Bercaw and KI Goldberg, *Organometallics*, 2010, 29, 2176
- [122] GA Crosby and JN Demas, *J Phys Chem*, 1971, 75, 991
- [123] SM Borisov, G Nuss, W Haas, R Saf, M Schmuck and I Klimant, *J Photochem Photobiol*, 2009, 201, 128
- [124] A J Lowe, G A Dyson and F M Pfeffer, *Eur J Org Chem*, 2008, 2008, 1559
- [125] Y. Simon and C. Weder, *J. Mater. Chem*, 2012, 22, 20793
- [126] S. H. Lee, D. C. Thévenaz, C. Weder and Y. Simon, *J. Polym. Sci. Pol. Chem.*, 2015, 53, 1629
- [127] T. Singh-Rachford and F. Castellano, *Coord. Chem. Rev.*, 2010, 254, 2560
- [128] F. Wang, R. Deng, J. Wang, Q. Wang, Y. Han, H. Zhu, X. Chen and X. Liu, *Nat. Mater.*, 2011, 10, 968
- [129] S. Mattiello, A. Monguzzi, J. Pedrini, M. Sassi, C. Villa, Y. Torrente, R. Marotta, F. Meinardi and L. Beverina, *Adv. Funct. Mater.*, 2016, 1
- [130] J. P. Vogel, *Physical Review Letters*, 1961, 7, 229
- [131] C. Ye, L. Zhou, X. Wang and Z. Liang, *Phys. Chem. Chem. Phys.*, 2016, 18, 10818
- [132] A. Monguzzi, S. M. Borisov, J. Pedrini, I. Klimant, M. Salvalaggio, P. Biagini, F. Melchiorre, C. Lelii and F. Meinardi, *Adv. Funct. Mater.*, 2015, 25, 5617
- [133] T. F. Schulze and T. W. Schmidt, *Energy Environ. Sci.*, 2015, 8, 103
- [134] T. N. Singh-Rachford and F. N. Castellano, *J. Phys. Chem. A*, 2008, 112, 3550
- [135] T. N. Singh-Rachford, A. Haefel, R. Ziessel and F. N. Castellano, *J. Am. Chem. Soc.*, 2008, 130, 16164
- [136] W. Wu, W. Wu, S. Ji, H. Guo and J. Zhao, *Dalton Trans.* 2011, 40, 5953
- [137] R. R. Islangulov, D. V. Kozlov and F. N. Castellano, *Chem. Commun.*, 2005, 30, 3776
- [138] A. Turshatov, D. Busko, S. Balushev, T. Miteva and K. Landfester, *New J. Phys.*, 2011, 13, 083035
- [139] C. A. Parher and C. G. Hatchard, *Nature*, 1965, 205, 1282
- [140] R. R. Islangulov, J. Lott, C. Weder and F. N. Castellano, *J. Am. Chem. Soc.*, 2007, 129, 12652
- [141] T. Gatti, L. Brambilla, M. Tommasini, F. Villafiorita-Monteleone, C. Botta, V. Sarritzu, A. Mura and G. Bongiovanni, *J. Phys. Chem. C*, 2015, 119, 17495
- [142] C. Ye, J. Wang, X. Wang, P. Ding, Z. Liang and X. Tao, *Phys. Chem. Chem. Phys.*, 2016, 18, 3430
- [143] H. Kouno, T. Ogawa, S. Amemori, P. Mahato, N. Yanai and N. Kimizuka, *Chem. Sci.*, 2016, 7, 5224
- [144] C. Wohnhaas, K. Friedemann, D. Busko, K. Landfester, S. Balushev, D. Crespy and A.

-
- Turshatov, *ACS Macro. Lett.*, 2013, 2, 446
- [145] P. Mahato, A. Monguzzi, N. Yanai, T. Yamada and N. Kimizuka, *Nat. Mater.*, 2015, 14, 924
- [146] J. Zimmermann, R. Mulet, G. D. Scholes, T. Wellens and A. Buchleitner, *J. Chem. Phys.*, 2014, 141, 18410
- [147] S. H. C. Askes, N. López Mora, R. Harkes, R. I. Koning, B. Koster, T. Schmidt, A. Kros and S. Bonnet, *Chem. Commun.*, 2015, 51, 9137
- [148] M. Poznik, U. Faltermeier, B. Dick and B. König, *RSC Adv.*, 2016, 6, 41947
- [149] Y. Murakami, T. Ito and A. Kawai, *J. Phys. Chem. B*, 2014, 118, 14442
- [150] M. Penconi, P. L. Gentili, G. Massaro, F. Elisei and F. Ortica, *Photochem. Photobiol. Sci.*, 2014, 13, 48
- [151] C. Ye, B. Wang, R. Hao, X. Wang, P. Ding, X. Tao, Z. Chen, Z. Liang and Y. Zhou, *J. Mater. Chem. C*, 2014, 2, 8507
- [152] Q. Liu, B. Yin, T. Yang and Y. Yang, *J. Am. Chem. Soc.*, 2013, 135, 5029
- [153] A. Turshatov, D. Busko, S. Balushev, T. Miteva and K. Landfester, *New. J. Phys.*, 2011, 13, 083035
- [154] K. Tanaka, K. Inafuku and Y. Chujo, *Chem. Commun.*, 2010, 46, 4378
- [155] A. J. Tilley, B. E. Robotham, R. P. Steer and K. P. Ghiggino, *Chem. Phys. Lett.*, 2015, 618, 198
- [156] K. Katta, D. Busko, Y. Avlasevich, R. Muñoz-Espí, S. Balushev and K. Landfester, *Macromol. Rapid. Commun.*, 2015, 36, 1084
- [157] C. Wohnhaas, V. Mailänder, M. Dröge, M. Filatov, D. Busko, Y. Avlasevich, S. Balushev, T. Miteva, K. Landfester, and A. Turshatov, *Macromol. Biosci.*, 2013, 13, 14220
- [158] J. Zhou, Q. Liu, W. Feng, Y. Sun and F. Li, *Chem. Rev.* 2015, 115, 395
- [159] J. H. Olivier, Y. Bai, H. Uh, H. Yoo, M. J. Therien and F. N. Castellano, *J. Phys. Chem. A*, 2015, 119, 5642
- [160] R. Andernach, H. Utzat, S. D. Dimitrov, I. McCulloch, M. Heeney, J. R. Durrant and H. Bronstein, *J. Am. Chem. Soc.*, 2015, 137, 10383
- [161] J. Sun, J. Yang, C. Zhang, H. Wang, J. Li, S. Su, H. Xu, T. Zhang, Y. Wu, W. Y. Wong, B. Xu, *New J. Chem.*, 2015, 39, 5180
- [162] S. Yu, Y. Zeng, J. Chen, T. Yu, X. Zhang, G. Yang and Y. Li, *RSC Adv.*, 2015, 5, 70640 [163 D. C. Thévenaz, A. Monguzzi, D. Vanhecke, R. Vadrucchi, F. Meinardi, Y. C. Simon and C. Weder, *Mater. Horiz.*, 2016, 3, 602
- [164] X. Yu, X. Cao, X. Chen, N. Ayres and P. Zhang, *Chem. Commun.*, 2015, 51, 588
- [165] C. Fan, W. Wu, J. J. Chruma, J. Zhao and C. Yang, *J. Am. Chem. Soc.*, 2016, DOI: 10.1021/jacs.6b07946

-
- [166] P.C. Boutin, K. P. Ghiggino, T. L. Kelly, R. P. Steer, *J. Phys. Chem. Lett.* 2013, 4, 4113-4118.
- [167] A. J. Tilley, M. J. Kim, M. Chen, K. P. Ghiggino. *Polymer*, 2013, 54, 2865-2872
- [168] E. Khosravi, in: "Handbook of Metathesis", R. H. Grubbs, Ed., Wiley-VCH, Weinheim 2003, 3, 72 and 255
- [169] A. Leitgeb, J. Wapple and C. Slugovc, *Polymer*, 2010, 51, 2927
- [170] M. Hollauf, G. Trimmel and A. C. Knall, *Monatsh. Chem.*, 2015, 146, 1063
- [171] M. Hollauf, M. Cajlakovič, M. Tscherner, S. Köstler, A. C. Knall and G. Trimmel, *Monatsh. Chem.*, 2016, DOI: 10.1007/s00706-016-1887-3
- [172] M. Sandholzer, A. Lex, G. Trimmel, R. Saf, F. Stelzer, C. Slugovc *J. Polym. Sci. Part A: Polym. Chem.* 2007, 45, 1336-1348
- [173] S. M. Borisov, C. Larndorfer, I. Klimant, I., *Adv. Funct. Mater.*, 2012, 22, 4360
- [174] C. A. Hunter and J. K. M. Sanders, *J. Am. Chem. Soc.*, 1990, 112, 5525
- [175] P. Rothmund, *J. Am. Chem. Soc.*, 1936, 157, 625
- [176] A. D. Adler, F. R. Longo, J. D. Finarelli, J. Goldmacher, J. Assour and L. Korsakoff, *J. Org. Chem.*, 1967, 32, 476
- [177] S. J. Lindsey, I. C. Schreiman, H. C. Hsu, P. C. Kearney and A. M. Marguerettaz, *J. Org. Chem.*, 1987, 52, 827
- [178] O. S. Finikova, A. V. Cheprakov, I. P. Beletskaya, P. J. Carroll and S. A. Vinogradov, *J. Org. Chem.*, 2004, 69, 522
- [179] C. Borek, K. Hanson, P. I. Djurovich, M. E. Thompson, K. Aznavour, R. Bau, Y. Sun, S. R. Forrest, J. Brooks and L. Michalski, *Angew. Chem. Int. Ed.* 2007, 46, 1109
- [180] K. Ichimura, M. Sakuragi, H. Morii, M. Yasuike, M. Fukui and O. Ohno, *Inorg. Chim. Acta*, 1991, 182, 83
- [181] L. H. Hutter, B. J. Müller, K. Koren, S. M. Borisov and I. Klimant, *J. Mater. Chem. C*, 2014, 2, 7589
- [182] X. Cui, J. Zhao, P. Yang and J. Sun, *Chem. Commun.*, 2013, 49, 10221
- [183] B. Neises, W. Steglich W., *Org. Synth.*, 1978, 7, 93
- [184] L. H. Hutter, B. J. Müller, K. Koren, S. M. Borisov and I. Klimant, *J. Mater. Chem. C*, 2014, 2, 7589
- [185] D. Burtscher , C. Lexer , K. Mereiter , R. Winde , R. Karch , C. Slugovc , *J. Polym. Sci., Part A: Polym. Chem.* 2008, 46, 4630.
- [186] X. Yu, X. Cao, X. Chen, N. Ayres and P. Zhang, *Chem. Commun.*, 2015, 51, 588
- [187] Y. Y. Cheng and T. Houry, *Phys. Chem. Chem. Phys.*, 2010, 12, 66
- [188] I. B. Rietveld, E. Kim and S. A. Vinogradov, *Tetrahedron* 2003, 59, 3821

-
- [189] G. R. Fulmer, A. J. M. Miller, N. H. Sherden, H. E. Gottlieb, A. Nudelman, B. M. Stoltz, J. E. Bercaw and K. I. Goldberg, *Organometallics*, 2010, 29, 2176
- [190] G. A. Crosby and J. N. Demas, *J. Phys. Chem.*, 1971, 75, 991
- [191] S. M. Borisov, G. Nuss, W. Haas, R. Saf, M. Schmuck and I. Klimant, *J. Photochem. Photobiol.*, 2009, 201, 128
- [192] R. Wang, Z. Shi, C. Zhang, A. Zhang, J. Chen, W. Guo and Z. Sun, *Dyes and Pigments*, 2013, 98, 450
- [193] B. Balaganesan, W. J. Shen and C. H. Chen, *Tetrahedron Lett.*, 2003, 44, 5747
- [194] B. Neises and W. Steglich, *Angew. Chem. Int. Ed. Engl.*, 1978, 17, 522
- [195] A. J. Lowe, G. A. Dyson and F. M. Pfeffer, *Eur. J. Org. Chem.*, 2008, 2008, 1559
- [196] Xiao P, Dumur F, Graff B, Gignes D, Fouassier JP, Lalevée J (2014) *Macromolecules* 47:601
- [197] Liu J, Shao S, Chen L, Xie Z, Cheng Y, Geng Y, Wang L, Jing X, Wang F (2007) *Adv Mater* 19:1863
- [198] Morgado J, Grüner J, Walcott SP, Yong TM, Cervini R, Moratti SC, Holmes AB, Friend RH (1998) *Synthetic Metals* 95:113
- [199] Zhang J, Zhang X, Xiao H, Li G, Liu Y, Li C, Huang H, Chen X, Bo Z *ACS Appl Mater Interfaces* (2016) 8:5475
- [200] Wang Y, Zhang X, Han B, Peng J, Hou S, Huang Y, Sun H, Xie M, Lu Z (2010) *Dyes and Pigments* 86:190
- [201] Srivastava AK, Singh AK, Lallan Mishra L, *J Phys Chem A*, DOI: 101021/acsjpca6b05355
- [202] Cho DW, Cho DW (2014) *New J Chem* 38:2233
- [203] Cao H, Chang V, Hernandez R, Heagy MD (2005) *J Org Chem* 70:4929
- [204] Jia X, Yang Y, Xu Y, Qian X (2014) 86(7):1237
- [205] Tian H, Gan J, Chen K, He J, Song QL, Hou XY (2002) *J Mater Chem* 12:1262
- [206] Grabchev I, Yordanova S, Stoyanov S, Petkov I (2014) *Journal of Chemistry*, 79321
- [207] Xu J-H, Hou Y-M, Ma Q-J, Wu X-F, Wei X-J (2013) *Spectrochimica Acta Part A: Molecular and Biomolecular Spectroscopy* 112:116
- [208] He C, Zhu W, Xu Y, Chen T, Qian X (2009) *Anal Chim Acta* 651:227
- [209] Guo X, Qian X, Jia L (2004) *J Am Chem Soc* 126:2272
- [210] Zhou J, Liu H, Jin B, Liu X, Fu H, Shangguan D (2013) *J Mater Chem C* 1:4427
- [211] Alaei P, Rouhani S, Gharanjig K, Ghasemi J (2012) *Spectrochimica Acta Part A* 90:85
- [212] Trupp S, Schweitzer A, Mohr GJ, (2006) *Org Biomol Chem* 4:2965
- [213] Kumar S, Koh J (2013) *Carbohydrate Polymers* 94:221
- [214] Yin H, Zhu W, Xu Y, Dai M, Qian X, Li Y, Liu J (2011) *Eur J Med Chem* 46:3030

-
- [215] Liang S, Yu H, Xiang J, Yang W, Chen X, Liu Y, Gao C, Yan G (2012) *Spectrochimica Acta Part A: Molecular and Biomolecular Spectroscopy* 97:359
- [216] Rouhani S, Nahavandifard F (2014) 197:185
- [217] Wagner R, Wan W, Biyikal M, Benito-Peña, Moreno-Bondi MC, Lazraq I, Rurack K, Sellergren B (2013) *J Org Chem* 78:1377
- [218] Li C, Hu Z, Aldred MP, Zhao L-X, Yan H, Zhang G-F, Huang Z-L, Li ADQ, Zhu M-Q (2014) *Macromolecules* 47:8594
- [219] Leitgeb A, Wappel J, Slugovc C (2010) *Polymer* 51:2927
- [220] Hauser L, Knall A-C, Roth M, Trimmel G, Edler M, Griesser T, Kern W (2012) *Monatsh Chemie Monthly* 143(11):1551
- [221] Hollauf M, Trimmel G, Knall AC, *Monatsh Chemie* 146 (7):1063
- [222] Gallas K, Knall AC, Scheicher SR, Fast DE, Saf R, Slugovc C (2013) *Macromol Chem Phys* 215(1):76
- [223] Bardajee GR, Li AY, Haley JC, Winnik MA (2008) *Dyes and Pigments* 79:24
- [224] Breul AM, Hager MD, Schubert US (2013) *Chem Soc Rev* 42:5366
- [225] Zhou J, Liu H, Jin B, Liu X, Fu H, Shangguan D (2013) *J Mater Chem C* 1:4427
- [226] Gan J, Chen K, Chang CP, Tian H (2003) *Dyes and Pigments* 57:21 Gan J, Tian H, Wang Z, Chen K, Hill J, Lane PA, Rahn MD, Fox AM, Bradley DDC (2002) *J Organomet Chem* 645:168
- [227] Saha S, Samanta A (2002) *J Phys Chem A*, 106:4763
- [217] Nandhikonda P, Paudel S, Heagy MD (2009) *Tetrahedron* 65:2173
- [218] Trupp S, Hoffmann P, Henkel T, Mohr GJ (2008) *Org Biomol Chem* 6:4319
- [230] Grabchev I, Konstantinova T (1997) 33(3):197
- [231] de Silva A P , Gunaratne H Q N , Habib-Jiwan J L , McCoy C P , Rice T E , Soumillion J P, *Angew Chem Int Ed Engl* 1995, 34, 1728
- [232] G Jiaan, C Kongchang, C Chen-Pin, T He, *Dyes and Pigments*, 2003, 57, 21
- [233] J H Xu, Y M Hou, Q J Ma, X F Wu, X J Wei, *Spectrochim Acta Mol Biomol Spectrosc*, 2013, 112, 116
- [234] M Sandholzer, G Fritz-Popovski and C Slugovc *J Polym Sci A Polym Chem*, 2008, 46, 401
- [235] S C G Biagini, R G Davies, V C Gibson, M R Giles, E L Marshall and M North, *Polymer*, 2001, 42, 6669
- [236] Grubbs, R H *Handbook of Metathesis*; Wiley- VCH: Weinheim, 2003, 277
- [237] C Lexer, R Saf and C Slugovc, *J Polym Sci Part A: Polym Chem*, 2009, 47, 299
- [238] R M Owen, J E Gestwicki, T Young, L L Kiessling, *Org Lett*, 2002, 4, 2293
- [239] G R Fulmer, A J M Miller, N H Sherden, H E Gottlieb, A Nudelman, B M Stoltz, J E Bercaw and

